

Novel insights into PIN polarity regulation during *Arabidopsis* development

by

Huibin Han

September, 2020

*A thesis presented to the
Graduate School
of the
Institute of Science and Technology Austria, Klosterneuburg, Austria
in partial fulfillment of the requirements
for the degree of
Doctor of Philosophy*



Institute of Science and Technology

The dissertation of Huibin Han, titled Novel insights into PIN polarity regulation during *Arabidopsis* development, is approved by:

Supervisor: Prof. Jiří Friml, IST Austria, Klosterneuburg, Austria

Signature: _____

Committee Member: Prof. Eva Benková, IST Austria, Klosterneuburg, Austria

Signature: _____

Committee Member: Prof. Bartel Vanholme, VIB, Gent, Belgium

Signature: _____

Exam Chair: Prof. Michael Sixt, IST Austria, Klosterneuburg, Austria

Signature: _____

Signed page is on file

© by Huibin Han, September, 2020

All Rights Reserved

IST Austria Thesis, ISSN: 2663-337X

I hereby declare that this dissertation is my own work and that it does not contain other people's work without this being so stated; this thesis does not contain my previous work without this being stated, and the bibliography contains all the literature that I used in writing the dissertation.

I declare that this is a true copy of my thesis, including any final revisions, as approved by my thesis committee, and that this thesis has not been submitted for a higher degree to any other university or institution.

I certify that any republication of materials presented in this thesis has been approved by the relevant publishers and co-authors.

Signature: _____

Huibin Han
September 30, 2020

Signed page is on file

Abstract

The plant hormone auxin plays indispensable roles in plant growth and development. An essential level of regulation in auxin action is the directional auxin transport within cells. The establishment of auxin gradient in plant tissue has been attributed to local auxin biosynthesis and directional intercellular auxin transport, which both are controlled by various environmental and developmental signals. It is well established that asymmetric auxin distribution in cells is achieved by polarly localized PIN-FORMED (PIN) auxin efflux transporters. Despite the initial insights into cellular mechanisms of PIN polarization obtained from the last decades, the molecular mechanism and specific regulators mediating PIN polarization remains elusive. In this thesis, we aim to find novel players in PIN subcellular polarity regulation during *Arabidopsis* development. We first characterize the physiological effect of piperonylic acid (PA) on *Arabidopsis* hypocotyl gravitropic bending and PIN polarization. Secondly, we reveal the importance of SCF^{TIR1/AFB} auxin signaling pathway in shoot gravitropism bending termination. In addition, we also explore the role of myosin XI complex, and actin cytoskeleton in auxin feedback regulation on PIN polarity.

In **Chapter 1**, we give an overview of the current knowledge about PIN-mediated auxin fluxes in various plant tropic responses. In **Chapter 2**, we study the physiological effect of PA on shoot gravitropic bending. Our results show that PA treatment inhibits auxin-mediated PIN3 repolarization by interfering with PINOID and PIN3 phosphorylation status, ultimately leading to hyperbending hypocotyls. In **Chapter 3**, we provide evidence to show that the SCF^{TIR1/AFB} nuclear auxin signaling pathway is crucial and required for auxin-mediated PIN3 repolarization and shoot gravitropic bending termination. In **Chapter 4**, we perform a phosphoproteomics approach and identify the motor protein Myosin XI and its binding protein, the MadB2 family, as an essential regulator of PIN polarity for auxin-canalization related developmental processes. In **Chapter 5**, we demonstrate the vital role of actin cytoskeleton in auxin feedback on PIN polarity by regulating PIN subcellular trafficking.

Overall, the data presented in this PhD thesis brings novel insights into the PIN polar localization regulation that resulted in the (re)establishment of the polar auxin flow and gradient in response to environmental stimuli during plant development.

Acknowledgments

First of all, I would like to thank Prof. Friml for giving me the opportunity to be a member of his group and also for his support and guidance during my PhD. I learned a lot about science such as thinking and writing, and also how to present in the best possible way.

Second, I would also like to acknowledge my internal and external committee members for their time and efforts to read, to evaluate and to suggest improvements for my PhD thesis.

I also want to thank the China Scholarship Council for supporting my study during the year from 2015 to 2019.

My great acknowledge to my family for their understanding and support during my time at IST.

I also want to thank all the lab members Lesia, Inge, Maciek, Lanxin, Jakub et al for their kind help, suggestions, and discussions. I also want to thank IST facilities – the Bioimaging facility, the media kitchen, the plant facility and all of the campus services, for their support.

Time flies fast, but all the memory at IST will stay forever in my mind.

Thank you all for all your help and support.

About the Author

Huibin Han completed the BSc in life sciences at Huanggang Normal University (China) and MSc in plant science at Shaanxi Normal University (China), before joining Prof. Friml group at IST Austria in October 2015. His main research interests focus on auxin exporter PIN protein polarity regulation during plant development. In 2017, he gave a talk about genetic screen for new factors-mediating PIN polarization during hypocotyl gravitropism at Ghent auxin meeting. He also presented his work about actin cytoskeleton in PIN polarity regulation at European Plant Cytoskeletal Club meeting in 2019.

List of Publications Appearing in Thesis

1. **Huibin Han**, Hana Rakusová, Inge Verstraeten, Yuzhou Zhang, Jiří Friml (2019) SCF^{TIR1/AFB} auxin signaling for termination of shoot gravitropism. **Plant Physiology** 183: 37-40

Manuscripts in preparation

1. **Huibin Han**, Maciek Adamowski, Linlin Qi, Jiří Friml. PIN-polarization dependent auxin transport in plant tropic response.

2. **Huibin Han**, Lesia Rodriguez, Inge Verstraeten, Shutang Tan, Behrokh Shojaie, Bartel Vanholme, Wout Boerjan, Jiří Friml. Piperonylic acid inhibits PIN3 polarization dependent auxin transport during *Arabidopsis* hypocotyl gravitropism.

3. **Huibin Han**, Inge Verstraeten, Mark Roosjen, Jakub Hajný, Ewa Mazur, Nikola Rýdza, Dolf Weijers, Jiří Friml. Rapid auxin-mediated phosphorylation of acto-myosin complex mediates polar auxin fluxes in *Arabidopsis* development

4. **Huibin Han**, Ewa Mazur, Nikola Rýdza, Jiří Friml. Actin cytoskeleton for auxin feedback regulation on PIN polarity.

Table of Contents

Abstract	v
Acknowledgments	vi
List of Figures	xi
List of Tables	xiv
List of Symbols/Abbreviations	xv
1 PIN-polarization dependent auxin transport in plant tropic response	1
1.1 INTRODUCTION	1
1.2 PIN-MEDIATED POLAR AUXIN FLUXES DURING TROPIC RESPONSES	2
1.3 SUBCELLULAR PIN TRAFFICKING AND KINASE-MEDIATED PIN PHOSPHORYLATION FOR PIN POLARITY SWITCHES IN TROPISMS	6
1.4 INTEGRATION OF DIFFERENT ENVIRONMENTAL CUES INTO PIN POLARITY SWITCHES TO INITIATE TROPISMS	10
1.5 AUXIN FEEDBACK ON PIN POLARITY TO TERMINATE SHOOT GRAVITROPIC BENDING	13
1.6 INTERACTIONS AMONG DIFFERENT TROPISMS	13
1.7 CONCLUDING REMARKS AND FUTURE PERSPECTIVES	15
1.8 REFERENCES	16
2 Piperonylic acid inhibits PIN polarization dependent auxin transport during Arabidopsis hypocotyl gravitropism	23
2.1 INTRODUCTION	23
2.2 RESULTS	25
2.2.1 Piperonylic acid (PA) causes hypocotyl overbending in a dose-dependent manner	25
2.2.2 PA perturbs auxin distribution in Arabidopsis hypocotyl	26
2.2.3 PA inhibits auxin- but not gravity-induced PIN3 repolarization	27
2.2.4 Defective Lignification is not the basis of PA impact on hypocotyl bending and PIN3 repolarization	29
2.2.5 Phenolic profiling analysis reveals flavonoids as downstream targets of C4H	29
2.2.6 Flavonoid negatively regulates hypocotyl bending and PIN3 polarization	30
2.2.7 Flavonoid is the downstream target of C4H in hypocotyl gravitropism	32
2.2.8 PA affects PIN3 phosphorylation status	33
2.3 DISCUSSION	35
2.4 MATERIALS AND METHODS	38
2.5 REFERENCES	42
2.6 SUPPLEMENTARY FIGURES	45
3 SCF^{TIR1/AFB} auxin signaling for bending termination during shoot gravitropism	56
3.1 INTRODUCTION	56
3.2 RESULTS AND DISCUSSION	56
3.3 MATERIALS AND METHODS	61
3.4 REFERENCES	64
3.5 SUPPLEMENTARY FIGURES	65
4 Auxin-mediated rapid phosphorylation of myosin complex mediates polar auxin fluxes in Arabidopsis development	72
4.1 INTRODUCTION	72
4.2 RESULTS	74
4.2.1 A novel and rapid phosphorylation response to auxin	74
4.2.2 Auxin-mediated phosphorylation of Myosin XI and Myosin-binding proteins	76
4.2.3 Myosin XI is required for auxin-senesitive PIN endomembrane trafficking	77

4.2.4	<i>Auxin-mediated Myosin XI phosphorylation regulates PIN endomembrane trafficking</i>	77
4.2.5	<i>Auxin-mediated phosphorylation of Myosin is required for auxin-mediated feedback on PIN polarity</i>	81
4.2.6	<i>MadB2 myosin binding proteins are required for auxin-mediated regulation of PIN polarity and trafficking</i>	82
4.2.7	<i>Auxin-mediated Myosin phosphorylation in shoot gravitropic bending termination</i>	82
4.2.8	<i>Auxin-mediated Myosin phosphorylation in auxin canalization-mediated vasculature formation and regeneration</i>	87
4.3	DISCUSSION	88
4.3.1	<i>Auxin-mediated rapid protein phosphorylation by different signaling pathways</i>	89
4.3.2	<i>Auxin regulates PIN trafficking and polarity via phosphorylation of myosin complex</i>	89
4.3.3	<i>Developmental roles of auxin feedback on directional auxin transport</i>	90
4.4	MATERIALS AND METHODS.....	92
4.5	REFERENCES.....	98
4.6	SUPPLEMENTARY FIGURES	103
5	Actin cytoskeleton for auxin feedback regulation on PIN polarity	119
5.1	INTRODUCTION	119
5.2	RESULTS	121
5.2.1	<i>The actin cytoskeleton is involved in auxin-mediated PIN rearrangement in Arabidopsis root</i> .	121
5.2.2	<i>Defective auxin feedback on PIN1 polarization in actin2 and arp3 mutants root</i>	122
5.2.3	<i>Defective auxin feedback on PIN3 polarization in actin2 and arp3 mutants during shoot gravitropism</i>	122
5.2.4	<i>Defective leaf venation patterning, auxin canalization, regeneration in actin2 and arp3 mutants</i> 124	
5.2.5	<i>Trafficking defects in actin2 and arp3 mutants</i>	126
5.2.6	<i>ACTIN2 and ARP3 mutations cause defective PIN trafficking</i>	126
5.3	DISCUSSION	127
5.3.1	<i>Requirement of actin cytoskeleton for auxin feedback regulation on PIN polarity</i>	130
5.3.2	<i>The actin cytoskeleton is a component of auxin canalization</i>	131
5.3.3	<i>The actin cytoskeleton dependent PIN trafficking</i>	132
5.4	MATERIALS AND METHODS.....	134
5.5	REFERENCES.....	138
5.6	SUPPLEMENTARY FIGURES	142
6	Conclusions and future Perspectives	145
6.1	CONCLUSIONS	145
6.2	FURTHER PERSPECTIVES	145

List of Figures

Chapter 1

Figure 1. PIN-mediated auxin fluxes during plant tropic response.

Figure 2. Simplified model of PIN subcellular trafficking.

Figure 3. Summary of kinase-mediated PIN phosphorylation sites.

Chapter 2

Figure 1. PA promotes hypocotyl bending requires its target C4H.

Figure 2. PA interferes auxin-mediated PIN3 repolarization.

Figure 3. Phenolic profiling of PA treated Arabidopsis seedlings after 24 hours gravity stimulation.

Figure 4. PA promotes PID and PIN3 phosphorylation.

Supplementary Figure S1. The map of the phenylpropanoid pathway in plants.

Supplementary Figure S2. PA effects on hypocotyl bending is independent of CA.

Supplementary Figure S3. PA doesn't affect gravity-induced PIN3 polarization.

Supplementary Figure S4. Normal gravity-induced PIN3 polarization in *c4h* mutant.

Supplementary Figure S5. *p*-CA rescues defective auxin-mediated PIN3 polarization upon PA treatment.

Supplementary Figure S6. *p*-CA rescues defective auxin-mediated PIN3 polarization in *c4h* mutant.

Supplementary Figure S7. Lignin perturbation is not the basis for PA effects on hypocotyl bending and PIN3 polarization.

Supplementary Figure S8. Lignin perturbation is not the basis for the defective hypocotyl bending and PIN3 polarization in *c4h* mutant.

Supplementary Figure S9. PA treatment reduces flavonoid content in hypocotyl.

Supplementary Figure S10. Inhibition of flavonoid biosynthesis doesn't affect gravity-induced PIN3 polarization.

Supplementary Figure S11. Inhibition of flavonoid inhibits auxin-mediated PIN3 repolarization.

Supplementary Figure S12. Flavonoid overcomes PA effects on hypocotyl bending and auxin-mediated PIN3 polarization.

Supplementary Figure S13. Flavonoid overcomes PA effects on auxin-mediated PIN3 polarization.

Chapter 3

Figure 1. Hypocotyl gravitropic bending termination depends on TIR1/AFB signaling.

Figure 2. TIR1/AFB signaling mediates auxin feedback on PIN3 repolarization.

Supplementary Figure S1. ABP1 is not involved in hypocotyl gravitropic bending termination.

Supplementary Figure S2. Modification of TIR1/AFB pathway doesn't affect amyloplasts sedimentation in Arabidopsis hypocotyl endodermal cells.

Supplementary Figure S3. Auxin-induced AUX/IAA protein degradation is not required for gravity-induced PIN3 polarization.

Supplementary Figure S4. Compromised TIR1/AFB signaling doesn't affect gravity-induced PIN3 polarization.

Supplementary Figure S5. Normal PIN3-GFP repolarization in non-induced *HS::axr3-1* hypocotyls after 24 hours gravity stimulation.

Supplementary Figure S6. Auxin-induced AUX/IAA protein degradation is required for auxin-mediated PIN3 repolarization.

Supplementary Figure S7. Normal gravity response and gravity-induced PIN3 polarization in *ccvTIR1* and *cTIR1* hypocotyls.

Supplementary Figure S8. Normal auxin-induced PIN3 repolarization in *cTIR1* mutant.

Chapter 4

Figure 1. Phosphoproteomic analysis reveals rapid phosphorylation-dependent auxin response.

Figure 2. Identification of Myosin XI-K and MadB2 as phosphotargets of auxin signaling.

Figure 3. Myosin XI proteins are involved in auxin-mediated PIN trafficking.

Figure 5. Phosphorylation of myosin XI proteins contributes to auxin-mediated PIN polarity regulation.

Figure 6. Phosphorylation of myosin XI proteins contributes to auxin-mediated PIN polarity regulation to terminate hypocotyl bending.

Figure 7. Defects in auxin-canalization related phenotype in *myosin xik xif* mutant.

Supplementary Figure S1. Comparison of different protein precipitation and phosphopeptide enrichments strategies.

Supplementary Figure S2. TIR1-dependent and -independent rapid auxin response.

Supplementary Figure S3. Analysis of phosphopeptide datasets.

Supplementary Figure S4. Conserved phosphorylation site at myosin XI protein family.

Supplementary Figure S5. Phosphorylation assay of the phospho-deficient and phospho-mimic myosin mutants (Col-0 background).

Supplementary Figure S6. PIN trafficking in phospho-deficient and phospho-mimic myosin mutants (Col-0 background).

Supplementary Figure S7. PIN trafficking in phospho-deficient and phospho-mimic myosin mutants (*myosin xik xif mutant* background).

Supplementary Figure S8. Fm4-64 uptake assay in phospho-deficient and phospho-mimic myosin mutants (*myosin xik xif mutant* background).

Supplementary Figure S9. Auxin-induced PIN1 lateralization in phospho-deficient and phospho-mimic myosin mutants (Col-0 background).

Supplementary Figure S10. Auxin-induced PIN1 lateralization in phospho-deficient and phospho-mimic myosin mutants (*myosin xik xif mutant* background).

Supplementary Figure S11. Auxin canalization related phenotype of *madb 4ko* mutant.

Supplementary Figure S12. The Madb2 myosin binding protein contribute to PIN trafficking and polarity regulation.

Supplementary Figure S13. Gravity-induced PIN3 polarization in *myosin xik xif* mutant hypocotyl.

Supplementary Figure S14. Gravity-induced PIN3 polarization in phospho-deficient and phospho-mimic myosin mutations in Col background.

Supplementary Figure S15. Auxin-induced PIN3 polarization in phospho-deficient and phospho-mimic myosin mutants in Col background.

Supplementary Figure S16. Leaf venation patterns defects in phospho-deficient and phospho-mimic mutants in Col background.

Chapter 5

Figure 1. Actin cytoskeleton is required for auxin feedback on PIN1 lateralization in primary root.

Figure 2. Auxin-induced PIN1 lateralization requires ACTIN2 and ARP3.

Figure 3. Auxin-induced PIN3 repolarization requires actin cytoskeleton, ACTIN2 and ARP3.

Figure 4. Defective leaf venation, regeneration in *actin2* and *arp3* mutants.

Figure 5. Auxin-canalization requires actin cytoskeleton, ACTIN2 and ARP3 protein function.

Figure 6. Decreased FM4-64 uptake in *actin2* and *arp3* mutants.

Figure 7. Defective intracellular PIN1 trafficking in *actin2* and *arp3* mutants upon BFA treatment.

Supplementary Figure S1. Normal gravity-induced PIN3 polarization in *arp3* mutant.

Supplementary Figure S2. Root phenotypes of *actin2* and *arp3* mutant upon auxin treatment.

Supplementary Figure S3. Defective trafficking to TGN/EE in *actin2* and *arp3* mutants.

Supplementary Figure S4. Actin cytoskeleton, ACTIN2 and ARP3 are involved in late endosomes movement.

List of Tables

Chapter 2

Supplementary Tab S1. Identification of metabolites in DMSO or PA treated etiolated hypocotyls with or without gravity stimulation.

Chapter 4

Supplementary Tab S1. Identification of phosphorylated proteins following IAA, PEO-IAA, cvxIAA treatment in *Arabidopsis* root.

List of Symbols/Abbreviations

AUX1/LAX: AUXIN-RESISTANT1/LIKE AUX1
ABCB: ATP-binding cassette subfamily B
BFA: Brefeldin A
ARF-GEFs: ADP-ribosylation factor guanine-nucleotide exchange factors
CME: Clathrin-mediated endocytosis
CHC: Clathrin Heavy Chain
CLC: Clathrin Light Chain
MAPK: Mitogen-Activated Protein Kinase
CRK: Ca²⁺/calmodulin-dependent protein kinase-related kinase
PID: PINOID
D6PK: D6 Protein Kinase
D6PKL: D6 Protein Kinase-like
PDK: 3-Phosphoinositide-Dependent Protein Kinase
BUD1: Bushy and Dwarf1
MKK7: MAP KINASE KINASE7
NPH3: Non-phototropic Hypocotyl
TOC complex: Outer envelope membrane of Chloroplasts complex
ARG1: Altered Response to Gravity 1
ARL2: ARG1-Like 2
NGR: Negative Gravitropic Response of Root
LZY: LAZY1-like
RLD: RCC1-like Domain
MIZ1: Mizu-Kussei 1
PA: Piperonylic acid
C4H: Cinnamate-4-hydroxylase
CA: Cinnamic Acid
***p*-CA:** *p*-coumaric acid
DMSO: Dimethyl sulfoxide
SDT: Sodium Diethyldithiocarbamate Trihydrate
DPBA: 2-aminoethyl diphenylborinate
***trans*-CA:** *trans*-Cinnamic acid
***cis*-CA:** *cis*-Cinnamic acid
SA: Salicylic acid
***p*-IBA:** *p*-iodobenzoic acid
PAA: phenylacetic acid
PIA: 5-(1,3-Benzodioxol-5-yl)-2,4-pentadienoic acid
DART: Drug Affinity Responsive Target Stability
ABP1: Auxin Binding Protein 1
***cvx*IAA:** convex-IAA
***ccv*TIR1:** concave-TIR1
***c*TIR1:** controlTIR1
GTD: Globular Tail Domain

1 PIN-polarization dependent auxin transport in plant tropic response

Huibin Han, Maciek Adamowski, Linlin Qi, Jiří Friml

Institute of Science and Technology Austria, 3400 Klosterneuburg, Austria

1.1 Introduction

Plants are unable to move in response to environmental stimulus. Instead, plants have evolved a robust system of tropic responses, to quickly adapt their growth in the changing local environment. Tropisms are directional growth adaptations to light (phototropism), gravity (gravitropism), obstacles (obstacle avoidance), salinity (halotropism), and water (hydrotropism). Phototropism is light-dependent growth that enable plants to react to the changes in light direction by bending shoot towards the light source, or root away from it (de Wit et al., 2016; Harmer and Brooks, 2018). Gravitropism orients plant growth direction along the gravity vector, so that root grows down, and shoot grows up, in order to correctly position of the plant body and obtain resources for organ development (Rakusová et al., 2015). Obstacle avoidance helps plant roots to reorient growth when encountering obstacles in soil (Lee et al., 2019). Halotropism and hydrotropism enable plants to sense salinity and water potential in the local environment and direct root growth accordingly (Dietrich, 2018; Harmer and Brooks, 2018).

In most tropic responses, cell to cell directional auxin movement is the main mechanism for maintaining the asymmetric auxin gradient and differential cell elongation. It is well established that asymmetric auxin distribution in plant tissues is achieved by polarly localized PIN auxin efflux carriers (Petrášek et al., 2006; Wiśniewska et al., 2006). The influx carriers, AUXIN-RESISTANT1/LIKE AUX1 (AUX1/LAX) (Band et al., 2014), and some B subclass of ATP-binding cassette (ABCB) efflux carriers (Geisler and Murphy, 2006) also contribute to the polar auxin flow. Several studies support the notion that PIN-mediated directional auxin flow is crucial for plant phototropism (Friml et al., 2002; Ding et al., 2011), root and shoot gravitropism (Friml et al., 2002; Abas et al., 2006; Kleine-Vehn et al., 2010; Rakusová et al., 2011), obstacle avoidance (Lee et al., 2019), halotropism (Galvan-Ampudia et al., 2013), and maybe also for hydrotropism (Nakajima et al., 2017).

In this review, we assess PIN-mediated polar auxin transport in phototropism, gravitropism, obstacle avoidance, halotropism and hydrotropism. We also discuss the underlying molecular mechanisms of PIN polarity switch in these tropic responses. We also

discuss the upstream signals controlling tropisms, and the interactions between distinct tropic responses.

1.2 PIN-mediated polar auxin fluxes during tropic responses

Light is an essential environmental source for plant development. Plants can detect light quality, intensity and direction, resulting in cellular responses to optimize growth and survival (Chen et al., 2004). Light-mediated phototropic bending was first observed in dark-grown seedlings of oat (*Avena sativa*) and canary grass (*Phalaris canariensis*), and this phenomenon was termed as phototropism (Darwin, 1880). The early experiments indicated that during phototropism, an unknown signal moves from the irradiated side of the seedling to the shaded side, and triggers the differential growth, and thus bending (Darwin, 1880; Went, 1928). Later, the plant hormone auxin was identified as the mobile signal responsible for plant phototropism (Kogl and Haagen-Smits, 1931). Together with this early work, the Cholodny-Went hypothesis was established to explain the plant phototropic response (Christie and Murphy, 2013). A key concept embedded within the Cholodny–Went hypothesis is that of polar auxin transport. Several studies confirmed the lateral auxin movement during phototropism, but the mechanism remained unknown for a long time (Briggs et al., 1957; Briggs, 1963; Pickard and Thimann, 1963).

Later, the auxin exporters of the PIN family have been suggested to mediate polar auxin transport during phototropism (Friml et al., 2002; Ding et al., 2011). Among the PINs, PIN3 is the major player mediating lateral auxin flow during phototropism (Ding et al., 2011). By default, PIN3 displays an apolar localization in endodermal cells of etiolated hypocotyls. However, upon unilateral blue light stimulation, PIN3 gradually polarizes towards to the shaded hypocotyl side, and is stabilized at the shaded side of endodermal cells (Figure 1A; Ding et al., 2011). Thus, the asymmetric distribution of PIN3 directs auxin flow to the shaded side of the hypocotyl, as can be visualized by an auxin response reporter (Ding et al., 2011). In de-etiolated *Arabidopsis* seedlings, the red/far red (R/FR) light receptor, phytochrome B (phyB) regulates phototropism by modulating auxin biosynthesis and transport (Figure 1B; Goyal et al., 2016). Recently, UV-B light was also observed to induce a phototropic response in the *Arabidopsis* stem via the UVR8 receptor, through effects on auxin responses and transport (Figure 1B; Vanhaelewyn et al., 2019). However, it is not known whether PIN-mediated auxin transport is involved in UVB- or R/FR-induced phototropic response.

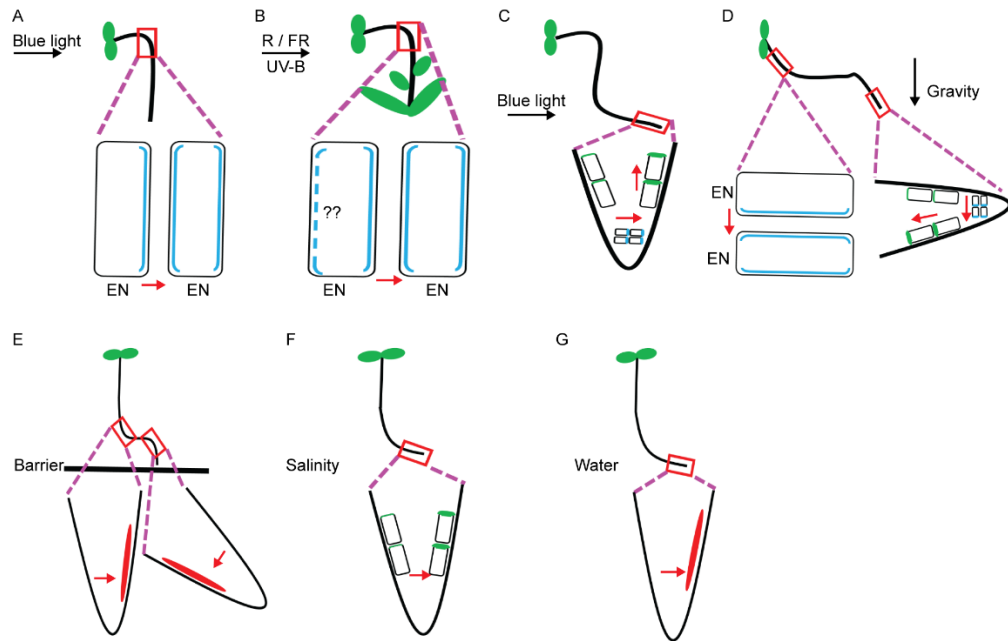


Figure 1. PIN-mediated auxin fluxes during plant tropic response.

(A) PIN3-mediated auxin movement during shoot phototropism. In etiolated hypocotyls, PIN3 polarizes gradually to shaded hypocotyl side and is stabilized at inner side of endodermal cells upon unilateral blue light stimulation. The asymmetric PIN3 distribution then directs auxin movement to shaded side, and hypocotyl bends to the light direction.

(B) In de-etiolated hypocotyls or in stem, UV-B or R / FR light illumination also induce phototropic response. However, it is not known whether PIN polarizes to the shaded side. Blue dashed line indicates PIN polarization to lateral side of endodermal cells.

(C) PIN-mediated auxin movement during root phototropic response. Upon blue light stimulation, PIN3 polarizes to shaded side in columella cells resulted in an asymmetric distribution of PIN3. PIN2 is differentially distributed between the vacuole and the plasma membrane at the irradiated and shaded sides of the root. As a result, auxin is asymmetric accumulated at the shaded root side, root grows away from light direction.

(D) PIN-mediated auxin transport during gravitropism. In etiolated shoot, PIN3 polarizes to outer side of endodermis cells at lower shoot side upon gravity stimulation, and auxin moves from upper side to lower side, resulted in auxin accumulation at lower side and shoot grows upwards. In root, PIN3 polarizes to lower side of columella cells; PIN2 abundance at upper side of root is decreased, while it becomes increased at the lower root side. Thus, the change of PIN3 polarity in columella cells and PIN2 abundance at epidermal cells leading to auxin accumulation at lower side and root grows downwards.

(E) Auxin asymmetric distribution in root obstacle avoidance. Two different bending events are observed during root obstacle avoidance. In the first bending response, auxin (The red) accumulates at concave side. In the second bending response, auxin accumulates at convex side. However, it is not clear which PIN protein mediates this two different auxin movements. Red arrow indicates auxin transport direction.

(F) PIN2-mediated auxin asymmetric distribution during Halotropism. Salinity induces an internalization of PIN2 at the side of the root facing the higher salt concentration, and through this mechanism, the differential PIN2 distribution redirects auxin flow to the root side without salt. Subsequently, the root grows away from a high salt concentration. Green line indicates PIN2 at epidermal cells. Red arrow indicates auxin transport direction.

(G) Auxin distribution in hydrotropism. Auxin (The red) is asymmetric distributed at lower water potential side, root grows away from high water potential. However, the auxin symmetric distribution in root hydrotropism is controversial. Blue solid line indicates PIN3 distribution in endodermal cells; green line indicates PIN2 at epidermal cells; red arrow indicates auxin transport direction. EN: endodermal cells. Red arrow indicates auxin transport direction.

Compared to the positive response to light in the shoot, the root exhibits a negative phototropic response, thereby avoiding a suboptimal environment (Figure 1C; Kutschera and Briggs, 2012). Blue light-mediated reorientation of root growth requires a local response in

the transition zone of the root meristem, and utilizes auxin efflux transporters in the root tip to establish an asymmetric auxin accumulation (Wan et al., 2012; Zhang et al., 2013). Light illumination inhibits the PIN2 vacuolar degradation, resulting in the accumulation of PIN2 at the plasma membrane (Wan et al., 2012). Thus, PIN2 is differentially distributed between the vacuole and the plasma membrane at the irradiated and shaded sides of the root, leading to a differential auxin distribution across the organ (Wan et al., 2012). In turn, PIN3 is by default apolar in the root columella cells, but upon blue light illumination it polarizes to the outer lateral membrane, also contributing to the accumulation of auxin at the shaded side and direction growth away from light (Zhang et al., 2013). Thus, light influences PIN3 polarization or PIN2 abundance at the plasma membrane to control polar auxin movement in root negative phototropism (Figure 1C).

Similarly to light, gravity also modulates plant growth, rendering root to grow downwards and shoot upwards. The asymmetric auxin distribution between the opposite sides of a gravistimulated shoot or root is also achieved via differential PIN subcellular distribution, resulting in organ bending (Friml et al., 2002; Abas et al., 2006; Kleine-Vehn et al., 2010; Rakusová et al., 2011; Baster et al., 2013). The strong agravitropic root phenotype of the *pin2* mutant indicates that PIN2 is the main player mediating auxin transport in root gravitropism (Abas et al., 2006; Baster et al., 2013). Upon gravity stimulation, the abundance of PIN2 in the epidermis of the upper root side is decreased, while it becomes increased at the lower root side. Thus, this asymmetric abundance of PIN2 causes a polar auxin movement to the lower root side, and root grows downwards (Abas et al., 2006; Baster et al., 2013). In addition to PIN2, PIN3 and PIN7 also participate in root gravitropism. By default, these transporters both are localized at the plasma membrane in columella cells in an apolar manner. Following gravistimulation, PIN3 and PIN7 polarize to the bottom side of columella cells, thus driving auxin flow from the upper side to the lower side of columella cells (Figure 1D; Kleine-Vehn et al., 2010). Thus, gravity-induced PIN polarization in columella cells and PIN abundance at the plasma membrane of epidermal cells are essential for asymmetric auxin distribution during root gravitropism.

In etiolated hypocotyls, PIN3 is the key player redirecting auxin flow for shoot gravitropism (Rakusová et al., 2011). PIN3 exhibits an apolar distribution in hypocotyl endodermal cells. Following gravistimulation, PIN3 relocates to the lower side of endodermal cells, presumably redirecting auxin flow to the lower hypocotyl side, and initiating hypocotyl

bending (Figure 1D; Rakusová et al., 2011). Additionally, PIN4 and PIN7 contribute to polar auxin transport in the absence of PIN3 (Rakusová et al., 2011).

Root growth is directed down through gravitropism to acquire nutrients and water and anchor the plant body in the soil. However, root reorients its growth when encountering obstacles (Massa and Gilroy, 2003; Lee et al., 2019). A recent study shows that PIN-mediated polar auxin transport promotes root bending during obstacle avoidance (Figure 1E; Lee et al., 2019). During obstacle avoidance, an asymmetric auxin distribution is detected between the concave and convex root sides (Lee et al., 2019). However, it is hard to distinguish which PIN protein is specifically affected to direct auxin flow during obstacle avoidance, even though the *pin2* mutant shows a clear bending defect as well as a defective auxin distribution (Lee et al., 2019).

Apart from the normal development, auxin is also involved in stress responses (Blakeslee et al., 2019). Salinity, a devastating abiotic stress, affects root growth (Liu et al., 2015), root gravity response (Sun et al., 2008), and auxin distribution (Hu et al., 2019; Wang et al., 2019). The phenomenon where the root grows away from a high salt concentration is termed as halotropism (Galvan-Ampudia et al., 2013). Salinity induces an internalization of PIN2 at the side of the root facing the higher salt concentration, and through this mechanism, the differential PIN2 distribution redirects auxin flow to the root side without salt. Subsequently, root grows away from a high salt concentration (Figure 1F; Galvan-Ampudia et al., 2013). However, the other PINs, such as PIN1 and PIN3, as well as the influx transporter AUX1, play dispensable roles in halotropism (Galvan-Ampudia et al., 2013). It has also been proposed that PIN regulators play essential roles in halotropism (van den Berg et al., 2016; Han et al., 2017).

Besides salinity in the local environment, water potential in the local environment also influences root growth. Roots mediate water uptake from soil and have developed a robust adaptive response called hydrotropism in order to sense different water potentials in the local environment and then direct root growth accordingly (Figure 1G; Dietrich, 2018; Harmer and Brooks, 2018). Pharmacological studies indicate that auxin transport is required for hydrotropism in some species, but not in *Arabidopsis* (Shkolnik et al., 2016; Nakajima et al., 2017; Morohashi et al., 2017). In *Arabidopsis*, auxin transport inhibitors TIBA and NPA don't interfere with hydrotropism, and the auxin response reporters remain unaffected during the root hydrotropic response (Shkolnik et al., 2016). However, the putative cucumber PIN

orthologue, *CSPIN5*, may direct auxin flow in hydrotropism (Morohashi et al., 2017). Even though polar auxin transport is not necessary in *Arabidopsis* root hydrotropism, the auxin response components are required (Dietrich, 2018). Additionally, abscisic acid (ABA) has been shown to play an essential role in hydrotropism by modulating PIN2 expression level and auxin transport (Xu et al., 2013).

To sum up, the accumulated evidence supports the notion that PIN-mediated polar auxin transport is crucial for most tropic responses and instances of organ bending (Figure 1A- 1G). However, in some cases, the involvement of polar auxin transport is inconclusive and requires further examination.

1.3 Subcellular PIN trafficking and kinase-mediated PIN phosphorylation for PIN polarity switches in tropisms

PIN-mediated auxin transport is vital for plant tropic responses, but how is the subcellular localization of PIN proteins controlled to establish auxin fluxes? Accumulating evidence supports the subcellular PIN trafficking (Figure 2) and kinase-mediated PIN phosphorylation (Figure 3) as conserved mechanisms that enable rapid changes in PIN polarities and redirections of auxin movement during tropic responses.

PIN proteins are thought to dynamically cycle between the plasma membrane and endosomal compartments in a process termed endocytic recycling. The exocytotic step of endocytic recycling is inhibited by the fungal toxin Brefeldin A (BFA) (Figure 2; Geldner et al., 2001, 2003; Friml, 2010). BFA inhibits some of the ADP-ribosylation factor guanine-nucleotide exchange factors (ARF-GEFs), which are essential for vesicle formation and other aspects of the endomembrane system function. The ARF-GEF GNOM has been identified as the target of BFA-mediated inhibition of PIN trafficking (Geldner et al., 2003). It has been observed that BFA treatment interferes with gravity- or light-mediated PIN polarization, resulting in defective organ bending (Kleine-Vehn et al., 2010; Ding et al., 2011; Rakusová et al., 2011). However, BFA-resistant *GNOM*^{M696L} mutant shows a normal PIN polarization and bending response to gravity or light (Kleine-Vehn et al., 2010; Ding et al., 2011; Rakusová et al., 2011). These observations indicate that GNOM-mediated PIN trafficking is essential for PIN polarity switches in tropisms. Interestingly, MIZ2/GNOM-mediated trafficking has been also reported to play important roles in root hydrotropism, albeit by a mechanism distinct from its role in polar auxin transport (Miyazawa et al., 2009).

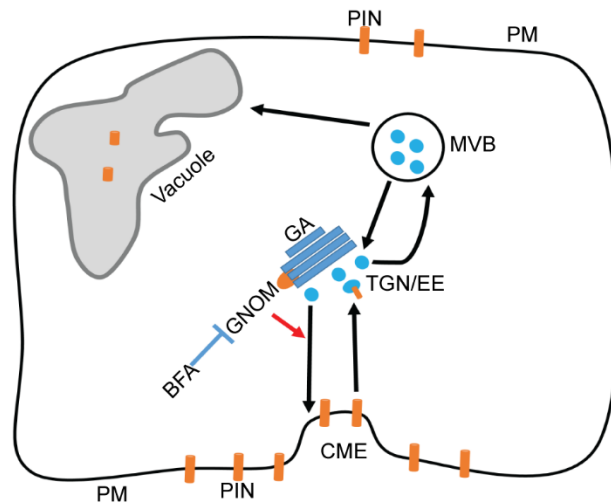


Figure 2. Simplified model of PIN subcellular trafficking.

Plasma membrane (PM) localized PINs are undergoing endocytic trafficking. Subcellular PIN trafficking is mediated by the BFA-sensitive target GNOM or clathrin-mediated endocytosis (CME). PINs undergo trafficking through multivesicular body (MVB) for degradation in the lytic vacuole. MVB, multivesicular body; EE, early endosome; TGN, *trans*-Golgi network; GA, Golgi apparatus.

As part of endocytic recycling, PIN proteins undergo continuous internalization from plasma membrane via Clathrin-Mediated Endocytosis (CME) (Dhonukshe et al., 2007). The vesicular clathrin coat is composed of Clathrin Heavy Chain (CHC) and Clathrin Light Chain (CLC) proteins. The *chc* or *clc* mutants display strong defects in PIN trafficking, PIN polar localization, auxin distribution and tropic responses (Kitakura et al., 2011; Wang et al., 2013; Zhang et al., 2017). The dominant-negative *chc1* mutant exhibits an agravitropic root and hypocotyl with an altered PIN localization and auxin distribution (Kitakura et al., 2011). The loss-of-function *clc2 clc3* double mutant exhibits a defective light-mediated PIN3 repolarization, as well as reduced phototropic bending (Zhang et al., 2017). In addition, the *clc2 clc3* double mutant also shows a reduced root gravitropic bending and defective PIN2 trafficking (Wang et al., 2013). Furthermore, clathrin-mediated PIN2 endocytosis is crucial for the asymmetric auxin distribution associated with halotropism (Galvan-Ampudia et al., 2013).

With these observations in mind, it must be noted that clathrin coats are involved not only in endocytosis, but also in the formation of vesicles participating in other trafficking events, specifically in the vacuolar pathway and potentially, in some forms of exocytosis (Robinson and Pimpl, 2014). In turn, the ARF-GEF GNOM has also been implicated in endocytosis (Naramoto et al., 2010). Thus, in some instances it is difficult to conclude precisely by which means the factors discussed above contribute to the PIN polarity control.

Nonetheless, PIN trafficking is clearly required for PIN relocations and subsequent formation of auxin gradients during tropic responses.

Additional observations in support of the relocation of PIN proteins by means of endocytic recycling during tropisms come from studies of PIN trafficking focused on a process termed transcytosis, defined as the movement of a protein cargo from one polar domain, to another (Kleine-Vehn et al., 2008). It has been observed that in gravistimulated roots or hypocotyls, inhibition of protein synthesis does not affect gravity-induced PIN3 polarization to the bottom cell side, suggesting that PIN3 is indeed translocated from the preexisting PIN pools. (Kleine-Vehn et al., 2010; Rakusová et al., 2011). Thus, it is suggested that transcytosis of PINs is an essential step for rapid modulation of auxin transport in tropisms.

Beside the importance of PIN trafficking for the control of its polarity during tropisms, kinase-mediated PIN phosphorylation has also been suggested as a regulatory mechanism for PIN polarity regulation (Barbosa et al., 2018). Phosphorylation of PIN proteins at the central hydrophilic loop is sufficient to modulate PIN polarity and polar auxin transport (Michniewicz et al., 2007; Huang et al., 2010; Zhang et al., 2010; Ganguly, et al., 2012). Several protein kinase families, such as the AGCVIII family, Mitogen-Activated Protein Kinase (MAPK) family, and the Ca^{2+} /calmodulin-dependent protein kinase-related kinase (CRK) family, phosphorylate PIN proteins and control PIN polarity or transport activity during plant development (Figure 3; Barbosa et al., 2018).

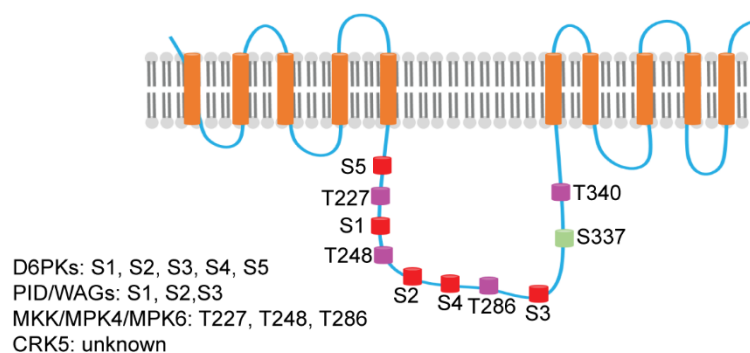


Figure 3. Summary of kinase-mediated PIN phosphorylation sites.

Multiple phosphorylation sites are uncovered in PIN hydrophilic loop. D6PKs phosphorylate S1 to S5 sites. PID/WAGs phosphorylate S1 to S3 sites. MPK4/MPK6 phosphorylates T227, T248, T286 sites. MPK3/MPK6 phosphorylates S337. CRK5 phosphorylates unknown site.

Among the AGCVIII kinase family, PINOID (PID) and its paralogs WAG1 and WAG2 are well studied in PIN polarity regulation. PID and WAGs directly phosphorylate PINs at three conserved serine site S1-S3, and this phosphorylation triggers PIN polarity changes (Figure 3A; Friml et al, 2004; Huang et al., 2010; Dhonukshe et al., 2010). PID loss-of-function or gain-of-

function mutants exhibit defective PIN polarizations as well as bending defects in response to light (Ding et al., 2011). The PID gain-of-function mutant displays a strong defects in hypocotyl bending and PIN3 polarization (Rakusová et al., 2011). Hence, PID-mediated PIN3 phosphorylation is essential for establishing auxin gradient during phototropic and gravitropic responses (Rakusová et al., 2011; Ding et al., 2011; Grones et al., 2018). Additionally, Protein Phosphatase 2A (PP2A) mediates PIN de-phosphorylation is also vital for root gravitropism (Sukumar et al., 2009).

Another group of AGCVIII kinases, D6 Protein Kinase (D6PK) and D6 Protein kinase-Likes (D6PKLs) have also been implicated in polar auxin transport regulation. Loss of D6PK and D6PKLs activity lead to typical auxin-related phenotypes that correlated with altered polar auxin transport (Willige et al., 2013; Zourelidou et al., 2014; Barbosa et al., 2016; Weller et al., 2017). D6PK phosphorylates PIN protein at serines S1-S3 and two additional serine sites S4 and S5 and this phosphorylation is independent of the PID kinase (Figure 3; Zourelidou et al., 2014; Barbosa et al., 2018). D6PK phosphorylates PIN proteins, but in contrast to PID, do not affect their polarity (Willige et al., 2013). Instead, D6PK regulates PIN transport activity (Willige et al., 2013; Zourelidou et al., 2014). This reduced PIN transport capacity in *d6pk* or *d6pkl* mutants correlates with defective gravitropic and phototropic responses (Willige et al., 2013; Barbosa et al., 2016; Weller et al., 2017).

In addition, the *Arabidopsis* 3-Phosphoinositide-Dependent Protein Kinase1 (PDK1) and PDK2, which also belong to the AGCVIII kinase family, have been shown to modulate the activity of PID and D6PK (Zegzouti et al., 2006; Armengot et al., 2016; Tan et al., 2020), indicating another layer in PIN polarity and activity regulation. To sum up, AGCVIII family kinases likely have both different and partially overlapping functions in regulating PIN polarity and auxin transport during tropisms.

MAPK cascades play essential roles in plant growth and development (Xu and Zhang, 2015). Auxin activates unknown MAPKs in the root (Mockaitis and Howell, 2000), and MAPKs repress auxin signaling (Kovtun et al., 1998), indicating an interaction between auxin and MAPKs. The *bushy and dwarf1 (bud1)* gain-of-function of MAP KINASE KINASE7 (MKK7) mutant displays a defective hypocotyl gravitropic bending (Dai et al., 2006). MPK6 has been shown to be the substrate of MKK7 (Jia et al., 2016). MKK7-MPK6 cascade directly phosphorylates Ser 337 of PIN1, a conserved phosphorylation site present in PIN3 at site S317 (Jia et al., 2016). However, there is not much evidence linking PIN3 polarity regulation to the

MKK7-MPK6 cascade during shoot gravitropic response. It is also known that T227, T248 and T286 in the PIN hydrophilic loop can be phosphorylated by MPK6 (Dory et al., 2018). The three threonines are part of TPRXS (N/S) motifs in the S1-S3 phosphorylation sites, pointing at a possible link between AGCVIII and MAPK kinases in the regulation of PIN polarity via phosphorylation (Barbosa et al., 2018).

A rapid transient increase of Ca^{2+} concentration in the root is observed upon auxin treatment (Monshausen et al., 2011) and after gravity stimulation (Tatsumi et al., 2014). Increasing of Ca^{2+} level suppresses the *PIN1* gain-of-function phenotypes and leads to defects in basal PIN1 localization (Zhang et al., 2011), suggesting a possible involvement of Ca^{2+} signaling pathway in PIN polarity regulation. The Ca^{2+} /Calmodulin-Dependent Kinase-Related Kinase 5 (CRK5) may be one possible protein that can translate Ca^{2+} levels into altered PIN polarity in root gravitropism (Rigó et al., 2013). CRK5 phosphorylates PIN2 hydrophilic loop *in vitro*, and this defective phosphorylation of PIN2 in *crk5* mutant explains the delayed root gravitropic response (Rigó et al., 2013). CRK5 is able to phosphorylate the hydrophilic loop of PIN3 *in vitro* as well (Baba et al., 2019). However, the phosphorylation site for CRK5 on PINs is unknown.

1.4 Integration of different environmental cues into PIN polarity switches to initiate tropisms

Plants employ different means to regulate and maintain PIN polarities and auxin gradients. One unanswered question is how plants integrate the environmental signal into PIN polarity switches to initiate tropic responses.

During shoot phototropism, the blue light receptors phototropins sense blue light at the upper part of the shoot and initiate shoot phototropic bending (Preuten et al., 2013; Liscum et al. 2014). It has been assumed that the signal transducer Non-phototropic Hypocotyl 3 (NPH3) integrates the light signal and lateral auxin gradient establishment during shoot phototropic response (Haga et al., 2005, 2015; Christie et al., 2018). An observation of no asymmetric auxin distribution in rice *nph3/cpt* mutant upon blue light illumination further supports the essential role of NPH3 for auxin gradient formation during phototropism (Haga et al., 2005). NPH3 is localized at plasma membrane and interacts with phototropin1, and the interaction is transiently disrupted by light (Haga et al., 2015). Light illumination also induces NPH3 internalization from the plasma membrane to cytoplasm microdomain aggregates (Haga et al., 2015). This phototropin1-driven NPH3 subcellular localization switch correlates

with the phosphorylation status of NPH3 (Pedmale and Liscum, 2007). In darkness, NPH3 is phosphorylated, while it becomes rapid dephosphorylated upon light illumination (Pedmale and Liscum, 2007). The reversible light-induced phototropin1-NPH3 interaction, NPH3 subcellular localization changes, and phosphorylation, are proposed to be parts of a signaling mechanism that determines the PIN-mediated lateral auxin distribution in phototropism. Even though, there is no direct evidence to show PIN polarization defects in *nph3* mutant (Haga et al., 2005, 2015; Pedmale and Liscum, 2007; Christie et al., 2018). Notable, Light-induced PIN2 asymmetric distribution at plasma membrane requires NPH3 function during root phototropic response (Wan et al., 2012). Moreover, etiolated seedlings lacking the Phytochrome Interacting Basic Helix-Loop-Helix Factors (PIFs) display reduced NPH3 dephosphorylation and altered auxin distribution (Sun et al., 2013; Sullivan et al., 2019), providing additional clues for the mechanisms of PIN polar localization and auxin distribution in phototropism. Besides, phototropin1 also interacts with the ATP-Binding Cassette B19 (ABCB19) and phosphorylates ABCB19 (Christie et al., 2011). The phosphorylated ABCB19 protein exhibits a reduced auxin efflux transport activity. Thereby, the increased auxin is subsequently channeled by PIN3 to elongation zone (Christie et al., 2011). Light also represses the transcription level of PID, contributing to PIN3 polarization during phototropism (Ding et al., 2011). However, D6PK kinases do not affect light-induced de-phosphorylation of NPH3, but repress PIN3 phosphorylation and activity leading to a defective phototropic response (Willige et al., 2013). Thus, light-induced the phosphorylation gradient via NPH3, PID, and D6PKs is crucial for PIN polarization and activity, which suggested to be part of the mechanism driving lateral auxin distribution during phototropism (de Wit et al., 2016).

It is well known that plants sense gravity via statoliths, starch-filled organelles present in root columella cells and shoot endodermal cells (Vandenbrink and Kiss, 2019). Following gravity stimulation, statoliths settle to the gravity direction, thus providing directional information to plants. The settling of statoliths triggers biochemical cascade to initiate asymmetric auxin distribution, resulting in the differential root or shoot growth. Some evidences support that the plant cell cytoskeleton, lipids, and the Translocon on the outer chloroplast membrane complex (TOC) play essential roles in gravity signal transduction (Vandenbrink and Kiss, 2019). The J-domain protein Altered Response to Gravity 1 (ARG1) and its paralog ARG1-Like 2 (ARL2) are expressed in root statocytes (gravity sensing cells), and *ARG1* and *ARL2* mutation causes a defective gravity sensing and PIN polarization (Guan et al.,

2003; Harrison and Masson, 2008). It has been suggested that root gravitropism depends on Negative Gravitropic Response of Root (NGR) protein, also referred as LAZY1-like (LZY) protein (Taniguchi et al., 2017). The *ngr1,2,3/lzy2,3,4* triple mutant shows a normal starch sedimentation, but PIN3 polarizes to the upper root side after gravity stimulation, thus root grows upwards (Ge and Chen, 2019). The LAZY protein is localized at the plasma membrane of columella cells (Furutani et al., 2020). After gravity stimulation, the LAZY protein polarizes to bottom columella cell side, and then recruits the RLD proteins (RCC1-like Domain) to form a complex (Furutani et al., 2020). This LAZY-RLD complex then guides PIN polarization and auxin flow (Furutani et al., 2020). Thus, gravity-sensing cell localized LAZY1-RLD protein complex bridges the gap between the sedimentation of amyloplasts and gravity-induced polar auxin movement (Furutani et al., 2020). In shoot, isolation of a series of *shoot gravitropism* (*sgr*) mutants provide vital insights into the function of actin cytoskeleton in shoot gravity sensing and PIN polarity regulation (Fukaki et al., 1996, 1998; Yamauchi et al., 1997; Yano et al., 2003; Morita et al., 2006; Nakamura et al., 2011). Those newly identified genes contribute to the understanding of the transition between gravity sensing and PIN-mediated auxin transport.

Great efforts have been made to understand the mechanism of salt perception and signal transduction. Phosphatidic acid, a minor membrane phospholipid, is essential for plant growth and development in response to salinity (Wang et al., 2019). Phosphatidic acid binds to PID and enhances PID-dependent PIN2 phosphorylation under salt treatment (Wang et al., 2019). Inhibition of phosphatidic acid generation also alters PIN localization and the halotropic response (Korver et al., 2019). Phosphatidic acid has also been shown to modulate CME (Antonescu et al., 2010). Hence, it is likely that plants sense the changes of phosphatidic acid, and then recruit PID or CME to modulate PIN-mediated auxin distribution during the halotropic response.

A considerable amount of research has been carried out to explore where and how plants sense the water gradient in the root. Identification of key genes in hydrotropism provide some new insights (Eapen et al., 2003; Kobayashi et al., 2007; Miyazawa et al., 2009; Saucedo et al., 2012; Dietrich et al., 2018). A novel report suggests that the root elongation zone senses the water gradient, leading to the differential growth of the cortex cells (Dietrich et al., 2017). The *mizu-kussei 1* (*miz1*) mutant shows a reduced hydrotropic response, and MIZ1 plays roles in sensing water potential at the early phase of hydrotropism (Kobayashi et

al., 2007; Dietrich et al., 2017). Furthermore, the role of water uptake and transport in root hydrotropism was explored. It has been shown that the Plasma membrane intrinsic proteins (PIPs), a subfamily of plasma membrane located aquaporin channels, contribute to water transport, root hydraulic conductivity and hydrotropism (Sutka et al., 2011; Li et al., 2014; Dietrich et al., 2018). Thus, a hypothetical model for water potential perception is proposed (Dietrich et al., 2017, 2018). In this model, MIZ1 senses the water potential (Kobayashi et al., 2007; Dietrich et al., 2017), and low water potential affects membrane presence or activity of PIPs (Dietrich et al., 2018). The altered aquaporin activity or presence results in an alteration of hydraulic conductivity or ABA concentration, ultimately leading to differential cell elongation and root bending. Meanwhile, MIZ2/GNOM is required for rapid cycling of PIPs and the interaction between PIPs and Receptor-Like Kinases (RLKs) to maintain the aquaporin activity and presence during hydrotropism (Dietrich et al., 2018).

1.5 *Auxin feedback on PIN polarity to terminate shoot gravitropic bending*

Plants sense and transduce environmental clues to initiate tropic growth. Interestingly, the hypocotyl bending response is terminated by a mechanism involving a feedback control of auxin on PIN polarity (Rakusová et al., 2016). In this model, auxin accumulated at the lower hypocotyl side triggers PIN3 repolarization to the inner side of endodermal cells, as such leading to a symmetric PIN distribution, and restoration of symmetric auxin distribution, across the organ. This auxin-mediated feedback on PIN repolarization requires SCF^{TIR1/AFB} auxin signaling pathway (Han et al., 2020), PIN endocytosis by CME, GNOM-mediated trafficking, PID-mediated phosphorylation (Rakusová et al., 2016) and actin cytoskeleton (Rakusová et al., 2019). Thus auxin feedback mechanism ensures fine-tuning of auxin fluxes for terminating asymmetric growth during gravitropic response.

1.6 *Interactions among different tropisms*

Plants are exposed to an intricate environment, and have to balance the cellular actions in response to various environmental cues for an adaptive growth. Several studies have been carried out to dissect the interactions among different tropisms, aiming to understand plant adaptive growth in a more natural environment.

Light plays predominant roles in hypocotyl tropic growth. Light-grown plants have to integrate light and gravity signal to guide growth. Several studies demonstrate that light inhibits the shoot gravitropic response to promote phototropism through different light

receptors (Lariguet and Fankhauser, 2004; Ohgishi et al., 2004; Kim et al., 2011). The multiple blue light receptor mutant displays random negative gravitropism, indicating that light is important to maintain a proper gravitropism (Lariguet and Fankhauser, 2004; Ohgishi et al., 2004). Red light illumination inhibits shoot gravitropism by triggering a conversion of gravity-sensing endodermal amyloplasts into chloroplastic plastids in a manner that depends on phytochromes and PIFs (Kim et al., 2011). These plastids lacking a gravity sensing function resulted in a reduced gravitropic response (Kim et al., 2011). Light also modulates the actin cytoskeleton organization via the Rice Morphology Determinant (RMD) protein to control statolith mobility and auxin distribution, and thus negatively regulating gravitropism (Song et al., 2019). In summary, based on the available data, light promotes phototropism though inhibition of gravitropism by modulating gravity sensing or actin organization.

An interaction between salinity and gravitropism has been described, in which NaCl treatments lead to a reduced root gravitropic bending curvature (Sun et al., 2008). This salt-induced reduction of root gravitropic response correlates with a rapid degradation of the amyloplasts, and with a repression of PIN2 endocytic recycling and degradation in an ion gradient sensing pathway-dependent manner (Sun et al., 2008). In turn, light has been suggested to attenuate root halotropism by preventing the perception of salinity gradient by an unknown mechanism (Yokawa et al., 2014).

In order to maintain the hydrotropic growth, roots have to overcome gravitropism. It has been revealed that a moisture gradient or water stress trigger reductions in the starch content and rapid degradation of amyloplasts in root columella cells (Takahashi et al., 2003). This mechanism partially helps root overcome gravitropism to promote hydrotropism. In turn, the phospholipase encoding protein PLD ζ 2 participates in root hydrotropism through a PIN2-mediated suppression of root gravitropism (Taniguchi et al., 2010). Furthermore, light also influences hydrotropic growth. Seedlings grown in light or dark behave differently during a hydrotropic response (Moriwaki et al., 2012). Dark-grown seedlings show a reduced hydrotropic curvature compared to light-grown seedlings, and it was proposed that this is due to the regulation of subcellular localization and expression of MIZ1 in the root cap by light (Moriwaki et al., 2012).

Overall, the research summarized above provides valuable insights into the molecular and cellular mechanisms of interactions among various tropic responses under a complicated

environment. However, the role of PIN-mediated polar auxin transport in these interactions awaits further investigation.

1.7 Concluding remarks and future perspectives

Tropisms, reorientations of plant growth in response to environmental stimuli, are robust adaptive features for plants to coordinate their growth with the changing environment. In most cases, PIN-mediated asymmetric auxin distribution plays an indispensable role in maintaining the auxin gradient at the stimulated organs. Polar auxin fluxes determined by PIN polarity switches and the regulation of PIN abundance are intricate and conserved mechanisms in tropic responses. The application of new tools and approaches expand our understanding of the molecular mechanisms of PIN polarizations under various environmental stimuli.

The PIN-mediated cell-to-cell polar auxin movement is required for organ bending or growth in most tropic responses. However, the signaling pathways which plants employ to activate the PIN polarity switches, or to modulate PIN abundance by altering PIN trafficking pathways, are still not well understood. Moreover, how these multi-level regulations, including specific trafficking and phosphorylation events, are integrated during these processes, is not fully answered. Multidisciplinary approaches utilizing genetics, biochemistry, advanced imaging tools and other cutting-edge techniques will be helpful for a better understanding of PIN polarity regulation in tropisms in future studies.

Under natural environment, plants are subject to multiple and sometimes conflicting environmental cues to regulate their growth. To gain the optimum fitness under complicated environment, plants need to integrate the different environmental clues to coordinate the cellular response and growth. The question of how plants coordinate a response to these often conflicting stimuli is a particularly interesting one. Elucidating the mechanisms by which complicated PIN polarity regulations resulting from distinct tropic stimuli are integrated will greatly help us to understand how plants adapt to the changing environment.

Overall, full understanding of PIN-mediated directional auxin transport in plant tropic responses will require not only the unraveling of the complex signaling pathways outlined above, but also how these pathways interact with each other. The basic knowledge gained from *Arabidopsis* will provide essential insights to modify crops for better growth and yield in adverse environmental conditions.

1.8 References

- Abas L, Benjamins R, Malenica N, Paciorek T, Wiśniewska J, Moulinier-Anzola JC, Sieberer T, Friml J, Luschnig C** (2006) Intracellular trafficking and proteolysis of the *Arabidopsis* auxin-efflux facilitator PIN2 are involved in root gravitropism. *Nat Cell Biol* 8: 249
- Antonescu CN, Danuser G, Schmid SL** (2010) Phosphatidic acid plays a regulatory role in clathrin-mediated endocytosis. *Mol Boil Cell* 21: 2944-2952
- Armengot L, Marquès-Bueno MM, Jaillais Y** (2016) Regulation of polar auxin transport by protein and lipid kinases. *J Exp Bot* 67: 4015-4037
- Briggs WR, Tocher RD, Wilson JF** (1957) Phototropic auxin redistribution in corn coleoptiles. *Science* 126: 210-212.
- Briggs WR** (1963) Mediation of phototropic responses of corn coleoptiles by lateral transport of auxin. *Plant Physiol* 38: 237-247
- Baster P, Robert S, Kleine-Vehn J, Vanneste S, Kania U, Grunewald W, et al** (2013) SCF^{TIR1/AFB}-auxin signalling regulates PIN vacuolar trafficking and auxin fluxes during root gravitropism. *The EMBO J* 32: 260-274
- Band LR, Wells DM, Fozard JA, Ghetiu T, French AP, Pound MP, Wilson MH, Yu L, Li W, Hijazi HI, Oh J, Pearce SP, Perez-Amador MA, Yun J, Kramer E, Alonso JM, Godin C, Vernoux T, Hodgman TC, Pridmore TP, Swarup R, King JR, Bennett MJ** (2014) Systems analysis of auxin transport in the *Arabidopsis* root apex. *Plant Cell* 26: 862-875
- Barbosa IC, Shikata H, Zourelidou M, Heilmann M, Heilmann I, Schwechheimer C** (2016) Phospholipid composition and a polybasic motif determine D6 PROTEIN KINASE polar association with the plasma membrane and tropic responses. *Development* 143: 4687-4700
- van den Berg T, Korver RA, Testerink C, ten Tusscher KH** (2016) Modeling halotropism: a key role for root tip architecture and reflux loop remodeling in redistributing auxin. *Development* 143: 3350-3362.
- Barbosa IC, Hammes UZ, Schwechheimer C** (2018) Activation and polarity control of PIN-FORMED auxin transporters by phosphorylation. *Trends Plant Sci* 23: 523-538
- Blakeslee JJ, Spatola Rossi T, Kriechbaumer V** (2019) Auxin biosynthesis: spatial regulation and adaptation to stress. *J Exp Bot* 70: 5041-5049
- Chen M, Chory J, Fankhauser C** (2004) Light signal transduction in higher plants. *Annu Rev Genet* 38: 87-117
- Christie JM, Yang H, Richter GL, Sullivan S, Thomson CE, Lin J, Titapiwatanakun B, Ennis M, Kaiserli E, Lee OR, Adamec J, Peer WA, Murphy AS** (2011) phot1 inhibition of ABCB19 primes lateral auxin fluxes in the shoot apex required for phototropism. *PLoS Biol* 9: e1001076
- Christie JM, Murphy AS** (2013) Shoot phototropism in higher plants: new light through old concepts. *Am J Bot* 100: 35-46
- Christie JM, Suetsugu N, Sullivan S, Wada M** (2018) Shining light on the function of NPH3/RPT2-like proteins in phototropin signaling. *Plant Physiol* 176: 1015-1024
- Darwin C** (1880) *The power of movement in plants*. John Murray, London, UK
- Dhonukshe P, Aniento F, Hwang I, Robinson DG, Mravec J, Stierhof YD, Friml J** (2007) Clathrin-mediated constitutive endocytosis of PIN auxin efflux carriers in *Arabidopsis*. *Curr Biol* 17: 520-527
- Dhonukshe P, Huang F, Galvan-Ampudia CS, Mähönen AP, Kleine-Vehn J, Xu J, Quint A, Prasad K, Friml J, Scheres B, Offringa R** (2010) Plasma membrane-bound AGC3 kinases

- phosphorylate PIN auxin carriers at TPRXS(N/S) motifs to direct apical PIN recycling. *Development* 137:3245-3255
- Ding Z, Galván-Ampudia CS, Demarsy E, Łangowski Ł, Kleine-Vehn J, Fan Y, Morita MT, Tasaka M, Fankhauser C, Offringa R, Friml J** (2011) Light-mediated polarization of the PIN3 auxin transporter for the phototropic response in *Arabidopsis*. *Nat Cell Biol* 13: 447
- Dai Y, Wang H, Li B, Huang J, Liu X, Zhou Y, Mou Z, Li J** (2006) Increased expression of MAP KINASE KINASE7 causes deficiency in polar auxin transport and leads to plant architectural abnormality in *Arabidopsis*. *Plant Cell* 18: 308-320
- Dietrich D, Pang L, Kobayashi A, Fozard JA, Boudolf V, Bhosale R, et al** (2017) Root hydrotropism is controlled via a cortex-specific growth mechanism. *Nat Plants*, 3: 17057
- Dietrich D** (2018) Hydrotropism: how roots search for water. *J Exp Bot* 69: 2759-2771
- Dory M, Hatzimasoura E, Kállai BM, Nagy SK, Jäger K, Darula Z, Nádai TV, Mészáros T, López-Juez E, Barnabás B, Palme K, Bögre L, Ditengou FA, Dóczy R** (2018) Coevolving MAPK and PID phosphosites indicate an ancient environmental control of PIN auxin transporters in land plants. *FEBS Lett* 592: 89-102
- Eapen D, Barroso ML, Campos ME, Ponce G, Corkidi G, Dubrovsky JG, Cassab GI** (2003) A no hydrotropic response root mutant that responds positively to gravitropism in *Arabidopsis*. *Plant Physiol*, 131: 536-546
- Fukaki H, Fujisawa H, Tasaka M** (1996) SGR1, SGR2, and SGR3: novel genetic loci involved in shoot gravitropism in *Arabidopsis thaliana*. *Plant Physiol* 110: 945-955
- Fukaki H, Wysocka-Diller J, Kato T, Fujisawa H, Benfey PN, Tasaka M** (1998) Genetic evidence that the endodermis is essential for shoot gravitropism in *Arabidopsis thaliana*. *The Plant J* 14: 425-430
- Friml J, Wiśniewska J, Benková E, Mendgen K, Palme K** (2002) Lateral relocation of auxin efflux regulator PIN3 mediates tropism in *Arabidopsis*. *Nature* 415: 806
- Friml J, Yang X, Michniewicz M, Weijers D, Quint A, Tietz O, et al** (2004) A PINOID-dependent binary switch in apical-basal PIN polar targeting directs auxin efflux. *Science* 306: 862-865
- Friml J** (2010) Subcellular trafficking of PIN auxin efflux carriers in auxin transport. *Eur J Cell Biol* 89: 231-235
- Furutani M, Hirano Y, Nishimura T, Nakamura M, Taniguchi M, Suzuki K, et al** (2020) Polar recruitment of RLD by LAZY1-like protein during gravity signaling in root branch angle control. *Nat Commun* 11: 1-13
- Geldner N, Friml J, Stierhof YD, Jürgens, G, Palme K** (2001) Auxin transport inhibitors block PIN1 cycling and vesicle trafficking. *Nature* 413: 425
- Geldner N, Anders N, Wolters H, Keicher J, Kornberger W, Muller P, Delbarre A, Ueda T, Nakano A, Jürgens G** (2003) The *Arabidopsis* GNOM ARF-GEF mediates endosomal recycling, auxin transport, and auxin-dependent plant growth. *Cell* 112: 219-230
- Guan C, Rosen ES, Boonsirichai K, Poff KL, Masson PH** (2003) The ARG1-LIKE2 gene of *Arabidopsis* functions in a gravity signal transduction pathway that is genetically distinct from the PGM pathway. *Plant Physiol* 133: 100-112
- Geisler M, Murphy AS** (2006) The ABC of auxin transport: the role of p-glycoproteins in plant development. *FEBS Lett* 580: 1094-1102
- Ganguly A, Sasayama D, Cho HT** (2012) Regulation of the polarity of protein trafficking by phosphorylation. *Mol Cells* 33: 423-430

- Ge L, Chen R** (2016) Negative gravitropism in plant roots. *Nat Plants* 2: 16155
- Ge L, Chen R** (2019) Negative gravitropic response of roots directs auxin flow to control root gravitropism. *Plant Cell Environ* 42: 2372-2383
- Galvan-Ampudia CS, Julkowska MM, Darwish E, Gandullo J, Korver RA, Brunoud G, Haring MA, Munnik T, Vernoux T, Testerink C** (2013) Halotropism is a response of plant roots to avoid a saline environment. *Curr Biol* 23: 2044-2050
- Goyal A, Karayekov E, Galvão VC, Ren H, Casal JJ, Fankhauser C** (2016). Shade promotes phototropism through phytochrome B-controlled auxin production. *Curr Biol* 26: 3280-3287
- Grones P, Abas M, Hajný J, Jones A, Waidmann S, Kleine-Vehn J, Friml J** (2018) PID/WAG-mediated phosphorylation of the Arabidopsis PIN3 auxin transporter mediates polarity switches during gravitropism. *Sci Rep* 8: 10279
- Haga K, Takano M, Neumann R, Iino M** (2005) The rice COLEOPTILE PHOTOTROPISM1 gene encoding an ortholog of Arabidopsis NPH3 is required for phototropism of coleoptiles and lateral translocation of auxin. *The Plant Cell* 17: 103-115
- Harrison BR, Masson PH** (2008) ARL2, ARG1 and PIN3 define a gravity signal transduction pathway in root statocytes. *Plant J* 53: 380-392
- Huang F, Zago MK, Abas L, van Marion A, Galván-Ampudia, CS, Offringa R** (2010) Phosphorylation of conserved PIN motifs directs Arabidopsis PIN1 polarity and auxin transport. *Plant Cell* 22: 1129-1142
- Haga K, Tsuchida-Mayama T, Yamada M, Sakai T** (2015) Arabidopsis ROOT PHOTOTROPISM2 contributes to the adaptation to high-intensity light in phototropic responses. *The Plant Cell* 27: 1098-1112
- Han EH, Petrella DP, Blakeslee JJ** (2017) Bending models of halotropism: incorporating protein phosphatase 2A, ABCB transporters, and auxin metabolism. *J Exp Bot* 68: 3071-3089
- Harmer SL, Brooks CJ** (2018) Growth-mediated plant movements: hidden in plain sight. *Curr Opin Plant Biol* 41: 89-94
- Hu H, Fu Y, Yang Y, Chen S, Ning N** (2019) *Arabidopsis* IAR4 modulates primary root growth under salt stress through ROS-mediated modulation of auxin distribution. *Front Plant Sci* 10: 522
- Han H, Rakusová H, Verstraeten I, Zhang Y, Friml J** (2020) SCF^{TIR1/AFB} auxin signaling for bending termination during shoot gravitropism. *Plant Physiol* 183: 37-40
- Jia W, Li B, Li S, Liang Y, Wu X, Ma M, Wang J, Gao J, Cai Y, Zhang Y, Wang Y, Li J, Wang Y** (2016) Mitogen-activated protein kinase cascade MKK7-MPK6 plays important roles in plant development and regulates shoot branching by phosphorylating PIN1 in *Arabidopsis*. *PLoS Biol* 14: e1002550
- Kogl, F., and A. J. Haagen-Smits.** (1931) I. Mitteilung über pflanzliche wachstumsstoffe. Über die chemie des euchsstoffs. *Proceedings Koninklijke Nederlandse Akademie van Wetenschappen* 34: 1411– 1416.
- Kovtun Y, Chiu WL, Zeng W, Sheen J** (1998) Suppression of auxin signal transduction by a MAPK cascade in higher plants. *Nature* 395: 716
- Kobayashi A, Takahashi A, Kakimoto Y, Miyazawa Y, Fujii N, Higashitani A, Takahashi H** (2007) A gene essential for hydrotropism in roots. *Proc Natl Acad Sci USA* 104: 4724-4729

- Kleine-Vehn J, Dhonukshe P, Sauer M, Brewer PB, Wiśniewska J, Paciorek T, Benková E, Friml J** (2008) ARF GEF-dependent transcytosis and polar delivery of PIN auxin carriers in *Arabidopsis*. *Curr Biol* 18: 526-531
- Kleine-Vehn J, Ding Z, Jones AR, Tasaka M, Morita MT, Friml J** (2010) Gravity-induced PIN transcytosis for polarization of auxin fluxes in gravity-sensing root cells. *Proc Natl Acad Sci USA* 107: 22344-22349
- Kitakura S, Vanneste S, Robert S, Löffke C, Teichmann T, Tanaka H, Friml J** (2011) Clathrin mediates endocytosis and polar distribution of PIN auxin transporters in *Arabidopsis*. *Plant Cell* 23: 1920-1931
- Kim K, Shin J, Lee SH, Kweon HS, Maloof JN, Choi G** (2011) Phytochromes inhibit hypocotyl negative gravitropism by regulating the development of endodermal amyloplasts through phytochrome-interacting factors. *Proc Natl Acad Sci USA* 108: 1729-1734
- Kutschera U, Briggs WR** (2012). Root phototropism: from dogma to the mechanism of blue light perception. *Planta* 235: 443-452
- Korver RA, van den Berg T, Meyer AJ, Galvan-Ampudia CS, ten Tusscher KH, Testerink C** (2020) Halotropism requires Phospholipase D ζ 1-mediated modulation of cellular polarity of auxin transport carriers. *Plant Cell Environ* 43:143-158
- Lariguet P, Fankhauser C** (2004) Hypocotyl growth orientation in blue light is determined by phytochrome A inhibition of gravitropism and phototropin promotion of phototropism. *Plant J* 40: 826-834
- Li, G., Santoni, V., & Maurel, C.** (2014). Plant aquaporins: roles in plant physiology. *Biochim Biophys Acta* 1840: 1574-1582
- Liscum E, Askinosie SK, Leuchtman DL, Morrow J, Willenburg KT, Coats DR** (2014) Phototropism: growing towards an understanding of plant movement. *Plant Cell* 26: 38-55
- Liu W, Li RJ, Han TT, Cai W, Fu ZW, Lu YT** (2015) Salt stress reduces root meristem size by nitric oxide-mediated modulation of auxin accumulation and signaling in *Arabidopsis*. *Plant Physiol* 168: 343-356
- Lee HJ, Kim HS, Park JM, Cho HS, Jeon JH** (2019) PIN-mediated polar auxin transport facilitates root obstacle avoidance. *New Phytol* 225: 1285-1296
- Mockaitis K, Howell SH** (2000) Auxin induces mitogenic activated protein kinase (MAPK) activation in roots of *Arabidopsis* seedlings. *Plant J* 24: 785-796
- Massa GD, Gilroy S** (2003) Touch modulates gravity sensing to regulate the growth of primary roots of *Arabidopsis thaliana*. *The Plant J* 33: 435-445
- Morita MT, Sakaguchi K, Kiyose SI, Taira K, Kato T, Nakamura M, Tasaka M** (2006) A C2H2-type zinc finger protein, SGR5, is involved in early events of gravitropism in *Arabidopsis* inflorescence stems. *The Plant J* 47: 619-628
- Michniewicz M, Zago MK, Abas L, Weijers D, Schweighofer A, Meskiene I, Heisler MG, Ohno C, Zhang J, Huang F, Schwab R, Weigel D, Meyerowitz EM, Luschnig C, Offringa R, Friml J** (2007) Antagonistic regulation of PIN phosphorylation by PP2A and PINOID directs auxin flux. *Cell* 130: 1044-1056
- Miyazawa Y, Takahashi A, Kobayashi A, Kaneyasu T, Fujii N, Takahashi H** (2009) GNOM-mediated vesicular trafficking plays an essential role in hydrotropism of *Arabidopsis* roots. *Plant Physiol* 149: 835-840
- Monshausen GB, Miller ND, Murphy AS, Gilroy S** (2011) Dynamics of auxin-dependent Ca²⁺ and pH signaling in root growth revealed by integrating high-resolution imaging with automated computer vision-based analysis. *Plant J* 65: 309-318

- Moriwaki T, Miyazawa Y, Fujii N, Takahashi H** (2012) Light and abscisic acid signalling are integrated by MIZ1 gene expression and regulate hydrotropic response in roots of *Arabidopsis thaliana*. *Plant Cell Environ* 35: 1359-1368
- Morohashi K, Okamoto M, Yamazaki C, Fujii N, Miyazawa Y, Kamada M, Kasahara H, Osada I, Shimazu T, Fusejima Y, Higashibata A, Yamazaki T, Ishioka N, Kobayashi A, Takahashi H** (2017) Gravotropism interferes with hydrotropism via counteracting auxin dynamics in cucumber roots: clinorotation and spaceflight experiments. *New Phytol* 215: 1476-1489
- Naramoto S, Kleine-Vehn J, Robert S, Fujimoto M, Dainobu T, Paciorek T, et al** (2010) ADP-ribosylation factor machinery mediates endocytosis in plant cells. *Proc Natl Acad Sci USA* 107: 21890-21895
- Nakajima Y, Nara Y, Kobayashi A, Sugita T, Miyazawa Y, Fujii N, Takahashi H** (2017) Auxin transport and response requirements for root hydrotropism differ between plant species. *J Exp Bot* 68: 3441-3456
- Ohgishi M, Saji K, Okada K, Sakai T** (2004) Functional analysis of each blue light receptor, cry1, cry2, phot1, and phot2, by using combinatorial multiple mutants in *Arabidopsis*. *Proc Natl Acad Sci USA* 101: 2223-2228
- Pickard BG, Thimann KV** (1963) Immediate cause of phototropic curvature in the maize seedling. *Science* 140: 384-384
- Petrášek J, Mravec J, Bouchard R, Blakeslee JJ, Abas M, Seifertová D, et al** (2006) PIN proteins perform a rate-limiting function in cellular auxin efflux. *Science* 312: 914-918
- Pedmale UV, Liscum E** (2007) Regulation of phototropic signaling in *Arabidopsis* via phosphorylation state changes in the phototropin 1-interacting protein NPH3. *J Bio Chem* 282: 19992-20001
- Preuten T, Hohm T, Bergmann S, Fankhauser C** (2013) Defining the site of light perception and initiation of phototropism in *Arabidopsis*. *Curr Biol* 23: 1934-1938
- Rakusová H, Gallego-Bartolomé J, Vanstraelen M, Robert HS, Alabadí D, Blázquez MA, Benková E, Friml J** (2011) Polarization of PIN3-dependent auxin transport for hypocotyl gravitropic response in *Arabidopsis thaliana*. *Plant J* 67: 817-826
- Rigó G, Ayaydin F, Tietz O, Zsigmond L, Kovács H, Páy A, Salchert K, Darula Z, Medzihradzsky KF, Szabados L, Palme K, Koncz C, Cséplő A** (2013) Inactivation of plasma membrane-localized CDPK-RELATED KINASE5 decelerates PIN2 exocytosis and root gravitropic response in *Arabidopsis*. *Plant Cell* 25: 1592-1608
- Robinson DG, Pimpl P** (2014) Clathrin and post-Golgi trafficking: a very complicated issue. *Trends Plant Sci* 19: 134-139
- Rakusová H, Fendrych M, Friml J** (2015) Intracellular trafficking and PIN-mediated cell polarity during tropic responses in plants. *Curr Opin Plant Biol* 23: 116-123
- Rakusová H, Abbas M, Han H, Song S, Robert HS, Friml J** (2016) Termination of shoot gravitropic responses by auxin feedback on PIN3 polarity. *Curr Biol* 26: 3026-3032
- Rakusová H, Han H, Valošek P, Friml J** (2019) Genetic screen for factors mediating PIN polarization in gravistimulated *Arabidopsis thaliana* hypocotyls. *Plant J* 98:1048-1059
- Sun F, Zhang W, Hu H, Li B, Wang Y, Zhao Y, Li K, Liu M, Li X** (2008) Salt modulates gravity signaling pathway to regulate growth direction of primary roots in *Arabidopsis*. *Plant Physiol* 146: 178-188.
- Sukumar P, Edwards KS, Rahman A, DeLong A, Muday GK** (2009) PINOID kinase regulates root gravitropism through modulation of PIN2-dependent basipetal auxin transport in *Arabidopsis*. *Plant Physiol* 150: 722-735

- Sutka M, Li G, Boudet J, Boursiac Y, Doumas P, Maurel C** (2011) Natural variation of root hydraulics in *Arabidopsis* grown in normal and salt-stressed conditions. *Plant Physiol* 155: 1264-1276
- Saucedo M, Ponce G, Campos ME, Eapen D, García E, Luján R, et al** (2012) An *altered hydrotropic response (ahr1)* mutant of *Arabidopsis* recovers root hydrotropism with cytokinin. *J Exp Bot* 63: 3587-3601
- Sun J, Qi L, Li Y, Zhai Q, Li C** (2013) PIF4 and PIF5 transcription factors link blue light and auxin to regulate the phototropic response in *Arabidopsis*. *The Plant Cell* 25: 2102-2114
- Shkolnik D, Krieger G, Nuriel R, Fromm H** (2016) Hydrotropism: root bending does not require auxin redistribution. *Mol Plant* 9: 757-759
- Sullivan S, Kharshiing E, Laird J, Sakai T, Christie JM** (2019) Deetiolation enhances phototropism by modulating NON-PHOTOTROPIC HYPOCOTYL3 phosphorylation status. *Plant Physiol* 180: 1119-1131.
- Song Y, Li G, Nowak J, Zhang X, Xu D, Yang X, et al** (2019) The rice actin-binding protein RMD regulates light-dependent shoot gravitropism. *Plant Physiol* 181: 630-644
- Tan S, Zhang X, Kong W, Yang X., Molnár G, Vondráková Z, et al** (2020). The lipid code-dependent phosphoswitch PDK1–D6PK activates PIN-mediated auxin efflux in *Arabidopsis*. *Nature Plants* 1-14.
- Takahashi N, Yamazaki Y, Kobayashi A, Higashitani A, Takahashi H** (2003) Hydrotropism interacts with gravitropism by degrading amyloplasts in seedling roots of *Arabidopsis* and radish. *Plant Physiol* 132: 805-810
- Taniguchi YY, Taniguchi M, Tsuge T, Oka A, Aoyama T** (2010) Involvement of *Arabidopsis thaliana* phospholipase D ζ 2 in root hydrotropism through the suppression of root gravitropism. *Planta* 231: 491
- Tatsumi H, Toyota M, Furuichi T, Sokabe M** (2014) Calcium mobilizations in response to changes in the gravity vector in *Arabidopsis* seedlings: possible cellular mechanisms. *Plant Signal Behav* 9: e29099
- Taniguchi M, Furutani M, Nishimura T, Nakamura M, Fushita T, Iijima K, Baba K, Tanaka H, Toyota M, Tasaka M, Morita MT** (2017) The *Arabidopsis* LAZY1 family plays a key role in gravity signaling within statocytes and in branch angle control of roots and shoots. *Plant Cell* 29: 1984-1999
- Tan S, Zhang X, Kong W, Yang XL, Molnár G, Friml J, Xue, HW** (2020). A lipid code-dependent phosphoswitch directs PIN-mediated auxin efflux in *Arabidopsis* development. *Nat Plants*
- Vanhaelewyn L, Viczián A, Prinsen E, Bernula P, Serrano AM, Arana MV, Ballaré CL, Nagy F, Van Der Straeten D, Vandenbussche F** (2019) Differential UVR8 signal across the stem controls UV-B-induced inflorescence phototropism. *Plant Cell* 31: 2070-2088
- Vandenbrink JP, Kiss JZ** (2019) Plant responses to gravity. *Semin Cell Dev Biol* 92:122-125
- Went FW (1928) Wuchsstoff und wachstum. *Rec Trav Bot Neerl* 25: 1-116
- Wiśniewska J, Xu J, Seifertová D, Brewer PB, Růžička K, Blilou I, et al** (2006) Polar PIN localization directs auxin flow in plants. *Science* 312: 883-883
- Wan Y, Jasik J, Wang L, Hao H, Volkmann D, Menzel D, Mancuso S, Baluška F, Lin J** (2012) The signal transducer NPH3 integrates the phototropin1 photosensor with PIN2-based polar auxin transport in *Arabidopsis* root phototropism. *Plant Cell* 24: 551-565
- Willige BC, Ahlers S, Zourelidou M, Barbosa IC, Demarsy E, Trevisan M, Davis PA, Roelfsema MR, Hangarter R, Fankhauser C, Schwechheimer C** (2013) D6PK AGCVIII kinases are

- required for auxin transport and phototropic hypocotyl bending in *Arabidopsis*. *Plant Cell* 25: 1674-1688
- Wang C, Yan X, Chen Q, Jiang N, Fu W, Ma B, Liu J, Li C, Bednarek SY, Pan J** (2013) Clathrin light chains regulate clathrin-mediated trafficking, auxin signaling, and development in *Arabidopsis*. *Plant Cell* 25: 499-516
- de Wit M, Galvão VC, Fankhauser C** (2016) Light-mediated hormonal regulation of plant growth and development. *Annu Rev Plant Biol* 67: 513-537
- Weller B, Zourelidou M, Frank L, Barbosa IC, Fastner A, Richter S, Jürgens G, Hammes UZ, Schwechheimer C** (2017) Dynamic PIN-FORMED auxin efflux carrier phosphorylation at the plasma membrane controls auxin efflux-dependent growth. *Proc Natl Acad Sci USA* 114: E887-E896
- Wang P, Shen L, Guo J, Jing W, Qu Y, Li W, Bi R, Xuan W, Zhang Q, Zhang W** (2019) Phosphatidic Acid Directly Regulates PINOID-Dependent Phosphorylation and Activation of the PIN-FORMED2 Auxin Efflux Transporter in Response to Salt Stress. *Plant Cell* 31: 250-271
- Xu W, Jia L, Shi W, Liang J, Zhou F, Li Q, Zhang J** (2013). Abscisic acid accumulation modulates auxin transport in the root tip to enhance proton secretion for maintaining root growth under moderate water stress. *New Phytol* 197: 139-150
- Xu J, Zhang S** (2015) Mitogen-activated protein kinase cascades in signaling plant growth and development. *Trends Plant Sci* 20: 56-64
- Yamauchi Y, Fukaki H, Fujisawa H, Tasaka M** (1997) Mutations in the SGR4, SGR5 and SGR6 loci of *Arabidopsis thaliana* alter the shoot gravitropism. *Plant Cell Physiol* 38: 530-535
- Yano D, Sato M, Saito C, Sato MH, Morita MT, Tasaka M** (2003) A SNARE complex containing SGR3/AtVAM3 and ZIG/VTI11 in gravity-sensing cells is important for *Arabidopsis* shoot gravitropism. *Proc Natl Acad Sci USA* 100: 8589-8594
- Yokawa K, Fasano R, Kagenishi T, Baluška F** (2014) Light as stress factor to plant roots—case of root halotropism. *Front Plant Sci* 5: 718
- Zhang J, Vanneste S, Brewer PB, Michniewicz M, Grones P, Kleine-Vehn J, Löffke C, Teichmann T, Bielach A, Cannoot B, Hoyerová K, Chen X, Xue HW, Benková E, Zažímalová E, Friml J** (2011) Inositol trisphosphate-induced Ca²⁺ signaling modulates auxin transport and PIN polarity. *Dev Cell* 20: 855-866
- Zhang KX, Xu HH, Yuan TT, Zhang L, Lu YT** (2013) Blue-light-induced PIN 3 polarization for root negative phototropic response in *Arabidopsis*. *Plant J* 76: 308-321
- Zourelidou M, Absmanner B, Weller B, Barbosa IC, Willige BC, Fastner A, Streit V, Port SA, Colcombet J, de la Fuente van Bentem S, Hirt H, Kuster B, Schulze WX, Hammes UZ, Schwechheimer C** (2014). Auxin efflux by PIN-FORMED proteins is activated by two different protein kinases, D6 PROTEIN KINASE and PINOID. *elife* 3: e02860
- Zhang Y, Yu Q, Jiang N, Yan X, Wang C, Wang Q, Liu J, Zhu M, Bednarek SY, Xu J, Pan J** (2017) Clathrin regulates blue light-triggered lateral auxin distribution and hypocotyl phototropism in *Arabidopsis*. *Plant Cell Environ* 40: 165-176
- Zegzouti H, Anthony RG, Jahchan N, Bögre L, Christensen SK** (2006) Phosphorylation and activation of PINOID by the phospholipid signaling kinase 3-phosphoinositide-dependent protein kinase 1 (PDK1) in *Arabidopsis*. *Proc Natl Acad Sci USA* 103: 6404-6409

2 Piperonylic acid inhibits PIN polarization dependent auxin transport during *Arabidopsis* hypocotyl gravitropism

Huibin Han¹, Lesia Rodriguez¹, Inge Verstraeten¹, Shutang Tan¹, Behrokh Shojaie¹, Bartel Vanholme^{2, 3}, Wout Boerjan^{2, 3}, Jiří Friml¹

¹ Institute of Science and Technology (IST) Austria, 3400 Klosterneuburg, Austria

² Department of Plant Systems Biology, VIB, B-9052 Gent, Belgium

³ Department of Plant Biotechnology and Bioinformatics, Ghent University, B-9052 Gent, Belgium

2.1 Introduction

Gravitropic bending both in root and shoot is initiated by asymmetric distribution of the phytohormone auxin (Friml et al., 2002; Rakusová et al., 2015). During gravitropic response, the asymmetric auxin distribution is mainly achieved by polarity switch of PIN auxin efflux transporters (Friml et al., 2002; Kleine-Vehn et al., 2010; Rakusová et al., 2011). Among the PINs, PIN3 plays the central role in hypocotyl gravitropic response (Friml et al., 2002; Rakusová et al., 2011, 2016, 2019; Han et al., 2020). PIN3 undergoes two distinct polarization events during hypocotyl gravitropism: (i) Following gravistimulation, PIN3 polarizes to the lower side of hypocotyl endodermal cells, thus driving auxin flow to and corresponding auxin accumulation at the lower hypocotyl side, leading to hypocotyl bending initiation (Rakusová et al., 2011). (ii) At the later stage of gravitropic response, PIN3 at the lower side of endodermal cells is specifically targeted for lytic degradation in response to higher auxin level, resulting in PIN3 symmetrical distribution at both side of endodermal cells. Subsequently, the symmetric distribution of auxin is restored and hypocotyl terminates bending (Rakusová et al., 2016, 2019; Han et al., 2020). Thus, gravity-induced PIN3 polarization is essential for bending initiation (Rakusová et al., 2011), and auxin-mediated feedback on PIN3 re-localization is vital for bending termination (Rakusová et al., 2016, 2019; Han et al., 2020).

To date, factors-mediating PIN polarity switch during hypocotyl gravitropism are uncovered. Clathrin-Mediated Endocytosis (CME) and the ARF-GEF GNOM-mediated constitutive PIN trafficking are involved in intracellular PIN3 polarity regulation (Kleine-Vehn et al., 2010; Naramoto et al., 2010; Rakusová et al., 2011, 2016). PINOID (PID) and related WAG1 and WAG2 serine/threonine protein kinases activity is also needed for both gravity- and auxin-induced PIN3 polarization (Rakusová et al., 2011, 2016). Gravity-induced PIN3 relocation doesn't require protein degradation and *de novo* protein synthesis (Rakusová et

al., 2011). However, vacuolar targeting PIN degradation (Baster et al., 2013) is required for auxin feedback on PIN3 polarization (Rakusová et al., 2016). Actin cytoskeleton is also essential for auxin feedback on PIN3 polarity and bending termination (Rakusová et al., 2019). Notably, auxin-mediated PIN3 polarization and bending termination requires the SCF^{TIR1/AFB} signaling pathway (Han et al., 2020). Despite these initial insights into cellular mechanisms of PIN polarization, the molecular mechanism and specific factors mediating both gravity- and auxin-induced PIN3 polarization remain elusive.

To gain novel insights into PIN3 polarity regulation during shoot gravitropic response, we performed a 24 hours hypocotyl bending assay using metabolites or inhibitors derived from the phenylpropanoid pathway (Supplementary Figure S1; Vanholme et al., 2012), which has been reported to perturb auxin response, transport and biosynthesis (Steenackers et al., 2016, 2017; Kurepa et al., 2018; Mehmood et al., 2019). Our findings revealed that piperonylic acid (PA), an inhibitor of the CINNAMATE-4-HYDROXYLASE (C4H) (Schalk et al., 1998; Steenackers et al., 2016), triggered hypocotyl hyperbending in a dose-dependent manner. PA treatment inhibited auxin-mediated PIN3 repolarization, resulted in continuous accumulation of auxin at the lower side of hypocotyl during shoot gravitropism. As a consequence, hypocotyls were hyperbending (Rakusová et al., 2016, 2019). Genetic mutation of *C4H*, the PA target, also led to similar hypocotyl hyperbending and a defective auxin-mediated PIN3 repolarization. In addition, lignin perturbation caused by PA treatment or *C4H* mutation is not the basis for the hypocotyl overbending and the defective auxin-mediated PIN3 repolarization. Metabolic analysis showed that flavonoids act as the downstream target of C4H. Exogenous application of quercetin, one of the main flavonoids, rescued the defective hypocotyl bending and auxin-mediated PIN3 polarization upon PA treatment as well as in the *c4h* mutant. We also demonstrated that PA affected PIN3 phosphorylation status via modulating PINOID (PID) kinase phosphorylation. Hence, we introduce a novel physiological effect of PA on *Arabidopsis* shoot gravitropism by modulating PIN polarization dependent directional auxin transport.

2.2 Results

2.2.1 *Piperonylic acid (PA) causes hypocotyl overbending in a dose-dependent manner*

As previously reported, metabolites or inhibitors derived from phenylpropanoid pathway perturb plant growth by interfering with auxin response, transport and biosynthesis (Steenackers et al., 2016, 2017; Kurepa et al., 2018; Mehmood et al., 2019). We thus performed a 24 hours bending assay to test their role in shoot gravitropic response (Supplementary Figure S1). We uncovered that PA triggered hypocotyl overbending in a dose-dependent manner (Figure 1A, 1B), and this overbending hypocotyl was not due to a fast hypocotyl growth (Supplementary Figure S2A). Similarly, genetic disruption of the PA target, CINNAMATE-4-HYDROXYLASE (C4H) (Schalk et al., 1998; Steenackers et al., 2016), also resulted in hypocotyl overbending (Figure 1A, 1C). However, other inhibitors or intermediates derived from the same pathway showed no obvious effects on hypocotyl bending (Supplementary Figure S2B; Van de Wouwer et al., 2016; Steenackers et al., 2016).

Inhibition of C4H leads to the accumulation of many products such as Cinnamic acid (CA) and *p*-Coumaric acid (*p*-CA) (Steenackers et al., 2016). Both *cis*-CA and *trans*-CA treatment showed no obvious effects on hypocotyl bending (Supplementary Figure S2B), we then examined whether *p*-CA, can complement PA effect on hypocotyl bending. Exogenous application of *p*-CA has no obvious effects on the hypocotyl bending, but it complemented the hyperbending hypocotyls triggered by PA treatment as well as the overbending hypocotyl of *c4h* mutant (Supplementary Figure S2C, S2D).

Taken together, our results reveal the novel physiological effect of PA in *Arabidopsis* hypocotyl gravitropism (Figure 1A - 1C), but upstream compounds of C4H are not the basis for PA effect on hypocotyl bending (Supplementary Figure S1; Supplementary Figure S2B). Our data also indicates that an unknown downstream metabolite of C4H is responsible for PA effect on hypocotyl bending (Supplementary Figure S2C, S2D).

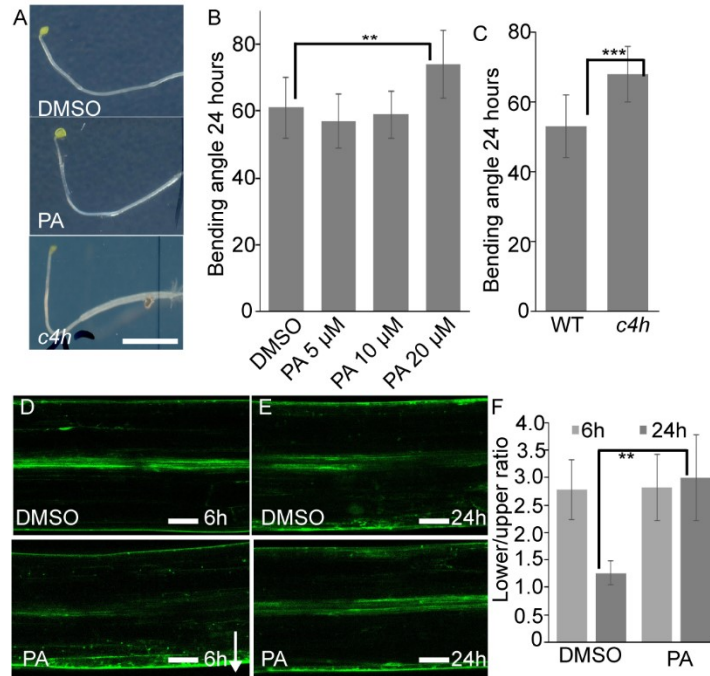


Figure 1. PA triggers *Arabidopsis* hypocotyl hyperbending via modulating auxin distribution.

(A) Represented images of 24 hours gravity stimulated wild type hypocotyl upon DMSO or PA treatment, and *c4h* mutant. Scale bars = 1 cm. (B - C) Quantification of hypocotyl bending angle upon various concentration of PA treatment in wild type seedlings (B), and in *c4h* mutant (C). (D - E) Represented images of *DR5rev::GFP* signal in hypocotyls under DMSO or PA treatment after 6 hours (D) and 24 hour (E) gravity stimulation. Scale bars = 20 μ M. (F) Quantification of GFP signal under DMSO or PA treatment after 6 hours or 24 hours gravity stimulation. The ratio was calculated between lower and upper side of hypocotyls. Data are means \pm SD, n = 30 – 40 for bending angle quantification, n = 15 for *DR5rev::GFP* signal quantification, *** $P < 0.01$ or ** $P < 0.05$ determined by Students t-test. Arrow indicates gravity direction.

2.2.2 PA perturbs auxin distribution in *Arabidopsis* hypocotyl

Next, we wondered whether PA perturbs auxin distribution during hypocotyl gravitropism (Friml et al., 2002; Rakusová et al, 2011). Thus, we studied PA impact on auxin distribution by detecting *DR5rev::GFP* signal in hypocotyls after gravity stimulation. Consistent with previous results (Rakusová et al., 2011), a strong *DR5rev::GFP* signal was detected at the lower side of hypocotyl under DMSO and PA treatment after 6 hours gravity stimulation (Figure 1D, 1F). After 24 hours gravity stimulation, the *DR5rev::GFP* signal was almost equal at both side of DMSO treated hypocotyls; whereas a strong *DR5rev::GFP* signal at the lower hypocotyl side was still observed in PA treated hypocotyls (Figure 1E, 1F). Collectively, these data supports that PA inhibits auxin asymmetrical distribution at the later stage of hypocotyl gravitropic response, leading to hypocotyl overbending (Figure 1A - 1F; Rakusová et al., 2016, 2019).

2.2.3 ***PA inhibits auxin- but not gravity-induced PIN3 repolarization***

We next addressed whether the defective auxin distribution triggered by PA treatment (Figure 1E, 1F) correlates with a defective PIN3 polarization during hypocotyl gravitropism (Rakusová et al., 2011, 2016). We first investigated PA effect on gravity-induced PIN3 polarization. Without gravity stimulation, PIN3-GFP symmetrically distributed at both side of hypocotyl endodermal cells under PA treatment, thus steady-state PIN3 localization was not affected by PA treatment (Supplementary Figure S3A, S3F; Rakusová et al., 2011). After 6 hours gravity stimulation, PIN3-GFP polarized to the outer side of endodermal cells at lower hypocotyl side following DMSO and PA treatment (Supplementary Figure S3B, S3C, S3F), implying that PA treatment didn't affect gravity-induced PIN3 polarization. After 24 hours gravity stimulation, a strong PIN3-GFP signal was still detected at the outer side of endodermal cells at lower hypocotyl side in PA treated hypocotyls; whereas PIN3-GFP signal at the lower side disappeared in DMSO treated hypocotyls (Supplementary Figure S3D, S3E, S3G). In addition, PIN3-GFP distributed symmetrically in the *c4h* mutant without gravity stimulation (Supplementary Figure S4A, S4D). We observed a normal gravity-induced PIN3-GFP polarization after 6 hours gravity stimulation (Supplementary Figure S4B, S4D); but a persistence of PIN3-GFP asymmetry, with strong signal at the lower side of hypocotyl endodermal cells was observed after 24 hours gravistimulation in *c4h* mutant (Supplementary Figure S4C, S4D). These data indicated that PA interfered with auxin-mediated but not gravity-induced PIN3 repolarization (Supplementary Figure S3A – S3G; Supplementary Figure S4A – S4D).

We also examined whether PA treatment interferes with exogenous auxin effect on PIN polarization. In line with previous results (Rakusová et al., 2016, 2019), exogenous auxin treatment induced PIN3-GFP relocation to inner side of endodermal cells (Figure 2A, 2B, 2E). However, PA treatment inhibited the auxin-mediated PIN3 repolarization as evident by a strong PIN3-GFP signal at the outer side of endodermal cells (Figure 2D, 2E). Similarly, auxin failed to induce PIN3-GFP repolarization to inner side of endodermal cells in *c4h* mutant (Figure 2F - 2H). Collectively, these data further supports that PA perturbs auxin-mediated PIN3 repolarization.

As *p*-CA rescued the defective hypocotyl bending upon PA treatment as well as in *c4h* mutant (Supplementary Figure S2C, S2D). We then tested *p*-CA effect on PIN3 polarization in presence of PA or in *c4h* mutant. We first studied gravity-induced PIN3 polarization. After 6

hours gravity stimulation, a normal gravity-induced PIN3 polarization was observed in hypocotyls co-treated with *p*-CA and PA (Supplementary Figure S5A, S5C) or in *p*-CA treated *c4h* mutant hypocotyls (Supplementary Figure S6A, S6C). However, the auxin-mediated PIN3 repolarization was normal in hypocotyls co-treated with *p*-CA and PA or in the *c4h* mutant after 24 hours gravity stimulation (Supplementary Figure S5B, S5C; Supplementary Figure S6B, S6C). In addition, the inhibitory effect of PA on exogenous auxin treatment induced PIN3 inner-lateralization was also complemented by adding *p*-CA (Supplementary Figure S5D – S5F). We also observed that the defective exogenous auxin treatment induced PIN3 inner-lateralization in *c4h* mutant was also complemented *p*-CA (Supplementary Figure S6D – S6E).

Together with these results indicate that PA causes hypocotyl overbending by inhibiting auxin-mediated PIN3 repolarization at the later stage of gravitropic response. Our data also demonstrate that an unknown downstream metabolite of C4H is needed for the PA effect on PIN3 polarization.

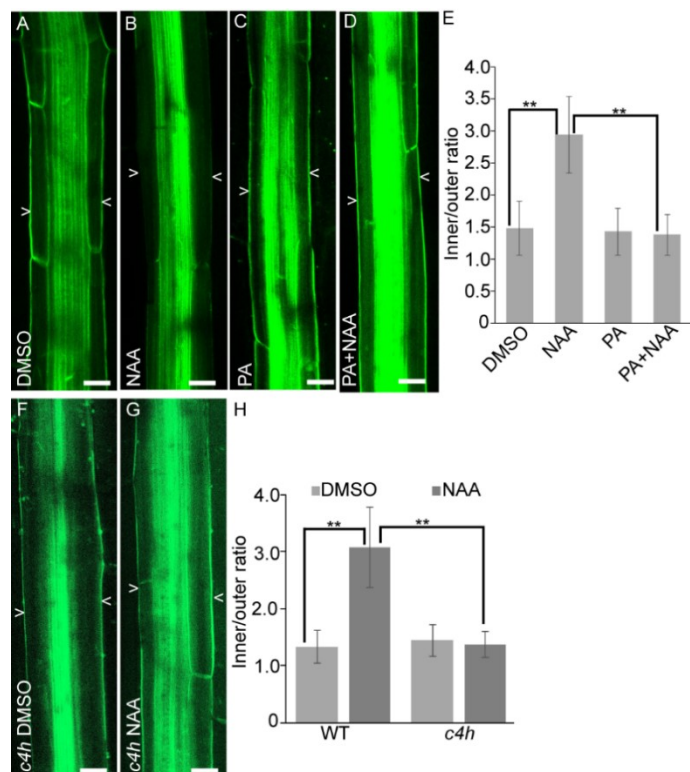


Figure 2. PA interferes auxin-mediated PIN3 repolarization.

(A - D) Represented images of PIN3-GFP in wild type seedlings under DMSO treatment (A), 10 μM of NAA treatment (B), 20 μM of PA treatment (C), PA and NAA co-treatment (D). (E) Quantification of PIN3-GFP signal upon PA treatment. The ratio was calculated between inner and outer side of endodermal cells. (F - G) Represented images of PIN3-GFP upon DMSO (F) and NAA (G) treatment in *c4h* mutant. (E) Quantification of PIN3-GFP signal upon NAA treatment in *c4h* mutant. The ratio was calculated between inner and outer side of endodermal cells. Data are means ± SD, n = 15, ** P < 0.05 determined by Student's t-test. Scale bars = 20 μm. Arrowheads depict PIN3-GFP at outer side of endodermal cells.

2.2.4 ***Defective Lignification is not the basis of PA impact on hypocotyl bending and PIN3 repolarization***

It has been reported that PA treatment reduces root lignification and can be restored by adding monolignols (Naseer et al., 2012). We wondered whether the reduced lignin deposition could be the basis for PA effect on hypocotyl bending and PIN3 polarization. Monolignols had no obvious effect on hypocotyl bending (Supplementary Figure S7A). Interestingly, the overbending hypocotyls caused by PA treatment or *C4H* mutation could not be restored by adding monolignols (Supplementary Figure S7A; Supplementary Figure S8A).

We next tested the impact of monolignols on both gravity- and auxin-induced PIN3 polarization in PA treated hypocotyls or in the *c4h* mutant. We observed a strong PIN3-GFP signal at the outer side of endodermal cells at the lower hypocotyl side by adding monolignols to the PA treated hypocotyls (Supplementary Figure S7B, S7D) or in the *c4h* mutant (Supplementary Figure S8B, S8D) after 6 hours gravity stimulation. After 24 hours gravity stimulation, the PIN3-GFP signal still retained at the outer side of endodermal cells at the lower side of the hypocotyl under PA and monolignols co-treatment (Supplementary Figure S7C, S7E) as well as in the *c4h* mutant (Supplementary Figure S8C, S8D). Additionally, monolignols could not rescue auxin-mediated PIN3-GFP repolarization to the inner side of the endodermal cells in the presence of PA (Supplementary Figure S7F, S7G, S7H) or in the *c4h* mutant (Supplementary Figure S8E, S8F).

Based on these observations, we conclude that PA treatment or mutation in *C4H* reduces lignin deposition (Naseer et al., 2012), but this reduced lignin deposition is not the basis for the observed hypocotyl overbending or the defective auxin-induced PIN3 repolarization.

2.2.5 ***Phenolic profiling analysis reveals flavonoids as downstream targets of C4H***

To further characterize the possible downstream compound of C4H during hypocotyl gravitropism, we performed a phenolic profiling of DMSO and PA treated etiolated Col-0 seedlings with or without 24 hours gravity stimulation by using ultra-high-pressure liquid chromatography-mass spectrometry (UHPLC-MS) method (Steenackers et al., 2016). Univariate statistical analysis was applied to select peaks with significantly different abundance ($P < 0.01$, 2-fold difference) between DMSO and PA treatment. Without gravity

stimulation, a total of 311 peaks were increased in abundance and 211 were reduced in abundance. After 24 hours gravity stimulation, 254 peaks were increased and 216 were reduced in abundance (Figure 3A). Among the identified peaks, 60 peaks were unique upon PA treatment following gravity stimulation, which may reflect a unique response to PA treatment during hypocotyl gravity response (Figure 3A). Based on the library, the content of flavonoid conjugates showed a significant reduction upon PA treatment (Figure 3B), indicating an involvement of flavonoids in PA triggered gravitropism response. The remarkably high number of identified unknown metabolites might reflect the developmental shift caused by PA treatment during shoot gravitropic response (Figure 3B; Supplementary Tab S1). On the other hand, our metabolomic analysis also provides novel insights into the role of phenylpropanoid pathway during young seedling development.

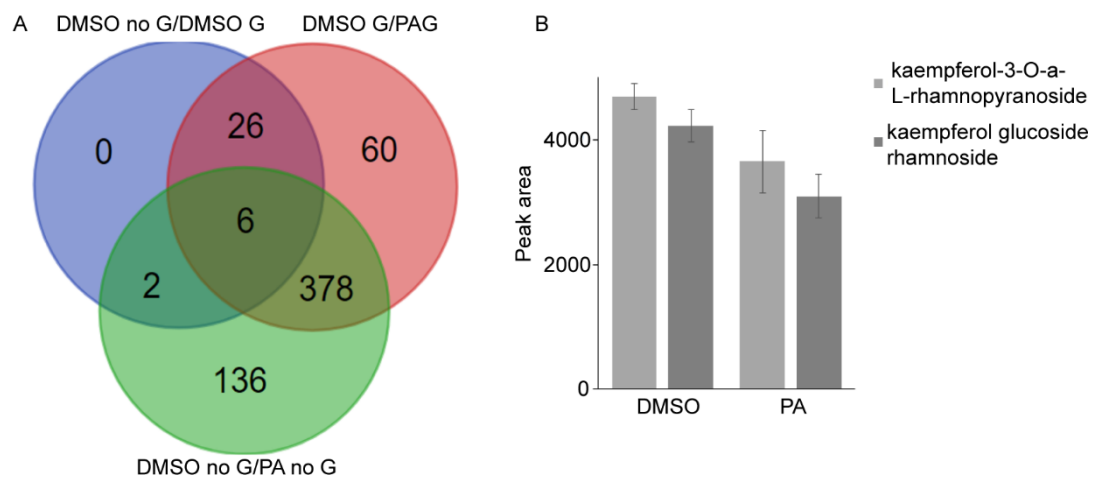


Figure 3. Phenolic profiling of PA treated *Arabidopsis* seedlings after 24 hours gravity stimulation. (A) Summary of differential shifts of metabolites upon DMSO and PA treatment with or without gravity stimulation. (B) Reduced content of flavonoids upon PA treatment after 24 hours gravity stimulation. $P < 0.05$ determined by Students t-test.

2.2.6 ***Flavonoid negatively regulates hypocotyl bending and PIN3 polarization***

It has been reported that flavonoids are an endogenous regulator of auxin transport (Brown et al., 2001), and flavonoid mutants show defects in root gravitropism (Buer and Muday, 2004; Buer et al., 2013) probably due to a mis-localization of PIN proteins or the altered PIN expression level (Peer et al., 2004). Gravity stimulation also increases flavonoid content in root (Buer and Muday, 2004). Notably, *pin2* mutant is agravitropic with a reduced flavonoid content at root elongation zone. Exogenous application of flavonoid partially rescues the agravitropic response and auxin distribution of *pin2* mutant (Santelia et al., 2008),

indicating an involvement of flavonoid during root gravitropism. However, its role in hypocotyl gravitropism is unclear. On the other hand, our phenolic profiling analysis revealed a decrease of flavonoids concentration after PA treatment (Figure 3B) as well as in the *c4h* mutant (Vanholme et al., 2012), indicating that flavonoids would act as downstream target of C4H. To test the hypothesis, we first assessed the flavonoid content in PA treated hypocotyls as well as in the *c4h* mutant hypocotyls with or without gravity stimulation. Our staining result showed that flavonoid content was decreased in both PA treated hypocotyls and in the *c4h* mutant hypocotyls without gravity stimulation (Supplementary Figure S9A – S9C, S9G). After 24 hours gravity stimulation, flavonoid content was increased in DMSO treated hypocotyls, but PA treated hypocotyls or the *c4h* mutant hypocotyls showed no increase of flavonoid content (Supplementary Figure S9D – S9F, S9G). These data indicate that the reduced flavonoid content could be one reason for the hypocotyl hyperbending of *c4h* mutant and PA treatment.

Next, we dissected the role of flavonoid in hypocotyl gravitropism by applying flavonoid biosynthesis inhibitors and the biosynthesis mutants. Diethyldithiocarbamate acts as flavonoid biosynthesis inhibitor targeting FLAVANONE-3-HYDROXYLASE (Forkmann and Stotz, 1981, 1984). We transferred 3 days old etiolated seedlings to new plates supplied with various concentration of sodium diethyldithiocarbamate trihydrate (SDT) then gravity stimulated for 24 hours. Our result showed that SDT treatment caused hypocotyl hyperbending in a concentration dependent manner (Supplementary Figure S10A), but SDT doesn't affect hypocotyl growth under our experimental condition (Supplementary Figure S10B). Additionally, we observed a similar overbending hypocotyl in *tt6* mutant after 24 hours gravity stimulation (Supplementary Figure S10C).

We then examined whether the defective flavonoid biosynthesis would also lead to a defective auxin-mediated PIN3 polarization. First, we examined SDT effect on gravity-induced PIN3 polarization. PIN3-GFP symmetrically distributed at both side of endodermal cells upon SDT treatment without gravity stimulation (Supplementary Figure S10D), and PIN3-GFP polarized to the outer side of endodermal cells after 6 hours gravity stimulation under DMSO or SDT treatment (Supplementary Figure S10E, S10G). After 24 hours gravistimulation, a strong PIN3-GFP signal was still detected at the outer side of endodermal cells under SDT treatment but not under DMSO treatment (Supplementary Figure S10F, S10G). Similarly, a

normal gravity-induced PIN3-GFP polarization was detected in *tt6* mutant (Supplementary Figure S10H, S10I, S10K). However, PIN3-GFP still retained at the outer side of endodermal cells at the lower side of *tt6* mutant hypocotyls after 24 hours gravity stimulation (Supplementary Figure S10J, S10K).

We also tested SDT effect on auxin-mediated PIN3 polarization. We transferred 3 days old etiolated seedlings to new plates supplied with 40 μ M of SDT for 2 hours, then co-treated the seedlings with 10 μ M NAA for another 4 hours. We observed that PIN3-GFP localization was retained at the outer side of the endodermal cells when flavonoid biosynthesis was inhibited (Supplementary Figure S11A, S11B). Similarly, *tt6* mutant also showed a defective auxin-mediated PIN3-GFP repolarization upon auxin treatment (Supplementary Figure S11C, S11D).

Overall, inhibition of flavonoid biosynthesis either in biosynthesis mutant or by applying chemical inhibitor resulted in hypocotyl hyperbending and defective auxin-mediated PIN3 polarization but not gravity-induced PIN3 polarization (Supplementary Figure S10; Supplementary Figure S11). These data demonstrates a negative role of flavonoid in auxin transport dependent hypocotyl gravitropism.

2.2.7 ***Flavonoid is the downstream target of C4H in hypocotyl gravitropism***

To exam whether flavonoids play an important role in response to gravity stimuli downstream of C4H, we first tested whether the exogenous application of flavonoid can rescue PA effect on hypocotyl bending. We transferred 3 days old etiolated seedlings to new plates supplied with quercetin and PA, and then gravistimulated the seedlings for 24 hours. Concentration up to 40 μ M of quercetin did not affect wild type hypocotyl gravitropic bending (Supplementary Figure S12A). However, quercetin rescued the overbending hypocotyls caused by PA treatment (Supplementary Figure S12A). Quercetin also rescued hyperbending hypocotyl of the *c4h* mutant (Supplementary Figure S12B).

We next tested whether flavonoid can rewrite PA effect on PIN3 polarization. We transferred 3 days etiolated seedlings to new plates supplied with 40 μ M of quercetin together with 20 μ M of PA, then seedlings were gravity stimulated for 6 hours or 24 hours. Quercetin had no effect on PIN3-GFP polarization with or without PA after 6 hours gravity stimulation (Supplementary Figure S12C, S12D, S12G), whereas quercetin revised the PA

effect on PIN3-GFP repolarization after 24 hours gravity stimulation (Supplementary Figure 12E, S12F, S12G). Quercetin also had no obvious effects on PIN3-GFP polarization in *c4h* mutant after 6 hours gravity stimulation (Supplementary Figure S12H, S12J), but the defective auxin-mediated PIN3 polarization was reversed by quercetin in *c4h* mutant after 24 hours gravity stimulation (Supplementary Figure S12I, S12J).

PA treatment or mutation in the *C4H* leads to a defective auxin-mediated PIN3 repolarization (Figure 2A - 2H), we then questioned whether quercetin can also rescue PA effect on auxin-mediated PIN3 polarization. In line with the 24 hours gravistimulation results (Supplementary Figure S12), quercetin also complemented the defective auxin-mediated PIN3 polarization triggered by PA treatment or *C4H* mutation in presence of exogenous auxin treatment (Supplementary Figure S13A – S13D).

Taken together, DPBA staining reveals a decrease of flavonoids content after gravity stimulation upon PA treatment as well as in the *c4h* mutant (Supplementary Figure S9A – S9G). Additionally, exogenous application quercetin rescues the defective hypocotyl bending and PIN3 polarization under PA treatment as well as in *c4h* mutant (Supplementary Figure S12; Supplementary Figure S13). This data shows that flavonoids act as downstream target of C4H to modulate PIN-mediated polar auxin transport during hypocotyl gravitropism.

2.2.8 ***PA affects PIN3 phosphorylation status***

Phosphorylation of PIN proteins at different sites by kinases is crucial for PIN polarity and activity regulation. It has been reported that PID and related WAG1 and WAG2 serine/threonine protein kinases activity contribute to PIN3 polarization during hypocotyl gravitropism (Rakusová et al., 2011, 2016; Groner et al., 2018). Flavonoid has been shown to bind to PID kinase and inhibits PID autophosphorylation activity (Henrichs et al., 2012). Our profiling data and DPBA staining assay showed that flavonoid content was decreased upon PA treatment as well as in *c4h* mutant (Figure 3B; Supplementary Figure S9A – S9G). Hence, it is likely that PA would potentially affect PIN3 phosphorylation by modulating flavonoid content and PID kinase phosphorylation.

To test the binding between flavonoid and PID kinase (Henrichs et al., 2012), we performed the Drug Affinity Responsive Target Stability (DARTS) assay (Lomenick et al., 2009) to further confirm the binding of flavonoid to PID kinase. DARTS assay using extracts of

PID::PID-YFP seedlings or the *E. coli* expressed PID protein revealed that quercetin treatment resulted in an obvious protection of PID kinase against pronase (mixture of proteases) degradation (Figure 4A, 4B). Hence, our results suggest that flavonoid binds to PID both *in vivo* and *in vitro*.

To further explore whether quercetin affects PID kinase activity (Henrichs et al., 2012), we carried out an *in vitro* kinase assay (Zegzouti et al., 2009). We first cloned the PIN3 hydrophilic loop with His tag (His-PIN3HL), and PID with His tag (His-PID) and expressed them in *E. coli*, then we purified both proteins from *E. coli* culture. We treated the PID protein or the mixture of PID and PIN3HL protein with quercetin and PA at room temperature for 1 hour. Our results revealed that quercetin reduced PID activity, but PA increased PID activity. However, PA treatment abolished quercetin effect on PID activity (Figure 4C). This reduced or increased PID activity also correlated with PID-mediated PIN3 phosphorylation activity (Figure 4C).

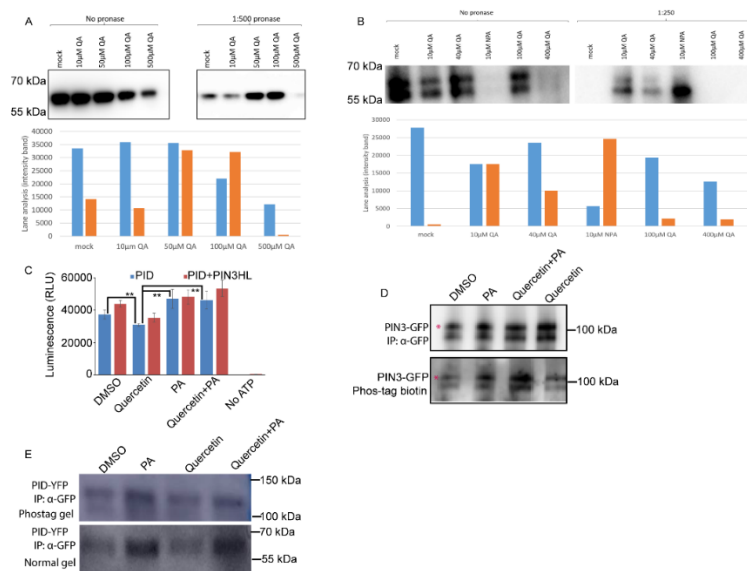


Figure 4. PA promotes PID and PIN3 phosphorylation.

(A) Flavonoid binds to PID *in vivo* by DARTS assay. The 7 days old *PID::PID-YFP* seedlings were collected and PID protein was extracted. The PID protein was treated with different concentration of quercetin with or without pronase. Then binding intensity was quantified. (B) Flavonoid binds to PID *in vitro*. The *E. coli* expressed PID protein was treated with different concentration of quercetin with or without pronase. Binding intensity was quantified. (C) Kinases assay *in vitro*. The *E. coli* expressed PID and PIN3-HL protein was treated with 20 µM of PA and 10 µM of quercetin, or the combination for 1 hour, then the luminescence was quantified. (D) PA increases PIN3 phosphorylation. The *PIN3::PIN3-GFP* seedlings were treated with 20 µM PA, 40 µM quercetin or the combination for 7 days, then the samples were collected and protein was extracted. The phos-tag botin antibody (1 : 1000) was used to detect phosphorylated PIN3 protein. (E) PA increases PID phosphorylation. The *PID::PID-YFP* seedlings were treated with DMSO, 20 µM PA, 40 µM quercetin or PA together with quercetin for 7 days, then seedlings were harvested and protein was extracted. The PID protein was added to phostag gel to detect the PID phosphorylation status. The GFP-HRP (1 : 1000) antibody was used to detect PID protein.

Our binding assay and *in vitro* kinase assay indicate that PA may influence the PIN3 phosphorylation status (Figure 4A - 4C). To test this, we performed an *in vivo* PIN3 phosphorylation assay. We treated *PIN3::PIN3-GFP* seedlings with DMSO, PA, quercetin or the combination for 7 days, whereupon the whole plants were collected for the phosphorylation assay. The western blot assay revealed that PIN3 was more phosphorylated upon PA treatment (Figure 4D). In addition, PA-triggered PIN3 phosphorylation was inhibited by quercetin (Figure 4D).

To test whether the increased PIN3 phosphorylation is caused by an altered PID phosphorylation, we then performed an *in vivo* phosphorylation assay to test PA effect on PID phosphorylation. We treated *PID::PID-YFP* seedlings with DMSO, PA, quercetin or the combination for 7 days, then the whole plants were collected. The western bolt assay showed that PA treatment led to an increase of PID phosphorylation; whereas, quercetin reduced the PID phosphorylation (Figure 4E).

Overall, PA treatment causes a decrease of flavonoids content in the hypocotyl (Figure S9A – S9G), resulting in a shift of PID kinase activity (Figure 4A - 4C). Consequently, the altered PID kinase phosphorylation triggers an altered PIN3 phosphorylation status (Figure 4D, 4E), ultimately leading to defects in auxin-mediated PIN3 repolarization (Grones et al., 2018), and hypocotyls are hyperbending.

2.3 Discussion

To search novel players in PIN polarity regulation in response to environmental stimuli, we carried out a 24 hours bending assay by treating *Arabidopsis* etiolated seedlings with various compounds derived from the phenylpropanoid pathway (Supplementary Figure S1; Steenackers et al., 2016, 2017; Kurepa et al., 2018; Mehmood et al., 2019). To this end, we introduced a novel physiological effect of PA on *Arabidopsis* shoot gravitropism. PA is a natural molecule extracted from the bark of Paracoto tree, and it acts as an inhibitor of C4H, a key enzyme of the phenylpropanoid pathway (Steenackers et al., 2016, 2017). Our detailed investigations reveal that PA modulates PIN polarization dependent directional auxin transport by modulating flavonoid content and PID kinase phosphorylation.

We observed that etiolated hypocotyls treated with PA bent more after 24 hours gravistimulation and a similar hyperbending hypocotyl was also observed in *c4h* mutant. It

seems that PA had a special effect on hypocotyl gravitropism, because other compounds derived from the same pathway had no obvious effects. The asymmetric auxin distribution during hypocotyl gravitropism is required for bending (Friml et al., 2002; Rakusová et al., 2011), the hyperbending hypocotyls caused by PA application indicates a defective auxin transport. Indeed, PA application caused a defective auxin distribution at the later stage of hypocotyl gravitropic response as manifested by a strong *DR5rev::GFP* signal at the lower hypocotyl side. The polar auxin transport is achieved by the polarly localized PIN efflux transporters (Wisniewska et al., 2006). The defective auxin distribution under PA treatment in gravitostimulated hypocotyls, suggests that PA would affect PIN3 subcellular polarity, the major player in shoot gravitropism (Rakusová et al., 2011, 2016, 2019). The direct evidence comes from the PIN3-GFP polarization observations under PA treatment or in *c4h* mutant after gravistimulation or following auxin treatment. PA treatment didn't affect gravity-induced PIN3 polarization, but inhibits auxin-mediated PIN3 polarization, resulting in a continuous accumulation of auxin at the lower side of the hypocotyl. As a consequence, hypocotyls are hyperbending. A similar PIN3 polarization defect was also observed in the *c4h* mutant. Together, these data support that PA and its target C4H play an essential role in modulating PIN3-polarization dependent auxin transport in gravity stimulated hypocotyls.

As the content of many products in phenylpropanoid pathway are changed in the *c4h* mutant (Vanholme et al., 2012), we then evaluated how the carbon flux over this pathway is redirected in hypocotyls upon PA treatment following gravity stimulation. To this end, we found 60 unique metabolites, differently accumulated upon PA treatment. Among the 60 compounds, we further confirmed that flavonoids act as downstream target of C4H during shoot gravitropism. Flavonoids have been reported as an endogenous auxin transport inhibitor, but its action differs from NPA (N-1-Naphthylphthalamic acid). The flavonoid biosynthesis mutants show defects in root gravitropism (Buer and Muday, 2004; Buer et al., 2013) probably due to a mis-localization of PIN proteins or changed PIN expression levels (Peer et al., 2004). Our profiling data shows that the flavonoid content is decreased upon PA treatment. In addition, the *c4h* mutant also shows a decreased flavonoid content (Vanholme et al., 2012). Furthermore, inhibition flavonoid biosynthesis resulting in a hyperbending hypocotyl with a defective auxin-mediated feedback on PIN3 repolarization. Complementary assay by exogenous application of quercetin showed that flavonoids act as downstream target

of *C4H* in hypocotyl gravitropism. Hence, our data showed that flavonoids act as downstream of *C4H* in hypocotyl gravitropism.

As proposed, flavonoid regulates PID and PP2A activity, which are essential players controlling PIN polarity by phosphorylation or de-phosphorylation PINs (Kuhn et al., 2017). Indeed, quercetin has been shown to bind to PID and reduce its activity (Henrichs et al., 2012). Decrease the content of flavonoids by PA treatment would lead to the change of PID-mediated PIN3 phosphorylation (Henrichs et al., 2012; Grones et al., 2018). Our binding assay further confirms that flavonoid binds to PID kinase. And *in vitro* kinase assay implies a shift of PID and PIN3 phosphorylation status upon PA treatment. Our *in vivo* assay also reveals that PA modulates PIN3 phosphorylation via regulating PID phosphorylation. However, we cannot exclude the possibility that PA also affects IAA-oxidase due to the reduced flavonoid content (Mathesius, 2001; Jansen et al., 2001) resulting in a shift of free IAA content in cells which will perturb the auxin effects on PIN polarity (Rakusová et al., 2016). On the other hand, PDKs (3-Phosphoinositide-Dependent Protein Kinases) also has been indicated to regulation PID activity (Armengot et al., 2016). In addition, other kinases also has been reported to affect PIN phosphorylation status or activity to maintain PIN polarity in particular developmental processes (Willige et al., 2013; Barbosa et al., 2016; Jia et al., 2016). Hence, we assume that PA may have effects on other kinases which may alter PIN polarization and polar auxin movement during hypocotyl gravitropism.

In conclusion, we demonstrate the crucial and novel physiological effect of PA on shoot gravitropism by inhibiting PIN-polarization dependent auxin transport. To our knowledge, PA is an example of various secondary metabolites that play essential roles in response to environmental factors by perturbing polar auxin transport.

2.4 Materials and Methods

Plant material and growth conditions

The following transgenic and mutant lines were used: Col-0, *PIN3::PIN3-GFP* (Col-0, Žádníková et al., 2010); *DR5rev::GFP* (Col-0, Friml et al., 2003); *PID::PID-YFP* (Col-0, Michniewicz et al., 2007); *c4h* (Col-0, GABI_753B06); *tt6-2* (Col-0, CS2105575). Mutant combinations with *PIN3::PIN3-GFP* were generated through genetic crosses. Seeds were sterilized and were sown on plates with half-strength Murashige and Skoof medium with 1% sucrose agar and stratified at 4°C for 3 days, and then cultivation at 21°C.

Gravity stimulation

To monitor hypocotyl gravitropic responses, plates with 3 days old etiolated seedlings were turned 90° and were scanned after 24 hours gravistimulation. Bending angles were measured by ImageJ with more than 30 seedlings (NIH; <http://rsb.info.nih.gov/ij>).

Chemical treatment for hypocotyl bending angle measurement

The piperonylic acid (PA, 20 μM), *trans*-cinnamic acid (*trans*-CA, 40 μM), *cis*-cinnamic acid (*cis*-CA, 40 μM) and salicylic acid (SA, 40 μM; Steenackers et al., 2016, 2017), *p*-iodobenzoic acid (*p*-IBA, 40 μM, Van de Wouwer et al., 2016), Coumarin (40 μM), *p*-coumaric acid (*p*-CA, 50 μM), phenylacetic acid (PAA, 40 μM), 5-(1,3-Benzodioxol-5-yl)-2,4-pentadienoic acid (PIA, 40 μM), Umbelliferone (40 μM), Scopoletin (40 μM), sodium diethyldithiocarbamate trihydrate (SDT, 5 μM, 10 μM, 20 μM, 40 μM, 60 μM; Sigma), quercetin (40 μM; Sigma), monolignols (coniferyl alcohol 50 μM; sinapyl alcohol 50 μM; Sigma) were used at indicated concentration. For bending assay, 3 days old etiolated hypocotyls were transferred to new plates with the chemicals or combinations at indicated concentration, then seedlings were gravity stimulated for 24 hours, bending angle was measured.

Chemical treatment for PIN3-GFP quantification

For gravity-induced PIN3-GFP localization, 3 days old etiolated hypocotyls were transferred onto new plates with DMSO, PA, quercetin, *p*-coumaric acid, SDT, monolignols or combinations at indicated concentration, then hypocotyls were gravity stimulated for 6 hours or 24 hours. The PIN3-GFP signal ratio was calculated between outer side of endodermal cells at lower and upper side of horizontally placed hypocotyls after gravity stimulation (Rakusová et al., 2019). For auxin-mediated PIN3-GFP localization, 3 days old etiolated hypocotyls were transferred onto new plates with DMSO, NAA (10 μM), PA, quercetin, *p*-CA and SDT, coniferyl alcohol and sinapyl alcohol combinations with NAA at the indicated concentration and

hypocotyls were incubated in darkness for 4 hours, then PIN3-GFP the ratio was calculated between inner and outer side of endodermal cells (Rakusová et al., 2019).

Flavonoid staining

3 days etiolated seedlings were transferred to new plates containing 20 μ M of PA, and the same amount of DMSO, or c4h mutant. The seedlings were kept in darkness for 24 hours with or with gravity stimulation. Then seedlings were stained with 2-aminoethyl diphenylborinate (DPBA, Sigma) for 15 minutes, and wash with water for 3 times. DPBA stock was prepared as described previous (Santelia et al., 2008). The GFP channel was selected to observe Kaempferol pattern in hypocotyls where we observe the PIN3-GFP localization at upper part of hypocotyls (Rakusová et al., 2019). The fluorescence intensity was quantified using ImageJ.

Microscopy

The *DR5rev::GFP*, PIN3-GFP or flavonoid staining was captured after gravity stimulation or auxin treatment by using an inverted Zeiss LSM-700 or LSM-800 microscope. For any single experiment, the settings were the same.

Phenolic profiling analysis by UHPLC-MS

In brief, 3 days old etiolated seedlings were transferred onto new plates with DMSO or 20 μ M of PA with or without 24 hours gravity stimulation. Seedlings were collected and phenolic profiling analysis was performed using UHPLC-MS as described previously (Steenackers et al., 2016). The data analysis was performed as described previously (Steenackers et al., 2016).

***In vivo* PIN3 phosphorylation**

PIN3::PIN3-GFP seedlings were grown on plates with DMSO, 20 μ M of PA, 40 μ M of quercetin, PA together with quercetin for 7 days. The whole plants were collected for phosphorylation assay. Samples were ground with liquid nitrogen, then protein extraction buffer (50 mM Tris-HCl, pH = 7.5; 1 protease inhibitor and 1 phosStop pill (Roche), 150 mM NaCl) was added and mixed well. Samples were centrifuged at 16000 g, for 20 minutes at 4 °C. The supernatant was removed and the sediment were re-suspended with detergent buffer (50 mM Tris-HCl, pH = 7.5; 150 mM NaCl, 1 protease inhibitor and 1 phosStop pill (Roche); 0.5% Triton-100; 0.5% NP40) and mixed well. The re-suspended samples were centrifuged at 13000 g, for 20 minutes at 4 °C. The supernatant was collected and protein level was determined with Bio-Rad Bradford reagent. 300 μ g of protein was incubated with 50 μ l of anti-GFP beads (MACS Molecular) for 1 hour to concentrate the PIN3 protein. Next, protein samples were mixed with preheated elution buffer at 95 °C, and loaded to Bio-Rad mini protean gel (10 %). After

electrophoresis, proteins were transferred to the PVDF membrane using Bio-Rad turbo transfer pack. Membrane was incubated with anti-GFP HRP antibody (MACS Molecular, 1:1000) over night at 4 °C to visualize the PIN3 protein in all treatment. For phosphorylation assay, the same membrane was incubated with the Phos-tag biotin antibody (1: 1000, BTL-111, Wako) at least 2 hours at room temperature. HRP activity was detected by the Supersignal Western Detection Reagents (Thermo Scientific) and imaged with a GE Healthcare Amersham 600RGB system.

***In vivo* PID phosphorylation assay**

PID::PID-YFP seedlings were grown on plates with DMSO, 20 µM of PA, 40 µM of quercetin, PA together with quercetin for 7 days. The whole plants were collected for phosphorylation test. Samples were ground with liquid nitrogen, then protein extraction buffer was added as described for *PIN3::PIN3-GFP* phosphorylation. 300 µg of PID protein was incubated with 50 µl of anti-GFP beads (MACS Molecular) for 90 minutes to concentrate the PID protein. Next, protein samples were mixed with preheated elution buffer at 95 °C, and loaded to Bio-Rad mini protean gel (10 %) or 12.5 % phostag gel (Wako). After electrophoresis, proteins were transferred to the PVDF membrane using Bio-Rad turbo transfer pack or wet transfer. Membrane was incubated with anti-GFP HRP antibody (MACS Molecular, 1:1000) over night at 4 °C to visualize the PID protein in all treatment. HRP activity was detected by the Supersignal Western Detection Reagents (Thermo Scientific) and imaged with a GE Healthcare Amersham 600RGB system.

Recombinant protein expression and purification

The pET28a-PIN3HL and pET28a-PID was expressed in *E. coli*. Strain BL21 (DE3) and protein expression was induced by adding 1 mM IPTG (Isopropyl β-D-1-Thiogalactopyranoside, 16°C, 12 h) to the cultured cells. The protein was purified using His Pur™ Ni-NTA Resin (Thermo Fisher) following the instructions. The purified protein was stored at 4°C for further analysis.

Drug Affinity Responsive Target Stability (DARTS) assay

The DARTS assay to test the binding of flavonoid to PID was performed as previously reported (Kania et al., 2018). The 7 days old *PID::PID-YFP* seedlings were used for total protein extraction. The sample were ground in liquid nitrogen, re-suspended in protein extraction buffer (25 mM Tris-HCl, pH 7.5; 150 mM NaCl; 0.1% IGEPAL CA-630, Roche cComplete protease, and one phosStop) with a 1:2 (w/v) ratio, and spun down to discard the cell debris. After quantifying the protein concentration (Quick Start™ Bradford Reagent, Bio-Rad), the cell

lysate was aliquoted and incubated with 0, 50 μM or 500 μM quercetin respectively for 30 min at 25°C, mixing at a low speed. The treated extracts or *E. coli* expressed PID protein were further aliquoted, and mixed with different concentrations of Pronase (Roche) in Pronase buffer (25 mM Tris-HCl, pH 7.5; 150 mM NaCl). After incubation at 25°C for 30 min, the proteolytic digestion was terminated by adding protease inhibitor cocktail (cOmplete, Roche) and the samples were kept on ice for 10 min. The protein samples were then analysed by Western blot. PID protein was detected by an anti-GFP HRP antibody (MACS Molecular, 1:1000) or anti-His antibody (1:600). HRP activity was detected by the Supersignal Western Detection Reagents (Thermo Scientific) and imaged with a GE Healthcare Amersham 600RGB system.

***In vitro* PID kinase activity assay**

10 μl of purified PID-His and PIN3HL protein or the mixture of both protein was incubated with DMSO, 10 μM of quercetin, and 20 μM PA with 100 μM ATP kinase buffer or without ATP for 1 hour at room temperature. Then the kinase assay was performed following the ADP-Glo kit instructions (ADP-Glo™ kinase Assay kit, Promega; Zegzouti et al., 2009). The Spectrophotometer Biotek SynergyH1 platereader was used to measure the luminescence.

Statistical analysis

Values that significantly differ from each other are indicated in figures according to Student's t-test, ** $P < 0.05$ or *** $P < 0.01$.

Author Contributions:

H. H. and J. F. conceived the project, designed the experiments, analyzed data; L. R. helped the PIN3 and PID phosphorylation assay; I. V. performed DARTS assay; S. T. provided the expression vectors of His-PID and His-PIN3HL; B. S. helped the flavonoid assay; B.V. and W.B. provided the chemicals, *c4h* mutant seed, helpful discussions, and performed the UHPLC-MS experiment and analyzed data. H. H. and J. F. wrote the article with all inputs from other authors.

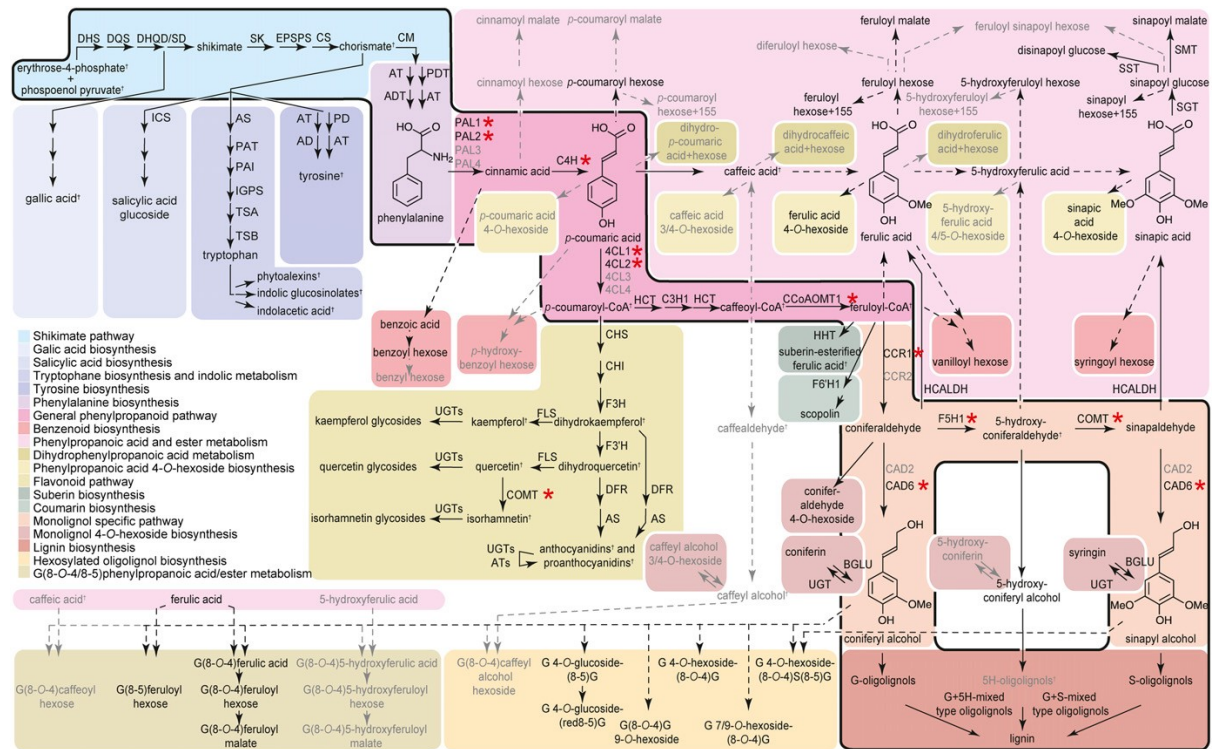
2.5 References

- Adamowski M, Friml J** (2015) PIN-dependent auxin transport: action, regulation, and evolution. *The Plant Cell* 27: 20- 32.
- Armengot L, Marquès-Bueno MM, Jaillais Y** (2016) Regulation of polar auxin transport by protein and lipid kinases. *J Exp Bot* 67: 4015-4037
- Brown DE, Rashotte AM, Murphy AS, Normanly J, Tague BW, Peer WA, Taiz L, Muday GK** (2001) Flavonoids act as negative regulators of auxin transport in vivo in *Arabidopsis*. *Plant Physiology* 126: 524- 535.
- Buer CS, Muday GK** (2004) The *transparent testa4* mutation prevents flavonoid synthesis and alters auxin transport and the response of *Arabidopsis* roots to gravity and light. *The Plant Cell* 16: 1191- 1205.
- Buer CS, Kordbacheh F, Truong TT, Hocart CH, Djordjevic MA** (2013) Alteration of flavonoid accumulation patterns in *transparent testa* mutants disturbs auxin transport, gravity responses, and imparts long-term effects on root and shoot architecture. *Planta* 238: 171- 189.
- Barbosa IC, Shikata H, Zourelidou M, Heilmann M, Heilmann I, Schwechheimer C** (2016) Phospholipid composition and a polybasic motif determine D6 PROTEIN KINASE polar association with the plasma membrane and tropic responses. *Development* 143: 4687- 4700.
- Barbosa IC, Hammes UZ, Schwechheimer C** (2018) Activation and polarity control of PIN-FORMED auxin transporters by phosphorylation. *Trends in Plant Science* 23: 523- 538.
- Dixon RA, Paiva NL** (1995) Stress-induced phenylpropanoid metabolism. *The Plant Cell* 7: 1085.
- Doyle SM, Rigal A, Grones P, Karady M, Barange DK, Majda M, et al** (2019) A role for the auxin precursor anthranilic acid in root gravitropism via regulation of PIN-FORMED protein polarity and relocalisation in *Arabidopsis*. *New Phytologist* 223:1420-1432.
- Forkmann G, Stotz G** (1981) Genetic control of flavanone 3-hydroxylase activity and flavonoid 3'-hydroxylase activity in *Antirrhinum majus* (Snapdragon). *Zeitschrift für Naturforschung C* 36: 411- 416.
- Forkmann G, Stotz G.** (1984) Selection and characterisation of flavanone 3-hydroxylase mutants of *Dahlia*, *Streptocarpus*, *Verbena* and *Zinnia*. *Planta* 161: 261- 265.
- Friml J, Wiśniewska J, Benková E, Mendgen K, Palme K** (2002) Lateral relocation of auxin efflux regulator PIN3 mediates tropism in *Arabidopsis*. *Nature* 415: 806.
- Grones P, Abas M, Hajný J, Jones A, Waidmann S, Kleine-Vehn J, Friml J** (2018) PID/WAG-mediated phosphorylation of the *Arabidopsis* PIN3 auxin transporter mediates polarity switches during gravitropism. *Scientific Reports* 8: 10279.
- Henrichs S, Wang B, Fukao Y, Zhu J, Charrier L, Bailly A, Oehring SC, Linnert M, Weiwad M, Endler A, Nanni P, Pollmann S, Mancuso S, Schulz A, Geisler M** (2012) Regulation of ABCB1/PGP1-catalysed auxin transport by linker phosphorylation. *The EMBO Journal* 31: 2965- 2980.
- Han H, Rakusová H, Verstraeten I, Zhang Y, Friml J** (2020) SCFTIR1/AFB auxin signaling for bending termination during shoot gravitropism. *Plant Physiology* 183: 37-40.
- Jansen M A, van den Noort RE, Tan MA, Prinsen E, Lagrimini LM, Thorneley RN** (2001) Phenol-oxidizing peroxidases contribute to the protection of plants from ultraviolet radiation stress. *Plant Physiology* 126: 1012- 1023.
- Jia W, Li B, Li S, Liang Y, Wu, Ma M, Wang J, Cao J, Zhang Y, Wang Y, Li J, Wang Y** (2016) Mitogen-activated protein kinase cascade MKK7-MPK6 plays important roles in plant

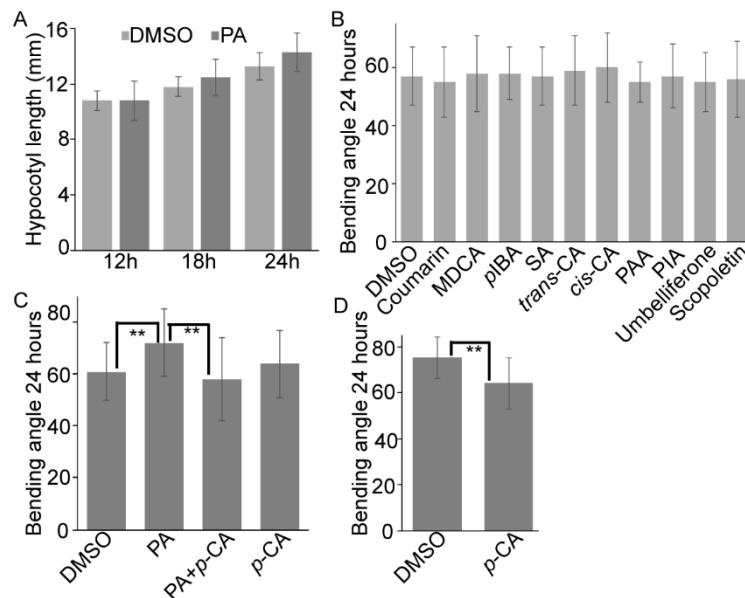
- development and regulates shoot branching by phosphorylating PIN1 in *Arabidopsis*. PLoS Biology 14: e1002550.
- Kuhn BM, Nodzyński T, Errafi S, Bucher R, Gupta S, Aryal B, Dobrev P, Bigler L, Geisler M, Zažímalová E, Friml J, Ringli C** (2017) Flavonol-induced changes in PIN2 polarity and auxin transport in the *Arabidopsis thaliana rol1-2* mutant require phosphatase activity. Scientific Reports 7: 41906.
- Kurepa J, Shull TE, Karunadasa SS, Smalle JA** (2018) Modulation of auxin and cytokinin responses by early steps of the phenylpropanoid pathway. BMC Plant Biology 18: 278.
- Kania U, Nodzyński T, Lu Q, Hicks GR, Nerinckx W, Mishev K, et al** (2018) The Inhibitor Endosidin 4 Targets SEC7 Domain-Type ARF GTPase Exchange Factors and Interferes with Subcellular Trafficking in Eukaryotes. The Plant Cell 30: 2553-2572.
- Karlsson R, Michaelsson A, Mattsson L** (1991) Kinetic analysis of monoclonal antibody-antigen interactions with a new biosensor based analytical system. Journal of Immunological Methods 145: 229-240.
- Lomenick B, Hao R, Jonai N, Chin RM, Aghajan M, Warburton S, et al** (2009) Target identification using drug affinity responsive target stability (DARTS). Proceedings of the National Academy of Sciences 106: 21984-21989.
- Mathesius U** (2001) Flavonoids induced in cells undergoing nodule organogenesis in white clover are regulators of auxin breakdown by peroxidase. Journal of Experimental Botany 52: 419- 426.
- Michniewicz M, Zago MK, Abas L, Weijers D, Schweighofer A, Meskiene I, et al.** (2007) Antagonistic regulation of PIN phosphorylation by PP2A and PINOID directs auxin flux. Cell 130: 1044-1056.
- Mierziak J, Kostyn K, Kulma A** (2014) Flavonoids as important molecules of plant interactions with the environment. Molecules 19: 16240- 16265.
- Mehmood A, Hussain A, Irshad M, Hamayun M, Iqbal A, Rahman H, Tawab A, Ahmad A, Ayaz S** (2019) Cinnamic acid as an inhibitor of growth, flavonoids exudation and endophytic fungus colonization in maize root. Plant Physiology and Biochemistry 135: 61- 68.
- Naseer S, Lee Y, Lapierre C, Franke R, Nawrath C, Geldner N** (2012) Casparian strip diffusion barrier in *Arabidopsis* is made of a lignin polymer without suberin. Proceedings of the National Academy of Sciences USA 109: 10101- 10106.
- Peer WA, Bandyopadhyay A, Blakeslee JJ, Makam SN, Chen RJ, Masson PH, Murphy AS** (2004) Variation in expression and protein localization of the PIN family of auxin efflux facilitator proteins in flavonoid mutants with altered auxin transport in *Arabidopsis thaliana*. The Plant Cell 16: 1898- 1911.
- Rakusová H, Gallego-Bartolomé J, Vanstraelen M, Robert HS, Alabadí D, Blázquez MA, Benková E, Friml, J** (2011) Polarization of PIN3-dependent auxin transport for hypocotyl gravitropic response in *Arabidopsis thaliana*. The Plant Journal 67: 817- 826.
- Schalk M, Cabello-Hurtado F, Pierrel MA, Atanassova R, Saindrenan P, Werck-Reichhart, D** (1998) Piperonylic acid, a selective, mechanism-based inactivator of the trans-cinnamate 4-hydroxylase: a new tool to control the flux of metabolites in the phenylpropanoid pathway. Plant Physiology 118: 209- 218.
- Santelia D, Henrichs S, Vincenzetti V, Sauer M, Bigler L, Klein M, Bailly A, Lee Y, Friml J, Geisler M, Martinoia E** (2008) Flavonoids redirect PIN-mediated polar auxin fluxes during root gravitropic responses. Journal of Biological Chemistry 283: 31218- 31226.

- Schilmiller AL, Stout J, Weng JK, Humphreys J, Ruegger MO, Chapple C** (2009) Mutations in the cinnamate 4-hydroxylase gene impact metabolism, growth and development in *Arabidopsis*. *The Plant Journal* 60: 771- 782.
- Steenackers W, Cesarino I, Klíma P, Quareshy M, Vanholme R, Corneillie S, Kumpf RP, Van de Wouwer D, Ljung K, Goeminne G, Novák O, Zažímalová E, Napier R, Boerjan W, Vanholme B** (2016) The allelochemical MDCA inhibits lignification and affects auxin homeostasis. *Plant Physiology* 172: 874- 888.
- Steenackers W, Klíma P, Quareshy M, Cesarino I, Kumpf RP., Corneillie, S., Araújo P, Viaene T, Goeminne G, Nowack MK, Ljung K, Friml J, Blakeslee JJ, Novák O, Zažímalová E, Napier R, Boerjan W, Vanholme B** (2017) *cis*-Cinnamic acid is a novel, natural auxin efflux inhibitor that promotes lateral root formation. *Plant Physiology* 173: 552- 565.
- Vanholme R, Storme V, Vanholme B, Sundin L, Christensen JH, Goeminne G, Halpin C, Rohde A, Morreel K, Boerjan W** (2012) A systems biology view of responses to lignin biosynthesis perturbations in *Arabidopsis*. *The Plant Cell* 24: 3506- 3529.
- Van de Wouwer D, Vanholme R, Decou R, Goeminne G, Audenaert D, Nguyen L, Höfer R, Pesquet E, Vanholme B, Boerjan W** (2016) Chemical genetics uncovers novel inhibitors of lignification, including p-iodobenzoic acid targeting CINNAMATE-4-HYDROXYLASE. *Plant Physiology* 172: 198- 220.
- Wisniewska J, Xu J, Seifertová D, Brewer PB, Ruzicka K, Blilou I, Rouquié D, Benková E, Scheres B, Friml J** (2006) Polar PIN localization directs auxin flow in plants. *Science* 312: 883-883.
- Willige BC, Ahlers S, Zourelidou M, Barbosa IC, Demarsy E, Trevisan M, Davis PA, Roelfsema MR, Hangarter R, Fankhauser C, Schwechheimer C** (2013) D6PK AGCVIII kinases are required for auxin transport and phototropic hypocotyl bending in *Arabidopsis*. *The Plant Cell* 25: 1674-1688.
- Zegzouti H, Zdanovskaia M, Hsiao K, & Goueli SA** (2009) ADP-Glo: a bioluminescent and homogeneous ADP monitoring assay for kinases. *Assay and Drug Development Technologies* 7: 560-572.
- Žádníková P, Petrášek J, Marhavý P, Raz V, Vandenbussche F, Ding Z, Schwarzerová K, Morita MT, Tasaka M, Hejátko J, Van Der Straeten D, Friml J, Benková E** (2010) Role of PIN-mediated auxin efflux in apical hook development of *Arabidopsis thaliana*. *Development* 137: 607- 617.
- Zegzouti H, Anthony RG, Jahchan N, Bögre L, Christensen SK** (2006) Phosphorylation and activation of PINOID by the phospholipid signaling kinase 3-phosphoinositide-dependent protein kinase 1 (PDK1) in *Arabidopsis*. *Proc Natl Acad Sci USA* 103: 6404-6409

2.6 Supplementary Figures



Supplementary Figure S1. The map of the phenylpropanoid pathway in plants. The map was referred to Vanholme et al., 2012.



Supplementary Figure S2. PA effects on hypocotyl bending is independent of CA.

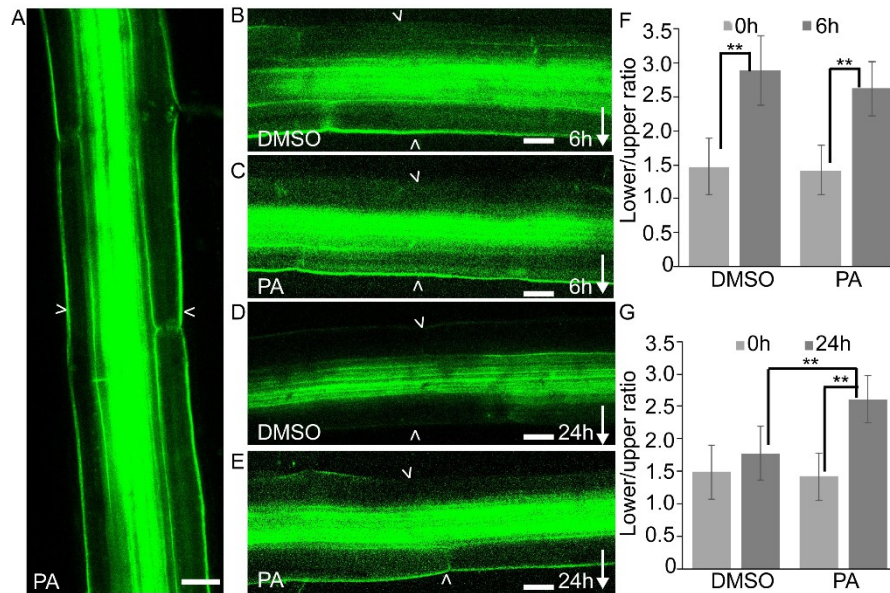
(A) Quantification of hypocotyl length upon DMSO and PA treatment.

(B) Quantification of bending angle of wild type hypocotyls upon 40 μ M of DMSO, Coumarin, MDCA, *p*IBA, SA, *trans*-CA, *cis*-CA, PAA, PIA, Umbelliferone, Scopoletin treatment.

(C) Combined effects of *p*-CA and PA on hypocotyl bending in wild type.

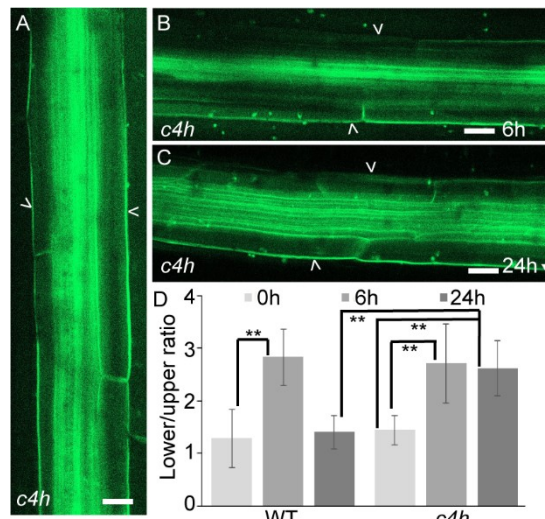
(D) Quantification of bending angle upon *p*-CA treatment in *c4h* mutant.

Data are means \pm SD, $n = 30 - 40$. ** $P < 0.05$ determined by Students t-test.



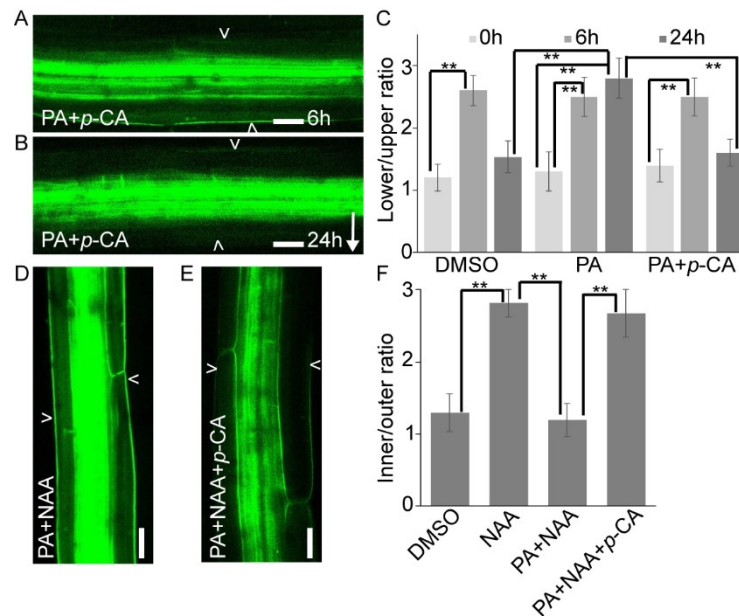
Supplementary Figure S3. PA doesn't affect gravity-induced PIN3 polarization.

(A- E) Confocal images of PIN3-GFP localization upon PA treatment without gravity stimulation (A), 6 hours gravity stimulation upon DMSO treatment (B) and PA treatment (C); 24 hours gravity stimulation upon DMSO treatment (D) and PA treatment (E). (F - G) Quantification of PIN3-GFP signal of wild type hypocotyls upon PA treatment after 6 hours (F) or 24 hours (G) gravity stimulation. The PIN3-GFP signal ratio was calculated at outer side of endodermal cells between lower and upper hypocotyl side. Data are means \pm SD, $n = 15$, $** P < 0.05$ determined by Students t-test. Scale bars = 20 μm . Arrowheads indicate PIN3-GFP at outer side of endodermal cells. Arrow indicates gravity direction.



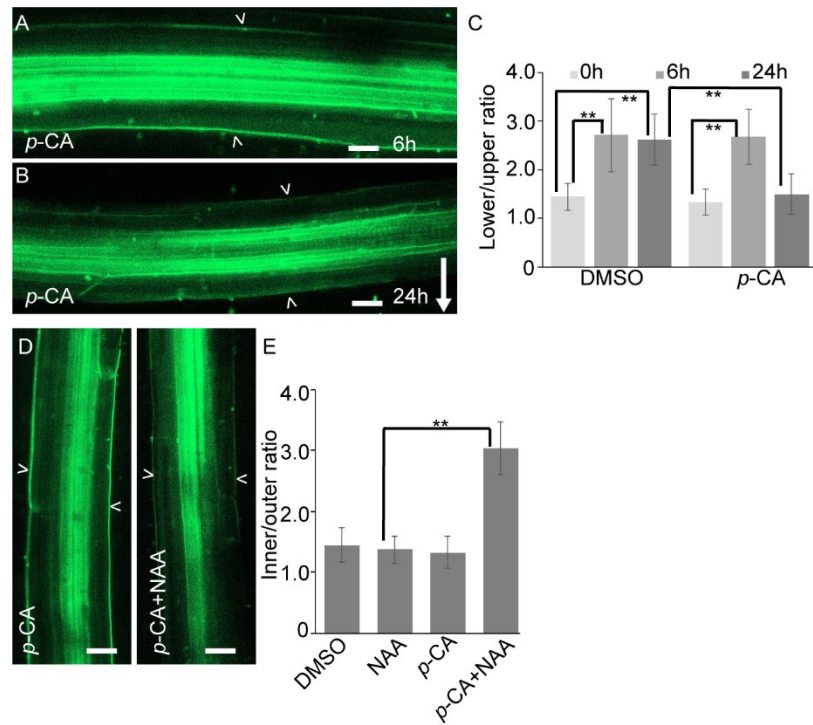
Supplementary Figure S4. Normal gravity-induced PIN3 polarization in *c4h* mutant.

(A - C) Confocal images of PIN3-GFP localization in *c4h* mutant without gravity stimulation (A), 6 hours (B) or 24 hours (C) gravity stimulation. (D) Quantification of PIN3-GFP signal after 6 hours or 24 hours gravity stimulation in *c4h* mutant. The PIN3-GFP signal ratio was calculated at outer side of endodermal cells between lower and upper hypocotyl side. Data are means \pm SD, $n = 15$, $** P < 0.05$ determined by Students t-test. Scale bars = 20 μm . Arrowheads indicate PIN3-GFP at outer side of endodermal cells. Arrow indicates gravity direction.



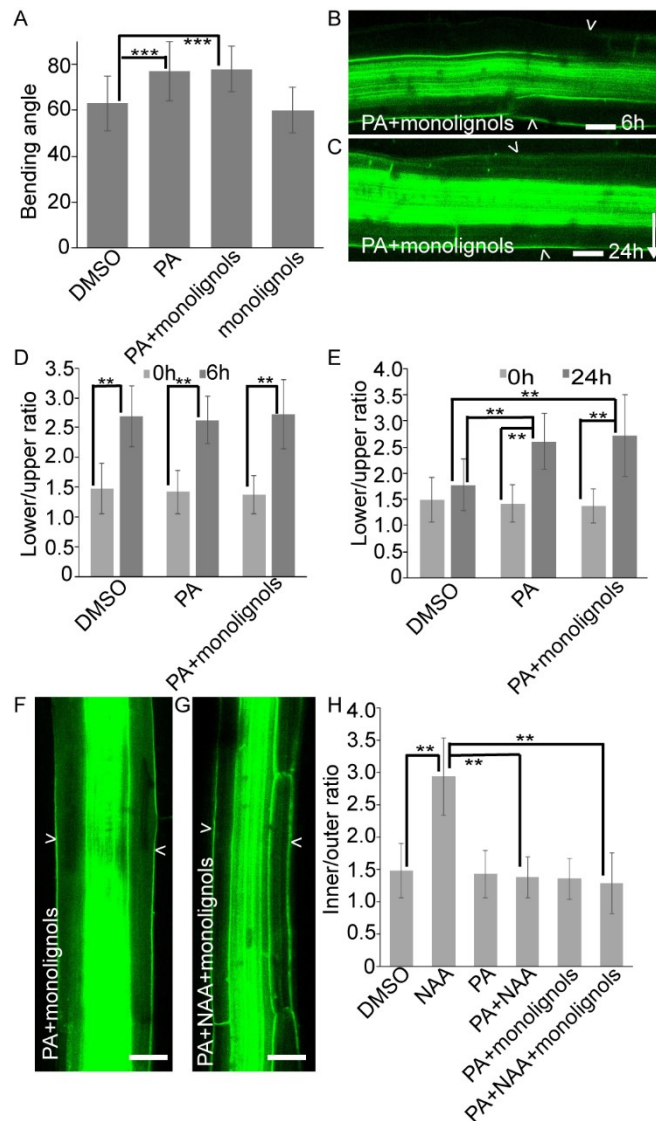
Supplementary Figure S5. *p*-CA rescues defective auxin-mediated PIN3 polarization upon PA treatment.

(A - B) Combined effect of *p*-CA and PA on PIN3-GFP localization after 6 hours (A) and 24 hours (B) gravity stimulation. (C) Quantification of PIN3-GFP upon PA and *p*-CA co-treatment after 6 hours or 24 hours gravity stimulation. The ratio was calculated at outer side of endodermal cells between lower and upper hypocotyl side. (D - E) Confocal images of PIN3-GFP localization under *p*-CA and NAA treatment (D) and under co-treatment with *p*-CA, PA, and NAA. (F) Quantification of PIN3-GFP upon PA, NAA, and *p*-CA co-treatment. The ratio was calculated between inner and outer side of endodermal cells. Data are means \pm SD, $n = 15$, ** $P < 0.05$ determined by Students t-test. Scale bars = 20 μm . Arrowheads indicate PIN3-GFP at outer side of endodermal cells. Arrow indicates gravity direction.



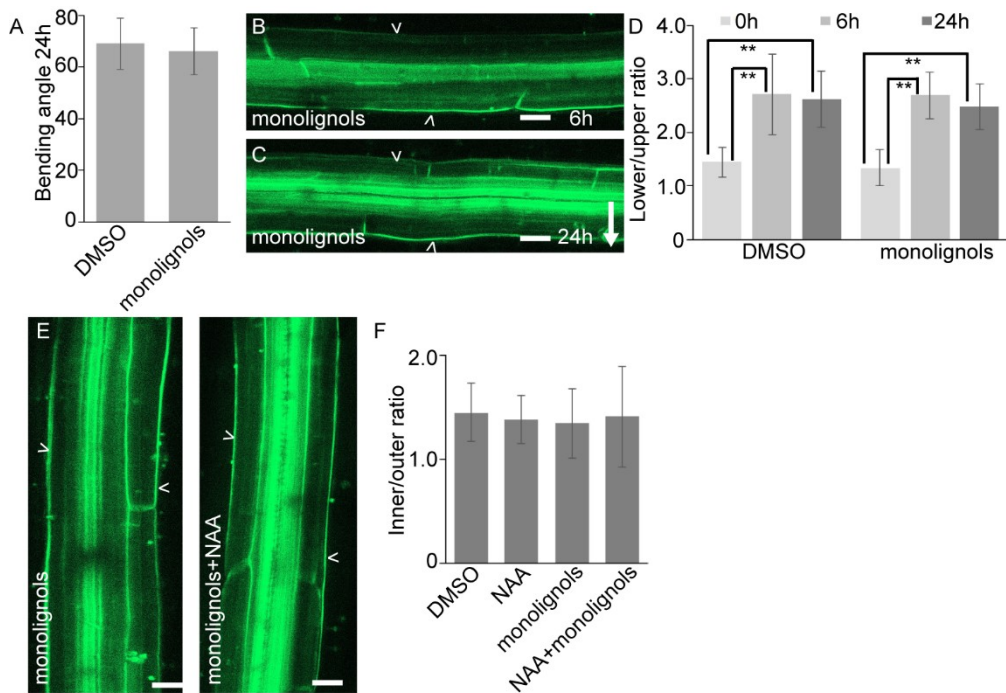
Supplementary Figure S6. *p*-CA rescues defective auxin-mediated PIN3 polarization in *c4h* mutant.

(A - B) Effect of *p*-CA on PIN3-GFP localization after 6 hours (A) and 24 hours (B) gravity stimulation in *c4h* mutant. (C) Quantification of PIN3-GFP signal upon *p*-CA treatment after 6 hours or 24 hours gravity stimulation in *c4h* mutant. The ratio was calculated at outer side of endodermal cells between lower and upper hypocotyl side. (D) Combined effect of *p*-CA and NAA on PIN3-GFP localization in *c4h* mutant. (E) Quantification of PIN3-GFP under *p*-CA and NAA co-treatment in *c4h* mutant. The ratio was calculated between inner and outer side of endodermal cells. Data are means



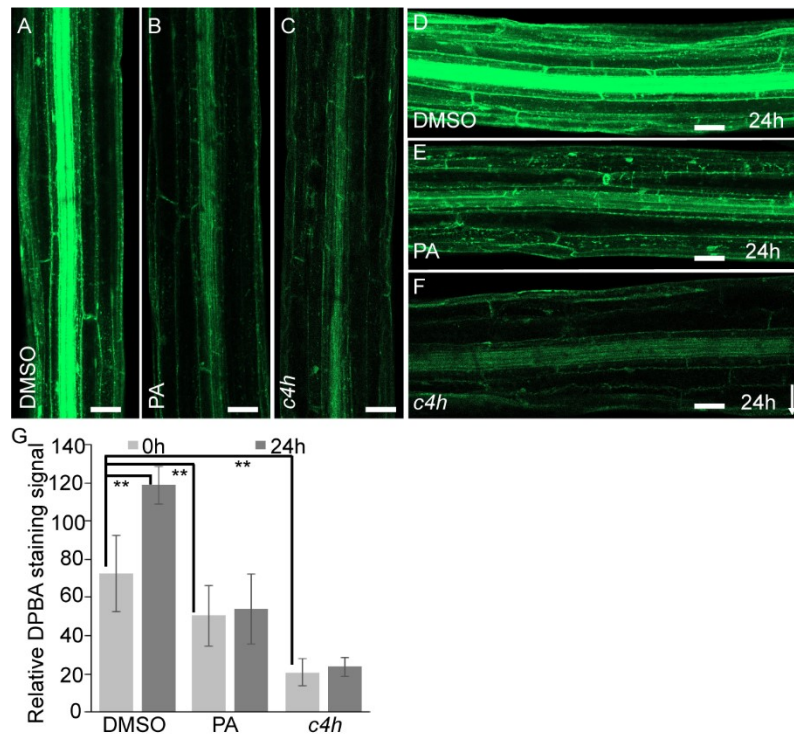
Supplementary Figure S7. Lignin perturbation is not the basis for PA effects on hypocotyl bending and PIN3 polarization.

(A) Combined effect of monolignols (50 μ M of each coniferyl alcohol and sinapyl alcohol) and PA on wild type hypocotyl bending. Bending angle was measured after 24 hours gravity stimulation. Data are means \pm SD, $n = 30 - 40$, *** $P < 0.01$ determined by Students t-test. (B - C) Combined effect of monolignols and PA on PIN3-GFP localization after 6 hours (B) and 24 hours (C) gravity stimulation. (D - E) Quantification of PIN3-GFP upon monolignols and PA treatment after 6 hours (D) and 24 hours (E) gravity stimulation. The ratio was calculated at outer side of endodermal cells between lower and upper hypocotyl side. Data are means \pm SD, $n = 15$, ** $P < 0.05$ determined by Students t-test. (F - G) Combined effect of monolignols, PA, NAA on PIN3-GFP localization. (H) Quantification of PIN3-GFP upon monolignols, PA, NAA treatment. The ratio was calculated between inner and outer side of endodermal cells. Data are means \pm SD, $n = 15$, ** $P < 0.05$ determined by Students t-test. Scale bars = 20 μ m. Arrowheads indicate PIN3-GFP at outer side of endodermal cells. Arrow indicates gravity direction.



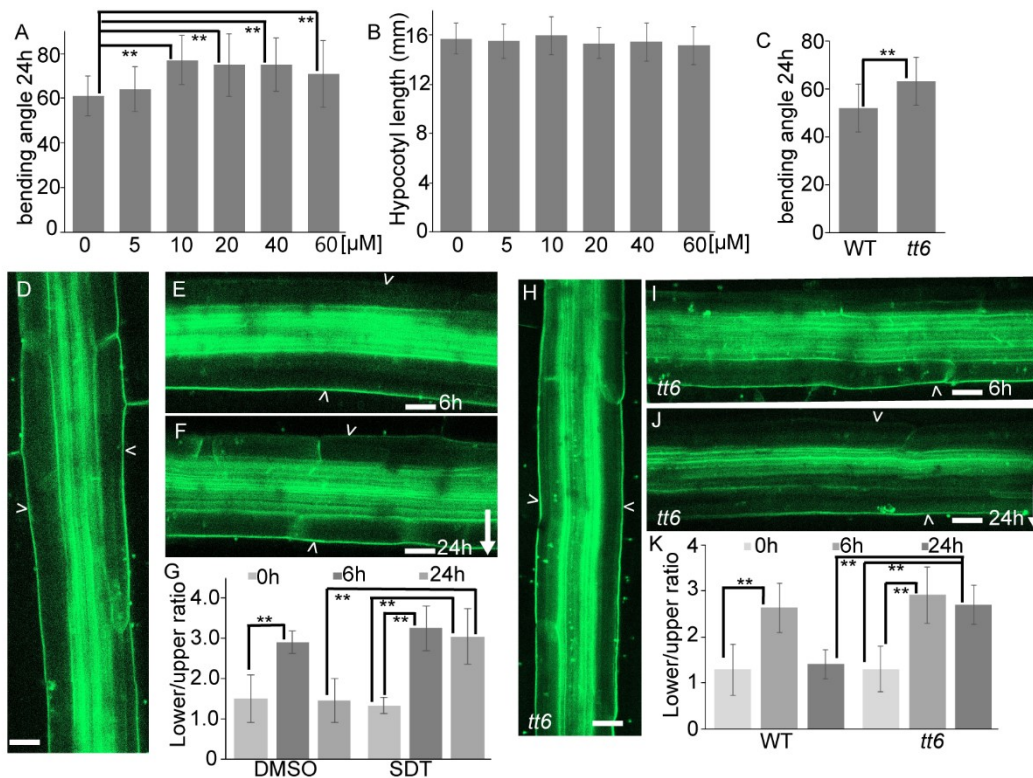
Supplementary Figure S8. Lignin perturbation is not the basis for the defective hypocotyl bending and PIN3 polarization in *c4h* mutant.

(A) Effects of monolignols on *c4h* mutant hypocotyl bending. Bending angle was quantified after 24 hours gravity stimulation. Data are means \pm SD, $n = 30 - 40$. (B - C) Effects of monolignols on PIN3-GFP localization in *c4h* mutant 6 hours gravity stimulation (B) and 24 hours gravity stimulation (C). (D) Quantification of PIN3-GFP signal upon monolignols treatment in *c4h* mutant after 6 hours or 24 hours gravity stimulation. The ratio was calculated at outer side of endodermal cells between lower and upper hypocotyl side. Data are means \pm SD, $n = 15$, $** P < 0.05$ determined by Students t-test. (E) Combined effects of monolignols and NAA on PIN3-GFP localization in *c4h* mutant. (F) Quantification of PIN3-GFP signal upon monolignols and NAA co-treatment in *c4h* mutant. The ratio was calculated between inner and outer side of endodermal cells. Data are means \pm SD, $n = 15$, $** P < 0.05$ determined by Students t-test. Scale bars = 20 μm . Arrowheads indicate PIN3-GFP at outer side of endodermal cells. Arrow indicates gravity direction.



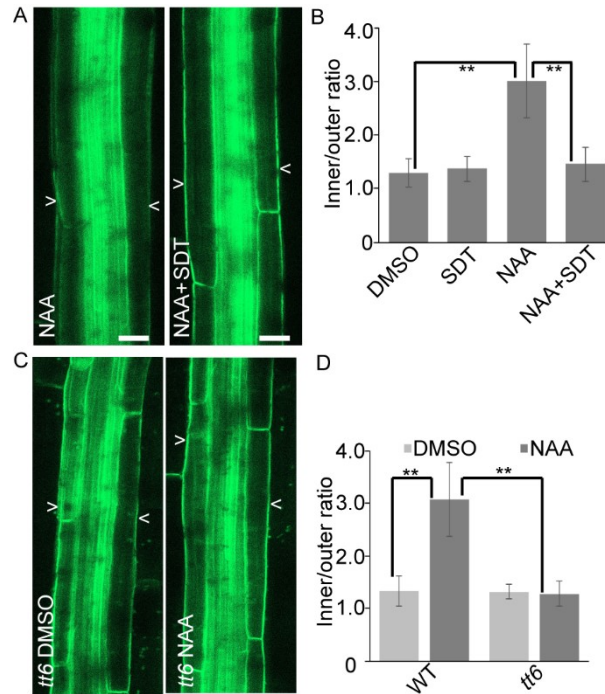
Supplementary Figure S9. PA treatment reduces flavonoid content in hypocotyl.

(A - C) Confocal images of showing flavonoid in hypocotyls under DMSO treatment (A), PA treatment (B) and in *c4h* mutant (C) without gravity stimulation. (D - F) Confocal images of showing flavonoid in hypocotyls under DMSO treatment (A), PA treatment (B) and in *c4h* mutant (C) after 24 hours gravity stimulation. (G) Quantification of flavonoid content in hypocotyls under DMSO and PA treatment, or in *c4h* mutant. Data are means \pm SD, n = 15, ** $P < 0.05$ determined by Students t-test. Scale bars = 20 μ m. Arrow indicates gravity direction.



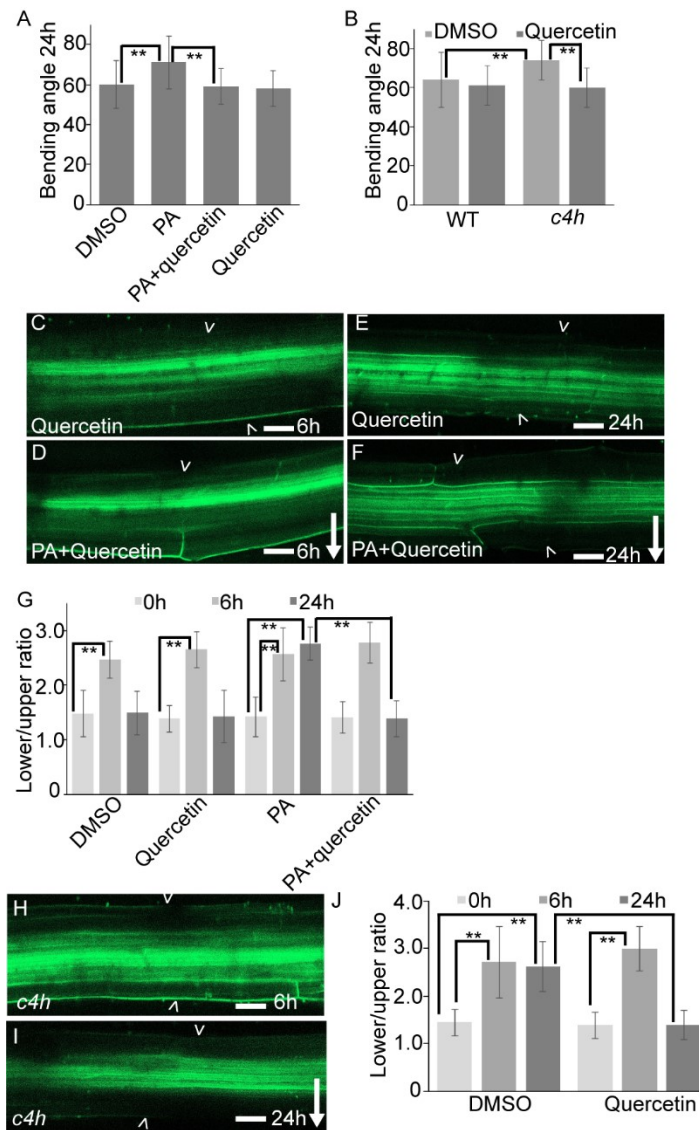
Supplementary Figure S10. Inhibition of flavonoid biosynthesis doesn't affect gravity-induced PIN3 polarization.

(A) Quantification of SDT effect on wild type hypocotyl bending after 24 hours gravity stimulation. Data are means \pm SD, $n = 30 - 40$, $** P < 0.05$ determined by Students t-test. (B) Quantification of SDT effect on hypocotyl growth. Data are means \pm SD, $n = 30 - 40$. (C) Quantification of hypocotyl bending in *tt6* mutant after 24 hours gravity stimulation. Data are means \pm SD, $n = 30 - 40$, $** P < 0.05$ determined by Students t-test. (D - F) Effects of SDT on PIN3-GFP localization in wild type without gravity stimulation (D), 6 hours (E) or 24 hours (F) gravity stimulation. (G) Quantification of PIN3-GFP signal upon SDT treatment. PIN3-GFP intensity was calculated at outer side of endodermal cells between lower and upper side of hypocotyl. Data are means \pm SD, $n = 15$, $** P < 0.05$ determined by Students t-test. (H - J) PIN3-GFP localization in *tt6* mutant without gravity stimulation (H), 6 hours (I) and 24 hours (J) gravity stimulation. (K) Quantification of PIN3-GFP signal in *tt6* mutant. PIN3-GFP intensity was calculated at outer side of endodermal cells between lower and upper side of hypocotyl. Data are means \pm SD, $n = 15$, $** P < 0.05$ determined by Students t-test. Scale bars = 20 μm . Arrowheads depict PIN3-GFP at outer side of endodermal cells. Arrow indicates gravity direction



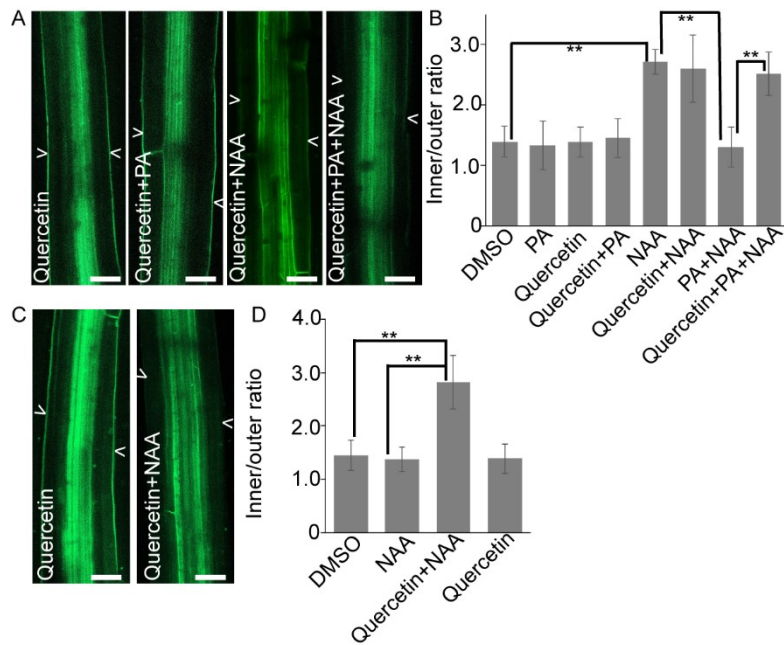
Supplementary Figure S11. Inhibition of flavonoid inhibits auxin-mediated PIN3 repolarization.

(A) Combined effects of NAA and SDT on PIN3-GFP localization. (B) Quantification of PIN3-GFP signal upon NAA and SDT co-treatment. PIN3-GFP intensity was calculated between inner and outer side of endodermal cells. Data are means \pm SD, n = 15, ** $P < 0.05$ determined by Students t-test. (C) PIN3-GFP localization in *tt6* mutant under DMSO and NAA treatment. (D) Quantification of PIN3-GFP signal upon DMSO and NAA treatment in *tt6* mutant. PIN3-GFP intensity was calculated between inner and outer side of endodermal cells. Data are means \pm SD, n = 15, ** $P < 0.05$ determined by Students t-test. Scale bars = 20 μ m. Arrowheads depict PIN3-GFP at outer side of endodermal cells.



Supplementary Figure S12. Flavonoid overcomes PA effects on hypocotyl bending and auxin-mediated PIN3 polarization.

(A) Combined effects of PA and quercetin on wild type hypocotyl bending after 24 hours gravity stimulation. Data are means \pm SD, $n = 30 - 40$, $** P < 0.05$ determined by Students t-test. (B) Effects of quercetin on hypocotyl bending in *c4h* mutant after 24 hours gravity stimulation. Data are means \pm SD, $n = 30 - 40$, $** P < 0.05$ determined by Students t-test. (C - F) Combined effects of quercetin and PA on PIN3-GFP localization after 6 hours (C, D) or 24 hours gravity stimulation (E, F). (G) Quantification of PIN3-GFP signal upon quercetin and PA co-treatment after 6 hours and 24 hours gravity stimulation. PIN3-GFP intensity was calculated at outer side of endodermal cells between lower and upper side of hypocotyl. Data are means \pm SD, $n = 15$, $** P < 0.05$ determined by Students t-test. (H - I) PIN3-GFP localization under quercetin treatment in *c4h* mutant after 6 hours (H) and 24 hours (I) gravity stimulation. (J) Quantification of PIN3-GFP signaling under quercetin treatment in *c4h* mutant after gravity stimulation. The PIN3-GFP intensity was calculated at outer side of endodermal cells between lower and upper side of hypocotyl. Data are means \pm SD, $n = 15$, $** P < 0.05$ determined by Students t-test. Scale bars = 20 μm . Arrowheads depict PIN3-GFP at outer side of endodermal cells. Arrow indicates gravity direction.



Supplementary Figure S13. Flavonoid overcomes PA effects on auxin-mediated PIN3 polarization.

(A) PIN3-GFP localization under quercetin treatment, quercetin and PA co-treatment, quercetin, PA and NAA co-treatment. (B) Quantification of PIN3-GFP signal under the co-treatment of PA, quercetin and NAA. The PIN3-GFP intensity was calculated between inner and outer side of endodermal cells. (C) PIN3-GFP localization under quercetin, and co-treatment with NAA in *c4h* mutant. (D) Quantification of PIN3-GFP signal under quercetin treatment in *c4h* mutant. The PIN3-GFP intensity was calculated between inner and outer side of endodermal cells. Data are means \pm SD, $n = 15$, ** $P < 0.05$ determined by Students t-test. Scale bars = 20 μ m. Arrowheads depict PIN3-GFP at outer side of endodermal cells.

3 SCF^{TIR1/AFB} auxin signaling for bending termination during shoot gravitropism

3.1 Introduction

Gravitropism is a plant adaptive response that involves asymmetric auxin distribution (Friml et al., 2002; Rakusová et al., 2015; Su et al., 2017). This auxin asymmetry leading to the shoot and root bending, is initiated by the gravity-induced subcellular relocalization of PIN auxin transporters (Friml et al., 2002; Kleine-Vehn et al., 2010; Rakusová et al., 2011). Bending termination is a much less characterized process, which depends on the re-establishment of the symmetrical auxin distribution due to auxin-mediated re-establishment of the symmetric PIN localization (Supplementary Figure S1A; Rakusová et al., 2016, 2019). Nonetheless, which auxin signaling pathway mediates this auxin feedback on PIN repolarization and bending termination is still unknown.

3.2 Results and discussion

To evaluate which auxin signaling machinery mediates auxin feedback on PIN3 repolarization for bending termination, we examined two most characterized auxin perception pathways: (i) the nuclear auxin receptors TIR1/AFB, which mediates both transcriptional and non-transcriptional responses (Salehin et al., 2015; Fendrych et al., 2016, 2018); and (ii) the AUXIN BINDING PROTEIN1 (ABP1) pathway with an unclear function (Gao et al., 2015; Grones et al., 2015). While *abp1* mutant showed a normal hypocotyl gravitropic response (Supplementary Figure S1B), the *tir1 afb2 afb3* triple hypocotyls were hyperbending (Figure 1A), suggesting a defect in termination response. Application of PEO-IAA that specifically interferes with auxin binding to TIR1 and inactivates TIR1 pathway (Hayashi et al., 2008), also triggered hypocotyl hyperbending (Figure 1B). The *HS::axr3-1* mutant carries a mutation in DII domain of the IAA17/AXR3 protein, a TIR1 co-receptor (Villalobos et al., 2012), and is conditionally expressed under a heat shock inducible promoter (Knox et al., 2003). The *HS::axr3-1* hypocotyls without heat shock induction displayed a normal gravitropic response (Supplementary Figure S1C); while after heat shock induction, *HS::axr3-1* hypocotyls were hyperbending (Figure 1C). These data collectively suggest that TIR1/AFB pathway is required for hypocotyl bending termination.

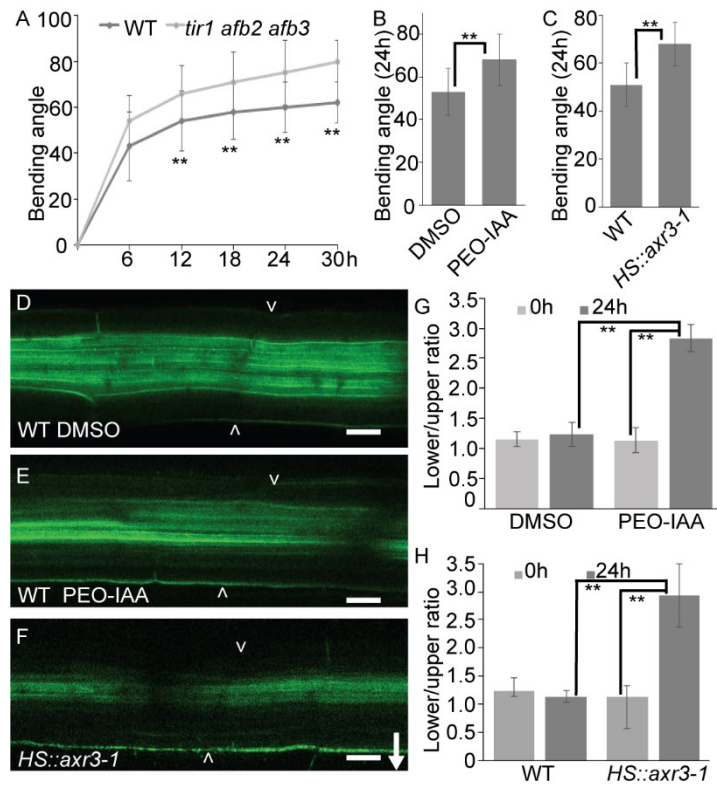


Figure 1. Hypocotyl gravitropic bending termination depends on TIR1/AFB signaling.

(A) Bending kinetics of wild type and *tir1afb2afb3* hypocotyls. (B) Bending angle of DMSO or 10 μ M PEO-IAA treated wild type hypocotyls after 24 hours gravistimulation. (C) Bending angle of heat shock induced *HS::axr3-1* hypocotyls after 24 hours gravistimulation. (D - F) PIN3-GFP localization after 24 hours gravistimulation. Wild type hypocotyls upon DMSO treatment (D) and 10 μ M PEO-IAA treatment (E), heat shock induced *HS::axr3-1* hypocotyls (F). (G - H) Quantification of PIN3-GFP intensity. PEO-IAA treated wild type hypocotyls after 24 hours gravistimulation (G); heat shock induced *HS::axr3-1* hypocotyls after 24 hours gravistimulation (H). The ratio was calculated by dividing the PIN3-GFP intensity at outer side of endodermal cells between lower and upper side of hypocotyls. Data and error bars represent the mean \pm SD. $n = 30 - 40$ for bending assay, $n = 15$ for PIN3-GFP intensity quantification. $** P < 0.05$ determined by Student's t-test. Arrowheads depict PIN3-GFP at outer side of endodermal cells, arrow indicates the gravity direction and hence determines lower and upper side of hypocotyl. Scale bar = 20 μ m.

Hypocotyl gravitropic bending is initiated by the sedimentation of amyloplasts in hypocotyl endodermal cells followed by the gravity-induced PIN3 polarization to the lower cell side (Fukaki et al., 1998; Rakusová et al., 2011). The bending termination involves the re-establishment of auxin-induced symmetrical PIN3 subcellular distribution at later stages (Supplementary Figure S1A; Rakusová et al., 2016, 2019). Therefore, we investigated these processes under conditions of compromised TIR1/AFB auxin signaling. Compromised TIR1/AFB pathway did not have any obvious impact on amyloplasts sedimentation in hypocotyl endodermal cells (Supplementary Figure S2). Next, we analyzed PIN3 polarization. Without gravity stimulation, PIN3-GFP is distributed symmetrically at both inner and outer side of hypocotyl endodermal cells in the wild type (Rakusová et al 2011), or in *HS::axr3-1* hypocotyls with or without heat shock induction (Supplementary Figure S3A, S3B). After 2

hours or 6 hours gravistimulation, PIN3-GFP polarized, as manifested by a stronger PIN3-GFP signal at lower sides of endodermal cells in wild type and *HS::axr3-1* hypocotyls with or without heat shock induction (Supplementary Figure S3C - S3H). Similarly, inhibition of TIR1/AFB auxin perception by PEO-IAA significantly affected the transcriptional auxin signaling in hypocotyls (Supplementary Figure S4A - S4B), but did not affect gravity-induced PIN3 polarization (Supplementary Figure S4C - S4H). Thus, steady state PIN3 localization and gravity-induced PIN3 polarization does not strongly depend on the TIR1/AFB signaling pathway.

We then investigated the involvement of TIR1/AFB pathway in the PIN3 repolarization at later stages of gravitropic response (Rakusová et al., 2016). After 24 hours gravity stimulation, PIN3-GFP repolarized to inner side of endodermal cells at the bottom side of the wild type hypocotyl (Figure 1D, 1G; Rakusová et al., 2016, 2019). In contrast, when TIR1/AFB pathway was inactivated by PEO-IAA or in the heat shock induced *HS::axr3-1* hypocotyls, we observed persistence of PIN3-GFP asymmetry, with strong signal at the lower side of hypocotyl endodermal cells (Figure 1E - 1H). As expected, we observed a normal PIN3-GFP polarization in the non-induced *HS::axr3-1* hypocotyls (Supplementary Figure S5A, S5B). These observations revealed an involvement of the TIR1/AFB auxin signaling in the re-establishment of symmetric PIN3 distribution during hypocotyl bending termination.

Exogenous auxin application also induces PIN3 inner-lateralization, similarly as observed at later stages of gravitropic response. As shown previously (Rakusová et al., 2016, 2019), PIN3-GFP relocated to inner side of endodermal cells after 4 hours of auxin (NAA) treatment (Figure 2A, 2B, 2H). In contrast, when TIR1/AFB pathway was inactivated by applying PEO-IAA, this relocation did not happen as evidenced by a strong PIN3-GFP signal at the outer side of endodermal cells (Figure 2C, 2H). Inactivation of TIR1/AFB pathway in the *HS::axr3-1* hypocotyls yielded the same result: in the heat shock induced hypocotyls, we observed a persisting PIN3-GFP signal at the outer side of endodermal cells after 4 hours NAA incubation (Supplementary Figure S6A, S6B, S6E); whereas it disappeared in *HS::axr3-1* hypocotyls without heat shock induction (Supplementary Figure S6C, S6D, S6F). This shows requirement of TIR1/AFB pathway for auxin-induced PIN3 relocation.

To test whether activation of TIR1/AFB is sufficient to mediate PIN3 relocation, we used an engineered convex-IAA/concave-TIR1 perception system (Uchida et al., 2018). For the concave TIR1 (ccvTIR1) and control TIR1 (cTIR1) auxin perception system, ccvTIR1 is less

sensitive to natural IAA, but binds to the synthetic cvxIAA, thus activating auxin response; whereas *cTIR1* is unable to bind to cvxIAA, thus not activating auxin response, but it responds normally to natural IAA. The *ccvTIR1* and *cTIR1* hypocotyls showed a normal gravity response and gravity-induced PIN3 polarization (Supplementary Figure S7A - S7H). The PIN3-GFP localization in *ccvTIR1* hypocotyls was normal (Figure 2D, 2I). IAA treatment induced PIN3-GFP repolarization to the inner side of endodermal cells in wild type hypocotyls (Figure 2I; Rakusová et al., 2016) as well as in *cTIR1* hypocotyls (Supplementary Figure S8A, S8B, S8D), however in the *ccvTIR1* hypocotyls the effect was less pronounced (Figure 2E, 2I). On the other hand, cvxIAA didn't induce PIN3-GFP repolarization to inner side of endodermal cells in the wild type (Figure 2F, 2J) or *cTIR1* hypocotyls (Supplementary Figure S8C, S8D) but induced strong PIN3-GFP repolarization to the inner side of endodermal cells in *ccvTIR1* hypocotyls (Figure 2G, 2J). These results show that a specific activation of the TIR1/AFB pathway is sufficient to repolarize PIN3 in hypocotyl endodermis (Figure 2K).

In conclusion, we demonstrate that genetic or chemical interference with TIR1/AFB signaling interferes with auxin-mediated re-establishment of symmetric PIN3 polarization during gravitropic response, leading to shoot overbending. Similarly, TIR1/AFB signaling is required for auxin-mediated PIN3 re-polarization. Furthermore, activation of TIR1 pathway using synthetic cvxIAA-*ccvTIR1* pair is sufficient to induce PIN3 re-polarization. Collectively, these observations reveal the essential role of SCF^{TIR1/AFB} auxin signaling pathway in mediating auxin feedback on auxin transport directionality for bending termination during plant adaptive development.

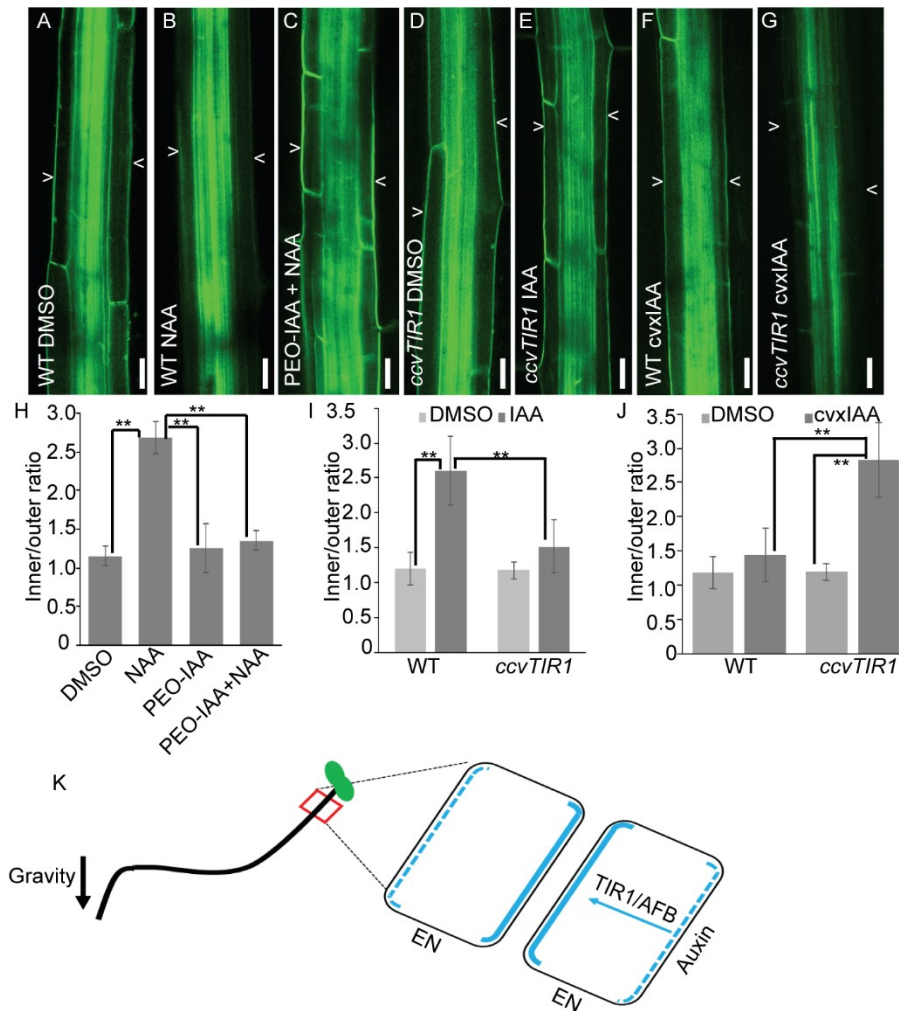


Figure 2. TIR1/AFB signaling mediates auxin feedback on PIN3 repolarization.

(A - G) PIN3-GFP localization in DMSO treated wild type hypocotyls (A), 10 μ M NAA treated wild type hypocotyls (B), 10 μ M PEO-IAA and 10 μ M NAA co-treated wild type hypocotyls (C), DMSO treated *ccvTIR1* hypocotyls (D), 10 μ M IAA treated *ccvTIR1* hypocotyls (E), 10 μ M cvxIAA treated wild type hypocotyls (F), 10 μ M cvxIAA treated *ccvTIR1* hypocotyls (G). (H - J) Quantification of PIN3-GFP intensity. Wild type hypocotyls treated with PEO-IAA (H); IAA treated *ccvTIR1* hypocotyls (I); cvxIAA treated *ccvTIR1* hypocotyls (J). The ratio was calculated by dividing the PIN3-GFP intensity at inner and outer side of hypocotyl endodermal cells. Data and error bars represent the mean \pm SD. N = 15, ** $P < 0.05$ determined by Student's test. Arrowheads depict PIN3-GFP at outer side of endodermal cells. Scale bar = 20 μ m. (K) Schematic diagram of auxin receptor TIR1/AFB mediated PIN3 repolarization for hypocotyl bending termination. At later stage of shoot gravitropism (24 hours), TIR1/AFB mediates auxin perception facilitates the repolarization of PIN3 to inner side of endodermal cells at the lower hypocotyl side, to equalize auxin distribution and thus terminate the hypocotyl bending. EN: endodermal cells; blue lines indicate PIN3 distribution at endodermal cells; blue arrow indicates auxin-TIR1/AFB mediated PIN3 repolarization from the outer side (blue dashed line) to inner side (blue solid line) at lower side hypocotyl endodermal cells; black arrow indicates gravity direction.

3.3 Materials and Methods

Plant material

Plant material used was as follows: Col-0, *PIN3::PIN3-GFP* (Col-0 background) (Žádníková et al., 2010), *DR5rev::GFP* (Col-0, Friml et al., 2003), *abp1-c1* (Col-0) and *abp1-TD1*(SK21825, Col-4) (Gao et al., 2015), *HS::axr3-1* (Col-0, Knox et al., 2003), *ccvTIR1* and *cTIR1* (*tir1-1 afb2-3*, Uchida et al., 2018). *HS::ax3-1*, *ccvTIR1* and *cTIR1* mutant combined with *PIN3::PIN3-GFP* were generated through genetic crosses.

Growth conditions

Seeds were grown on plates containing normal half-strength Murashige and Skoog medium and stratified at 4°C for 3 days. Plates were placed vertically in the growth room to induce germination under light for 16 hours, and then plates were covered by aluminum foil and kept growing at 21°C for 3 days. Light sources used were Philips GreenPower LED production modules combined with deep red (660 nm) / far red (720 nm) / blue (455 nm), with a photon density of about 140 $\mu\text{mol m}^{-2} \text{s}^{-1}$.

Hypocotyl gravitropic bending assay

For gravity stimulation, 3-day-old etiolated seedlings were turned 90 degree, and plates were scanned (EPSON V700) at the indicated time or after 24 hours. The bending angle was measured using ImageJ. The wild type and *HS::axr3-1* seedlings were both heat shock induced at 37°C or not induced at room temperature for 40 minutes as described previously (Fendrych et al., 2016). After heat shock induction, the same plates were turned 90 degree for 24 hours and bending angle was measured.

PEO-IAA treatment for *DR5rev::GFP* quantification in hypocotyl

3-day-old etiolated *DR5rev::GFP* seedlings were pretreated with 10 μM PEO-IAA or the same amount of DMSO for 5 hours in darkness, then the seedlings were transferred to new plates supplied with 10 μM NAA for another 2 hours in darkness. *DR5rev::GFP* signal in hypocotyl was captured and quantified.

PEO-IAA treatment for bending assay and *PIN3-GFP* quantification

For bending assay, 3-day-old etiolated wild type seedlings were pretreated with 10 μM PEO-IAA or DMSO for 2 hours, then the same plates were turned 90 degree for 24 hours, bending angle was measured. For *PIN3-GFP* quantification, wild type seedlings were pretreated with 10 μM PEO-IAA or DMSO for 5 hours, then the same plates were turned 90 degree for 2 hours, 6 hours or 24 hours, subsequently the *PIN3-GFP* localization in hypocotyl endodermal cells

was captured and GFP signal intensity was quantified. For the co-treatment with auxin, wild type seedlings pretreated with PEO-IAA or DMSO for 2 hours, the pretreated seedlings were transferred to new plates supplied with 10 μ M NAA and 10 μ M PEO-IAA or same amount of DMSO for another 4 hours in darkness, then PIN3-GFP localization in hypocotyl endodermal cells was detected immediately and GFP signal intensity was quantified.

Quantification of PIN3-GFP in *HS::axr3-1* hypocotyls as well as *ccvTIR1* and *cTIR1* hypocotyls
3-day-old etiolated wild type and *HS::axr3-1* seedlings were both incubated at 37°C for heat shock induction or at room temperature without induction for 40 minutes (Fendrych et al., 2016). 4 hours after induction, seedlings were gravistimulated for 2 hours, 6 hours and 24 hours, PIN3-GFP localization in hypocotyl endodermal cells was captured and GFP signal intensity was quantified. For auxin treatment, heat shock induced or non-induced wild type and *HS::axr3-1* seedlings were transferred to new plates with 10 μ M NAA or same amount of DMSO for another 4 hours in darkness, then PIN3-GFP localization in hypocotyl endodermal cells was captured, GFP signal intensity was quantified.

Similarly, 3-day-old etiolated wild type, *ccvTIR1*, *cTIR1* seedlings were gravistimulated for 6 hours or 24 hours respectively, then PIN3-GFP localization in hypocotyl endodermal cells was captured, GFP signal intensity was quantified. For auxin-induced PIN3-GFP quantification, 3-days-old etiolated wild type, *ccvTIR1* and *cTIR1* hypocotyls were transferred to new plates with DMSO, 10 μ M IAA or 10 μ M cvxIAA, respectively. Then seedlings were incubated in darkness for 4 hours, PIN3-GFP localization in hypocotyl endodermal cells was captured, and GFP signal intensity was quantified.

Amyloplasts sedimentation analysis

3-day-old etiolated seedlings were treated with DMSO, PEO-IAA, NAA, and cvx-IAA or heated shock induced as described above, subsequently seedlings were gravity stimulated for 10 minutes, 30 minutes, 1 hour, and 2 hours or without gravity stimulation. The seedlings were fixed with FAA solution (10% formaldehyde, 5% acetic acid and 50% ethanol; Fukaki et al., 1998) at 4°C overnight. After fixation, seedlings were rinsed in 50% ethanol three times, and then seedlings were stained with Lugol solution (Sigma-Aldrich) for 15 minutes in darkness. Seedlings were mounted on slides with clearing solution (chloral hydrate : glycerol : water (8:1:2, W:V:V)) for 2 hours at room temperature and then the images were captured by OLYMPUS BX53 microscopy.

Microscopy

All the confocal images were obtained by LSM 700 or LSM 800 inverted microscopy (Zeiss, <http://www.zeiss.com>). All the confocal experiments were performed in the dark to avoid any light effects on PIN3 polarization. In any single experiment, the settings were identical for all samples.

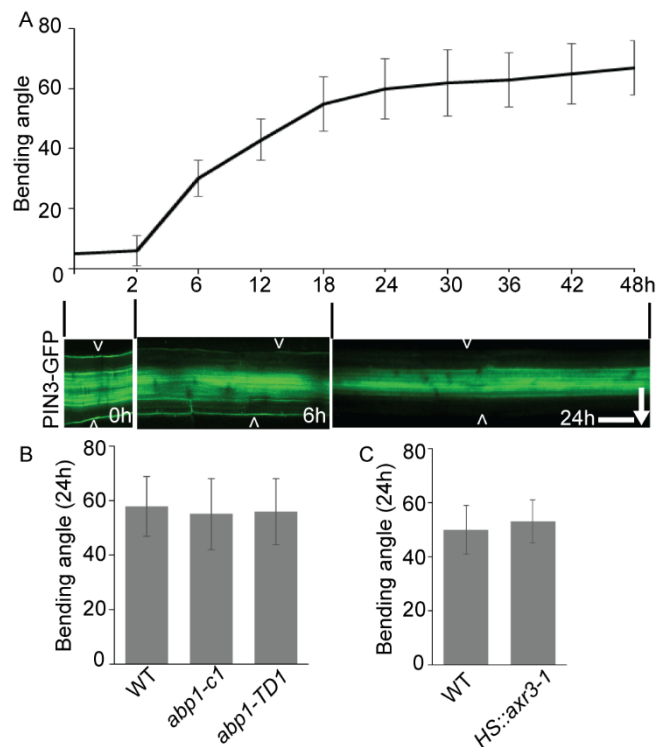
Quantitation of PIN3-GFP intensity

All measurements were performed using ImageJ software. For the quantification of PIN3-GFP polarization, the intensity of PIN3-GFP at endodermal cells was measured (Rakusová et al., 2019). After gravity stimulation, the ratio was calculated between the outer side of endodermal cells at lower and the upper side of horizontally placed hypocotyls (Rakusová et al., 2019). For auxin and co-treatment with other chemicals, the ratio was calculated between the inner side and outer side of endodermal cells (Rakusová et al., 2019). In all cases, at least 15 hypocotyls were measured and the ratio was calculated from the mean.

3.4 References

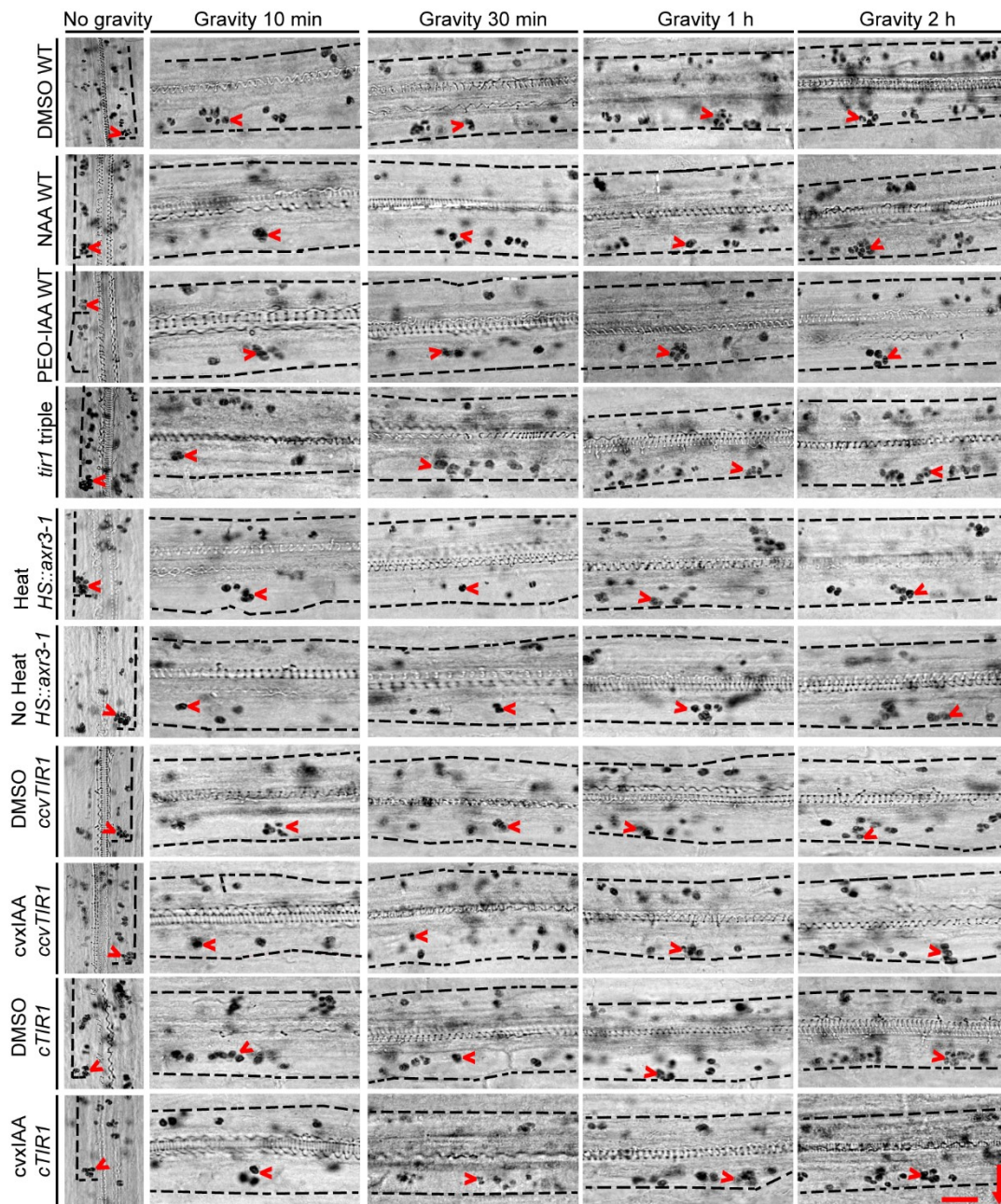
- Fukaki H, Wysocka-Diller J, Kato T, Fujisawa H, Benfey PN, Tasaka M** (1998) Genetic evidence that the endodermis is essential for shoot gravitropism in *Arabidopsis thaliana*. *Plant Journal* 14: 425-430
- Friml J, Wiśniewska J, Benková E, Mendgen K, Palme K** (2002) Lateral relocation of auxin efflux regulator PIN3 mediates tropism in *Arabidopsis*. *Nature* 415: 806
- Fendrych M, Leung J, Friml J** (2016) TIR1/AFB-Aux/IAA auxin perception mediates rapid cell wall acidification and growth of *Arabidopsis* hypocotyls. *elife* 5: e19048
- Fendrych M, Akhmanova M, Merrin J, Glanc M, Hagihara S, Takahashi K, Uchida N, Torii KU, Friml, J** (2018) Rapid and reversible root growth inhibition by TIR1 auxin signalling. *Nat Plants* 4: 453
- Gao Y, Zhang Y, Zhang D, Dai X, Estelle M, Zhao Y** (2015) Auxin binding protein 1 (ABP1) is not required for either auxin signaling or *Arabidopsis* development. *Proc Natl Acad Sci USA* 112: 2275-2280
- Grones P, Chen X, Simon S, Kaufmann WA, De Rycke R, Nodzyński T, et al** (2015) Auxin-binding pocket of ABP1 is crucial for its gain-of-function cellular and developmental roles. *J Exp Bot* 66: 5055-5065.
- Hayashi KI, Tan X, Zheng N, Hatate T, Kimura Y, Kepinski S, Nozaki H** (2008) Small-molecule agonists and antagonists of F-box protein–substrate interactions in auxin perception and signaling. *Proc Natl Acad Sci USA* 105: 5632-5637
- Knox K, Grierson CS, Leyser O** (2003) AXR3 and SHY2 interact to regulate root hair development. *Development* 130: 5769-5777
- Kleine-Vehn J, Ding Z, Jones AR, Tasaka M, Morita MT, Friml J** (2010) Gravity-induced PIN transcytosis for polarization of auxin fluxes in gravity-sensing root cells. *Proc Natl Acad Sci USA* 107: 22344-22349
- Rakusová H, Gallego-Bartolomé J, Vanstraelen M, Robert HS, Alabadí D, Blázquez MA, Benková E, Friml J** (2011) Polarization of PIN3-dependent auxin transport for hypocotyl gravitropic response in *Arabidopsis thaliana*. *Plant J* 67: 817-826
- Rakusová H, Fendrych M, Friml J** (2015) Intracellular trafficking and PIN-mediated cell polarity during tropic responses in plants. *Curr Opin Plant Biol* 23: 116-123
- Rakusová H, Abbas M, Han H, Song S, Robert HS, Friml J** (2016) Termination of shoot gravitropic responses by auxin feedback on PIN3 polarity. *Curr Biol* 26: 3026-3032
- Rakusová H, Han H, Valošek P, Friml J** (2019) Genetic screen for factors mediating PIN polarization in gravistimulated *Arabidopsis thaliana* hypocotyls. *Plant J* 98:1048-1059
- Salehin M, Bagchi R, Estelle M.** (2015) SCF^{TIR1/AFB}-based auxin perception: mechanism and role in plant growth and development. *Plant Cell* 27: 9-19
- Su SH, Gibbs NM, Jancewicz AL, Masson PH** (2017) Molecular mechanisms of root gravitropism. *Curr Biol* 27: R964-R972
- Uchida N, Takahashi K, Iwasaki R, Yamada R, Yoshimura M, Endo T A, et al** (2018) Chemical hijacking of auxin signaling with an engineered auxin–TIR1 pair. *Nat Chem Biol* 14: 299
- Villalobos LIAC, Lee S, De Oliveira C, Ivetac A, Brandt W, Armitage L, et al** (2012) A combinatorial TIR1/AFB–Aux/IAA co-receptor system for differential sensing of auxin. *Nature Chem Biol* 8: 477.

3.5 Supplementary Figures



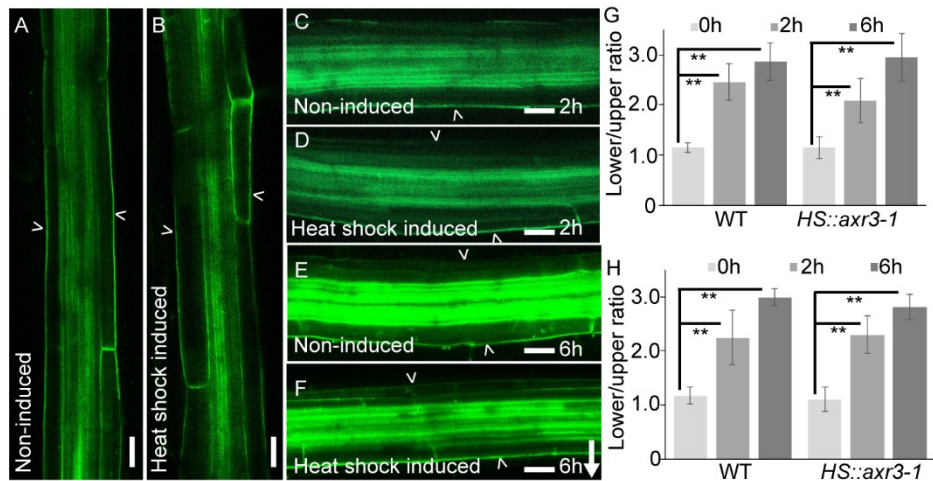
Supplementary Figure S1. *ABP1* is not involved in hypocotyl gravitropic bending termination.

(A) Time-line of wild type hypocotyls bending kinetics and PIN3 polarization events, data adapted from Rakusová et al. (2016). Arrowheads depict PIN3-GFP at outer sides of endodermal cells. Arrow indicates gravity direction. Scale bar = 20 μ m. (B) Bending angle of *abp1* hypocotyls after 24 hours gravistimulation. n = 30 - 40. (C) Bending angle of non-induced *HS::axr3-1* hypocotyls after 24 hours gravitimulation. n = 30 - 40.



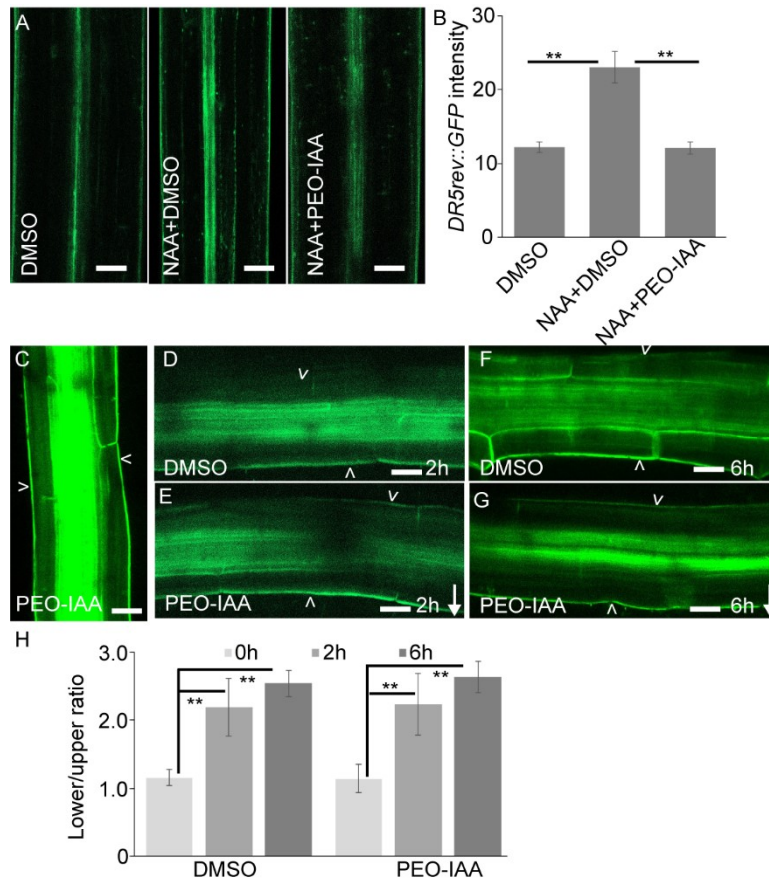
Supplementary Figure S2. Modification of TIR1/AFB pathway doesn't affect amyloplasts sedimentation in Arabidopsis hypocotyl endodermal cells.

3 days old etiolated wild type (WT, Col-0), *ccvTIR1*, *cTIR1* seedlings were transferred to new Arabidopsis medium plates supplied with DMSO, 10 μ M NAA, 10 μ M PEO-IAA, 10 μ M *cvxIAA*. Seedlings were gravity stimulated for 10 minutes, 30 minutes, 1 hour and 2 hours or without gravity stimulation. The heat-induced or non-induced *HS::axr3-1* seedlings were also gravity stimulated for 10 minutes, 30 minutes, 1 hour and 2 hours or without gravity stimulation. The amyloplast sedimentation in endodermal cells was observed. Arrowheads depict the amyloplast at endodermal cells. Arrow indicates gravity direction. Scale bar = 20 μ m.



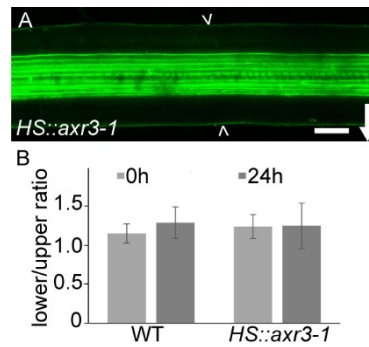
Supplementary Figure S3. Auxin-induced AUX/IAA protein degradation is not required for gravity-induced PIN3 polarization.

(A - B) PIN3-GFP localization in non-induced *HS::axr3-1* hypocotyls (A) and heat-shock induced *HS::axr3-1* hypocotyls (B) without gravity stimulation. (C - D) PIN3-GFP localization in non-induced *HS::axr3-1* hypocotyls (C) and heat shock induced *HS::axr3-1* hypocotyls (D) after 2 hours gravity stimulation. (E - F) PIN3-GFP localization in non-induced *HS::axr3-1* hypocotyls (E) and heat shock induced *HS::axr3-1* hypocotyls (F) after 6 hours gravity stimulation. (G - H) Quantification of PIN3-GFP intensity in non-induced *HS::axr3-1* hypocotyls (G) or heat shock induced *HS::axr3-1* hypocotyls (H) after 2 hours or 6 hours gravistimulation. The ratio was calculated by dividing the PIN3-GFP intensity at outer side of endodermal cells between lower and upper side of hypocotyls. Data and error bars represent the mean \pm SD. $n = 15$, ** $P < 0.05$ determined by Student's t-test. Arrowheads depict PIN3-GFP at outer sides of endodermal cells. Arrow indicates gravity direction. Scale bar = 20 μ m



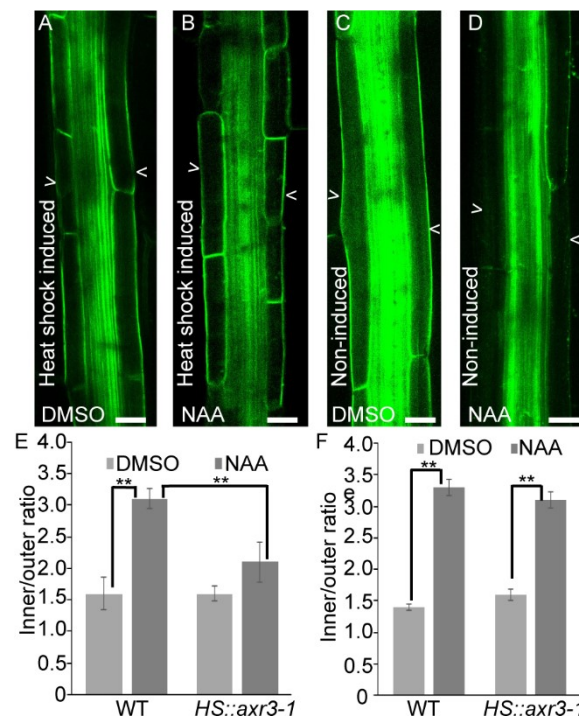
Supplementary Figure S4. Compromised TIR1/AFB signaling doesn't affect gravity-induced PIN3 polarization.

(A) *DR5rev::GFP* signal in hypocotyls upon DMSO treatment, 10 μ M NAA and DMSO co-treatment, 10 μ M NAA and 10 μ M PEO-IAA co-treatment. Scale bar = 20 μ m. (B) Quantification of *DR5rev::GFP* signal in hypocotyls. Data and error bars represent the mean \pm SD. $n = 15$, ** $P < 0.05$ determined by Student's t-test. (C) PIN3-GFP localization in non-gravity stimulated wild type hypocotyls upon 10 μ M PEO-IAA treatment. (D - E) PIN3-GFP localization in DMSO treated wild type hypocotyls (D), 10 μ M PEO-IAA treated wild type hypocotyls (E) after 2 hours gravity stimulation. (F - G) PIN3-GFP localization in DMSO treated wild type hypocotyls (F), 10 μ M PEO-IAA treated wild type hypocotyls (G) after 6 hours gravity stimulation. (H) Quantification of PIN3-GFP intensity in PEO-IAA treated wild type hypocotyls after 2 hours or 6 hours gravistimulation. The ratio was calculated by dividing the PIN3-GFP intensity at outer side of endodermal cells at the lower and upper side of hypocotyls. Data and error bars represent the mean \pm SD. $n = 15$, ** $P < 0.05$ determined by Student's t-test. Arrowheads depict PIN3-GFP at outer sides of endodermal cells. Arrow indicates gravity direction. Scale bar = 20 μ m.



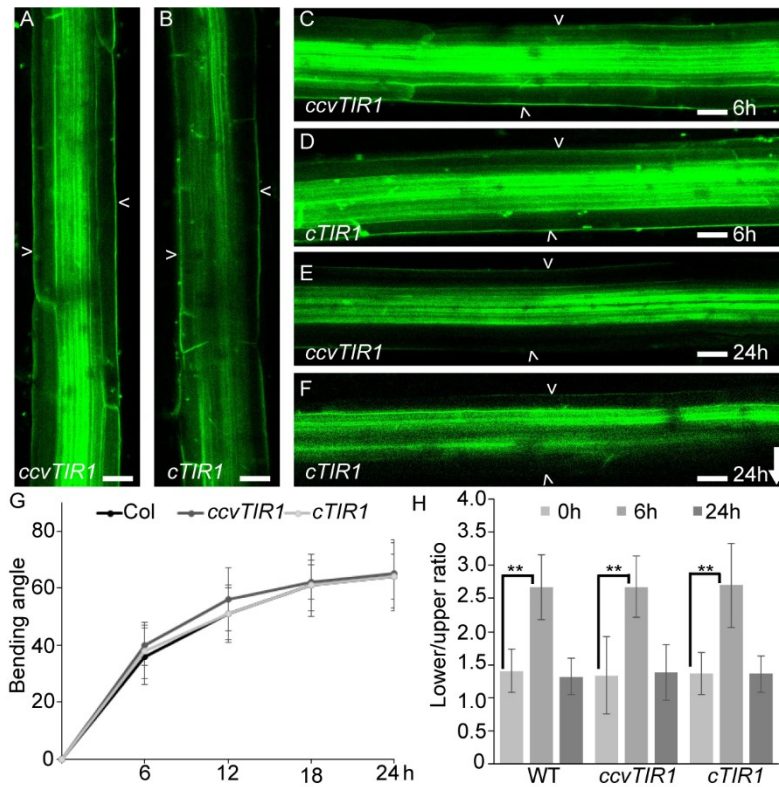
Supplementary Figure S5. Normal PIN3-GFP repolarization in non-induced *HS::axr3-1* hypocotyls after 24 hours gravity stimulation.

(A) PIN3-GFP localization in non-induced *HS::axr3-1* hypocotyls after 24 hours gravity stimulation. (B) Quantification of PIN3-GFP intensity in non-induced *HS::axr3-1* hypocotyls. The ratio was calculated by dividing the PIN3-GFP intensity at outer side of endodermal cells between lower and upper side of hypocotyls. Data and error bars represent the mean \pm SD. $n = 15$. Arrowheads depict PIN3-GFP at outer sides of endodermal cells. Arrow indicates gravity direction. Scale bar = 20 μ m.



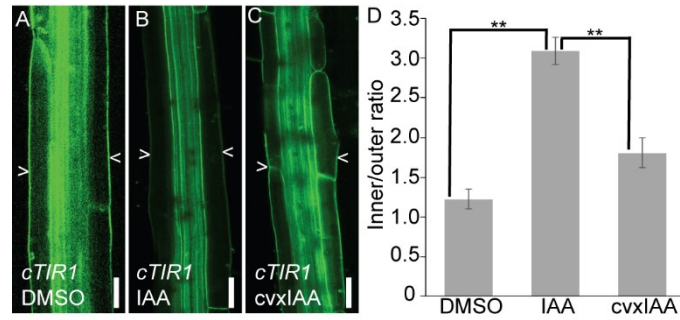
Supplementary Figure S6. Auxin-induced AUX/IAA protein degradation is required for auxin-mediated PIN3 repolarization.

(A - D) PIN3-GFP localization in DMSO or 10 μ M NAA treated heat shock induced *HS::axr3-1* hypocotyls (A - B); DMSO or NAA treated non-induced *HS::axr3-1* hypocotyls (C - D). (E - F) Quantification of PIN3-GFP intensity after 4 hours NAA treatment in heat shock induced *HS::axr3-1* hypocotyls (E) and non-induced *HS::axr3-1* hypocotyls (F). The ratio was calculated by dividing the PIN3-GFP intensity at inner and outer side of hypocotyl endodermal cells. Data and error bars represent the mean \pm SD. $n = 15$, ** $P < 0.05$ determined by Student's t -test. Arrowheads depict PIN3-GFP at outer side of endodermal cells. Scale bar = 20 μ m.



Supplementary Figure S7. Normal gravity response and gravity-induced PIN3 polarization in *ccvTIR1* and *cTIR1* hypocotyls.

(A - F) PIN3-GFP localization in non-gravity stimulated *ccvTIR1* hypocotyls (A) and *cTIR1* hypocotyls (B); PIN3-GFP in *ccvTIR1* hypocotyls (C) and *cTIR1* hypocotyls (D) after 6 hours gravity stimulation; PIN3-GFP in *ccvTIR1* hypocotyls (E) and *cTIR1* hypocotyls (F) after 24 hours gravity stimulation. (G) Quantification of bending kinetics of *ccvTIR1* and *cTIR1* hypocotyls. Data and error bars represent the mean \pm SD. $n = 30 - 40$ for bending assay. (H) Quantification of PIN3-GFP intensity after 6 hours and 24 hours gravistimulation in *ccvTIR1* and *cTIR1* hypocotyls. The ratio was calculated by dividing the PIN3-GFP intensity at outer side of endodermal cells at the lower and upper side of hypocotyls. Data and error bars represent the mean \pm SD. $n = 15$, $** P < 0.05$ determined by Student's t-test. Arrowheads depict PIN3-GFP at outer sides of endodermal cells. Arrow indicates gravity direction. Scale bar = 20 μ m.



Supplementary Figure S8. Normal auxin-induced PIN3 repolarization in *cTIR1* mutant.

(A - C) PIN3-GFP localization in DMSO treated *cTIR1* hypocotyls (A), 10 μ M IAA treated *cTIR1* hypocotyls (B) and 10 μ M cvxIAA treated *cTIR1* hypocotyls (C). (D) Quantification of PIN3-GFP intensity in *cTIR1* hypocotyls. The ratio was calculated by dividing the PIN3-GFP intensity at inner and outer side of hypocotyl endodermal cells. Data and error bars represent the mean \pm SD. n = 15, ** $P < 0.05$ determined by Student's t-test. Arrowheads depict PIN3-GFP at outer side of endodermal cells. Scale bar = 20 μ m.

4 Auxin-mediated rapid phosphorylation of myosin complex mediates polar auxin fluxes in *Arabidopsis* development

Huibin Han¹, Inge Verstraeten¹, Mark Roosjen², Jakub Hajný¹, Ewa Mazur³, Nikola Rýdza⁴, Dolf Weijers², Jiří Friml¹

¹ Institute of Science and Technology (IST) Austria, 3400 Klosterneuburg, Austria

² Laboratory of Biochemistry, Wageningen University, Stippeneng 4, 6708 Wageningen, the Netherlands.

³ Department of Cell Biology, Faculty of Biology and Environmental Protection, University of Silesia in Katowice, 40-032 Katowice, Jagiellońska 28, Poland

4.1 Introduction

The plant hormone auxin acts as a key regulator of plant development. It modulates plant growth and development by controlling multiple cellular processes. The complexity of auxin response is illustrated by the fact that numerous genes are controlled by auxin, and these auxin-responsive genes are differentially expressed across tissues and organs (Paponov et al., 2008; Salehin et al., 2015). Auxin regulates gene transcription through the canonical TIR1/AFB-Aux/IAA-ARF nuclear signaling pathway, and this pathway allows changes in transcription in response to auxin in a timeframe of 3 to 5 minutes (McClure et al., 1989; Abel and Theologis, 1996). However, there are recent demonstrations of rapid auxin actions depending on the TIR1/AFB receptor that are too fast to involve transcriptional regulation, such as the fast auxin-regulated root growth (Fendrych et al., 2018) or root hair elongation. Thus, TIR1/AFB auxin receptors, besides well-characterized mechanism of transcriptional regulation must have also a so far unknown non-transcriptional branch.

In addition, over decades of auxin research, there were repeated observations about rapid cellular auxin effects including plasma membrane hyperpolarization, H⁺-pump activation, cytosolic calcium or pH changes, protoplast swelling and others that were never connected to transcriptional responses or TIR1/AFB-Aux/IAA pathway (Badescu and Napier 2006). Prominent among those has been regulation of clathrin-mediated endocytosis by auxin as it clearly occurs independently of TIR1/AFB pathway and may serve as a part of feed-back mechanism between auxin and its intercellular flow (Paciorek et al., 2005; Robert et al., 2010). Also a newly identified auxin analogue, Pinstatic acid (PISA), does not require TIR1/AFB

receptors for its action, but still triggers distinct auxin responses including the effect on endocytosis and auxin transport (Oochi et al., 2019). All these observations show that a fast auxin response distinct from the well-studied nuclear TIR1/AFB-mediated mechanism exists and involves other, unknown modes of auxin perception (Paciorek et al., 2005; Robert et al., 2010; Gallei et al., 2020). The cell surface-localized TMK receptor-like kinases may contribute to this uncharacterized auxin signaling (Xu et al., 2014; Cao et al., 2019), but it remains uncertain and other knowledge on the mechanism of auxin perception and downstream cellular auxin effects is lacking.

Another essential level of regulation in auxin action is the directional auxin transport between cells (Vanneste and Friml, 2009). The establishment of auxin gradients and local maxima and minima in plant tissues (Vanneste and Friml, 2009) can be attributed to the local auxin biosynthesis (Morffy and Strader, 2020) and the directional, intercellular auxin transport (Adamowski and Friml, 2015). The directionality of auxin flow through tissues is achieved by the action of the PIN-FORMED (PIN) auxin efflux transporters and the polarity of their cellular localization at the plasma membrane (Petrášek et al., 2006; Wiśniewska et al., 2006). PIN polarization and abundance at plasma membrane depends on various vesicle transport-related processes, such as GNOM-mediated constitutive recycling and clathrin-mediated constitutive endocytosis (Geldner et al., 2001, 2003; Dhonukshe et al., 2007; Glanc et al., 2018), *de novo* secretion (Salanenska et al., 2018) and degradation in lytic vacuoles (Abas et al., 2006; Kleine-Vehn et al., 2008). Additionally, kinase-mediated PIN phosphorylation is also a key mechanism for PIN polarity or activity regulation (Zhang et al., 2010; Barbosa et al., 2018; Xiao and Offringa, 2020; Tan et al., 2020). The PIN-dependent auxin transport network and its subcellular dynamics have emerged as a prominent mechanism integrating multitude of endogenous (such as plant hormones) and exogenous (including light and gravity) signals and translating them into the auxin distribution-mediated development (Vanneste and Friml, 2009; Adamowski and Friml, 2015).

Auxin itself has an impact on PIN-mediated transport. A positive feedback between auxin signaling and transport directionality is a key pre-requisite of the so-called auxin canalization hypothesis (Sachs, 1981; Sauer et al., 2006; Wabnik et al., 2010, 2011). For this feedback regulation, auxin triggers coordinated PIN polarization to gradually establish directional auxin transport between source and sink tissue (Wabnik et al., 2010, 2011; Prát et al., 2018). Auxin canalization underlines several self-organizing processes, such as the vascular

strands formation (Sachs, 1981; Govindaraju et al., 2020), regeneration after wounding (Sauer et al., 2006; Mazur et al., 2016, 2020a, b), embryogenesis (Robert et al., 2013), shoot and root organogenesis (Benková et al., 2003; Heisler et al., 2005; Bhatia et al., 2016), and shoot gravitropic bending termination (Rakusová et al., 2016, 2019; Han et al., 2020). The genetic and cell biological studies suggested that auxin effect on PIN endocytic trafficking is central for canalization (Sauer et al., 2006; Paciorek et al., 2005; Robert et al., 2010; Zhang et al., 2020; Mazur et al., 2020a,b). Nonetheless, the auxin signaling and downstream cellular mechanism, by which auxin regulates both PIN polarity and subcellular trafficking crucial for the self-organizing canalization processes, still remains elusive.

Here, we applied a rapid phosphoproteomics approach to obtain components of the fast, non-transcriptional auxin responses. Among number of identified proteins that were rapidly phosphorylated in a TIR1/AFB-dependent and -independent manner, we further characterized the Myosin XI and MadB2 myosin binding proteins. We show that auxin-phosphorylation of the myosin complex is sufficient and crucial for auxin feedback on PIN auxin transporter trafficking and polarization ultimately involved in auxin canalization-mediated developmental processes such as flexible vasculature formation or regeneration. Overall, our study uncovers novel components of, so far elusive rapid auxin action and identifies a crucial part of the mechanism, by which auxin regulates its own transport during plant development.

4.2 Results

4.2.1 A novel and rapid phosphorylation response to auxin

Several responses to auxin occur within minutes or faster, and are too quick to be mediated by gene expression changes (Kubeš and Napier, 2019; Fendrych et al., 2018). For similarly rapid responses described for animal steroid hormones (Steinman and Trainor, 2010), or for osmotic stress in *Arabidopsis* (Stecker et al., 2014), changes in protein phosphorylation has been detected as prominent downstream signaling events. Therefore, we tested whether auxin can trigger rapid changes in protein phosphorylation. To maximize the depth of detecting phosphopeptides in plant extracts, we compared a number of protein extraction and phosphopeptide enrichment strategies. We found Filter-Aided Sample Preparation (FASP) to yield best results, identifying most proteins with the least co-purification of nucleic acids (Figure 1A; Supplementary Figures S1A – S1J). We next combined

FASP with various phosphopeptide enrichment strategies, and obtained superior recovery with magnetic Ti⁴⁺ beads, identifying nearly 1500 phosphopeptides from *Arabidopsis* root extracts (Supplementary Figures S1A, S1B, S1D). When compared with alternative methods, Ti⁴⁺ enrichment did not show a bias for charged peptides, yet mostly identified phosphoserines and -threonines (Supplementary Figures S1E – S1J).

We optimized the protocol to allow for a 2-minute treatment of *Arabidopsis* seedlings. We used 100 nM of the natural auxin Indole-3-Acetic Acid (IAA), and identified phosphopeptides by mass spectrometry (Figure 1A). This resulted in about 3100 phosphopeptides which were subjected to a sensitive hybrid data analysis approach (Nikonorova et al., 2018) that allows detection of differential abundance across samples despite missing values. The 2157 remaining phosphopeptides after filtering were subjected to FDR-controlled statistical comparison across treatments, resulting in about 10% differentially abundant phosphopeptides (FDR ≤ 0.05; Figure 1B). Global analysis showed that IAA mainly induces hyperphosphorylation, while limited hyperphosphorylation was detected (Figure 1B). The differential phosphopeptides map to 338 proteins (Supplementary Table S1), and among these are several proteins for which auxin-dependent phosphorylation has previously been shown (SNX, AHA2; Figure 1C). Importantly, comparison with an earlier phosphoproteome on roots treated with 10 μM NAA for 30 minutes showed that most of the early phosphosites are unique (Figure 1C). Comparison of the proteins that are differentially phosphorylated with genes that are transcriptionally regulated by auxin confirmed that the phosphoresponse targets a different and unique set of proteins (Figure 1D). Thus, auxin induces a very rapid phosphorylation of number of proteins within 2 minutes or shorter.

We next addressed whether the rapid phosphorylation response is mediated by TIR1/AFB pathway using either PEO-IAA, an anti-auxin for the TIR1 receptor (Hayashi et al., 2008) or the orthologous cvxIAA/ccvTIR1 system that specifically activates TIR1/AFB signaling (Uchida et al., 2018). Notably, cvxIAA induced some changes in phosphorylation, but the overlap with IAA-induced phosphorylation changes was minimal (Figures 1B, 1E; Supplementary Figures S2A, S2B) suggesting that a substantial portion of the auxin phosphoresponse was TIR1-independent. PEO-IAA also induced changes in phosphorylation within 2 minutes (Figures 1B, 1E), but these again overlapped minimally with IAA-dependent or TIR1-dependent phosphosites (Figure 1E; Supplementary Figures S2A, S2B). This suggests

that the auxin perception site cannot be efficiently inhibited by PEO-IAA and provides independent confirmation that the response is partly independent of TIR1/AFB. Thus, we identified a novel, ultra-rapid response to auxin that leads to the differential phosphorylation of a range of proteins, and that is largely mediated through yet unknown auxin perception and signaling mechanism.

4.2.2 ***Auxin-mediated phosphorylation of Myosin XI and Myosin-binding proteins***

The 338 proteins (Supplementary Table S1) predominately reside in the nucleus, cytosol and plasma membrane (Supplementary Figure S3A). The residues targeted by auxin-dependent phosphorylation were mostly serines (Supplementary Figure S3B). Some of the targets have reported roles in membrane trafficking (e.g. SYP132, BIG3, DRP2A/B, EPSIN2), microtubule regulation (e.g. MAP70-1, TOR1, NEK5) or chromatin biology (e.g. SUVR5, TPL, BRM, HDT1), but have not previously been associated with auxin-dependent processes. The candidates also include PDK1, an AGC kinase that activates PIN proteins (Xiao and Offringa, 2020; Tan et al., 2020). Thus, the phosphoproteome dataset represents a rich starting point for exploring fast auxin responses. Interestingly, among the identified candidates (Supplementary Tab S1), we found Myosin XIK, which is involved in trafficking processes (Peremyslov et al., 2008), was phosphorylated following auxin treatment. In the globular tail domain (GTD) of Myosin XIK, the serine at position 1234 (S1234) was hyper-phosphorylated upon auxin treatment, while this site was not phosphorylated upon PEO-IAA treatment (Figure 2A). Minor differential phosphorylation was observed with cvxIAA treatment on ccvTIR1, suggesting a (partial) dependence on TIR1 (Figure 2A). Protein alignment revealed that the phosphorylation site is also conserved in other myosin XI proteins (Supplementary Figure S4A). In addition to Myosin XIK, we also found the myosin binding protein MadB2/PHOX2 to be hyper-phosphorylated upon auxin treatment (Figure 2B).

The *Arabidopsis* genome contains 17 myosin members that are highly conserved (Reddy et al., 2001; Avisar et al., 2009). Myosin proteins have been shown to play roles in vesicle trafficking and endocytosis (Prokhnevsky et al., 2008; Peremyslov et al., 2008), auxin transport (Abu-Abied et al., 2019), auxin response (Ojangu et al., 2018) and gravitropism (Okamoto et al., 2015; Talts et al., 2016). MadB2 has been shown to bind to Myosin XIK but its function in plant development is less characterized (Kurth et al., 2017).

To examine auxin-mediated phosphorylation of Myosin XIK and XIF, we fused the globular tail domain (GTD) of myosin XIK and XIF with an RFP-tag, expressed this construct under the 35S promoter (*35S::MyosinXIK^{WT}*, *35S::MyosinXIF^{WT}*) and transformed it into both Col-0 and *myosin xik xif* plants. We then treated 7 days old *35S::MyosinXIK^{WT}* and *35S::MyosinXIF^{WT}* (Col background) seedlings with 10 μ M NAA for 30 minutes and collected the samples. Western blot analysis showed that Myosin XIK/XIF were more phosphorylated under auxin treatment (Figures 2C, 2D; Supplementary Figure 4B) thereby independently confirming the mass spectrometry data and extending this potential regulation to Myosin XIF.

4.2.3 ***Myosin XI is required for auxin-sensitive PIN endomembrane trafficking***

PIN polar localization is tightly regulated by its constitutive endocytic trafficking between plasma membrane and endosomes (Geldner et al., 2001, 2003; Dhonukshe et al., 2007; Kitakura et al., 2011; Glanc et al., 2018). We hence tested the involvement of Myosin XI proteins in PIN trafficking, which can be visualized by PIN intracellular aggregation into BFA bodies upon treatment with the trafficking inhibitor Brefeldin A (BFA) (Geldner et al., 2001, 2003). Upon BFA treatment, the *myosin xik xif* double mutant displayed less PIN1 aggregation into BFA bodies compared to the wild type (Figures 3A, 3B), implying defective PIN1 endocytic trafficking. Auxin shows an inhibitory effect on BFA body formation (Paciorek et al., 2005), however, *myosin xik xif* double mutant was less sensitive to auxin treatment (Figures 3A, 3B).

We next performed FM4-64 uptake assays (Bolte et al., 2004) to monitor endomembrane vesicles trafficking in *myosin xik xif* mutant. Quantification of FM4-64 uptake revealed a significantly reduced FM4-64 uptake in *myosin xik xif* mutant compared to the wild type (Figures 3C, 3D). Furthermore, auxin exhibited no additional inhibitory effect on FM4-64 uptake in *myosin xik xif* mutant (Figures 3C, 3D), indicating that Myosin XI is involved in auxin-mediated PIN endomembrane trafficking (Figures 3A – 3D; Paciorek et al., 2005).

4.2.4 ***Auxin-mediated Myosin XI phosphorylation regulates PIN endomembrane trafficking***

To further investigate the physiological relevance of the S1234 or S1256 phosphorylation site for Myosin XIK and Myosin XIF, respectively (Figures 2A - 2D), we mutated the Serine to Alanine to prevent phosphorylation, or to Aspartic acid to mimic phosphorylation. The resulting constructs *MyosinXIK^{S1234A}*, *MyosinXIK^{S1234D}*, *MyosinXIF^{S1256A}*

and *MyosinXIF^{S1256D}* were fused to a RFP tag, expressed under the 35S promoter and were introduced into Col-0 and *myosin xik xif* mutant plants. We then harvested the T3 seedlings of *35S::MyosinXIK^{S1234A}*, *35S::MyosinXIK^{S1234D}*, *35S::MyosinXIF^{S1256A}* and *35S::MyosinXIF^{S1256D}* plants (Col-0 background) to verify their expression in these phospho-deficient and phospho-mimic mutants. Western blot analysis showed that both phospho-deficient and phospho-mimic mutations of Myosin XIK/XIF were well expressed in plants (Figure 4A; Supplementary Figures S5A - S5D).

We next examined whether altered the phosphorylation status of Myosin XIK/XIF contribute to PIN trafficking. The phospho-deficient mutants (Col-0 background) exhibited less BFA bodies in the root (Figure 4B; Supplementary Figure S6A), less FM4-64 uptake (Figure 4C; Supplementary Figure S6B) and were also less sensitive to auxin treatment (Figures 4B, 4C; Supplementary Figures S6A, S6B). However, the phospho-mimic mutants showed normal BFA body formation, FM4-64 uptake and responded normally to exogenously applied auxin (Figure 4B, 4C; Supplementary Figures S6A, S6B). Although the phospho-mimic mutations partially complemented the defective BFA body formation and FM4-64 uptake in *myosin xik xif* mutant, the phospho-deficient mutations did not restore these defects (Supplementary Figures S7A - S7C; Supplementary Figures S8A - S8C).

Taken together, our results reveal that Myosin XI proteins are involved in PIN trafficking, and auxin-mediated phosphorylation of Myosin XI protein is a critical step for their function in PIN trafficking.

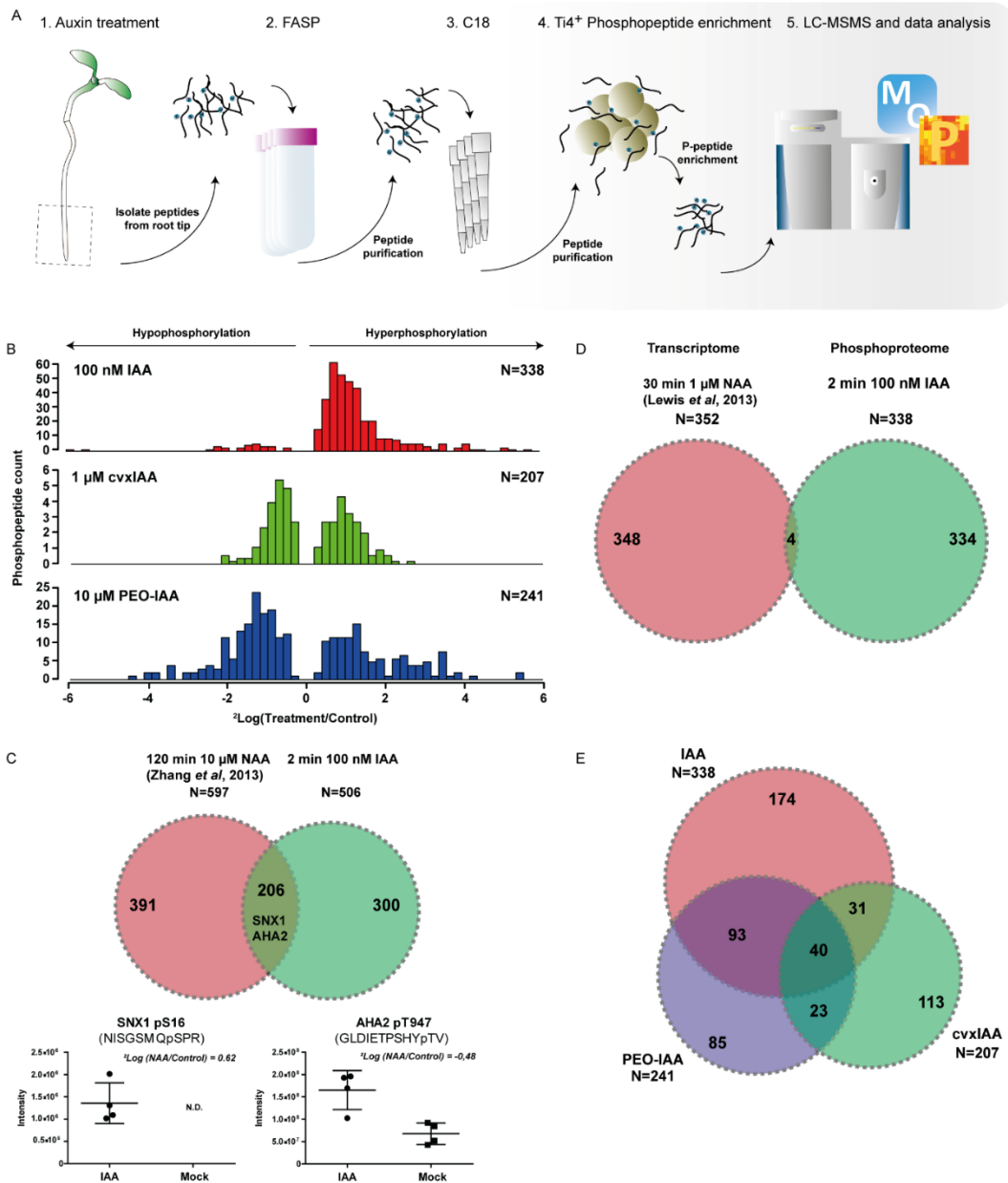


Figure 1. Phosphoproteomic analysis reveals rapid phosphorylation-dependent auxin response.

(A) Schematic depiction of the phosphopeptide enrichment protocol. Root tips of 5 day old seedlings were treated with either 100 nM IAA, 10 μM PEO-IAA on Col-0 or 1 μM cvxIAA on cTIR/ccvTIR1. Root tips were harvested, proteins were extracted and submitted to the optimized FASP-C18-Ti4⁺ phosphopeptide enrichment protocol.

(B) Histograms depict log₂ fold changes of significantly regulated phosphopeptides (FDR ≤0.05) in each treatment compared to control treatment.

(C) Comparison between IAA dataset including differentially regulated phosphopeptides (FDR ≤0.05), unique phosphopeptides for IAA and unique phosphopeptides for mock and previously published phosphoproteomics on 2 hours stimulated roots with 10μNAA (Zhang et.al. 2013). Inserts in graphs depict log₂ fold changes from Zhang et.al. (2013).

(D) Comparison between IAA differentially regulated phosphopeptides (FDR ≤0.05) and 30 min 1 μM IAA treated root transcriptome from Lewis et.al (2013).

(E) Venn diagram of overlapping significantly regulated phosphopeptides (FDR ≤0.05).

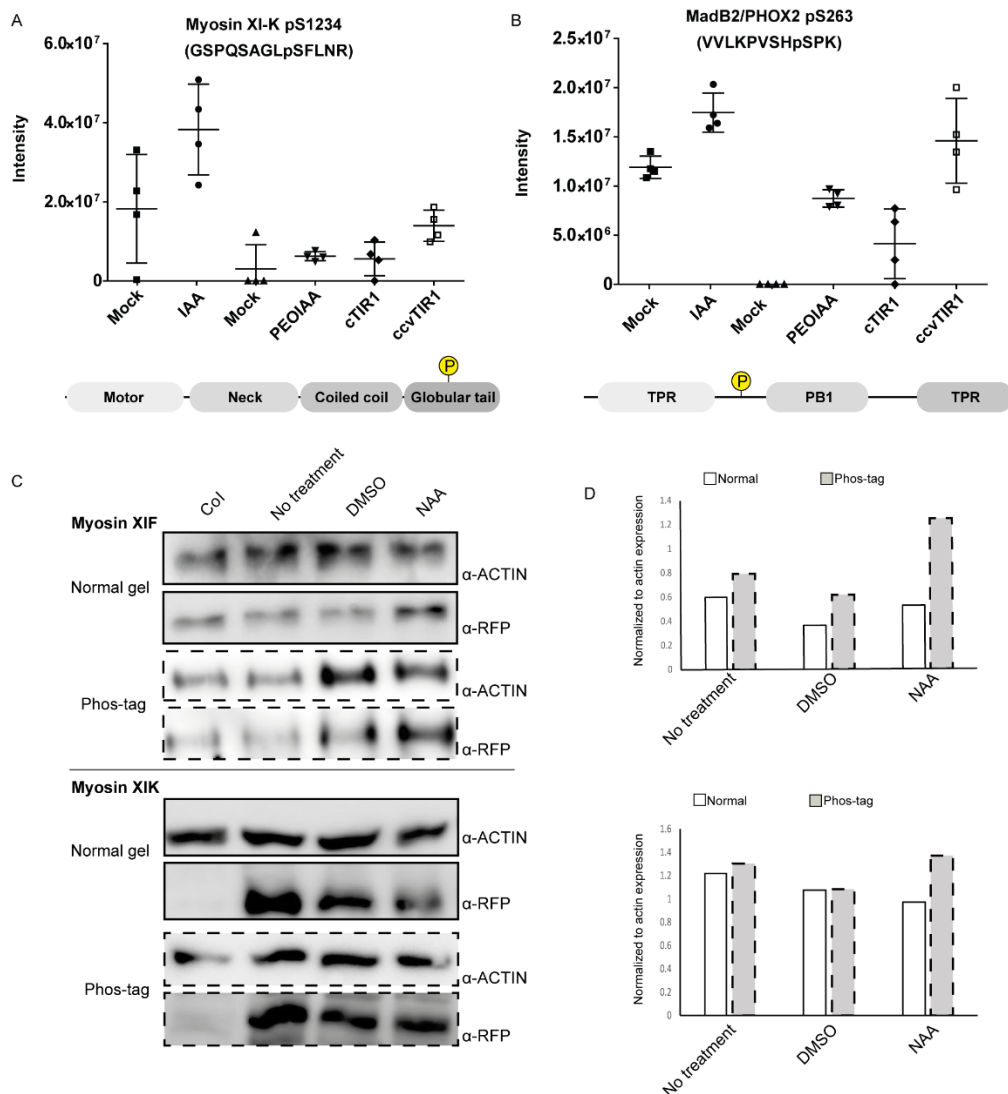


Figure 2. Identification of Myosin XI-K and MadB2 as phosphotargets of auxin signaling.

(A) Relative intensity of MS peak corresponding to the phosphopeptide surrounding S1234 in Myosin XI-K (sequence indicated) across various treatments (x-axis).

(B) Relative intensity of MS peak corresponding to the phosphopeptide surrounding S263 in MadB2/PHOX2 (sequence indicated) across various treatments (x-axis). Each dot corresponds to a single biological replicate. The phosphosites are indicated relative to protein domains in bottom panels.

(C - D) Phosphorylation of myosin XI proteins upon auxin treatment by immunoblot assay. 7 days old whole seedlings were treated with 10 μ M NAA or DMSO for 30 minutes. Whole plants were harvested and used for western blot assay.

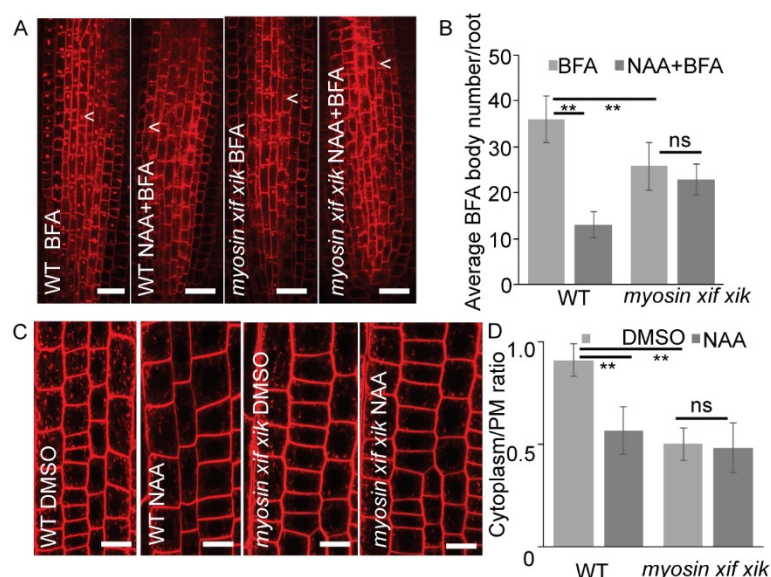


Figure 3. Myosin XI proteins are involved in auxin-mediated PIN trafficking.

(A) Representative images showing PIN1 trafficking in *myosin xif xif* mutant root.

(B) Quantification of BFA bodies in *myosin xif xif* root. The BFA body was counted in each root, and average BFA bodies were calculated. Data and error bars represent the mean \pm SD. $n > 15$, ** $P < 0.05$ determined by Student's t-test.

(C) Representative images showing FM4-64 uptake in *myosin xif xif* mutant root.

(D) Quantification of FM4-64 uptake in *myosin xif xif* mutant root. The ratio was calculated by dividing signal between cytoplasm and plasm membrane. Data and error bars represent the mean \pm SD. $n = 10$, more than 50 cells were quantified, ** $P < 0.05$ determined by Student's t-test. Arrowheads indicate BFA body in root. Scale bars, 20 μ m.

4.2.5 ***Auxin-mediated phosphorylation of Myosin is required for auxin-mediated feedback on PIN polarity***

Next, we investigated the requirement of Myosin XIK/XIF for auxin to repolarize PINs (Sauer et al., 2006; Prát et al., 2018). In line with previous results (Sauer et al., 2006; Prát et al., 2018), auxin induced a relocalization of PIN1 from the basal to the lateral side of endodermal cells in wild type roots (Figures 5A, 5B). However, auxin failed to induce PIN1 lateralization in the *myosin xif xif* mutant (Figures 5A, 5B).

We then tested the auxin impact on PIN1 repolarization in phospho-deficient and phospho-mimic mutants (Col background). Whereas auxin-mediated PIN1 repolarization in phospho-mimic mutants was similar to wild type, the phospho-deficient mutants were less responsive to exogenous auxin (Figures 5C, 5D; Supplementary Figure S9). In addition, the defective auxin-mediated PIN1 repolarization in *myosin xif xif* mutant, was rescued by introducing the phospho-mimic mutations in *myosin xif xif* mutant background, but not by the phospho-deficient mutations (Supplementary Figures S10A - S10C). This suggests that auxin-mediated phosphorylation is critical for the action of Myosin XIK/XIF while controlling dynamic PIN1 localization.

4.2.6 ***MadB2 myosin binding proteins are required for auxin-mediated regulation of PIN polarity and trafficking***

Multiple Myosin protein receptors or binding proteins with unknown function have been identified in plants (Peremyslov et al., 2013; Kurth et al., 2017). MadB2, a myosin binding protein, was previously shown to directly interact with Myosin XIK (Kurth et al., 2017), and was identified in our study to be hyper-phosphorylated upon auxin treatment (Figure 2B; Supplementary Tab S1). The MadB2 protein has three homologs that appear to act redundantly in root hair growth (Kurth et al., 2017). We thus investigated the *madb2* quadruple mutant (*madb 4ko*) for defects related to altered auxin responses and found decreased primary root growth and reduced auxin-dependent root growth inhibition (Supplementary Figures S11A - S11C). Furthermore, while the hypocotyl gravitropic response was normal (Supplementary Figure S11D), hypocotyl basipetal auxin transport was reduced (Supplementary Figure S11E). In the *madb 4ko* mutant, we did not observe any differences in number of loops nor in the distribution of the defects between the loops. However it had significantly more leaves with ectopic branches (Supplementary Figures S11F - S11H). These phenotypes strongly suggest a role for MadB2 proteins in polar auxin transport, thus we wondered whether the MadB2 family contributes to PIN polarity regulation and trafficking. We first tested auxin-mediated PIN1 lateralization in *madb 4ko* mutant root. Auxin treatment failed to repolarize PIN1 to the lateral side of endodermal cells in *madb 4ko* mutant (Supplementary Figures S12A, S12B). Under BFA treatment, *madb 4ko* mutant showed less BFA bodies and were less sensitive to auxin application (Supplementary Figures S12C, S12D). Quantification of FM4-64 uptake demonstrated that vesicle trafficking was impaired in *madb 4ko* mutant and auxin treatment showed no additional inhibitory effect on FM4-64 uptake in *madb 4ko* mutant (Supplementary Figures S12E, S12F).

Hence, our data further support that MadB2 family also play an essential role for PIN trafficking and polarity regulation. However, other myosin binding proteins may contribute to PIN polarity regulation in shoot gravitropism (Kurth et al., 2017).

4.2.7 ***Auxin-mediated Myosin phosphorylation in shoot gravitropic bending termination***

Auxin feedback on PIN polarity has also been shown crucial during hypocotyl gravitropic bending termination. In this context, auxin leads to relocation of PIN3 protein to

the inner lateral sides of shoot endodermis cells thus equalizing auxin gradient and asymmetric growth (Rakusová et al., 2016, 2019; Han et al., 2020). Indeed, the *myosin xik xif* mutant showed hypocotyl hyperbending (Supplementary Figure S13A; Okamoto et al., 2015) and impaired polar auxin transport in hypocotyl (Supplementary Figure S13B) and likewise, the phospho-deficient mutants also showed hypocotyl hyperbending in both Col-0 and *myosin xik xif* mutant background (Supplementary Figures S14A, S14B).

Given the hypocotyl hyperbending phenotype, we then assessed both gravity- and auxin-induced PIN3 polarization events (Rakusová et al., 2011, 2016) in *myosin xik xif* mutant. The steady-state of PIN3 polarity is not affected in *myosin xik xif* mutant (Supplementary Figures S13C, S13D). After 6 hours gravistimulation (Rakusová et al., 2011), we observed a normal gravity-induced PIN3 polarization in both wild type and *myosin xik xif* mutant hypocotyls (Supplementary Figures S13E, 13F, S13I); however, the auxin-mediated PIN3 repolarization at later stages was defective (Supplementary Figures S13G, S13H, S13I). Additionally, gravity-induced PIN3 polarization was normal in both phospho-deficient and phospho-mimic Myosin XIK/XIF mutants (Col-0 background) but the phospho-deficient mutants showed a defective auxin-mediated PIN3 repolarization, whereas the phospho-mimic mutants had normal PIN3 repolarization (Supplementary Figures S14C - S14G).

Auxin application induces a similar PIN3 repolarization which is observed at later stage of gravitropism response (Rakusová et al., 2016, 2019; Han et al., 2020). We observed auxin-induced PIN3 repolarization to the inner side of endodermal cells in wild type, but this auxin effect was defective in *myosin xik xif* mutant (Figures 6A, 6B) or phospho-deficient mutants (Figures 6C, 6D; Supplementary Figure S15). On the other hand, the phospho-mimic mutants showed normal PIN3 polarization in response to auxin treatment (Figures 6C, 6D; Supplementary Figure S15).

These observations demonstrate that auxin-mediated Myosin XI protein phosphorylation is also required for auxin-mediated PIN3 repolarization during shoot gravitropic bending termination providing a developmental context to the cellular role of Myosin XI in auxin-regulated PIN polarity.

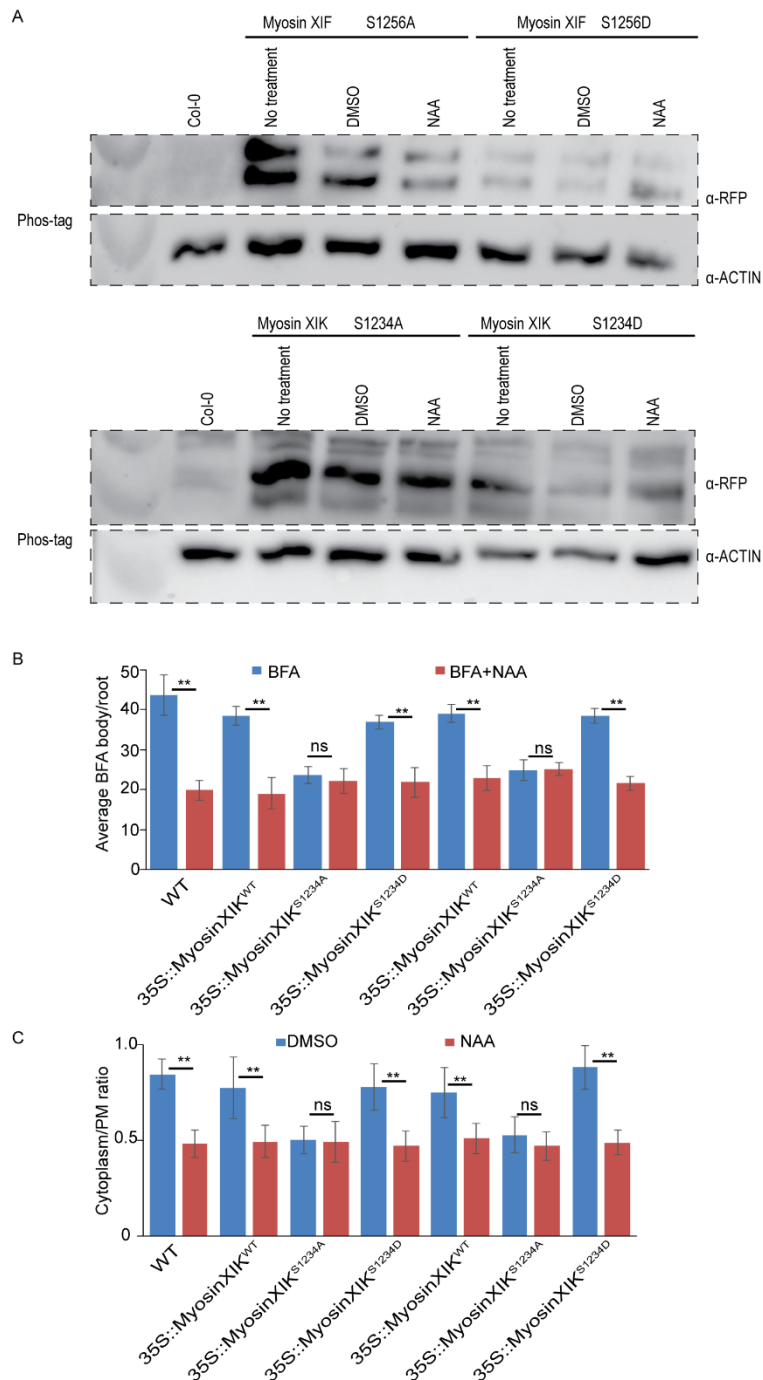
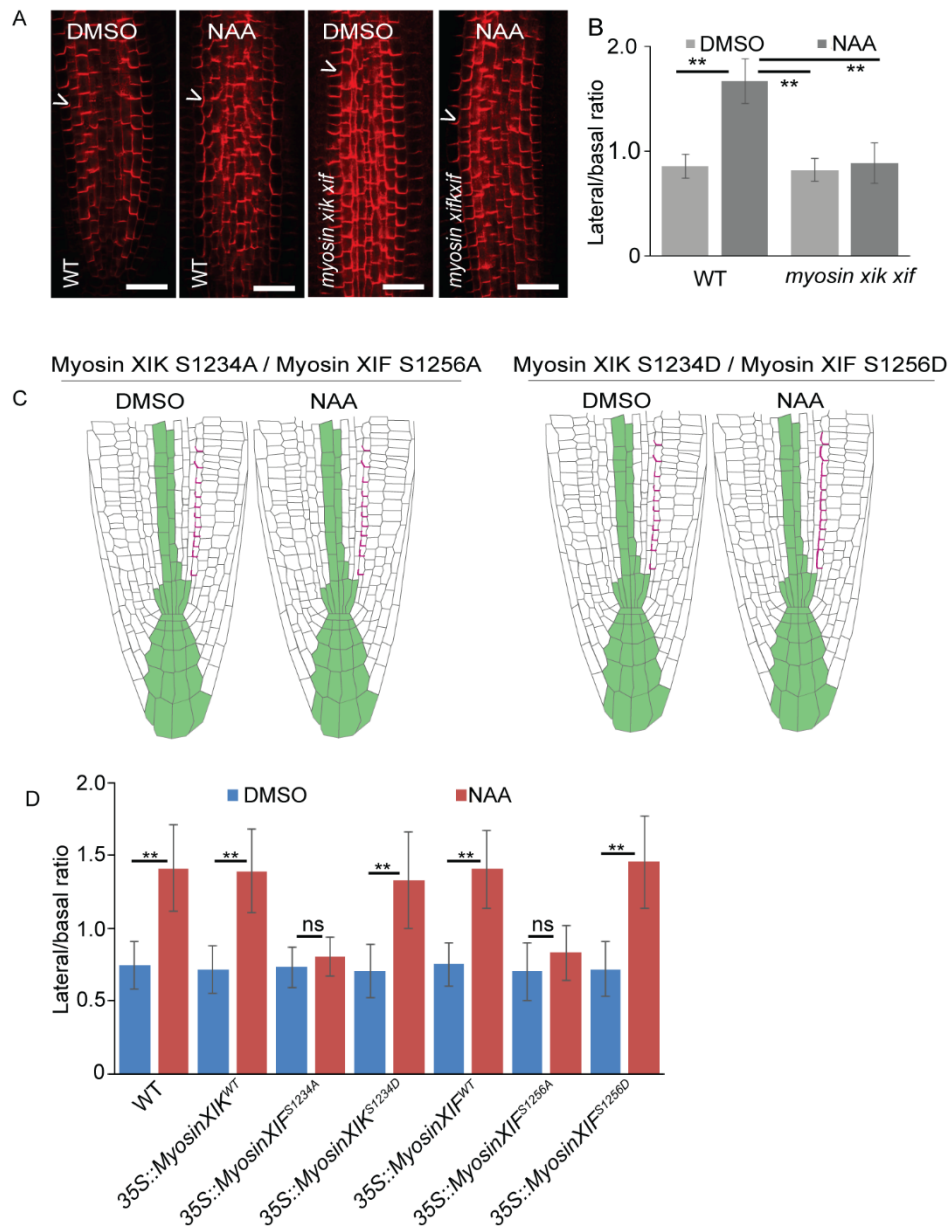


Figure 4. Auxin-mediated Myosin phosphorylation is required for PIN trafficking.

(A) Myosin XIk and XIk phosphorylation status in the phospho-deficient and phospho-mimic mutants (Col-0).

(B) Quantification of BFA bodies in phospho-deficient and phospho-mimic myosin mutant root (Col-0 background). The BFA body was counted in each root, average BFA bodies were calculated. Data and error bars represent the mean \pm SD. $n > 15$, ** $P < 0.05$ determined by Student's t-test.

(C) Quantification of FM4-64 uptake in phospho-deficient and phospho-mimic myosin mutant root (Col-0 background). The ratio was calculated by dividing signal between cytoplasm and plasm membrane. Data and error bars represent the mean \pm SD. $n = 10$, more than 50 cells were quantified, ** $P < 0.05$ determined by Student's t-test.



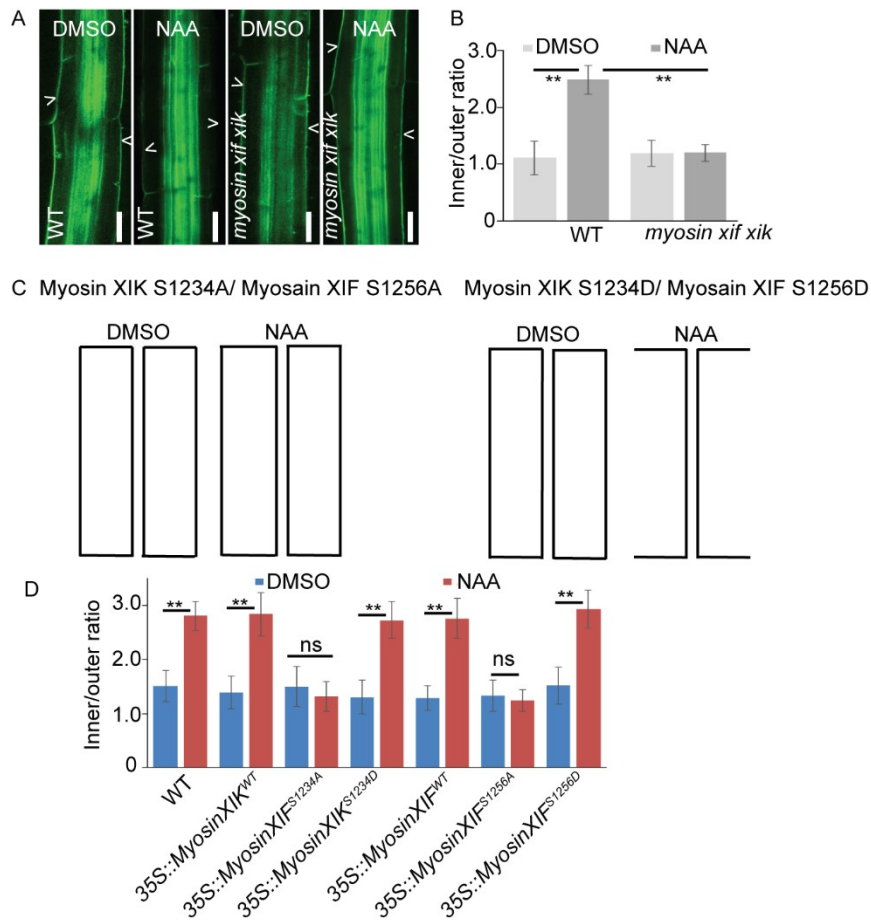


Figure 6. Phosphorylation of myosin XI proteins contributes to auxin-mediated PIN polarity regulation to terminate hypocotyl bending.

(A) Representative images showing PIN3-GFP localization in wild type, *myosin xif xif* mutant hypocotyl upon DMSO and auxin treatment.

(B) Quantification of auxin-mediated PIN3 repolarization in *myosin xif xif* mutant hypocotyls. The ratio was calculated by dividing PIN3-GFP signal between inner side and outer side of hypocotyl endodermal cells. Data and error bars represent the mean \pm SD. $n = 15$, ** $P < 0.05$ determined by Student's t-test.

(C) Schematic depiction of auxin-induced PIN3 repolarization in phospho-deficient and phospho-mimic myosin mutant hypocotyls (Col-0 background). This schematic shows the PIN3 pre-polarization in shoot endodermal cells. Following auxin treatment, PIN3 polarizes to inner side of the endodermal cells in the phospho-mimic mutants, but this auxin-mediated PIN3 repolarization does not happen in the phospho-deficient mutants.

(D) Quantification of auxin-mediated PIN3 repolarization in phospho-deficient and phospho-mimic myosin mutant hypocotyls. The ratio was calculated by dividing PIN3-GFP signal between inner side and outer side of hypocotyl endodermal cells. Data and error bars represent the mean \pm SD. $n = 15$, ** $P < 0.05$ determined

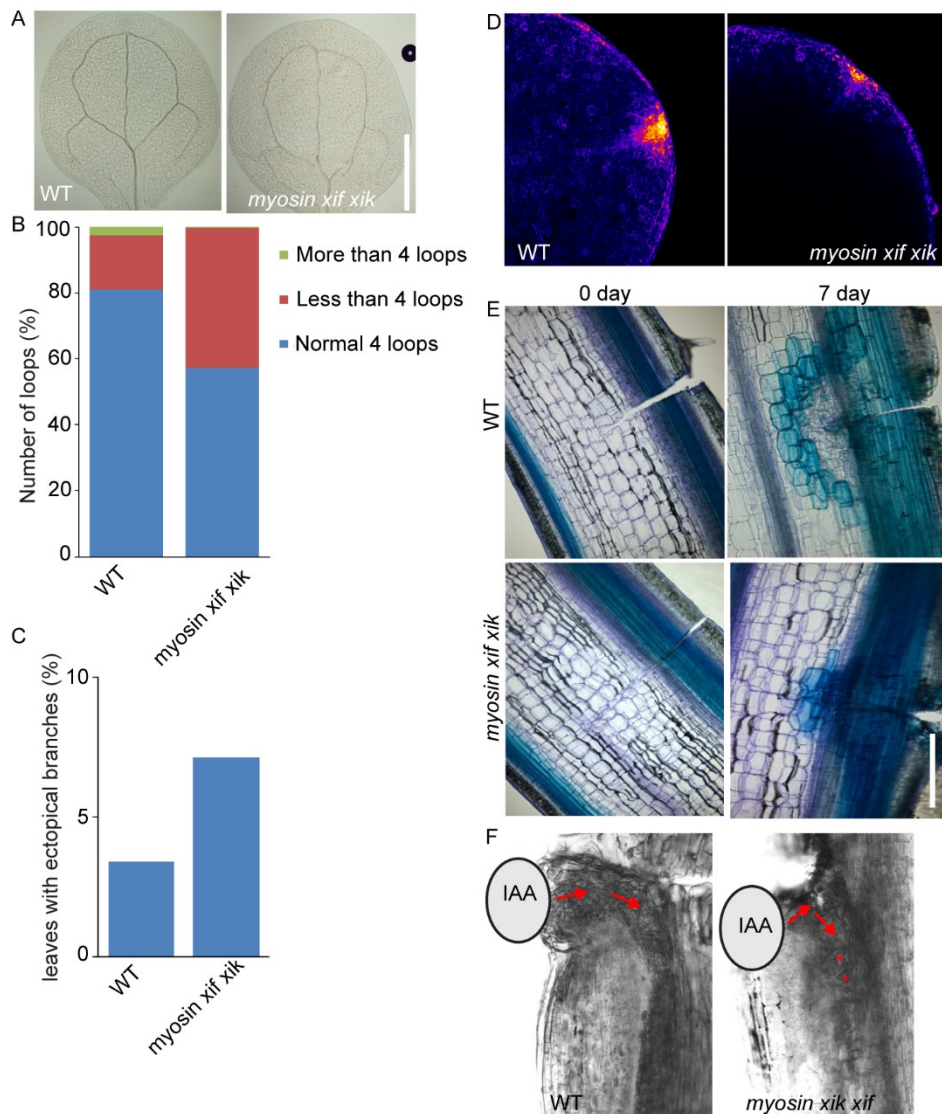


Figure 7. Defects in auxin-canalization related phenotype in *myosin xik xik* mutant.

- (A) Represented leaf venation defects in *myosin xik xik* mutant.
 (B) Quantification of loops defects in *myosin xik xik* mutant.
 (C) Quantification of ectopic branches in *myosin xik xik* mutant.
 (D) Decreased *DR5-GFP* signal in *myosin xik xik* mutant leaf.
 (E) Regeneration defects in *myosin xik xik* mutant stem after wounding.
 (F) Defects in auxin canalization in *myosin xik xik* mutant stem.

4.2.8 ***Auxin-mediated Myosin phosphorylation in auxin canalization-mediated vasculature formation and regeneration***

The classical auxin canalization hypothesis proposes auxin feed-back regulation of directional auxin transport as the key part underlying self-organizing aspects of plant development, such as spontaneously arising vasculature during leaf venation (Scarpella et al., 2009) and flexible regeneration of vasculature around wounding sites (Sauer et al., 2006; Mazur et al., 2016, 2020a, 2020b).

We first analyzed leaf venation patterns in the *myosin xik xif* mutant. Compared to the wild type leaves, *myosin xik xif* mutant had significantly more leaves with fewer loops and they showed abnormal vascular patterning with disconnected loops and extra branches (Figure 7A - 7C). To test if these venation defects were linked to altered auxin distribution (Scarpella et al., 2009), we analyzed the expression of the auxin-responsive reporter *DR5rev::GFP* in leaves. In *myosin xik xif* mutant, the DR5 activity was decreased compared to wild type (Figure 7D). Additionally, we analyzed the leaf venation in the phospho-mimic and -deficient mutants (Col-0 background). Without any mutation in the Myosin XIK and XIF phosphorylation site, we observed more defects in the lower loops and slightly more ectopic branches (Supplementary Figures S16A, S16B). However, the phospho-mimic mutant showed similar phenotypes as the wild type leaves, the phospho-deficient mutants showed defects in both discontinuity of the bottom loops of the vasculature and number of ectopic branches (Supplementary Figures S16A, S16B).

Next, we analyzed the extent of vasculature regeneration in *myosin xik xif* mutant, visualized by toluidine blue staining of regenerated vasculature in stem segments. In wild type stems, the vasculature was fully developed and connected (Figure 7E). In *myosin xik xif* mutant, regeneration was completed and connected, but the vessel cells were formed from parenchyma cells compared to wild type stems (Figure 7E). In addition, auxin-induced vascular formation was also impaired in *myosin xik xif* mutant (Figure 7F).

These results reveal that Myosin XI proteins is essential for auxin canalization-mediated vasculature formation and regeneration around the wounding.

4.3 Discussion

The molecular mechanism underlying auxin-mediated PIN polarity regulation in plant developmental processes are extensively studied over the past century (Adamowski and Friml, 2015), but it is still elusive. Here, we applied a phosphoproteomics approach to identify novel proteins potentially will play essential roles in PIN polarity regulation in a phosphorylation-dependent manner. In this study, we characterized the crucial roles of the myosin transport network in PIN polarity regulation and trafficking.

4.3.1 *Auxin-mediated rapid protein phosphorylation by different signaling pathways*

Protein phosphorylation and de-phosphorylation are suggested fast acting post-translational modification to control protein functions. It long has been suggested that the phospho-state of PIN proteins involved in polar auxin transport has an effect on their function, both activity and polarity and trafficking (Zhang et al., 2010; Barbosa et al., 2018). While inhibition of phosphatase activity by genetic and pharmacological approaches has led to defects in auxin transport and PIN polarization (Rashotte et al., 2001; Friml et al., 2004; Michniewicz et al., 2007; Huang et al., 2010). More recent findings have revealed a role for D6PK and its paralogs D6PK-LIKE1-3, PINOID/WAG1,2 AGCVIII kinases, mitogen-activated protein (MAP) kinases and Ca²⁺/calmodulin-dependent protein kinase-related kinases (CRKs) in PIN phosphorylation and polar localization (Barbosa et al., 2018; Weller et al., 2017; Rigo et al., 2013; Jia et al., 2016; Zourelidou et al., 2014; Lofke et al., 2013). The phosphatase PP2A displays antagonistic activity to PID activation, affecting the apical-basal targeting of PINs (Zhang et al., 2010; Michniewicz et al., 2007; Tan et al., 2020).

Here we performed a short auxin treatment followed by an extensive phosphoproteomics approach in order to identify fast players in post-translational modifications of proteins important in auxin responses. By using the available tools, such as the TIR1-specific anti-auxin PEO-IAA and the engineered receptor-ligand pair cvxIAA/ ccvTIR1, we identified auxin-induced rapid phosphorylation both dependent and independent of the canonical TIR1/AFB1 nuclear signaling pathway. The fast phosphorylation of myosin complex belongs to the candidates identified. Further analysis of their role and the role of auxin-mediated phosphorylation, in canalization-related processes proved that our approach was successful for the identification of novel and rapid regulators of PIN trafficking and polarity regulation.

4.3.2 *Auxin regulates PIN trafficking and polarity via phosphorylation of myosin complex*

A key condition for canalization is the feedback regulation of auxin transport, as manifested at a cellular level by the auxin effect on the subcellular localization of PIN auxin transporters. Constitutive trafficking and clathrin-mediated endocytosis of PINs have been suggested essential for this auxin feedback on PIN polarity (Paciorek et al., 2005; Robert et al., 2010; Mazur 2020a).

Here we show that the Myosin XI proteins play crucial roles in auxin-mediated PIN polarity rearrangement both in root, hypocotyl, because the loss-of-function the *myosin xik xif* mutant was strongly affected in these processes. These auxin-mediated PIN polarization defects were also revealed in the phospho-deficient mutants, which further suggests that auxin-mediated phosphorylation of Myosin XI proteins are required and essential for PIN polarity regulation. Additionally, the defective PIN trafficking in *myosin xik xif* mutant and phospho-deficient mutants suggests the importance of auxin-mediated phosphorylation of Myosin XI proteins in PIN trafficking.

The identification of large number of myosin interacting proteins indicates there is a series of specific interactions that allow myosin motors to operate on various cargoes, such as PIN proteins (Kurth et al., 2017). In this study, we demonstrate that the MadB2 myosin binding protein family contributes to PIN trafficking and polarity regulation in roots, but because of the lack of a hypocotyl phenotype, we postulate that other myosin binding proteins contribute to PIN polarity regulation in hypocotyl gravitropism (Peremyslov et al., 2013; Kurth et al., 2017). It is likely that PIN proteins would bind to the MadB2 family, thus PINs can be transported through the trafficking pathway via the myosin transport network to the desired cell side, thereby determining the directional auxin transport (Peremyslov et al., 2013; Kurth et al., 2017). However, it is still not clear how myosin binding proteins bind to PINs and transport PINs to the plasma membrane or to the endomembrane system. It is also essential to explore how myosin tail-binding proteins are employed by myosin proteins to carry out their transport ability and cellular functions to transport PINs (Peremyslov et al., 2013; Ryan et al., 2017).

4.3.3 Developmental roles of auxin feedback on directional auxin transport

PIN polarization defects at the cellular level revealed by the exogenous auxin application appears to be developmentally relevant. Auxin feedback on PIN1 polarization defects was seen in *myosin xik xif* mutants by defects in leaf venation pattern, regeneration after wounding in stem segments and in root morphogenesis. Similarly, auxin feedback on PIN3 polarization in the shoot was visualized by defects in shoot bending termination in *myosin xik xif* mutants. Furthermore, we also observed defects in auxin-mediated PIN polarization and canalization-related phenotypes in the myosin binding protein MadB2

mutant. Hence, our findings suggest that the myosin transport network plays an essential role in auxin feedback on PIN polarity.

In conclusion, our study demonstrates that Myosin XIK and XIF and MadB2 myosin binding proteins, as part of the myosin transport network, are required for auxin feedback on PIN polarity by mediating PIN trafficking. Furthermore, we also uncover that auxin-mediated phosphorylation of these myosin proteins is sufficient and required for their function in PIN trafficking and polarity regulation. Our work provides a novel and vital mechanism of PIN polarity regulation during plant development.

4.4 Materials and Methods

Plant material and growth

The following transgenic and mutant lines were used: Col-0, *PIN3::PIN3-GFP* (Žádníková et al., 2010), *myosin xik xif* (Okamoto et al., 2015), *madb 4ko* (Kurth et al., 2017). Mutant combinations with *PIN3::PIN3-GFP* were generated through genetic crosses. Seeds were sown on plates with half-strength Murashige and Skoog (½ MS) medium with 1% sucrose, 1% agar and stratified at 4°C for 2 days, and then cultivation at 21°C in standard long day lighting (16h : 8h, light : dark).

Protein extraction

Five days after germination, roots were treated with either 100 nM IAA, 10 µM PEO-IAA or 1 µM cvxIAA or their respective solvents in the respective dilution as mock. Root tips were directly harvested on liquid nitrogen. For IAA and PEO-IAA treatments, Col-0 wild-type was used, while for cvxIAA treatment, *ccvTIR1* was used (Uchida et al., 2018). The harvested root tips were ground to fine powder in liquid nitrogen with a mortar and pestle. Powder was suspended in SDS lysis buffer (100mM Tris pH8.0, 4%SDS and 10mM DTT). Protein extract was next sonicated using a cooled Biorupter (Diagenode) for 10 minutes using high power with 30 seconds on 30 seconds off cycle. Lysate was cleared by centrifugation at maximum speed (13,000xg) for 30 minutes. Protein concentrations were determined using Bradford reagent (Bio-Rad).

Protein precipitation

Acetone precipitation was done according to Humphrey et.al. (2015). Methanol chloroform precipitation was done according to Vu et.al. (2016). For trichloroacetic acid (TCA) precipitation 1 volume of ≥99% TCA was added to 4 volumes of protein lysate. Mixtures were incubated on ice for 10 minutes and spun down at maximum speed (13,000xg) for 5 minutes at 4°C. Pellet was washed twice with acetone at maximum speed (13,000xg) for 5 minutes at 4°C and then air dried and suspended in 50 mM ammoniumbicarbonate (ABC) (Sigma).

Filter aided sample preparation (FASP)

For FASP, 30 kDa cut-off amicon filter units (Merck Millipore) were used. Filters were first tested by applying 1000 µl urea buffer UT buffer (8 M Urea and 100mM Tris, pH=8.5) and centrifuging for 20 minutes on 6,000 RPM at 20°C. The desired amount of protein sample was next mixed with UT buffer to a volume of 5000 µl, applied to filter and centrifuged for 20 minutes at 6,000 RPM at 20°C. Filter was washed with UT buffer for 20 minutes at 6,000 RPM

at 20°C. Retained proteins were alkylated with 50 mM acrylamide (Sigma) in UT buffer for 30 minutes at 20°C while gently shaking. Filter was centrifuged and afterwards washed three times with UT buffer for 20 minutes on 6,000 RPM at 20°C. Next, filters were washed three times in 50 mM ABC buffer. After the last wash, proteins were cleaved by adding Trypsin (Roche) in a 1:100 trypsin:protein ratio. Digestion was completed overnight. Filter was transferred to a new tube and peptides were eluted by 20 minutes at 6,000 RPM at 20°C. Further elution was completed by two times adding 50 mM ABC buffer and centrifuging for 20 minutes on 6000 RPM at 20°C.

C18 Stagetip clean up

For peptide desalting and concentrating, 1000 µl tips were fitted with 2 plugs of C18 octadecyl 47mm Disks 2215 (Empore™) material and 1 mg : 10 µg of LiChroprep® RP-18 peptides (Merck). Tips were sequentially equilibrated with 100 % methanol, 80 % ACN in 0.1 % formic acid and twice with 0.1 % formic acid for 4 minutes at 1,500xg. After equilibration, peptides were loaded for 20 minutes at 400xg. Bound peptides were washed with 0.1 % formic acid and eluted with 80 % ACN in 0.1 % formic acid for 4 minutes at 1,500xg. Eluted peptides were subsequently concentrated using a vacuum concentrator for 30 minutes at 45°C and resuspended in 50 µl of 0.1 % formic acid.

Phosphopeptide enrichment

For magnetic Ti⁴⁺-IMAC (MagResyn) and TiO₂-MOAC (MagResyn) approaches manufacture's protocols were used without modifications (Resyn biosciences). For stage tip based TiO₂ Titansphere™ (GL Sciences) a 1:2 peptide to TiO₂ (µg/µg) was used. FASP eluted peptides were mixed with ACN and TFA to a concentration of 50 % ACN and 6 % TFA. TiO₂ columns were made with double C8 membrane and desired amount of beads in 100 % methanol. The columns were washed and equilibrated with 100 % ACN and 80 % ACN in 6 % TFA using centrifugation for 4 minutes at 1,500xg. Sample was loaded at 400xg for 30 minutes. Non-specifically bound peptides were washed with 80 % ACN in 6 % TFA by centrifugation for 4 minutes at 1,500xg and 2 times with 60 % ACN in 1 % TFA for 4 minutes at 1,500xg. Next, bound phosphopeptides were eluted three times in 40 % ACN and 15 % NH₄OH. After the last elution samples were concentrated using a vacuum concentrator for 30 minutes at 45°C. Samples were subsequently acidified using 10% TFA and processed with C18 Stagetip clean up.

Mass spectrometry and data analysis

Phosphopeptides were applied to online nanoLC-MS/MS using a 120 min acetonitrile gradient from 8-50 %. Spectra were recorded on a LTQ-XL mass spectrometer (Thermo Scientific) according to Wendrich et.al. (2017). Data analysis of obtained spectra was done in MaxQuant software package (Wendrich et al., 2017), with the addition of phosphorylation as a variable modification. Data analysis and visualization was performed in Perseus, Adobe Illustrator and R. Filtering of phosphopeptides was conducted using a hybrid data filtering approach as described previously (Nikonorova et al. 2018). Protein subcellular localisation analysis was performed using the Multiple Marker Abundance Profiling (MMAP) tool on the subcellular localisation database for Arabidopsis proteins (SUBA4) (Hooper et.al. 2017).

Myosin XIK and XIF phosphorylation mutagenesis

The Myosin XIK and XIF GTD sequences (from amino acid 1100 to the C terminus) (Peremyslov et al., 2008) with mutations S1234A (Myosin XIK^{S1234A}), S1234D (Myosin XIK^{S1234D}), S1256A (Myosin XIF^{S1256A}) and S1256D (Myosin XIF^{S1256D}) or in non-mutated version (Myosin XIK^{WT}, Myosin XIF^{WT}) were synthesized, respectively. Then the sequences were recombined into the pDONR221 gateway vector and the pB7RWG2 expression vector. All the constructs were re-sequenced to confirm the mutation sites and transformed into *Arabidopsis* plants using flower dip method.

Protein extraction and immunoblot assay

7 days old homozygous T3 seedlings of *35S::MyosinXIK^{WT}*, *35S::MyosinXIK^{S1234A}*, *35S::MyosinXIK^{S1234D}*, *35S::MyosinXIF^{WT}*, *35S::MyosinXIF^{S1256A}*, *35S::MyosinXIF^{S1256D}* were treated with DMSO or 10 µM NAA for 30 minutes and seedlings were harvested. Samples were frozen in liquid nitrogen, ground into powder, and homogenized in protein extraction buffer (50 mM Tris-HCl, pH=7.5; 150 mM NaCl; 0.15% NP40; 10 mM DTT (1, 4-dithiothreitol); 1 mM PMSF; containing protease inhibitor and phosphatase inhibitor). After 20 minutes of centrifugation (16,000 g) at 4 °C, total protein extract was collected and concentration was determined by Bradford Reagent (Bio-Rad). Lambda protein phosphatase treatment (New England Biolabs) was performed following the manufacturer's protocol. After adding an equal amount of loading buffer (5µl, 4× Laemmli Sample Buffer, Bio-Rad), 30 µg protein for each sample was boiled at 65°C for 10 minutes, then separated on a 10% normal or the Phos-tag SDS-PAGE (Phos-tag acrylamide AAL-107, Wako Pure Chemical Industries, #304-93521). Proteins were transferred to a PVDF membrane by wet blotting. The membranes were

incubated with primary rat monoclonal anti-5F8 antibody (Chromotek, 1:1000) and secondary bovine anti-rat HRP (horseradish peroxidase)-conjugated (1:5000) antibody. Following detection of the myosin protein, the membranes were stripped and incubated with primary plant Monoclonal Anti-Actin (Sigma, A0480, 1:1000) and secondary anti-mouse HRP (1:5000) antibody overnight. HRP activity was detected by the Supersignal Western Detection Reagents (Thermo Scientific) and imaged with a GE Healthcare Amersham 600RGB system.

Quantification of hypocotyl gravitropic bending angle

3 days old etiolated seedlings were turned 90°. To monitor gravitropic responses, plates were scanned 24 hours after gravistimulation or the bending was recorded at 1-h intervals and bending angle was measured by ImageJ (NIH; <http://rsb.info.nih.gov/ij>).

Quantification of root hair length

3 days old light grown seedlings were transferred to new plates supplied with 100 nM of NAA or the equivalent amount of DMSO for another 3 days. The plates were scanned and root hair length was quantified by ImageJ.

Quantitative analysis of PIN3-GFP polarization in hypocotyl

The PIN3-GFP intensity was measured by ImageJ. The fluorescence intensity of PIN3-GFP was measured at upper part of hypocotyl as described previously (Rakusová et al., 2019). After gravity stimulation, the ratio between lower and upper side endodermal cells was calculated. For auxin treatment, 3 days old etiolated seedlings were transferred to new plates with 10 µM of NAA, or the equivalent amount of DMSO for 4 hours in darkness. The inner/outer ratio was calculated for the relevant endodermal cells.

Hypocotyl basal-petal auxin transport assay

6 days etiolated seedlings were placed on new half MS plates. 15 seedlings for each mutant or treatment in 3 replicates were used. 3H-IAA was added into half MS medium (1.25% agar) to a final concentration of 1.5 µM. A 5 µl of 3H-IAA droplets was placed on the top of the hypocotyl from which the cotyledons were excised for 6 hours while the seedlings were kept in the dark. 10 µM N-1-Naphthylphthalamic acid (NPA) was used as a control. After 6 hours, roots and the top part of the hypocotyl in contact with the drop were removed. Samples were homogenized in liquid nitrogen and incubated overnight in Opti-Fluor scintillation cocktail (Perkin Elmer). The scintillation counter (Hidex 300SL) was used to measure the amount of 3H-IAA uptake by the hypocotyl and hence represents basipetal auxin transport. Measurements were performed in three technical and three biological replicates.

Leaf venation assay

7 days old light grown seedlings were used for leaf venation analysis. Cotyledons were cleared in 4% HCl and 20% methanol for 15 minutes at 65°C, followed by a 15 minutes incubation in 7% NaOH and 70% ethanol at room temperature. Next, seedlings were rehydrated by successive incubations in 70%, 50%, 25%, and 10% ethanol for 5 minutes each, followed by incubation in 25% glycerol and 5% ethanol for 2 days at room temperature. Finally, cotyledons were mounted in 50% glycerol and were monitored by differential interference contrast DIC microscopy (Olympus BX53).

Regeneration of stem after wounding

For regeneration, inflorescence stems were cut with a sharp razor blade 3 to 4 mm from the rosette in the transversal plane of the basal sectors to interrupt the longitudinal continuum of vascular cambium and secondary tissues. Plants were covered with an artificial weight. Axillary buds grown above the rosette were not removed, thus remaining a source of endogenous auxin. 7 days after wounding, stem segments were cut to 80 µm native sections by automated vibratome (Leica VT1200 S, Leica Microsystems Ltd., Wetzlar, Germany). These sections were stained with a 0.025 % Toluidine Blue O aqueous solution and regeneration was analyzed in stems with fully developed, closed cambial rings and secondary tissues. Observations were made using a wide field microscope at 10x magnification (Zeiss Axioscope.A1 ZENAxioCam 105).

Whole-mount in situ immunolocalization

For PIN1 localization in root, 3 days old primary roots were treated for 4h with 10 µM of NAA in liquid ½ MS medium. Immunolocalization was carried out as described previously (Sauer et al., 2006). The following antibodies were used: anti-PIN1 (1:1000), secondary goat anti-rabbit antibody coupled Cy3 (Sigma-Aldrich, 1:600). PIN1 localization was monitored by LSM 800 microscopy. Quantification of PIN1 lateralization was done as described (Sauer et al., 2006).

FM4-64 uptake assay

4 days old light grown seedlings were incubated with 10 µM NAA or the equivalent amount of DMSO for 30 minutes in ½ MS liquid medium. Then 2 µM FM4-64 was added to the medium for 15 minutes and roots were mounted and observed using LSM-800 Zeiss confocal microscope. Signal intensity at PM and cytoplasm was measured using ImageJ. The ratio

between cytoplasm and PM was calculated and statistical analysis was performed using t-tests.

BFA treatment assay

To monitor PIN trafficking in the root, 3 days old light grown seedlings were pretreated with 10 μ M NAA or the equivalent amount of DMSO in $\frac{1}{2}$ MS liquid medium for 30 minutes, and then co-treatment with 50 μ M BFA for another 60 minutes. Immunolocalization was carried out as described previously (Sauer et al., 2006). The average number of BFA bodies per root was quantified.

Statistical analysis

All statistical analysis was performed using student's test in excel (Microsoft 2010) with a significant difference ($P < 0.05$).

Author Contributions

H. H. and J. F. designed research. H. H. performed most of the experiment; I. V. helped to synthesize the Myosin XIK and XIF GTD sequences and performed western blot assay; M. R. and D. W. performed phosphoproteomics experiment and analyzed the data; J. H. carried out the auxin transport assay; E. M. and N. R. contributed to the regeneration assay. H. H. and J. F. wrote the manuscript with the inputs from all authors.

4.5 References

- Abel, S., and Theologis, A. (1996). Early genes and auxin action. *Plant Physiol.* *111*, 9.
- Abas, L., Benjamins, R., Malenica, N., Paciorek, T., Wiśniewska, J., Moulinier–Anzola, J. C., et al. (2006). Intracellular trafficking and proteolysis of the Arabidopsis auxin-efflux facilitator PIN2 are involved in root gravitropism. *Nat. Cell Biol.* *8*, 249-256.
- Avisar, D., Abu-Abied, M., Belausov, E., Sadot, E., Hawes, C., Sparkes, I.A. (2009). A comparative study of the involvement of 17 *Arabidopsis* myosin family members on the motility of Golgi and other organelles. *Plant Physiol.* *150*, 700-709.
- Adamowski, M., and Friml, J. (2015). PIN-dependent auxin transport: action, regulation, and evolution. *Plant Cell* *27*, 20-32.
- Abu-Abied, M., Belausov, E., Hagay, S., Peremyslov, V., Dolja, V., Sadot, E. (2018). Myosin XI-K is involved in root organogenesis, polar auxin transport, and cell division. *J. Exp. Bot.* *69*, 2869-2881.
- Benková, E., Michniewicz, M., Sauer, M., Teichmann, T., Seifertová, D., Jürgens, G., Friml, J. (2003). Local, efflux-dependent auxin gradients as a common module for plant organ formation. *Cell* *115*, 591-602.
- Bolte, S., Talbot, C., Boutte, Y., Catrice, O., Read, N.D., Satiat-Jeunemaitre, B. (2004). FM-dyes as experimental probes for dissecting vesicle trafficking in living plant cells. *J. Microsc.* *214*, 159-173.
- Badescu, G.O., Napier, R.M. (2006). Receptors for auxin: will it all end in TIRs?. *Trends Plant Sci.* *11*, 217-223.
- Benjamins, R., and Scheres, B. (2008). Auxin: the looping star in plant development. *Annu. Rev. Plant Biol.* *59*, 443-465.
- Bhatia, N., Bozorg, B., Larsson, A., Ohno, C., Jönsson, H., & Heisler, M. G. (2016). Auxin acts through MONOPTEROS to regulate plant cell polarity and pattern phyllotaxis. *Curr. Biol.* *26*, 3202-3208.
- Barbosa, I. C., Hammes, U. Z., Schwechheimer, C. (2018). Activation and polarity control of PIN-FORMED auxin transporters by phosphorylation. *Trends Plant Sci.* *23*, 523-538.
- Cao, M., Chen, R., Li, P., Yu, Y., Zheng, R., Ge, D., et al. (2019). TMK1-mediated auxin signalling regulates differential growth of the apical hook. *Nature* *568*, 240-243.
- Dhonukshe, P., Aniento, F., Hwang, I., Robinson, D. G., Mravec, J., Stierhof, Y. D., Friml, J. (2007). Clathrin-mediated constitutive endocytosis of PIN auxin efflux carriers in *Arabidopsis*. *Curr. Biol.* *17*, 520-527.
- Friml, J. (2010). Subcellular trafficking of PIN auxin efflux carriers in auxin transport. *Eur. J. Cell Biol.* *89*, 231-235.
- Fendrych, M., Akhmanova, M., Merrin, J., Glanc, M., Hagihara, S., Takahashi, K., Friml, J. (2018). Rapid and reversible root growth inhibition by TIR1 auxin signalling. *Nat. Plants* *4*, 453-459.
- Geldner, N., Friml, J., Stierhof, Y. D., Jürgens, G., Palme, K. (2001). Auxin transport inhibitors block PIN1 cycling and vesicle trafficking. *Nature* *413*, 425.
- Geldner, N., Anders, N., Wolters, H., Keicher, J., Kornberger, W., Muller, P., et al. (2003). The Arabidopsis GNOM ARF-GEF mediates endosomal recycling, auxin transport, and auxin-dependent plant growth. *Cell* *112*, 219-230.
- Glanc, M., Fendrych, M., Friml, J. (2018). Mechanistic framework for cell-intrinsic re-establishment of PIN2 polarity after cell division. *Nat. Plants* *4*, 1082-1088.
- Govindaraju, P., Verna, C., Zhu, T., Scarpella, E. (2020). Vein patterning by tissue-specific auxin transport. *Development* *147*, dev187666

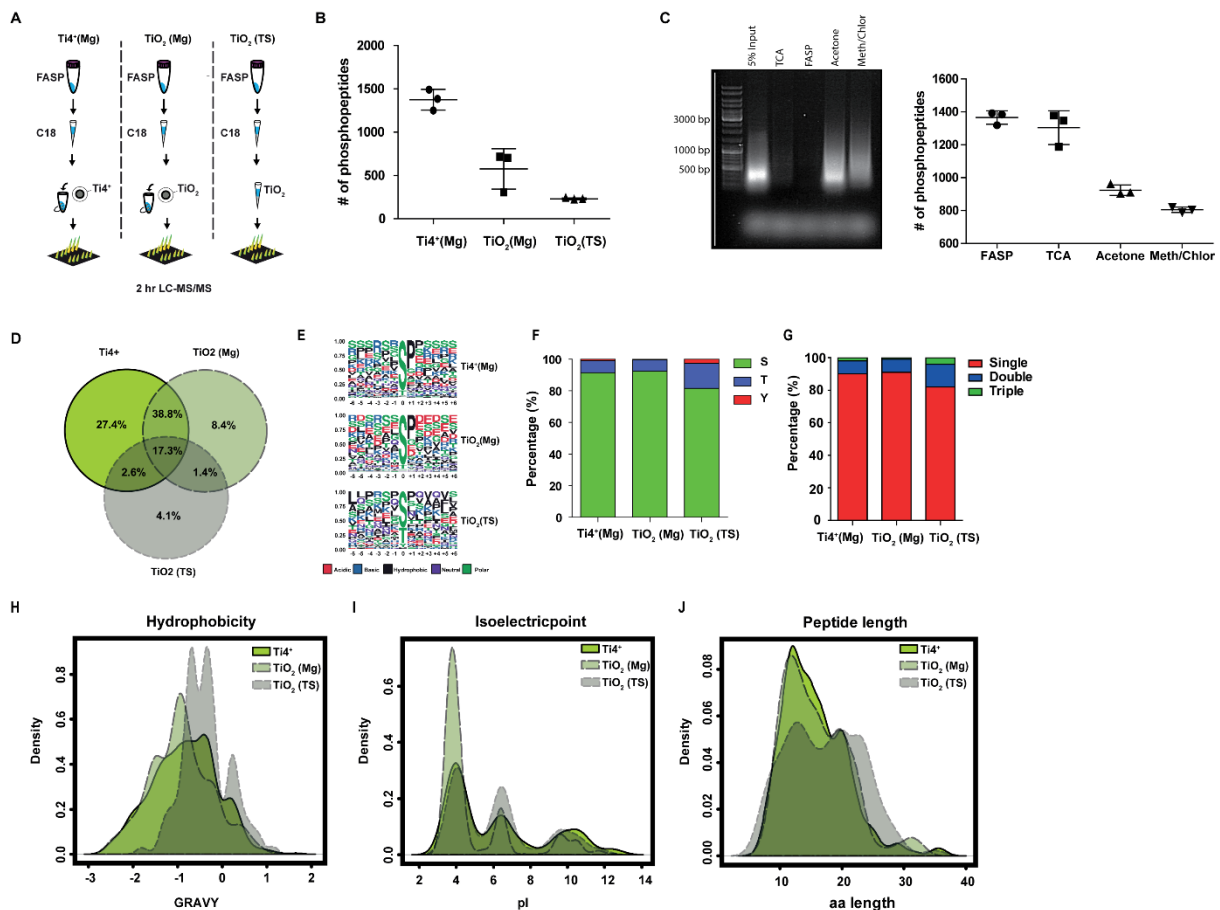
- Heisler, M. G., Ohno, C., Das, P., Sieber, P., Reddy, G. V., Long, J. A., Meyerowitz, E. M.** (2005). Patterns of auxin transport and gene expression during primordium development revealed by live imaging of the Arabidopsis inflorescence meristem. *Curr. Biol.* *15*, 1899-1911.
- Humphrey, S. J., Azimifar, S. B., Mann, M.** (2015). High-throughput phosphoproteomics reveals in vivo insulin signaling dynamics. *Nat. Biotechnol.* *33*, 990-995.
- Hooper, C. M., Castleden, I. R., Tanz, S. K., Aryamanesh, N., Millar, A. H.** (2017). SUBA4: the interactive data analysis centre for Arabidopsis subcellular protein locations. *Nucleic Acids Res.* *45*, D1064-D1074.
- Han, H., Rakusova, H., Verstraeten, I., Zhang, Y., Friml, J.** (2020). SCF^{TIR1/AFB} auxin signaling for bending termination during shoot gravitropism. *Plant Physiol.* *183*, 37-40
- Kleine-Vehn, J., Leitner, J., Zwiewka, M., Sauer, M., Abas, L., Luschig, C., Friml, J.** (2008). Differential degradation of PIN2 auxin efflux carrier by retromer-dependent vacuolar targeting. *Proc. Natl. Acad. Sci. USA* *105*, 17812-17817.
- Kitakura, S., Vanneste, S., Robert, S., Löffke, C., Teichmann, T., Tanaka, H., Friml, J.** (2011). Clathrin mediates endocytosis and polar distribution of PIN auxin transporters in *Arabidopsis*. *Plant Cell* *23*, 1920-1931.
- Kurth, E. G., Peremyslov, V. V., Turner, H. L., Makarova, K. S., Iranzo, J., Mekhedov, S. L., Koonin, E. V., Dolja, V. V.** (2017). Myosin-driven transport network in plants. *Proc. Natl. Acad. Sci. USA* *114*, E1385-E1394.
- Kubeš, M., Napier, R.** (2019). Non-canonical auxin signalling: fast and curious. *J. Exp. Bot.* *70*, 2609.
- Lewis, D. R., Olex, A. L., Lundy, S. R., Turkett, W. H., Fetrow, J. S., Muday, G. K.** (2013). A kinetic analysis of the auxin transcriptome reveals cell wall remodeling proteins that modulate lateral root development in Arabidopsis. *Plant Cell* *25*, 3329-3346.
- McClure, B. A., Hagen, G., Brown, C. S., Gee, M. A., Guilfoyle, T. J.** (1989). Transcription, organization, and sequence of an auxin-regulated gene cluster in soybean. *Plant Cell*, *1*, 229-239.
- Mazur, E., Benková, E., Friml, J.** (2016). Vascular cambium regeneration and vessel formation in wounded inflorescence stems of Arabidopsis. *Sci. Rep.* *6*, 33754.
- Mazur, E., Gallei, M., Adamowski, M., Han, H., Robert, H. S., Friml, J.** (2020a). Clathrin-mediated trafficking and PIN trafficking are required for auxin canalization and vascular tissue formation in Arabidopsis. *Plant Sci.* *293*, 110414.
- Mazur, E., Kulik, I., Hajný, J., Friml, J.** (2020b). Auxin canalization and vascular tissue formation by TIR1/AFB-mediated auxin signaling in Arabidopsis. *New Phytol.* *226*, 1375-1383.
- Morffy, N., and Strader, L. C.** (2020). Old Town Roads: routes of auxin biosynthesis across kingdoms. *Curr Opin Plant Biol.* *55*, 21-27.
- Okamoto, K., Ueda, H., Shimada, T., Tamura, K., Kato, T., Tasaka, M., Morita, M. T., Hara-Nishimura, I.** (2015). Regulation of organ straightening and plant posture by an actin-myosin XI cytoskeleton. *Nat. Plants* *1*, 15031.
- Nikonorova, N., Van den Broeck, L., Zhu, S., Van De Cotte, B., Dubois, M., Gevaert, K., et al.** (2018). Early mannitol-triggered changes in the Arabidopsis leaf (phospho) proteome reveal growth regulators. *J. Exp. Bot.* *69*, 4591-4607.
- Ojangu, E. L., Ilau, B., Tanner, K., Talts, K., Ihoma, E., Dolja, V. V., Paves, H., Truve, E.** (2018). Class XI myosins contribute to auxin response and senescence-induced cell death in *Arabidopsis*. *Front. Plant Sci.* *9*, 1570

- Oochi, A., Hajny, J., Fukui, K., Nakao, Y., Gallei, M., Quareshy, M., et al. (2019). Pinstatic acid promotes auxin transport by inhibiting PIN internalization. *Plant physiol.* *180*, 1152-1165.
- Paciorek, T., Zažímalová, E., Ruthardt, N., Petrášek, J., Stierhof, Y. D., Kleine-Vehn, J., Morris, A. D., Emans, N., Jürgens, G., Geldner, N., Friml, J. (2005). Auxin inhibits endocytosis and promotes its own efflux from cells. *Nature* *435*, 1251.
- Petrášek, J., Mravec, J., Bouchard, R., Blakeslee, J. J., Abas, M., Seifertová, D., et al. (2006). PIN proteins perform a rate-limiting function in cellular auxin efflux. *Science* *312*, 914-918.
- Prokhnovsky, A. I., Peremyslov, V. V., Dolja, V. V. (2008). Overlapping functions of the four class XI myosins in *Arabidopsis* growth, root hair elongation, and organelle motility. *Proc. Natl. Acad. Sci. USA* *105*, 19744-19749.
- Peremyslov, V. V., Prokhnovsky, A. I., Avisar, D., Dolja, V. V. (2008). Two class XI myosins function in organelle trafficking and root hair development in *Arabidopsis*. *Plant Physiol.* *146*, 1109-1116.
- Paponov, I. A., Paponov, M., Teale, W., Menges, M., Chakrabortee, S., Murray, J. A., Palme, K. (2008). Comprehensive transcriptome analysis of auxin responses in *Arabidopsis*. *Mol. Plant* *1*, 321-337.
- Peremyslov, V. V., Morgun, E. A., Kurth, E. G., Makarova, K. S., Koonin, E. V., Dolja, V. V. (2013). Identification of myosin XI receptors in *Arabidopsis* defines a distinct class of transport vesicles. *Plant Cell* *25*, 3022-3038.
- Prát, T., Hajný, J., Grunewald, W., Vasileva, M., Molnár, G., Tejos, R., Schmid, M., Sauer, M., Friml, J. (2018). WRKY23 is a component of the transcriptional network mediating auxin feedback on PIN polarity. *PLoS Genet.* *14*, e1007177.
- Reddy, A. S., Day, I. S. (2001). Analysis of the myosins encoded in the recently completed *Arabidopsis thaliana* genome sequence. *Genome Biol.* *2*, research0024.
- Rashotte, A. M., DeLong, A., & Muday, G. K. (2001). Genetic and chemical reductions in protein phosphatase activity alter auxin transport, gravity response, and lateral root growth. *Plant Cell*, *13*, 1683-1697.
- Robert, S., Kleine-Vehn, J., Barbez, E., Sauer, M., Paciorek, T., Baster, P., et al. (2010). ABP1 mediates auxin inhibition of clathrin-dependent endocytosis in *Arabidopsis*. *Cell* *143*, 111-121.
- Rakusová, H., Gallego-Bartolomé, J., Vanstraelen, M., Robert, H. S., Alabadí, D., Blázquez, M. A., et al. (2011). Polarization of PIN3-dependent auxin transport for hypocotyl gravitropic response in *Arabidopsis thaliana*. *Plant J.* *67*, 817-826.
- Robert, H. S., Grones, P., Stepanova, A. N., Robles, L. M., Lokerse, A. S., Alonso, J. M., et al. (2013). Local auxin sources orient the apical-basal axis in *Arabidopsis* embryos. *Curr. Biol.* *23*, 2506-2512.
- Rakusová, H., Abbas, M., Han, H., Song, S., Robert, H. S., Friml, J. (2016). Termination of shoot gravitropic responses by auxin feedback on PIN3 polarity. *Curr. Biol.* *26*, 3026-3032.
- Ryan, J. M., Nebenführ, A. (2017). Update on myosin motors: molecular mechanisms and physiological functions. *Plant Physiol.* *176*, 119-127.
- Rakusová, H., Han, H., Valošek, P., Friml, J. (2019). Genetic screen for factors mediating PIN polarization in gravistimulated *Arabidopsis thaliana* hypocotyls. *Plant J.* *98*, 1048-1059
- Sachs, T. The control of the patterned differentiation of vascular tissues. *Adv. Bot. Res.* *9*, 151-162 (1981).

- Scarpella, E., Marcos, D., Friml, J., Berleth, T.** (2006). Control of leaf vascular patterning by polar auxin transport. *Genes Dev.* *20*, 1015-1027.
- Sauer, M., Balla, J., Luschnig, C., Wiśniewska, J., Reinöhl, V., Friml, J., Benková, E.** (2006). Canalization of auxin flow by Aux/IAA-ARF-dependent feedback regulation of PIN polarity. *Genes Dev.* *20*, 2902-2911.
- Sattarzadeh, A., Franzen, R., Schmelzer, E.** (2008). The Arabidopsis class VIII myosin ATM2 is involved in endocytosis. *Cell Motil Cytoskeleton* *65*, 457-468.
- Steinman, M. Q. and Trainor, B. C.** (2010) Rapid Effects of Steroid Hormones on Animal Behavior. *Nature Education Knowledge* *3*, 1
- Stecker, K.E., Minkoff, B.B., Sussman, M. R.** (2014) Phosphoproteomic analyses reveal early signaling events in the osmotic stress response. *Plant Physiol.* *165*, 1171-1187.
- Salehin, M., Bagchi, R., Estelle, M.** (2015). SCF^{TIR1/AFB}-based auxin perception: mechanism and role in plant growth and development. *Plant Cell* *27*, 9-19.
- Shih, H. W., DePew, C. L., Miller, N. D., Monshausen, G. B.** (2015). The cyclic nucleotide-gated channel CNGC14 regulates root gravitropism in *Arabidopsis thaliana*. *Curr. Biol.* *25*, 3119-3125.
- Talts, K., Ilau, B., Ojangu, E. L., Tanner, K., Peremyslov, V. V., Dolja, V. V., Truve, E., Paves, H.** (2016). Arabidopsis myosins XI1, XI2, and XIK are crucial for gravity-induced bending of inflorescence stems. *Front. Plant Sci.* *7*, 1932
- Tan, S., Zhang, X., Kong, W., Yang, X. L., Molnár, G., Vondráková, Z., et al.** (2020). The lipid code-dependent phosphoswitch PDK1–D6PK activates PIN-mediated auxin efflux in Arabidopsis. *Nat. Plants* *6*, 556-569
- Vieten, A., Vanneste, S., Wiśniewska, J., Benková, E., Benjamins, R., Beeckman, T., et al.** (2005). Functional redundancy of PIN proteins is accompanied by auxin-dependent cross-regulation of PIN expression. *Development* *132*, 4521-4531.
- Vanneste, S., and Friml, J.** (2009). Auxin: a trigger for change in plant development. *Cell* *136*, 1005-1016.
- Vu, L. D., Stes, E., Van Bel, M., Nelissen, H., Maddelein, D., Inzé, D., De Smet, I.** (2016). Up-to-date workflow for plant (phospho) proteomics identifies differential drought-responsive phosphorylation events in maize leaves. *J. of proteome Res.* *15*, 4304-4317.
- Wiśniewska, J., Xu, J., Seifertová, D., Brewer, P. B., Růžička, K., Blilou, I., et al.** (2006). Polar PIN localization directs auxin flow in plants. *Science* *312*, 883-883.
- Wabnik, K., Kleine-Vehn, J., Balla, J., Sauer, M., Naramoto, S., Reinöhl, V., et al.** (2010). Emergence of tissue polarization from synergy of intracellular and extracellular auxin signaling. *Mol. Syst. Biol.* *6*, 447.
- Wabnik, K., Govaerts, W., Friml, J., Kleine-Vehn, J.** (2011). Feedback models for polarized auxin transport: an emerging trend. *Mol. Syst. Biol.* *7*, 2352-2359.
- Wu, L., Hu, X., Wang, S., Tian, L., Pang, Y., Han, Z., et al.** (2015). Quantitative analysis of changes in the phosphoproteome of maize induced by the plant hormone salicylic acid. *Sci. Rep.* *5*, 1-16.
- Wendrich, J. R., Boeren, S., Möller, B. K., Weijers, D., De Rybel, B.** (2017). In vivo identification of plant protein complexes using IP-MS/MS. *Methods Mol. Biol.* *1497*, 147-158.
- Xu, T., Dai, N., Chen, J., Nagawa, S., Cao, M., Li, H., et al.** (2014). Cell surface ABP1-TMK auxin-sensing complex activates ROP GTPase signaling. *Science* *343*, 1025-1028.
- Xiao, Y., Offringa, R.** (2020). PDK1 regulates auxin transport and Arabidopsis vascular development through AGC1 kinase PAX. *Nat. Plants* *6*, 544-555.

- Zhang, J., Nodzyński, T., Pěňčík, A., Rolčík, J., Friml, J.** (2010). PIN phosphorylation is sufficient to mediate PIN polarity and direct auxin transport. *107*(2), 918-922.
- Žádníková, P., Petrášek, J., Marhavý, P., Raz, V., Vandenbussche, F., Ding, Z., Schwarzerová, K., Morita, M. T., Tasaka, M., Hejátko, J., Van Der Straeten, D., Friml, J., Benková, E.** (2010). Role of PIN-mediated auxin efflux in apical hook development of *Arabidopsis thaliana*. *Development* *137*, 607-617.
- Zhang, H., Zhou, H., Berke, L., Heck, A. J., Mohammed, S., Scheres, B., Menke, F. L.** (2013). Quantitative phosphoproteomics after auxin-stimulated lateral root induction identifies an SNX1 protein phosphorylation site required for growth. *Mol. Cell Proteomics* *12*, 1158-1169.
- Zhang, W., Cai, C., Staiger, C.J.** (2019). Myosins XI Are Involved in Exocytosis of Cellulose Synthase Complexes. *Plant Physiol.* *179*, 1537-1555.
- Zhang, J., Mazur, E., Balla, J., Gallei, M., Kalousek, P., Medved'ová, Z., et al.,** (2020). Strigolactones inhibit auxin feedback on PIN-dependent auxin transport canalization. *Nat. Commun.* *11*, 1-10.

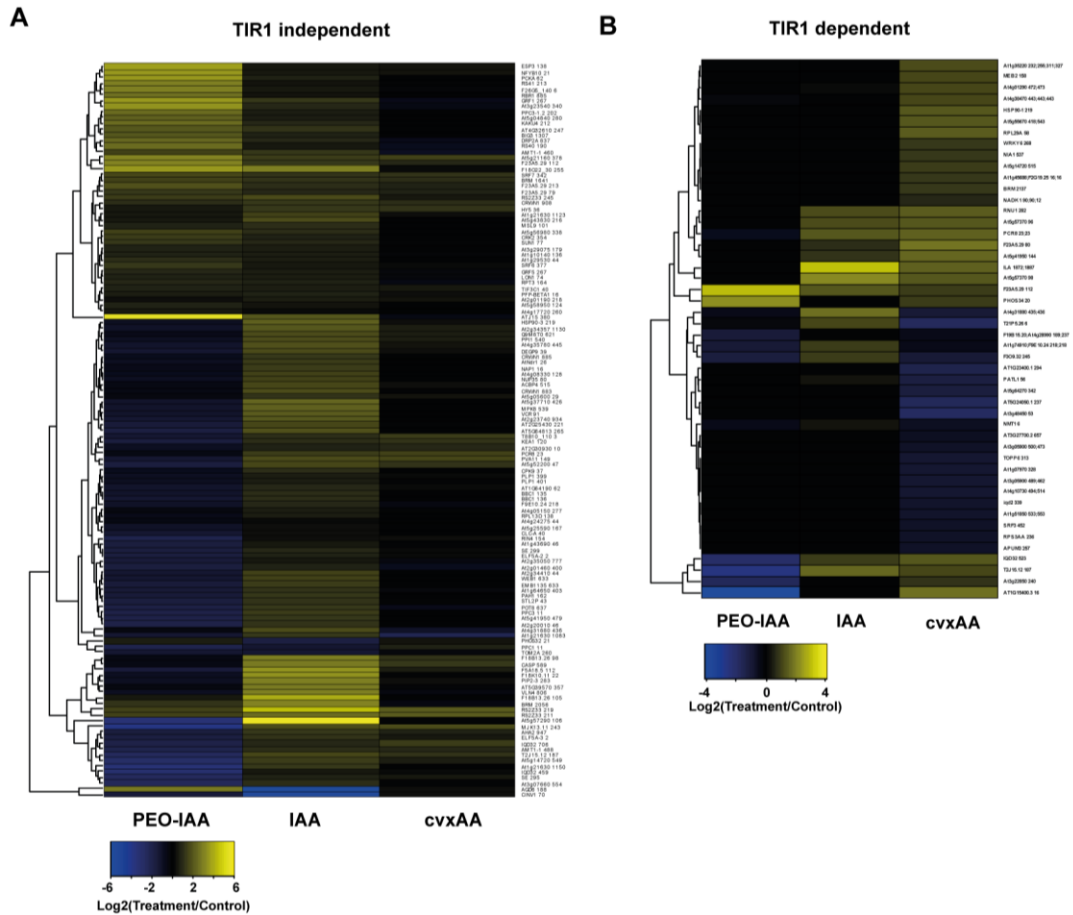
4.6 Supplementary Figures



Supplementary Figure 1. Comparison of different protein precipitation and phosphopeptide enrichment strategies.

(A, B) Magnetic IMAC, MOAC (Mg) and agarose MOAC (TS) enrichment strategies were compared for phosphopeptide enrichment performance. IMAC outperforms the MOAC method by identifying ~3 fold more phosphopeptides. All enrichments were conducted in technical triplicate. (C) Peptide digested samples were compared to 5 % protein lysate input material for nucleic acid interference on a DNA agarose gel. Phosphopeptide identifications supports DNA gel analysis by poor performance of acetone and methanol/chloroform precipitation techniques. All samples were performed in technical triplicate and phosphopeptides were enriched by the Ti^{4+} -IMAC method. (D) Venn diagram of enriched phosphopeptides show little overlap between the different enrichment methods.

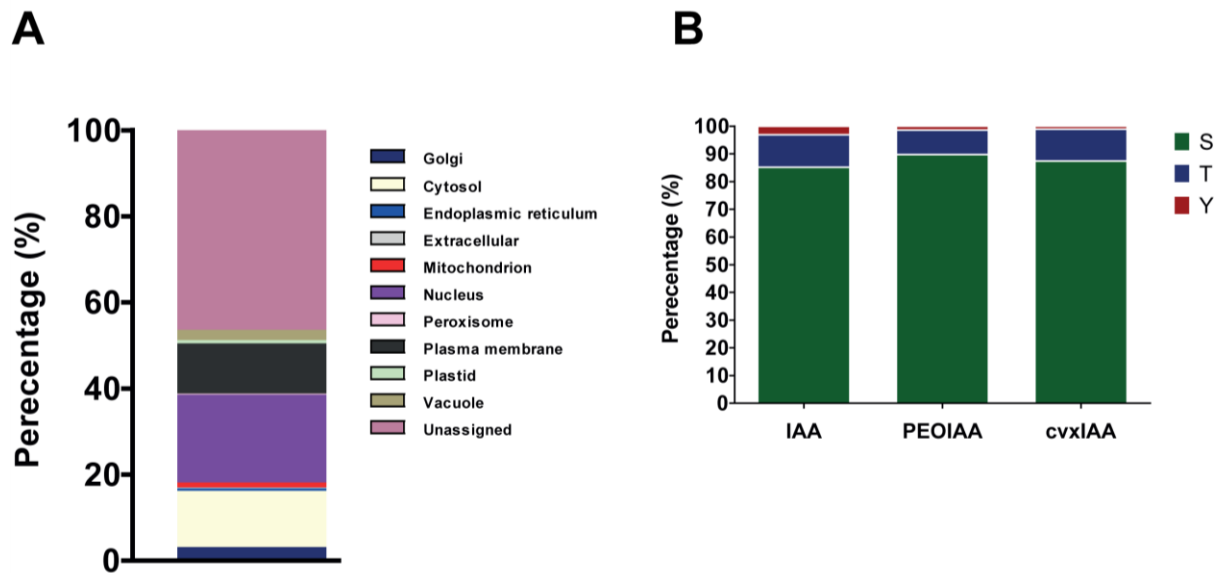
(E) Motif analysis from the specific enriched peptides shows a bias towards acidic peptides for TiO_2 (Mg). No discernible differences were observed in phosphorylated amino acid (F) or charge state (G). Biochemical properties of specific peptides show a bias in acidic peptides for TiO_2 (Mg) (H-J).



Supplementary Figure 2. TIR1-dependent and -independent rapid auxin response.

(A) Overlapping significantly regulated phosphopeptides of IAA and PEO-IAA dataset with the same phosphosite shows partial opposite regulation in a TIR1-independent manner. Corresponding sites show no regulation in the cvxIAA set as seen by predominantly black colour.

(B) Significant TIR1 dependent phosphosites (cvxIAA) mapped to phosphopeptides of IAA and PEO-IAA dataset. Only non-significant IAA and PEO-IAA phosphopeptides mapped to significantly regulated cvxIAA peptides



Supplementary Figure 3. Analysis of phosphopeptide datasets.

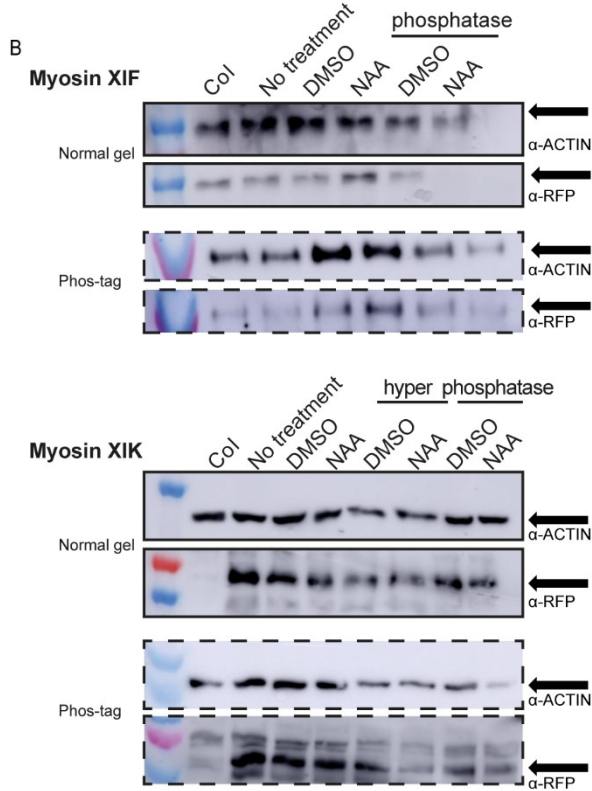
(A) Proteins represented by differentially regulated phosphopeptides (FDR ≤ 0.05) from the 100 nM IAA dataset show a predominant localization in the nucleus, cytoplasm and plasma membrane. (B) The overall nature of phosphorylated amino acids followed previously published percentages (Serine ~90%, Threonine ~7 and Tyrosine ~1%) Wu et.al. 2016.

A

```

XIG: LAYWLINTSALIFLLQKSLKPAGAGATASKKPPITTSFLGRMALSFRSSPNLAAAAEAAALAVIR
XIH: LAYWLINTSALIFLLQKSLKPAGAGATASKKPPITTSFLGRMALSFRSSPNLAAAAEAAALAVIR
XIB: LAYWLINTSALIFLLQKSLKPAGAGATASKKPPITTSFLGRMALSFRSSPNLAAAAEAAALAVIR
XIA: LINTSTLIFLLQSLRQSSSTGSSPTKPPQ-----PTSFFGRMTQGFRTSSPNLSTDVV
XID: LAYWLINTSTLIFLLQSLKSHSTTGASPKKPPQP-TSFFGRMTQGFRTSSASLSGDVV
XIF: LYLLQSTLKFSTNTNNAASRRNRSSHATLFGRLVQGMQPS---SVGLETSSGYSGMAGIPN
XII: LYLLQSTLKFSTNTNNAASRRNRSSHATLFGRLVQGMQPS---SVGLETSSGYSGMAGIPNDQ
XIC: LLFLQRTIKASGAAGMAPQRRSSSATLFGRMSQSFRTGAP---PGVNIAMINGAAGGADTFR
XIE: LLFLQRTIKASGAAGMAPQRRSSSATLFGRMTQSFRTGTP---QGVNIAMINGGVDTL
XIK: LLFLQRTIKATGAASLTPORRRTTASLFGRMSQGLRGSP---QSAGIFLNRQGLTKLDDLRL
XII: LLQRTLKAGATGSIITPRRGM-PSSLFGRVQSFRGSP-----QSAGFPFMTGRAIGGGLDELRL
XII: LRSNSFLNASAQSGRAAYGVKSPFKL-HGPDDGASHIEARYPALLFKQQLTACVEKIYGLIRD

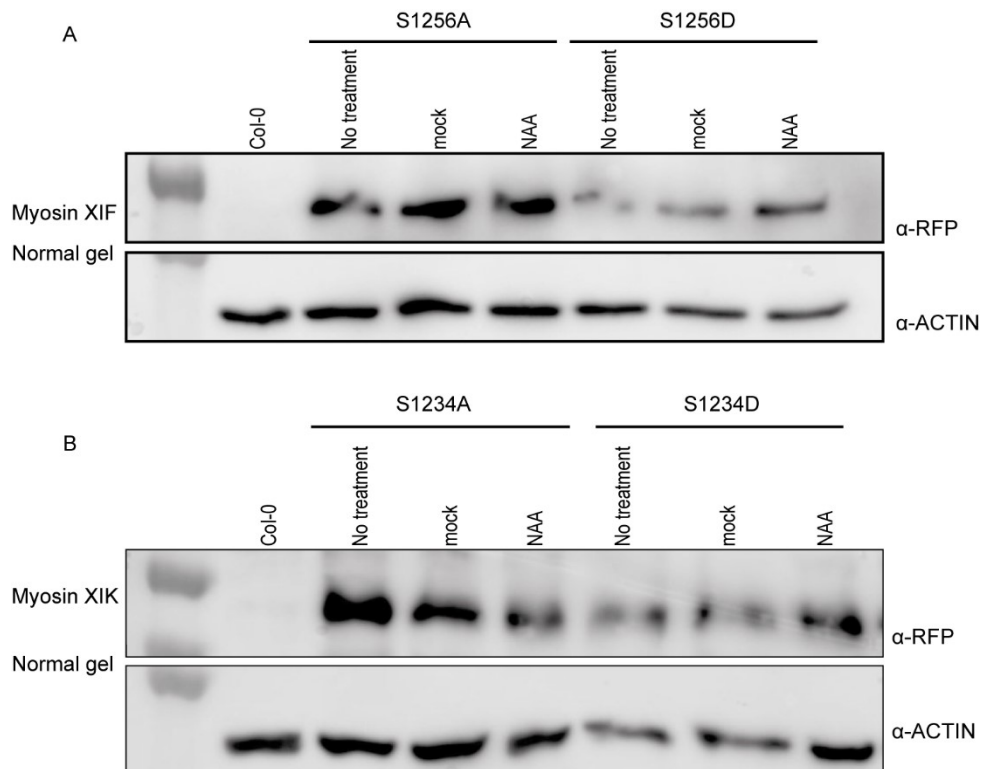
```



Supplementary Figure S4. Conserved phosphorylation site at myosin XI protein family.

(A) Protein alignment of some myosin XI proteins shows the conserved phosphorylation site at the GTD sequence.

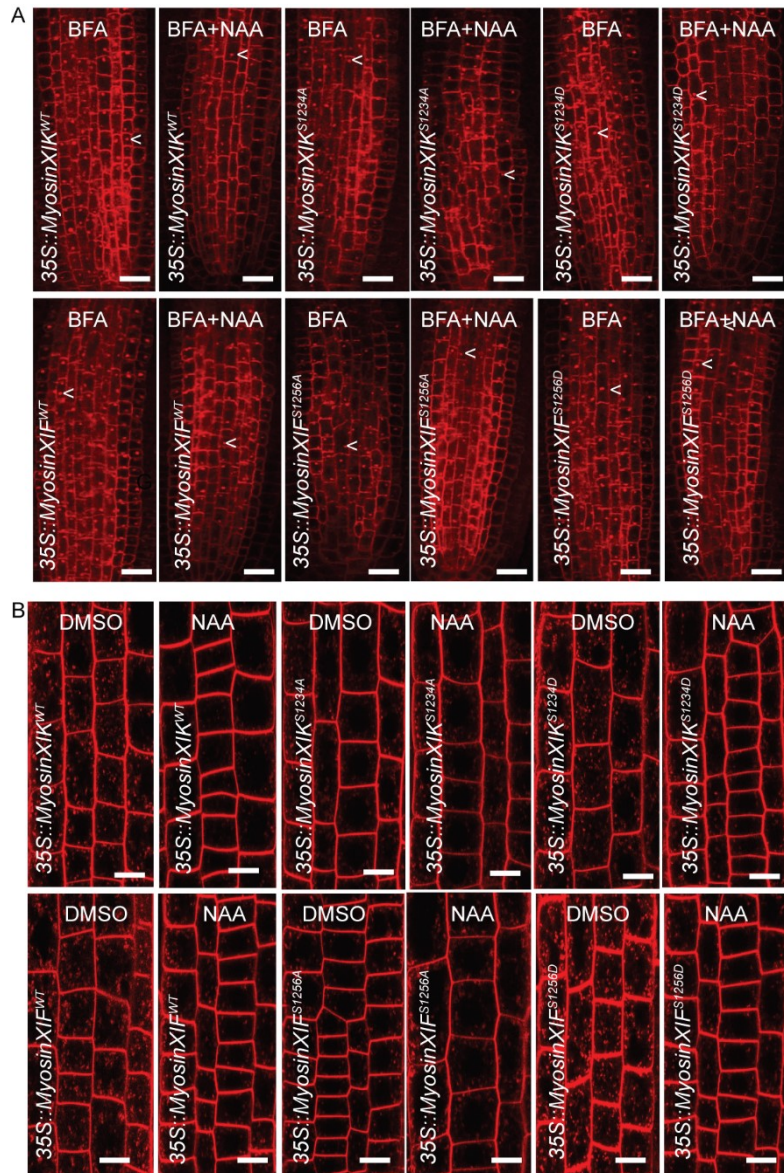
(B) Normal western blot assay of Myosin XIK and XIF and quantification of the phosphorylation ratio of Myosin XIK and XIF upon auxin treatment.



Supplementary Figure S5. Phosphorylation assay of the phospho-deficient and phospho-mimic myosin mutants (Col-0 background).

(A - B) Normal western blot assay of Myosin XIF and quantification of the phosphorylation ratio of phospho-deficient and phospho-mimic mutants upon auxin treatment.

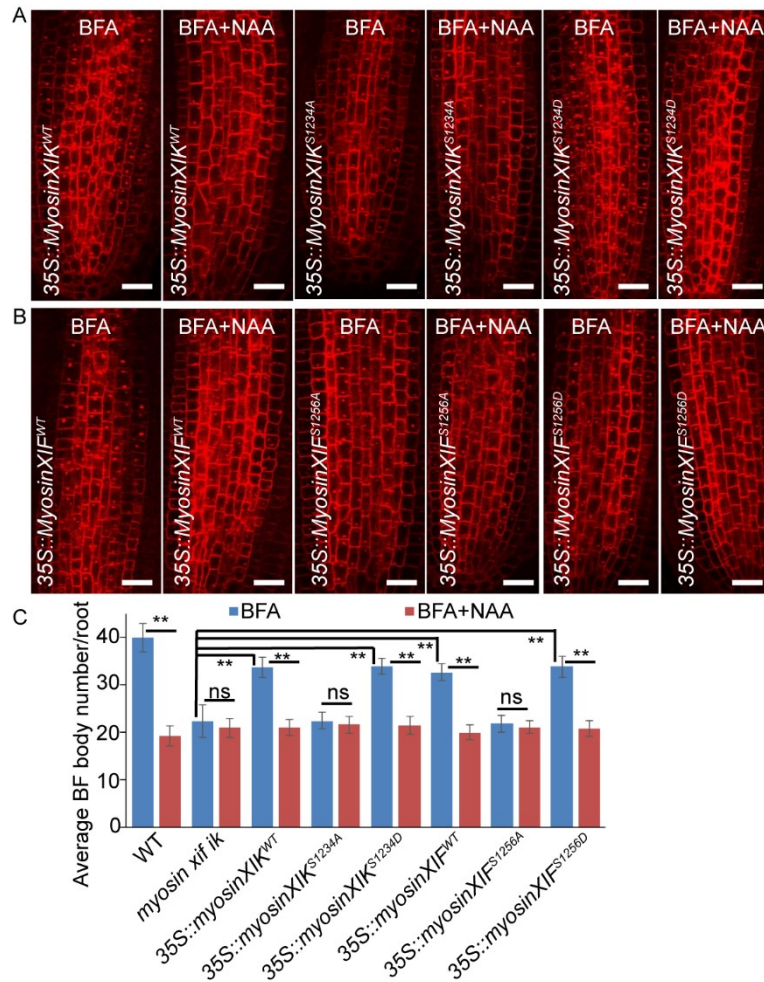
(C - D) Normal western blot assay of Myosin XIK and quantification of the phosphorylation ratio of phospho-deficient and phospho-mimic mutants upon auxin treatment.



Supplementary Figure S6. PIN trafficking in phospho-deficient and phospho-mimic myosin mutants (Col-0 background).

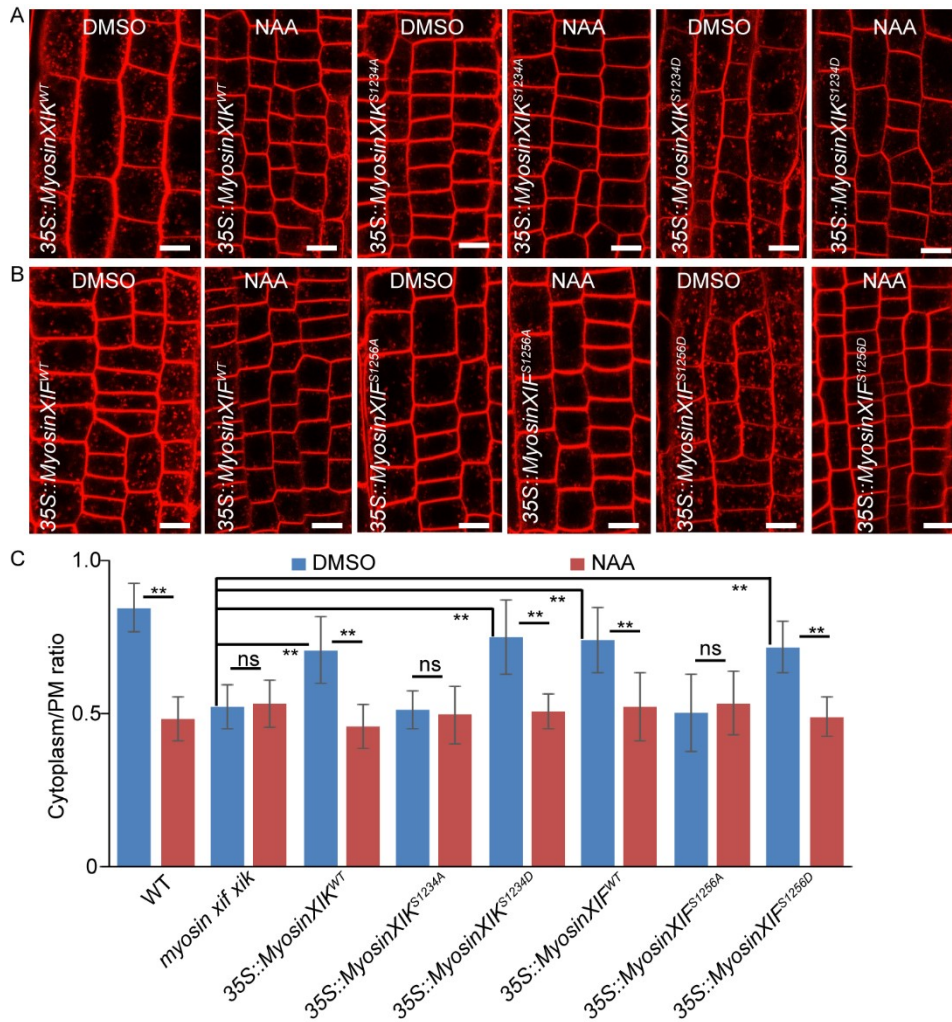
(A) Representative images showing BFA bodies in phospho-deficient and phospho-mimic myosin mutant root.

(B) Representative images showing FM4-64 uptake in phospho-deficient and phospho-mimic myosin mutant root. Arrowheads indicate BFA body in root. Scale bars, 20 μm.



Supplementary Figure S7. PIN trafficking in phospho-deficient and phospho-mimic myosin mutants (*myosin xik xif* mutant background).

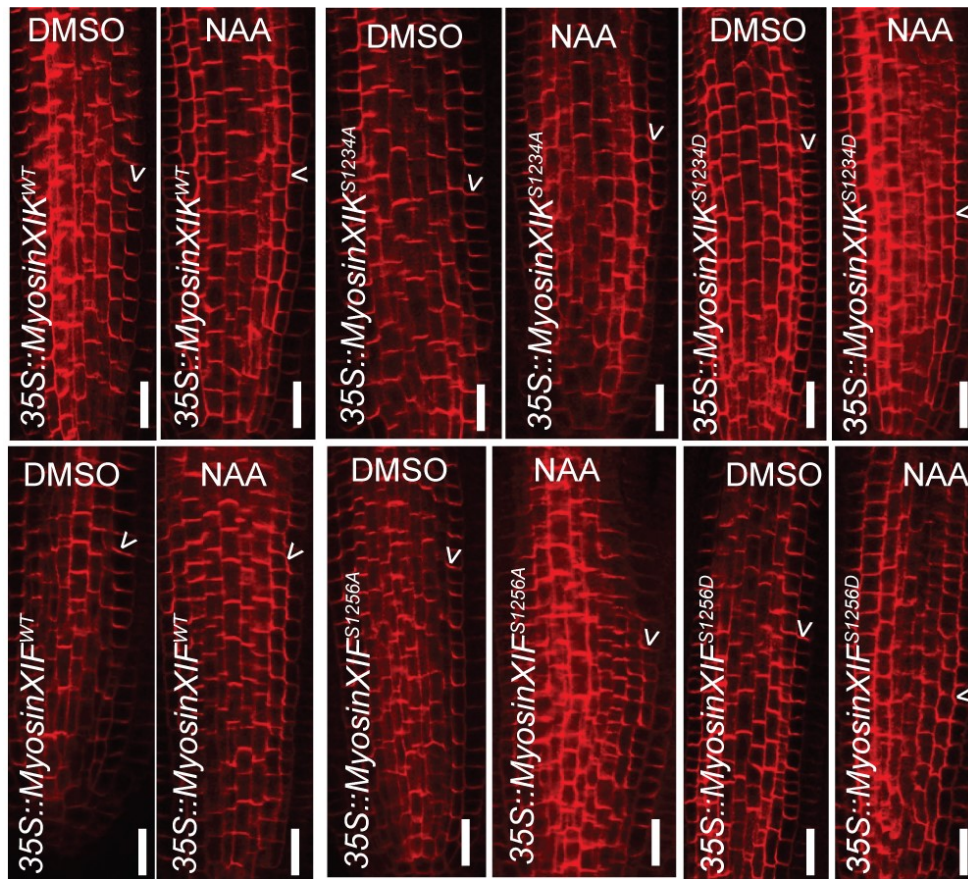
(A - B) Representative images showing BFA bodies in phospho-deficient and phospho-mimic myosin mutant root. (C) Quantification of BFA bodies in phospho-deficient and phospho-mimic myosin mutant root (*myosin xik xif* mutant background). The BFA body was counted in each root, average BFA bodies were calculated. Data and error bars represent the mean ± SD. n > 15, ** P < 0.05 determined by Student's t-test.



Supplementary Figure S8. Fm4-64 uptake assay in phospho-deficient and phospho-mimic myosin mutants (*myosin xik xif* mutant background).

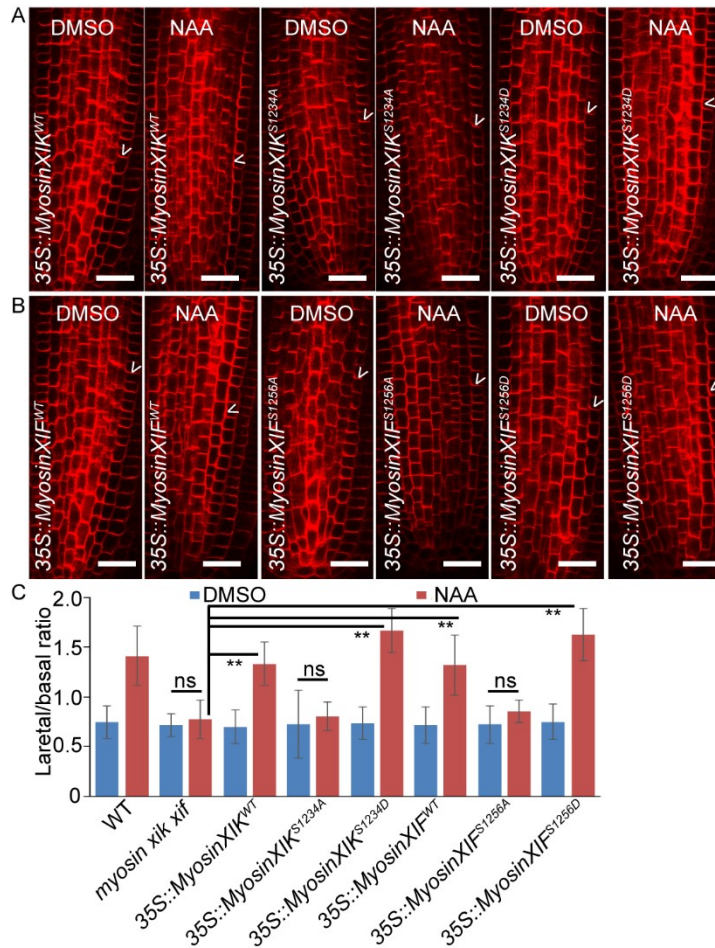
(A - B) Representative images showing FM4-64 uptake in phospho-deficient and phospho-mimic myosin mutant root.

(C) Quantification of FM4-64 uptake in phospho-deficient and phospho-mimic myosin mutant root (*myosin xik xif* mutant background). The ratio was calculated by dividing signal between cytoplasm and plasm membrane. Data and error bars represent the mean \pm SD. n = 10, more than 50 cells were quantified, ** $P < 0.05$ determined by Student's t-test.



Supplementary Figure S9. Auxin-induced PIN1 laterlization in phospho-deficient and phospho-mimic myosin mutants (Col-0 background).

Representative images showing PIN1 localization in phospho-deficient and phospho-mimic myosin mutant root. Arrowheads indicate PIN1 localization in root. Scale bars, 20 μm.

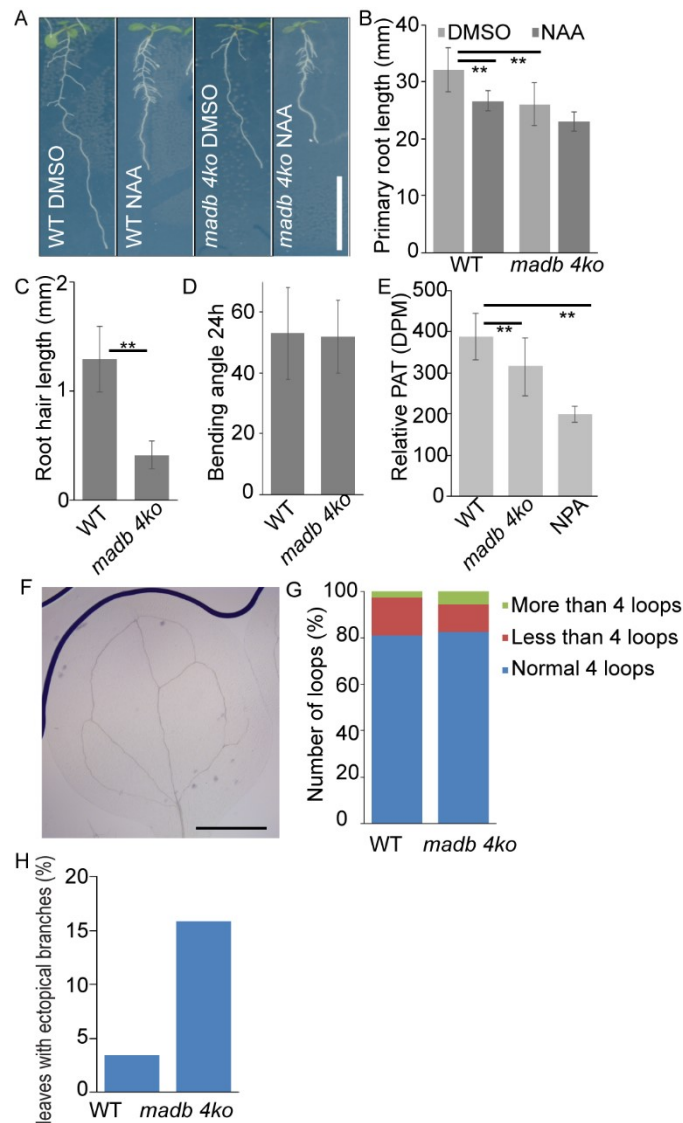


Supplementary Figure S10. Auxin-induced PIN1 lateralization in phospho-deficient and phospho-mimic myosin mutants (*myosin xik xif* mutant background).

(A – B) Representative images showing PIN1 localization in phospho-deficient and phospho-mimic myosin mutant root.

(C) Quantification of auxin-mediated PIN1 lateralization. The ratio was calculated by dividing PIN1 signal between lateral side and basal side in root endodermal cells. Data and error bars represent the mean \pm SD. n = 15, more than 50 cells were quantified, ** $P < 0.05$ determined by Student's t-test.

Arrowheads indicate PIN1 localization in root. Scale bars, 20 μ m.



Supplementary Figure S11. Auxin canalization related phenotype of *madb 4ko* mutant.

(A) Representative images showing root growth defects in *madb 4ko* mutant upon auxin treatment. (B) Quantification of primary root length in *madb 4ko* mutant upon auxin treatment. Data and error bars represent the mean \pm SD. n = 30 - 40, ** $P < 0.05$ determined by Student's t-test.

(C) Quantification of root hair length in *madb 4ko* mutant upon auxin treatment. Data and error bars represent the mean \pm SD. n = 30 - 40, ** $P < 0.05$ determined by Student's t-test.

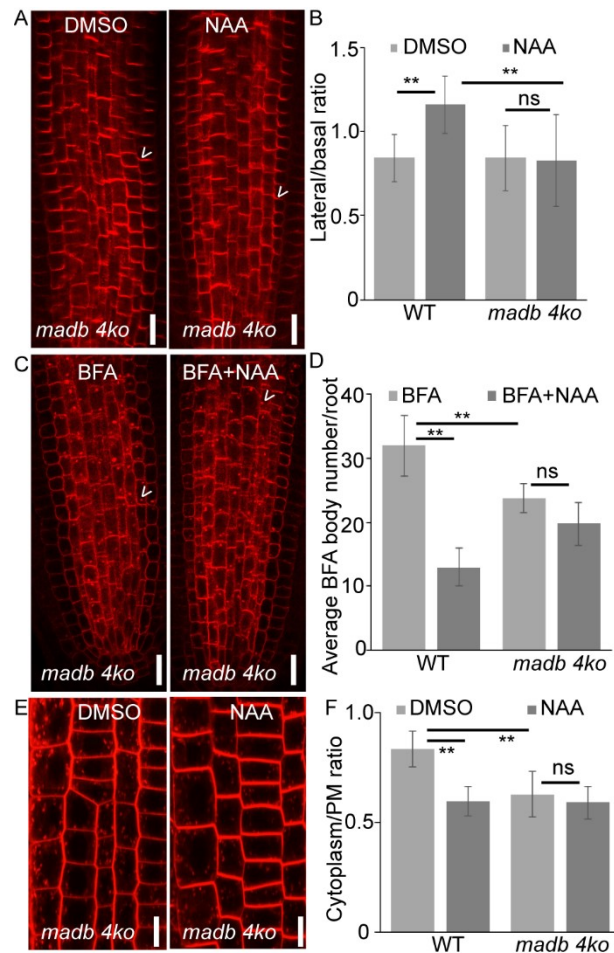
(D) Hypocotyl gravitropic bending after 24 hours gravity stimulation in *madb 4ko* mutant. 3 days old etiolated seedlings were gravistimulated for 24 hours, and bending angle was quantified.

(E) Polar auxin transport in *madb 4ko* mutant. Data and error bars represent the mean \pm SD. n = 15, ** $P < 0.05$ determined by Student's t-test.

(F) Represented Leaf venation defects in *madb 4ko* mutant.

(G) Quantification of loops defects in *madb 4ko* mutant.

(H) Quantification of ectopic branches in *madb 4ko* mutant.



Supplementary Figure S12. The Madb2 myosin binding protein contribute to PIN trafficking and polarity regulation.

(A) Representative images showing PIN1 localization in *madb 4ko* mutant upon auxin treatment. (B) Quantification of auxin-mediated PIN1 lateralization in *madb 4ko* mutant root. The ratio was calculated by dividing PIN1 signal between lateral side and basal side in root endodermal cells. Data and error bars represent the mean \pm SD. $n = 15$, more than 50 cells were quantified, ** $P < 0.05$ determined by Student's t-test.

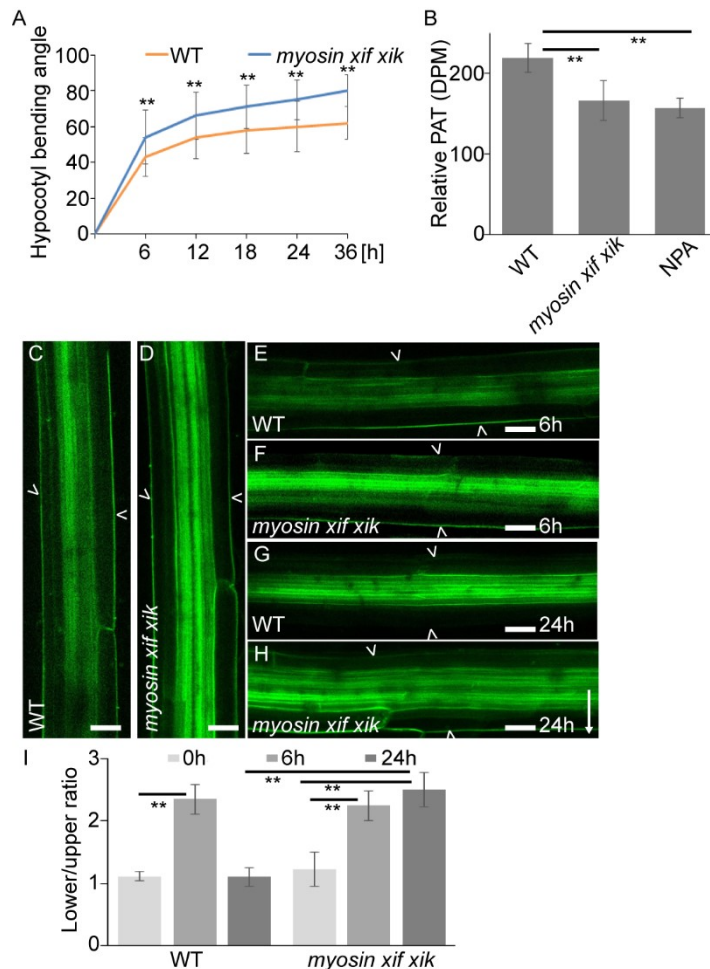
(C) Representative images showing PIN1 trafficking in *madb 4ko* mutant root.

(D) Quantification of BFA bodies in *madb 4ko* mutant root. The BFA body was counted in each root, average BFA bodies were calculated. Data and error bars represent the mean \pm SD. $n > 15$, ** $P < 0.05$ determined by Student's t-test.

(E) Representative images showing FM4-64 uptake in *madb 4ko* mutant root.

(F) Quantification of FM4-64 uptake in *madb 4ko* mutant root. The ratio was calculated by dividing signal between cytoplasm and plasm membrane. Data and error bars represent the mean \pm SD. $n = 10$, more than 50 cells were quantified, ** $P < 0.05$ determined by Student's t-test.

Arrowheads indicate PIN1 localization or BFA body in root. Scale bars, 20 μm .



Supplementary Figure S13. Gravity-induced PIN3 polarization in *myosin xik xik* mutant hypocotyl.

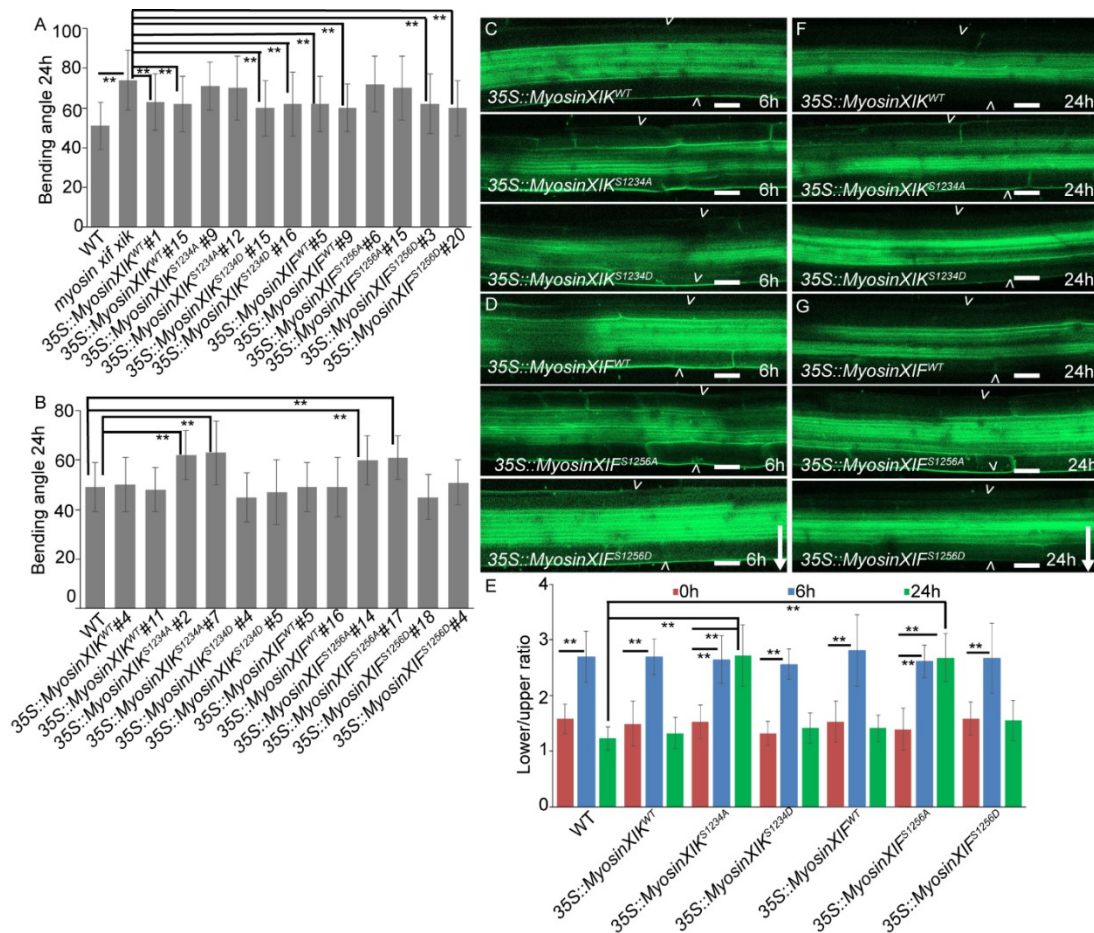
(A) Hypocotyl gravitropic bending kinetics of *myosin xik xik* mutant. The average bending curvatures were calculated. Data and error bars represent the mean \pm SD. $n = 30 - 40$, $** P < 0.05$ determined by Student's t-test.

(B) Polar auxin transport in *myosin xik xik* mutant hypocotyl. Data and error bars represent the mean \pm SD. $n = 15$, $** P < 0.05$ determined by Student's t-test.

(C - H) Representative images showing PIN3-GFP localization in no gravity stimulated wild type hypocotyls (C); no gravity stimulated *myosin xik xik* mutant hypocotyl (D); 6 hours gravity stimulated wild type hypocotyl (E) and *myosin xik xik* mutant hypocotyl (F); 24 hours gravity stimulated wild type (G) and *myosin xik xik* mutant hypocotyl (H). 3 days old etiolated seedlings were gravistimulated, and PIN3-GFP localization was captured.

(I) Quantification of gravity-induced PIN3 repolarization in *myosin xik xik* mutant hypocotyl. The ratio was calculated by dividing PIN3-GFP signal between inner side and outer side of hypocotyl endodermal cells. Data and error bars represent the mean \pm SD. $n = 15$, $** P < 0.05$ determined by Student's t-test.

Arrowheads indicate PIN3 at outer side of hypocotyl endodermal cells. Arrow indicates gravity direction. Scale bars, 20 μm .



Supplementary Figure S14. Gravity-induced PIN3 polarization in phospho-deficient and phospho-mimic myosin mutations in Col background.

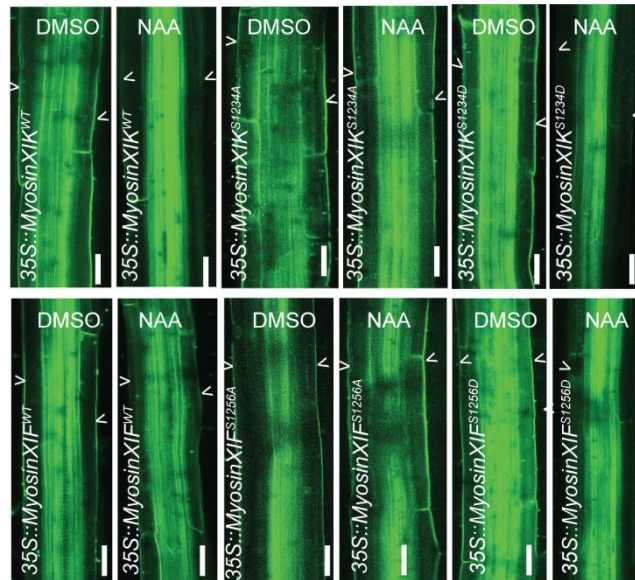
(A) Bending angle of phospho-deficient and phospho-mimic myosin mutations in Col background after 24 hours gravity stimulation. 3 days old etiolated seedlings were gravistimulated for 24 hours, and bending angle was quantified.

(B) Bending angle of phospho-deficient and phospho-mimic myosin mutations in *myosin xik xif* mutant background after 24 hours gravity stimulation. 3 days old etiolated seedlings were gravistimulated for 24 hours, and bending angle was quantified.

(C - G) Representative images showing PIN3-GFP localization in phospho-deficient and phospho-mimic myosin mutations in Col background after 6 hours (C, D) or 24 hours (F, G) gravity stimulation. 3 days old etiolated seedlings were gravistimulated for 6 hours or 24 hours, PIN3-GFP localization was captured.

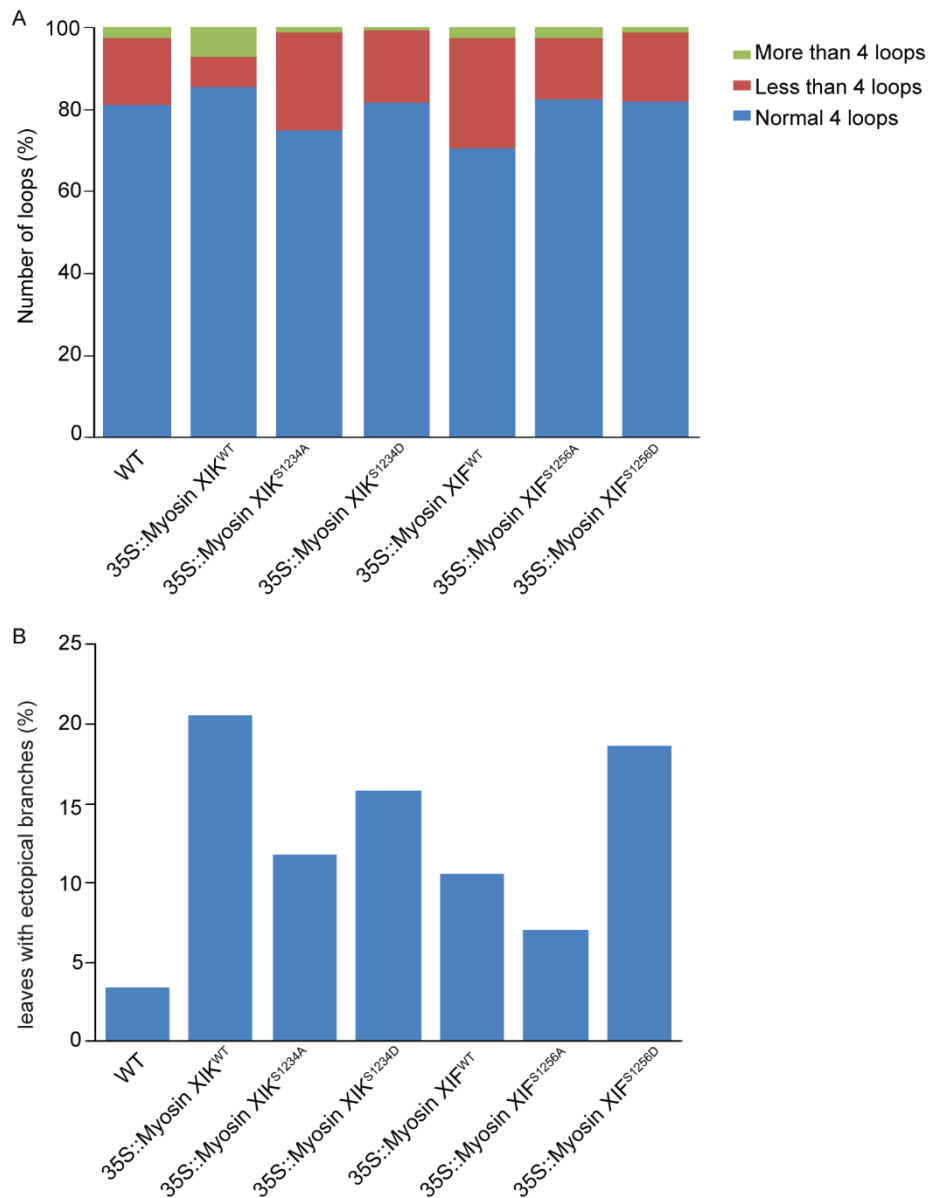
(E) Quantification of gravity-induced PIN3 repolarization in phospho-deficient and phospho-mimic Myosin XIK and XIF mutant hypocotyl. The ratio was calculated by dividing PIN3-GFP signal between lower side and upper side of hypocotyl endodermal cells. Data and error bars represent the mean \pm SD. $n = 15$, $** P < 0.05$ determined by Student's t-test.

Arrowheads indicate PIN3 at outer side of hypocotyl endodermal cells. Arrow indicates gravity direction. Scale bars, 20 μ m.



Supplementary Figure S15. Auxin-induced PIN3 polarization in phospho-deficient and phospho-mimic myosin mutants in Col background.

Representative images showing PIN3-GFP localization in phospho-mimic Myosin XIK and XIF mutant hypocotyl upon DMSO or auxin treatment. Arrowheads indicate PIN3 at outer side of hypocotyl endodermal cells. Scale bars, 20 μm .



Supplementary Figure S16. Quantification of leaf venation defects in phospho-deficient and phospho-mimic myosin mutants in Col background.

(A) Quantification of loops defects.

(B) Quantification of ectopical branches.

5 Actin cytoskeleton for auxin feedback regulation on PIN polarity

Huibin Han¹, Ewa Mazur², Nikola Rýdza³, Jiří Friml^{1, *}

¹ *Institute of Science and Technology (IST) Austria, 3400 Klosterneuburg, Austria*

² *Department of Cell Biology, Faculty of Biology and Environmental Protection, University of Silesia in Katowice, 40-032 Katowice, Jagiellońska 28, Poland*

³ *Central European Institute of Technology, Masaryk University, Brno, Czech Republic*

5.1 Introduction

Auxin is a regulatory phytohormone during plant development, which is characterized with polar transport within cells or tissues (Adamowski and Friml, 2015). The polar auxin transport depends on polarly localized PIN-FORMED (PIN) efflux transporters (Wiśniewsk et al., 2006). In the past decades, many novel genes, hormones, and environmental signals have been discovered to regulate the subcellular localization of PIN proteins and polar auxin fluxes that are essential for specific developmental processes (Adamowski and Friml, 2015). The canalization hypothesis indicates that the polarized PIN transporters forms a self-organizing patterns that determines auxin flows through tissues to establish the new polarity axes (Sachs, 1975; Sachs, 1986; Bennett et al., 2014; Smith and Bayer, 2009). Auxin canalization is involved in many developmental processes, such as vascular formation (Berleth and Sachs, 2001), regeneration after wounding (Sauer et al., 2006; Mazur et al., 2016), competitive regulation of apical dominance (Bennett et al., 2016), embryonic apical-basal axis establishment (Wabnik et al., 2013; Robert et al., 2013), organogenesis (Benková et al., 2003), and hypocotyl gravitropic bending termination (Rakusová et al., 2016, 2019). However, the molecular mechanism of auxin canalization is still not clear. The key hypothesis is either auxin has a direct feedback regulation on auxin transporters or the formation of auxin channels (Sachs, 1975). Evidence has been shown that auxin has a direct feedback regulation on PIN polarity (Sauer et al., 2006), and this probably due to auxin effect on clathrin-mediated endocytosis (CME) of PIN protein (Paciorek et al., 2005).

Auxin feedback regulation on PIN repolarization has been demonstrated in both root and hypocotyl. In root, PIN1 is localized at basal sides of endodermal cells, pericycle cells and vascular tissues (Friml et al., 2002a), whereas PIN2 displays a basal polarity in young cortex cells but an apical polarity in epidermal cells (Müller et al., 1998; Kleine-Vehn et al., 2008a). Upon auxin treatment, PIN1 rearranges its polarity from basal to inner-lateral side in root

endodermal and pericycle cells; whereas PIN2 polarity is shifted from basal to outer-lateral side of root cortex cells (Sauer et al., 2006, Prát et al., 2018). In the hypocotyl, PIN3 is expressed at endodermal cells with apolar distribution (Friml et al., 2002), and PIN3 repolarizes to inner side of hypocotyl endodermal cells upon auxin treatment (Rakusová et al., 2016, 2019). The detailed mechanism and biological significance of this auxin effect on PIN1 and PIN2 in root are still elusive, but it depends on SCF^{TIR1}-AUX/IAA-ARF auxin signaling pathway (Sauer et al., 2006), and requires the function of WRKY23 transcription factor (Prát et al., 2018). However, auxin feedback on PIN3 polarity at least is essential for hypocotyl gravitropic bending termination (Rakusová et al., 2016), and requires actin cytoskeleton function (Rakusová et al., 2019).

PIN proteins are undergoing recycling between plasma membrane and endosomal compartments (Geldner et al., 2001, 2003). The cycling is inhibited by the fungal toxin, brefeldin A (BFA), resulting in PIN internalization into the “BFA body” (Geldner et al., 2001). Actin inhibitor cytochalasin D abolishes the BFA-induced PIN internalization (Geldner et al., 2001). Cytochalasin D also induces a rapid PIN3 internalization (Friml et al., 2002b). Furthermore, actin inhibitor latrunculin B (Lat B) treatment leads a defective PIN1 polar localization in protophloem cells as well as a defective auxin-induced PIN3 repolarization in hypocotyl endodermal cells (Kleine-Vehn et al., 2006; Rakusová et al., 2019). Importantly, both apical and basal PIN targeting requires intact actin cytoskeleton (Kleine-Vehn et al., 2008b). Cortical actin microfilaments are also crucial for PIN1 asymmetric distribution in leaf epidermal pavement cells (Nagawa et al., 2012). However, the mechanism of actin cytoskeleton in auxin-mediated feedback on PIN polarity is not well understood.

Actin cytoskeleton function and organization require many actin-binding proteins, such as formin, actin-depolymerizing factor and Actin-Related-Protein 2/3 Complex (ARP2/3) (Staiger and Blanchoin, 2006). The ARP2/3 complex has been extensively studied in *Arabidopsis*, and mutations in ARP2/3 complex leads epidermal cell adhesion defects and distorted trichomes (Le et al., 2003; Mathur et al., 2003; El-Din El-Assal et al., 2004). The ARP2/3 complex mutants also exhibit cell wall defects as well as defects in polar auxin transport (Pratap Sahi et al., 2017). It also has been reported that ARP3 and ARPC2A shows different roles in gravitropism and phototropism (Reboulet et al., 2010). ARP3, one of the subunits of ARP2/3 complex, is involved in root gravitropism response by affecting amyloplast sedimentation and PIN-mediated polar auxin transport (Zou et al., 2016). Moreover, the *arp3*

mutant shows an overbending hypocotyl gravitropic response (Zou et al., 2016), indicating a possible role of ARP3 in regulation of PIN3 polarization during hypocotyl gravitropism.

In this study, we performed a detailed analysis to explore the roles of actin cytoskeleton and its organization protein, ACTIN2 and ARP3 in auxin feedback on PIN polarity. We conclude that actin cytoskeleton is involved in auxin feedback regulation on PIN repolarization in both root and hypocotyl. Disruption of the actin cytoskeleton or mutation in *ACTIN2* and *ARP3* genes resulting in a defective auxin-induced PIN rearrangement in roots and hypocotyls, ultimately lead to auxin-canalization related developmental defects. An uptake assay using the FM4-64 dye indicates that both *actin2* and *arp3* mutants defects in endomembrane trafficking. BFA treatment demonstrates that the actin cytoskeleton is involved in PIN trafficking. Overall, our results indicate the actin cytoskeleton plays an essential role in auxin feedback regulation of PIN polarity by affecting PIN trafficking.

5.2 Results

5.2.1 *The actin cytoskeleton is involved in auxin-mediated PIN rearrangement in Arabidopsis root*

Previously, we reveal that the actin cytoskeleton is required for auxin feedback on PIN3 repolarization during hypocotyl bending termination (Rakusová et al., 2019). To evaluate whether the actin cytoskeleton is also required for auxin-mediated PIN rearrangement in root, we studied the impacts of actin cytoskeleton inhibitors on auxin-mediated PIN1 rearrangement in roots (Sauer et al., 2006; Prát et al., 2018). We pretreated 3 days old light grown wild type seedlings with 10 μ M of latrunculin B (LatB) to disrupt the actin cytoskeleton or 5 μ M of jasplakinolide to stabilize the actin cytoskeleton for 30minutes, then co-treated with 10 μ M of 1-naphthaleneacetic acid (NAA) for another 4 hours. Consistent with previous results (Sauer et al., 2006; Prát et al., 2018), NAA induced PIN1 repolarization to the lateral side of endodermal cells in roots (Figure 1A, 1B, 1E), but NAA failed to induce PIN1 rearrangement when the actin cytoskeleton is disrupted by LatB or stabilized by Jasplakinolide (Figure 1C, 1D, 1E), these data indicate that the actin cytoskeleton is required for auxin-mediated PIN rearrangement in roots.

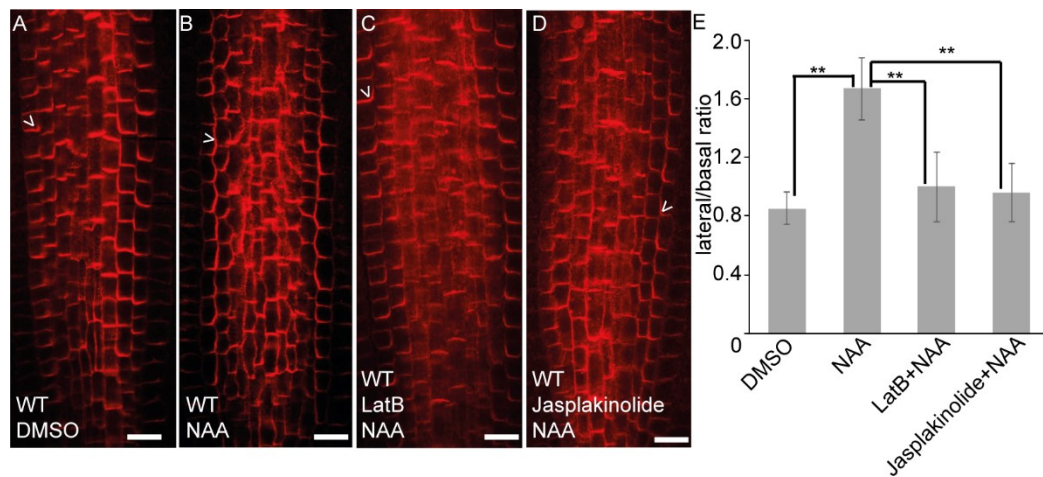


Figure 1. Actin cytoskeleton is required for auxin feedback on PIN1 lateralization in primary root.

3 days old light grown wild type seedlings were pre-treated with 10 μM of LatB, and 5 μM of jasplakinolide for 30 minutes, then co-treated with 10 μM of NAA for 4 hours. (A - D) Representative confocal images of PIN1 in root upon DMSO treatment (A), 10 μM of NAA treatment (B), 10 μM of LatB and NAA co-treatment (C), 5 μM of jasplakinolide and NAA co-treatment (D). (E) Quantification of PIN1 lateral-to-basal signal intensity in endodermal cells. The ratio was calculated between lateral and basal side of endodermal cells. Data are means ± the SD, N > 10, Students t-test, ** $P < 0.05$. Scale bars = 20 μm. Arrowheads depict PIN1 in endodermal cells

5.2.2 ***Defective auxin feedback on PIN1 polarization in actin2 and arp3 mutants root***

We next characterized actin cytoskeleton related mutants which would show the same PIN polarization defects. ACTIN2 and ARP3 are two good candidates with defects either in PIN repolarization or polar auxin transport (Zou et al., 2016; Pratap Sahi et al., 2017; Rakusová et al., 2019). Therefore, we assessed the auxin-induced PIN1 lateralization in *actin2* and *arp3* mutants. As shown, PIN1 relocated to the lateral side of endodermal cells after 4 hours of 10 μM of NAA treatment in wild type roots; whereas the auxin-induced PIN1 lateralization did not happen in both *actin2* and *arp3* mutants roots (Figure 2A - 2E), indicating that ACTIN2 and ARP3 are also required for auxin feedback on PIN repolarization in the root.

5.2.3 ***Defective auxin feedback on PIN3 polarization in actin2 and arp3 mutants during shoot gravitropism***

In contrast to roots, auxin also mediates PIN repolarization during hypocotyl gravitropism (Rakusová et al., 2016, 2019). As shown previously, either disruption of the actin cytoskeleton or mutation in ACTIN2 gene causes hypocotyl hyperbending with defects in auxin-mediated PIN3 repolarization (Figure 3A - 3G, 3J; Rakusová et al., 2019). In addition, the *arp3* mutant also shows overbending of the hypocotyl similar to *actin2* mutant and LatB treatment (Supplementary Figure S1E; Zou et al., 2016; Rakusová et al., 2019), we then addressed the role of ARP3 in PIN3 polarization regulation during hypocotyl gravitropism. We

first examined gravity-mediated PIN3 polarization in the *arp3* mutant (Rakusová et al., 2016). After 6 hours of gravity stimulation, a strong PIN3-GFP signal was observed at the lower side of endodermal cells in both wild type and in *arp3* mutant hypocotyls (Supplementary Figure S1A, S1B, S1F). However, after 24 hours gravity stimulation, a strong PIN3-GFP signal retained at the outer side of endodermal cells in the *arp3* mutant; whereas the PIN3-GFP signal disappeared at outer side of endodermal cells in the wild type hypocotyls (Supplementary Figure S1C, S1D, S1G). These data indicate a defective of auxin-mediated PIN3 repolarization at later stage of hypocotyl gravitropic response (Rakusová et al., 2016), but a normal gravity-mediated PIN3 polarization in the *arp3* mutant (Supplementary Figure S1A – S1G). Similar auxin-mediated PIN3 polarization defects are also observed in LatB treated hypocotyls and in the *actin2* mutant hypocotyls (Rakusová et al., 2019).

Exogenous application of auxin also induces PIN3 repolarization into the inner side of endodermal cells of the hypocotyl, as is observed at the later stage of gravitropic response (Rakusová et al., 2016, 2019). As reported previously, auxin-mediated PIN3 polarization doesn't happen in LatB treated hypocotyls and in the *actin2* mutant (Figure 3A - 3G, 3J; Rakusová et al., 2019). We then investigated the auxin effect on PIN3 polarization in the *arp3* mutant. We transferred 3 days old etiolated *arp3* mutant seedlings to new plates with 10 μ M of NAA or dimethyl sulfoxide (DMSO) for 4 hours. DMSO has no prominent effect on PIN3 polarity in both wild type and the *arp3* mutant (Figure 3A, 3H, 3K; Rakusová et al., 2016, 2019). The PIN3-GFP signal disappeared at outer side of endodermal cells in wild type after 4 hours NAA treatment (Figure 3B, 3E; Rakusová et al., 2016, 2019), but a strong PIN3-GFP signal was still observed at outer side of endodermal cells in the *arp3* mutant upon auxin treatment (Figure 3I, 3K), indicating a defective auxin-mediated PIN3 repolarization in the *arp3* mutant. Together with previous data (Figure 3A - 3K; Rakusová et al., 2019), our result supports that actin cytoskeleton is required for auxin feedback regulation of PIN polarity during hypocotyl gravitropic response.

The defective auxin feedback on PIN polarity also resulted in auxin canalization related phenotypes in *actin2* and *arp3* mutants. Upon auxin treatment, *actin2* and *arp3* mutants generated less lateral root, and short root hairs compared to wild type (Supplementary Figure S2A – S2D), this could be the consequence of less effective PIN repolarization in root upon auxin treatment (Figure 3A - 3E). The defective auxin feedback regulation on PIN3 polarity in *actin2* and *arp3* mutants is also demonstrated by hyperbending hypocotyls. In addition, LatB

treatment also causes hypocotyl hyperbending (Supplementary Figure S1E; Zou et al., 2016; Rakusová et al., 2019).

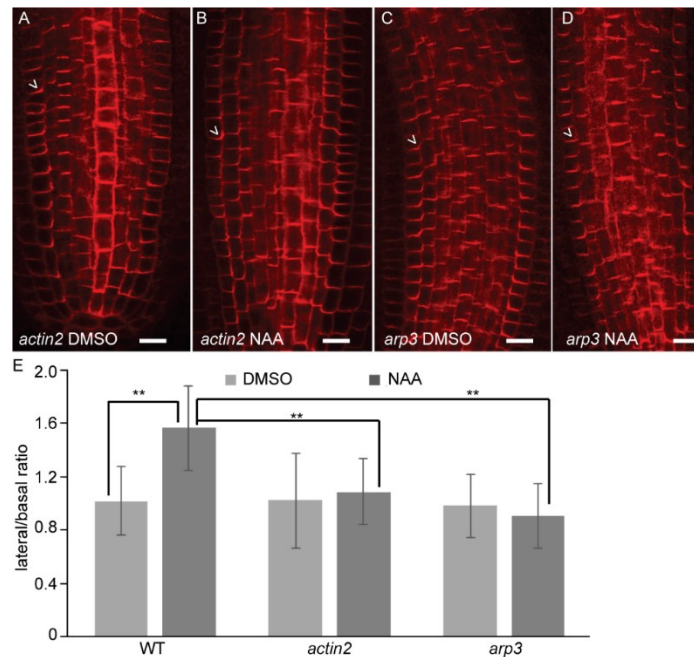


Figure 2. Auxin-induced PIN1 lateralization requires ACTIN2 and ARP3.

3 days light grown seedlings were treated with DMSO or 10 μ M of NAA for 4 hours. (A - D) Representative confocal images of PIN1 in DMSO treatment in *actin2* mutant (A) and *arp3* mutant (C) or NAA treated *actin2* mutant (B) and *arp3* mutant (D). (E) Quantification of PIN1 lateral-to-basal signal intensity in endodermal cells. The ratio was calculated between lateral and basal side of endodermal cells. Data are means \pm the SD, N > 10 seedlings, Students t-test, ** $P < 0.05$. Scale bars = 20 μ m. Arrowheads depict PIN1 in endodermal cells.

5.2.4 **Defective leaf venation patterning, auxin canalization, regeneration in *actin2* and *arp3* mutants**

Leaf vascular patterning requires auxin signaling and auxin flow (Berleth et al., 2006). The canalization hypothesis proposes the directional auxin flow as the main signal for vascular development and regeneration. To further emphasize the involvement of ACTIN2 and ARP3 in canalization, we examined the leaf venation patterning (Berleth and Sachs, 2001), regeneration after wounding (Sauer et al., 2006; Mazur et al., 2016) in *actin2* and *arp3* mutants.

We first quantified leaf vascular pattern of 7 days light-grown seedlings of wild type, *actin2* and *arp3* mutants. In wild type, only 13% of the leaves showed venation defects; whereas in the leaves of the *actin2* and *arp3* mutants the venation defects increased to 43.9% and 39.3%, respectively (Figure 4A, 4B).

Vasculature is regenerated in the wound neighborhood of primary tissues, according to the presumable new auxin flow direction (Aloni and Sachs, 1973; Sachs and Cohen, 1982; Flaishman et al., 2003; Sauer et al., 2006; Mazur et al., 2016). We then investigated

vasculature regeneration in the *actin2* and the *arp3* mutants stem after wounding. After 7 days, the new regenerated vessel was completely formed around the wound in wild type plants (Figure 4C, 4D). In the *actin2* mutant, 50% of seedlings displayed a completed regeneration of vessel cells; 50% of seedlings showed a slower development of vessel strands and the newly formed vessel strands were not connected (Figure 4C, 4D). In the *arp3* mutant, 30% of the seedlings showed single vessel cells, and 30% of seedlings exhibited incomplete vasculature regeneration (Figure 4C, 4D), indicating a defective regeneration of new vessels in the *arp3* and *actin2* mutants stem compared to wild type.

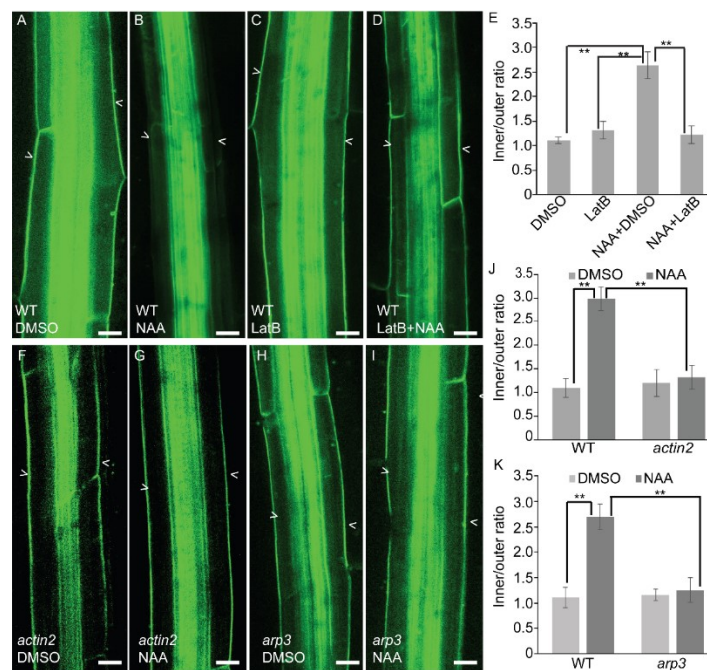


Figure 3. Auxin-induced PIN3 repolarization requires actin cytoskeleton, ACTIN2 and ARP3.

3 days etiolated seedlings were transferred to new plates with DMSO or 10 μ M of NAA for 4 hours in darkness. (A - D) Representative confocal images of PIN3-GFP in wild type hypocotyls under DMSO treatment (A), NAA treatment (B), LatB treatment (C), LatB and NAA co-treated (D). (E) Quantification of PIN3-GFP intensity upon LatB and auxin co-treatment. The PIN3-GFP intensity was calculated between inner and outer side of endodermal cells. (F - I) Representative confocal images of PIN3-GFP under DMSO treatment in *actin2* mutant (F) and *arp3* mutant (H), NAA treatment in *actin2* mutant (G) and *arp3* mutant (I). (J - K) Quantification of PIN3-GFP intensity upon auxin treatment in *actin2* mutant (J) and *arp3* mutant (K). The PIN3-GFP intensity was calculated between inner and outer side of endodermal cells. Data are means \pm the SD, N > 15, Students t-test, ** $P < 0.05$. Scale bars = 20 μ m. Arrowheads depict PIN3 at outer side of endodermal cells.

Local application of auxin after wounding is sufficient to induce vasculature formation along the auxin channel (Sauer et al., 2006; Mazur et al., 2016). We then studied auxin effect on vasculature formation in the *actin2* and *arp3* mutants after wounding. After 6 days, new vessels were completely formed from the local auxin source, the vessels were organized in continuous strand in wild type stems (Figure 5A, 5G, 5H). In *actin2* mutant, auxin-induced vessels formation decreased to 80%, and the vessels are unshaped, disorganized and did not

form continues strand (Figure 5B, 5G, 5H). In *arp3* mutants, the vessels formation decreased to 60%, vessels are observed in groups of cells and the strand were not connected (Figure 5C, 5G, 5H). In addition, we didn't observe vessels formation from the local applied auxin source when actin cytoskeleton was disrupted by LatB in wild type, the *actin2* and *arp3* mutants (Figure 5D, 5E, 5F, 5H). Taken together, these data indicate that actin cytoskeleton is involved in auxin canalization.

5.2.5 **Trafficking defects in *actin2* and *arp3* mutants**

Auxin feedback on PIN polarity is linked to auxin effects on clathrin-mediated endocytosis of PIN proteins (Paciorek et al., 2005). Accumulation of cortical actin microfilaments inhibits PIN endocytosis (Nagawa et al., 2012). The ARP2/3 complex has been reported to be involved in actin filament assembly, and it is also required for vesicle trafficking and endocytosis (Rotty and Bear, 2013; Sun et al., 2015; Zou et al., 2016). We then evaluated whether ACTIN2 and ARP3 are involved in endomembrane trafficking. The FM4-64 dye is widely used to investigate endomembrane trafficking of vesicles in living eukaryotic cells (Bolte et al., 2004). After incubation with 2 μ M of FM4-64 for 15 minutes, FM4-64 dye was internalized and substantial numbers of fluorescent vesicles were detected in the cytoplasm of wild type roots. Conversely, only a few vesicles were observed in the *actin2* and *arp3* mutants, indicating a defective trafficking in *actin2* and *arp3* mutants (Figure 6A, 6C, 6E, 6G; Zou et al., 2016). In addition, auxin has been shown to inhibit endomembrane trafficking (Figure 6B; Paciorek et al., 2005), however, *actin2* and *arp3* were less sensitive to auxin treatment (Figure 6D, 6F, 6G), indicating that ACTIN2 and ARP3 are involved in endomembrane trafficking.

5.2.6 **ACTIN2 and ARP3 mutations cause defective PIN trafficking**

PIN proteins are undergoing recycling between plasma membrane and endosomal compartments (Geldner et al., 2001). The cycling is inhibited by the fungal toxin, brefeldin A (BFA), resulting in PIN internalization into BFA bodies (Geldner et al., 2001). Auxin and actin inhibitors have been reported to inhibit BFA body formation (Geldner et al., 2001; Paciorek et al., 2005). To determine whether ACTIN2 and ARP3 are required for PIN trafficking, we studied PIN trafficking in the *actin2* and *arp3* mutant roots upon BFA treatment. After 50 μ M of BFA treatment for 60 minutes, we observed less BFA bodies in *actin2* and *arp3* mutants compared to wild type (Figure 7A, 7B, 7C, 7G), indicating a defective PIN trafficking. As

expected, auxin inhibited BFA body formation in wild type roots (Figure 7D, 7G), however, auxin has no additional effects in the *actin2* and *arp3* mutants root (Figure 7E - 7G). Altogether, actin cytoskeleton is required for PIN trafficking (Geldner et al., 2001; Figure 7A - 7C). Furthermore, our data at least support that ACTIN2 and ARP3 are involved in auxin-mediated inhibition of PIN trafficking (Paciorek et al., 2005).

BFA treatment also leads membrane proteins including PINs translocation from Golgi apparatus to *trans*-Golgi network (TGN)/early endosomes (EE) (Naramoto et al., 2014). Because less BFA bodies were observed in *actin2* and *arp3* mutants (Figure 7), it is likely that ACTIN2 and ARP3 are required for PIN translocation from the Golgi apparatus to the TGN/EE. To address this hypothesis, we performed immunolocalization in the *actin2* and *arp3* mutants roots using the anti-ARF1 antibody to mark TGN/EE. First, we investigated if actin cytoskeleton is required for PIN trafficking to TGN/EE. Pretreatment with 10 μ M of LatB for 30 minutes, and then co-treatment with 50 μ M of BFA, and LatB abolished the trafficking from Golgi apparatus to TGN/EE (Supplementary Figure S3A – S3D). Furthermore, the *actin2* and *arp3* mutants also showed defects in trafficking to TGN/EE upon BFA treatment (Supplementary Figure S3E – S3H). This assay suggests that actin cytoskeleton including ACTIN2 and ARP3 is required for protein trafficking to TGN/EE.

To further study the role of the actin cytoskeleton, ACTIN2 and ARP3 in trafficking, we monitored late endosomes movements, marked by *35S::GFP-ARA7* in *actin2* and *arp3* mutants roots (Ueda et al., 2004). When the actin cytoskeleton was disrupted by LatB, the endosomes movement were significantly reduced compared to DMSO treatment (Supplementary Figure S4). Similar endosomes movement defects were also observed in the *actin2* and *arp3* mutants, but not as strong as LatB treatment (Supplementary Figure S4), maybe due to the redundancy of the gene family. Our results demonstrate that actin cytoskeleton is essential for PIN trafficking to TGN/EE.

5.3 Discussion

The link between the actin cytoskeleton and polar auxin transport is complicated. On one hand, auxin modulates actin organization, and actin dynamics (Zhu and Geisler, 2015). On the other hand, the actin cytoskeleton is involved not only in the PIN recycling but also in PIN endocytosis. As a consequence, modulation of actin dynamics and organization either by chemical treatments, by hormones such as auxin, or by genetic mutants (including actin and

actin regulators) do affect PIN protein trafficking and endocytosis (Zhu and Geisler, 2015). In this study, we show that at least the actin cytoskeleton and its organization protein ACTIN2 and ARP3 are involved in auxin canalization with an essential role in auxin-mediated PIN polarity rearrangement by modulating PIN trafficking.

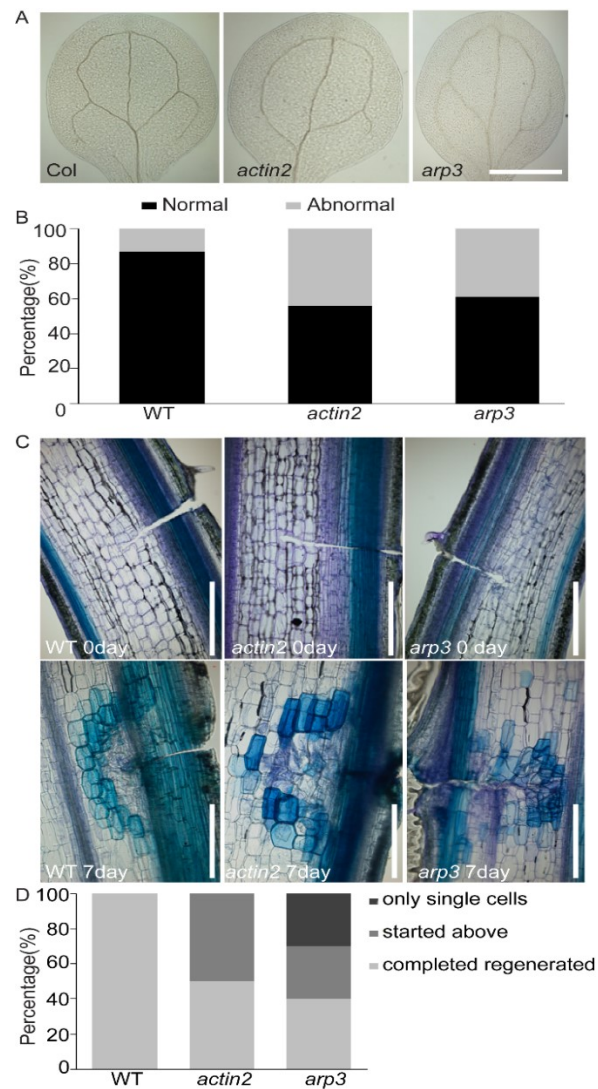


Figure 4. Defective leaf venation, regeneration in *actin2* and *arp3* mutants.

(A) Representative images of leaf venation defects in wild type, *actin2* and *arp3* mutant leaf. Scale bars = 1 cm. (B) Evaluation of cotyledon vasculature defects in *actin2* and *arp3* mutants. (C) Representative images of vasculature regeneration around wound after 7 days in wild type, *actin2* and *arp3* mutants. Vessels were fully regenerated around wound in wild type; vessels were not fully regenerated and slower than wild type in *actin2* mutant (50%); vessels were in grouped cells (30%) and vessels were not started (30%) in *arp3* mutant. Scale bars = 200 μ m. (D) Quantification of regeneration defects in *actin2* and *arp3* mutants. N = 10.

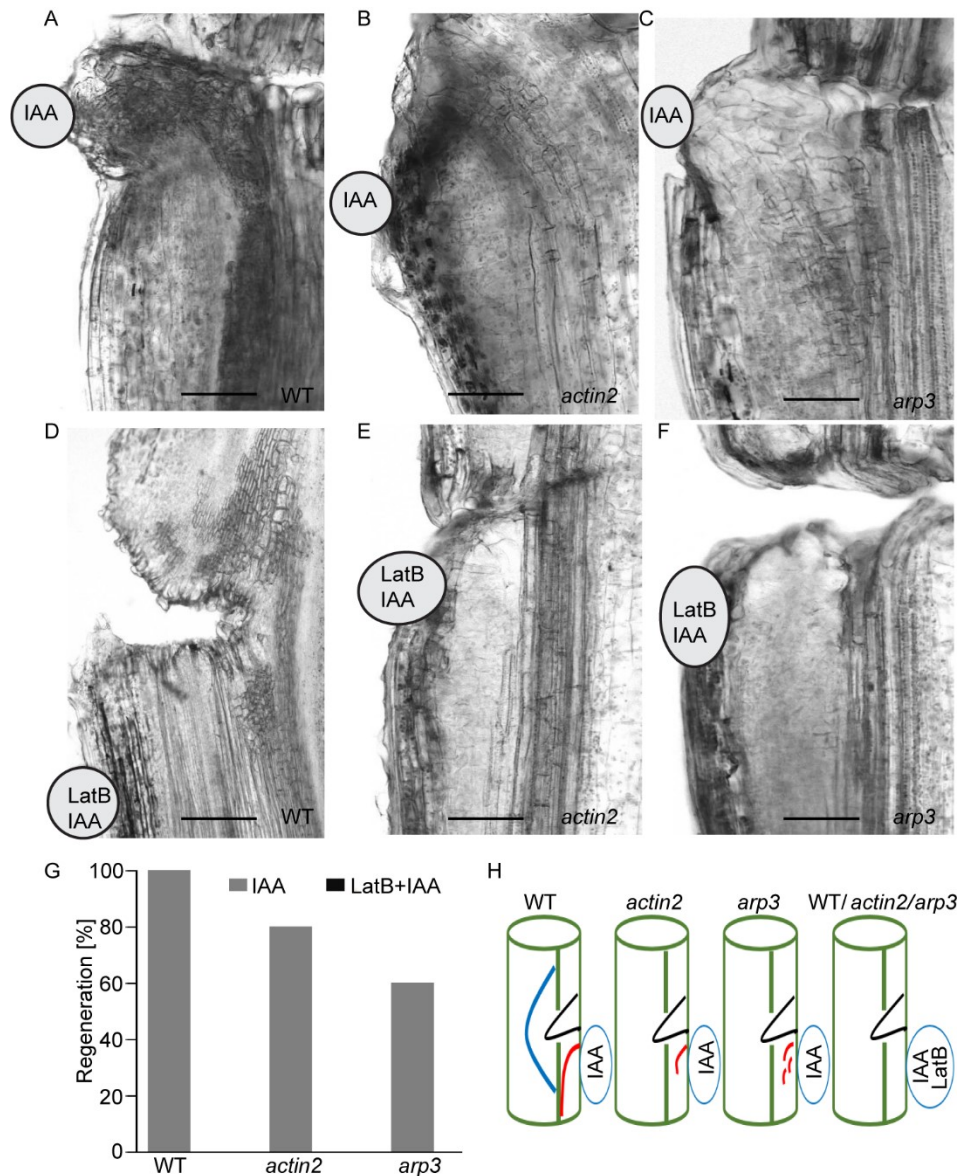


Figure 5. Auxin-canalization requires actin cytoskeleton, ACTIN2 and ARP3 protein function.

(A - C) Representative images of auxin induced vasculature regeneration in wild type (A), *actin2* mutant (B) and *arp3* mutant (C). The vessels are completely formed and connected with exist vasculature in wild type (A); the vessels are unshaped, disorganized and are not connected with vasculature in *actin2* mutant (B); the vessels are in grouped cells and are not connected with vasculature in *arp3* mutant (C). (D - F) Representative images of auxin induced vasculature regeneration upon LatB treatment in wild type (D), *actin2* mutant (E) and *arp3* mutant (F). Auxin failed to induce vessels formation in wild type, *actin2* and *arp3* mutants when actin cytoskeleton is disrupted by LatB (D - F). Scale bars = 200 μ m. (G) Quantification of vasculature regeneration upon auxin and LatB treatment in *actin2* and *arp3* mutants. N = 10. (H) Schemes of auxin canalization in *actin2* and *arp3* mutants. Auxin-induced vessels formation was completed and connected to exist vasculature in wild type (red line), and vessels were also formed around the wound in wild type (blue line) but not in *actin2* and *arp3* mutants. Auxin-induced vessels formation was defective in both *actin2* and *arp3* mutants (red line). LatB abolished auxin-induced vessels formation in wild type, *actin2* and *arp3* mutants.

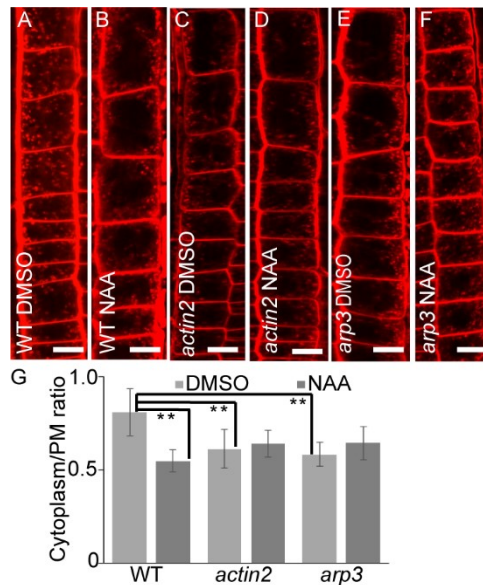


Figure 6. Decreased FM4-64 uptake in *actin2* and *arp3* mutants.

4 days light grown seedlings were used for FAM4-64 assay. (A - F) 30 minutes DMSO treatment in wild type (A), *actin2* mutant (C), and *arp3* mutant (E) or 10 μ M of NAA treatment in wild type (B), *actin2* mutant (D), and *arp3* mutant (F). (G) Quantification of FM4-64 internalization fluorescence intensity in *actin2* and *arp3* mutants. The ratio was calculated between cytoplasm and plasma membrane (PM). Data are means \pm the SD, N > 10, Students t-test, ** $P < 0.05$. Scale bars = 20 μ m.

5.3.1 Requirement of actin cytoskeleton for auxin feedback regulation on PIN polarity

The canalization hypothesis proposes that auxin has a feedback regulation on PIN polarity (Sachs, 1975; Smith and Bayer, 2009; Bennett et al., 2014), and this auxin feedback on PIN polarity has been demonstrated with experimental evidence in roots and hypocotyls (Sauer et al., 2006; Prát et al., 2018; Rakusová et al., 2016, 2019). In roots, PIN1 changes its polarity from the basal side to the lateral-inner side of endodermal cells upon auxin treatment (Sauer et al., 2006; Prát et al., 2018). However, auxin fails to induce PIN1 repolarization to lateral-inner side of endodermal cells when the actin cytoskeleton is disrupted or in *actin2* and *arp3* mutants roots (Figure 2A - 2E). Taken together, these direct evidence supports that actin cytoskeleton plays vital roles in auxin feedback regulation on PIN polarity.

Auxin feedback on PIN3 repolarization is essential for hypocotyl gravitropic bending termination (Rakusová et al., 2016, 2019), and the hyperbending hypocotyls of the *actin2* and *arp3* mutants suggest a possible role of ACTIN2 and ARP3 in PIN polarity regulation. Indeed, both *actin2* and *arp3* mutants showed defects in auxin-mediated PIN3 repolarization in hypocotyls (Figure 3F - 3K; Supplementary Figure S1C, S1D, S1G; Rakusová et al., 2019), but a normal gravity-induced PIN3 polarization (Supplementary Figure S1A, S1B, S1F; Rakusová et al., 2019). In addition, distribution of the actin cytoskeleton also shows similar auxin-mediated

PIN3 polarization defects (Figure 3A - 3E; Rakusová et al., 2019). All these data support a more specific role of actin cytoskeleton in auxin-mediated feedback on PIN3 polarization to terminate hypocotyl bending.

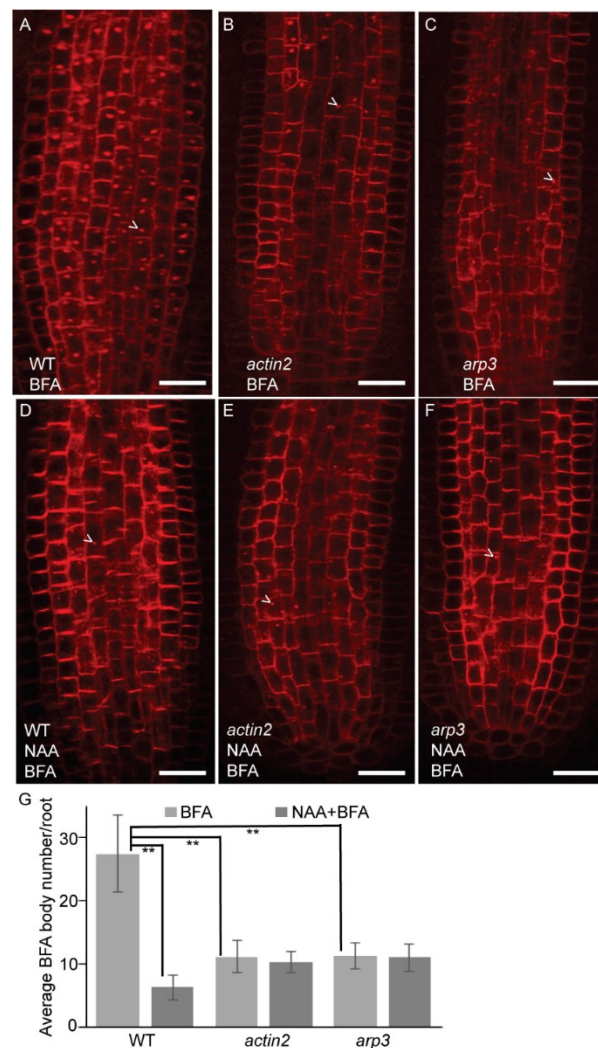


Figure 7. Defective intracellular PIN1 trafficking in *actin2* and *arp3* mutants upon BFA treatment.

3 days light grown seedlings were used for BFA treatment. (A - C) 60 minutes of 50 μ M of BFA treatment in wild type (A), *actin2* mutant (B), *arp3* mutant (C). (D - F) 30 minutes of 10 μ M NAA pretreatment then co treatment with 50 μ M of BFA for 60 minutes in wild type (D), *actin2* mutant (E), *arp3* mutant (F). (G) Quantification of BFA bodies in *actin2* and *arp3* mutants. Data are means \pm the SD. N > 15, Students t-test, ** P < 0.05. Scale bars = 20 μ m. Arrowheads depict BFA body.

5.3.2 ***The actin cytoskeleton is a component of auxin canalization***

Canalization is involved in many developmental processes (Berleth and Sachs, 2001; Sauer et al., 2006; Mazur et al., 2016). Auxin has been proposed to be the polarizing signal that mediates the directional channel formation underlying the spatio-temporal vasculature patterning and regeneration after wounding (Mazur et al., 2016). Feedback between auxin signaling and auxin flow is required for canalization (Mazur et al., 2016), but the mechanism behind is poorly understood. The *actin2* and *arp3* mutants show defects in leaf venation

patterning (Figure 4A, 4B), and they also show regeneration defects around the wound compared to wild type (Figure 4C, 4D). Furthermore, actin cytoskeleton inhibitor, LatB abolished auxin-induced formation of vascular in stem after wounding in wild type, *actin2* and *arp3* mutants (Figure 5D - 5G). Additionally, *actin2* and *arp3* mutants are insensitive to auxin application during regeneration after wounding (Figure 5A - 5C, 5G). These evidences support that actin cytoskeleton is a component of auxin-canalization, which is in line with previous report that LatB causes a defective PIN1 polar localization in protophloem cells (Kleine-Vehn et al., 2006).

5.3.3 ***The actin cytoskeleton dependent PIN trafficking***

The abundance and localization of PIN proteins at plasma membrane are finely regulated by different signals (Adamowski and Friml, 2015). PIN trafficking is crucial for PIN subcellular localization. Actin cytoskeleton has been shown to be involved in PIN trafficking (Geldner et al., 2001; Friml et al., 2002b; Nagawa et al., 2012). Clathrin-mediated endocytosis (CME) of PIN protein is a vital mechanism for manipulating PIN-mediated auxin distribution (Dhonukshe et al., 2007; Kitakura et al., 2011). In mammalian cells, actin cytoskeleton and ARP2/3 complex have been shown to transiently appear at clathrin-coated pits just prior to vesicle release (Yarar, et al; 2005). Our data provide evidence that ACTIN2 and ARP3 are also essential for trafficking (Figure 6A - 6G). However, the role of actin cytoskeleton in plant CME needs more investigation.

BFA treatment indicates that PIN recycling depends on the actin cytoskeleton (Figure 7A - 7G; Geldner et al., 2001). Disruption of actin cytoskeleton leads to a defective trafficking to TGN/EE. Similar defects are also observed in *actin2* and *arp3* mutants (Supplementary Figure S3A – S3H; Supplementary Figure S4). Taken together, our results demonstrate that ACTIN2 and ARP3 mediated actin organization participates in regulation of auxin distribution by inhibiting endosomes movement, resulting in a defective PIN trafficking.

In plants, the ARP2/3 complex is regulated by the nucleation promoting factors SCAR/WAVE regulatory complex and other proteins (Szymanski, 2005; Yanagisawa et al., 2013). SPIKE1 (SPK1) activating ROP-GTP signals that antagonize the SCAR regulatory complex resulting in activating of the ARP2/3 complex (Yanagisawa et al., 2013). On the other hand, some of the known membrane adaptor proteins do not have homologs in plants, therefore,

plants have evolved different protein complexes that localize at the cytoskeleton and mediated membrane trafficking or endocytosis (Wang and Hussey, 2015). We can't exclude the role of these proteins in auxin feedback on PIN polarity regulation, CME-mediated PIN endocytosis and trafficking. The next step would be important to investigate the function of these proteins such as the SCAR/WAVE complex, upstream of the ARP2/3 complex and other ARP2/3 complex subunits in PIN-mediated auxin transport, CME, and PIN trafficking processes. These novel findings would provide more insights to understand the basis of PIN polarity regulation. In addition, the actin-based myosin transport network drives long-distance intracellular transport in plant cells, the myosin motor proteins track toward to actin filament to deliver cargoes or proteins to specific cellular locations (Tominaga et al., 2003). Thus, it appears that myosin proteins may also important for PIN-mediated auxin transport (Abu-Abied et al., 2018), but the function of myosin proteins in auxin canalization especially in auxin feedback on PIN polarity needs more investigation.

In summary, our study reveals an essential aspect of the actin cytoskeleton in PIN subcellular localization regulation. We also demonstreat that actin cytoskeleton is also important for auxin canalization-related developmental processes.

5.4 Materials and Methods

Plant material and growth conditions

The following transgenic and mutant lines were used: Col-0 (wild type), *PIN3::PIN3-GFP* (Col-0 background, Žádníková et al., 2010); *35S::GFP-ARA7* (Ueda et al., 2004); *actin2* (SALK_048987, Rakusová et al., 2019), *arp3* (SALK_010045). Mutant combinations with *PIN3::PIN3-GFP* or *35S::GFP-ARA7* were generated through genetic crosses. Seeds were sown on plates with half-strength Murashige and Skoog (½ MS) medium with 1% sucrose, 1% agar and stratified at 4°C for 2 days, and then cultivation at 21°C.

Hypocotyl gravity stimulation

3 days old etiolated seedlings were turned 90°. To monitor gravitropic responses, plates were scanned 24 hours after gravistimulation, and bending angle was measured by ImageJ (NIH; <http://rsb.info.nih.gov/ij>). Each experiment was done at least three times with more than 30 seedlings to generate the same significant results.

Quantification of PIN3-GFP intensity

PIN3-GFP intensity was measured by ImageJ. The fluorescence intensity of PIN3-GFP were measured at upper part of hypocotyl as described previously (Rakusová et al., 2019). The ratio was calculated between outer side of endodermal cells at lower and upper side of hypocotyl after gravity stimulation for 6 hours or 24 hours (Rakusová et al, 2019). For auxin treatment, 3 days old etiolated seedlings were transferred onto new plates with 10 µM of NAA, and the same amount of DMSO for 4 hours. The ratio was calculated between inner and outer side of endodermal cells (Rakusová et al, 2016, 2019). Three biological repeats with more than 15 seedlings were performed to generate the same significant results.

Leaf venation assay

7 days old light grown seedlings were used for leaf venation analysis. Cotyledons were cleared in a solution containing 4% HCl and 20% methanol for 15 minutes at 65°C, followed by a 15 minutes incubation in 7% NaOH and 70% ethanol at room temperature. Next, seedlings were rehydrated by successive incubations in 70%, 50%, 25%, and 10% ethanol for 5 minutes, followed by incubation in a solution containing 25% glycerol and 5% ethanol for 2 days at room temperature. Finally, seedlings were mounted in 50% glycerol and were monitored by differential interference contrast DIC microscopy (Olympus BX53).

Canalization and regeneration of stem

The canalization and regeneration was performed as described previously (Mazur et al., 2016). Briefly, plants with immature inflorescence stems (9 to 10 cm tall) were used. Stems were decapitated with a sharp razor blade, the apical floral parts (1 to 2 cm) were removed, and the artificial weight, a 2.5 g lead ball connected with a plastic tube was applied. Decapitated stems covered by the artificial weight were additionally supported by a wood stick to avoid their bending. With this method, secondary tissue architecture could be obtained 6 days after weight application in the basal parts of previously immature *Arabidopsis* stems (5 mm segments above the rosette). Next, the stems were incised in the basal parts. 10 μ M of indole-3-acetic acid (IAA) and 10 μ M of Latrunculin B were mixed with lanolin paste and locally applied onto the wounded stems, beneath the wound.

For regeneration, inflorescence stems were cut precisely with a sharp razor blade 3 to 4 mm from the rosette in the transversal plane of the basal sectors with vascular cambium and secondary tissues to interrupt their longitudinal continuum. Plants were still covered with the artificial weight during this experimental step. Axillary buds grown above the rosette leaves were not removed, thus remaining the source of endogenous auxin. After 7 days after wounding, stems were cut by automated vibratome (Leica VT1200 S, Leica Microsystems Ltd., Wetzlar, Germany) and 80 μ m thick native sections were prepared. The native sections were stained with a 0.025 % Toluidine Blue O aqueous solution and regeneration was analyzed in stems with fully developed, closed cambial rings, and secondary tissues in their basal parts. The native sections were observed using a bright field microscope (Zeiss Axioscope.A1 ZEN) and pictures of vasculature were photographed with a camera (Axiocam 105) at 10x magnification. Only stems selected in this manner were used to study vasculature regeneration.

Whole-mount in situ immunolocalization

For PIN1 rearrangement in root upon auxin treatment, 3 days old primary roots were treated with 10 μ M of LatB and 5 μ M of Jasplakinolide for 30 minutes, then co-treated with 10 μ M of NAA for another 4 hours. The immunolocalization was carried out as described previously (Sauer and Friml, 2010). The antibodies were used as follows: anti-PIN1, 1 : 1000 (Paciorek et al., 2005). The second goat anti-rabbit antibody coupled Cy3 (Sigma-Aldrich) was diluted 1 : 600. PIN1 was monitored by inverted Zeiss confocal LSM-700. Quantification of PIN1 lateralization was performed in more than 50 endodermal cells for each root as described

before (Sauer et al., 2006). Three biological repeats were performed with a similar significant results.

FM4-64 assay and microscopy observation

4 days old light grown seedlings were incubated with 10 μM of NAA or same amount of DMSO for 30 minutes in $\frac{1}{2}$ MS liquid medium, then seedlings were transferred to new medium with 2 μM of FM4-64 for 15 minutes, and seedlings were mounted and observed using an inverted Zeiss confocal LSM-700 microscopy. Signal intensity was measured using ImageJ in more 50 cells. The ratio was calculated between cytoplasm and plasma membrane (PM). Three biological independent repeats with at least 10 seedlings were performed to generate the same significant results.

BFA treatment assay

To monitor PIN trafficking, 3 days old light grown seedlings were pretreated with 10 μM of latrunculin B (LatB), 10 μM of NAA or same amount of DMSO for 30 minutes, and then co-treatment with 50 μM of BFA in $\frac{1}{2}$ MS liquid medium for another 60 minutes, immunolocalization was carried out using anti-PIN1 or anti-ARF1 (ADP-ribosylation factor 1) antibody. Three biological independent repeats with at least 15 seedlings were performed to generate the same significant results.

Quantification of endosomes movements

4 days old light-grown seedlings were used for analysis. Seedlings were treated with 30 μM of latrunculin B and same amount of DMSO for 30 minutes, then an inverted LSM-800 microscopy was used to track the late endosomes movement with a setting of 4 millisecond per frame, in total 12 frames were recorded for each root. The TrackMate software was used to quantify endosomes movement using ImageJ (Jaqaman et al., 2008). The estimated blob diameter was set by 0.5 micron, with a threshold at 20, over 200 spots were quantified per root. Three biological independent repeats were performed to generate the same significant results.

Statistical analysis

All statistical analysis was performed using student's test in excel (Microsoft 2010) with a significant difference (** $P < 0.05$ or *** $P < 0.001$).

Author contributions:

H.H. and J.F. designed experiments; H.H. performed most the experiments; E.M. performed the auxin canalization experiment, and analyzed data, N.R. conducted the regeneration

experiment, and analyzed data; H.H. and J.F. wrote the manuscript with inputs from all authors.

5.5 References

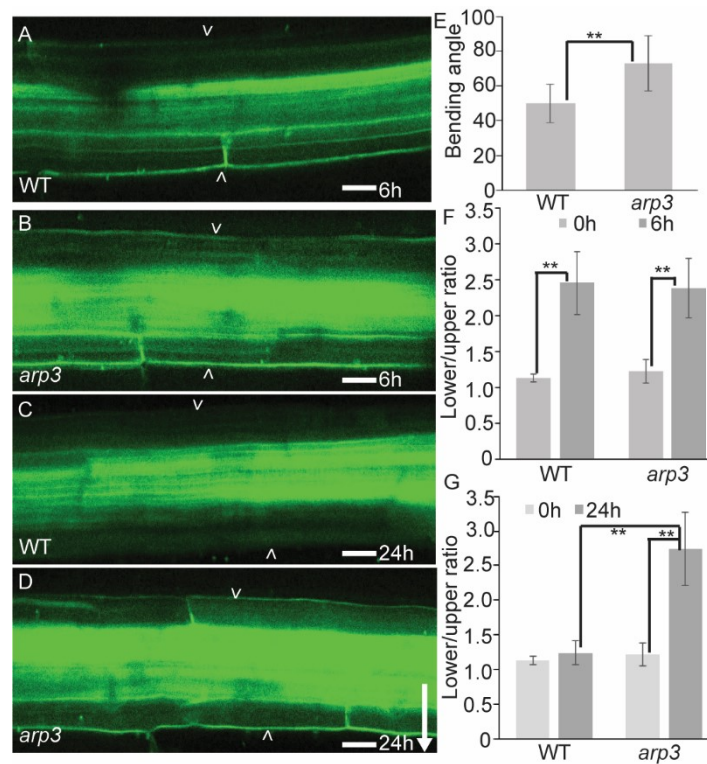
- Aloni R, Sachs T** (1973) The three-dimensional structure of primary phloem systems. *Planta* 113: 345-353.
- Adamowski M, Friml J** (2015) PIN-dependent auxin transport: action, regulation, and evolution. *The Plant Cell* 114.
- Abu-Abied M, Belausov E, Hagay S, Peremyslov V, Dolja V, Sadot E** (2018) Myosin XI-K is involved in root organogenesis, polar auxin transport, and cell division. *Journal of Experimental Botany* 69: 2869-2881.
- Berleth T, Sachs T** (2001) Plant morphogenesis: long-distance coordination and local patterning. *Current Opinion in Plant Biology* 4: 57-62.
- Benková E, Michniewicz M, Sauer M, Teichmann T, Seifertová D, Jürgens G, Friml J** (2003) Local, efflux-dependent auxin gradients as a common module for plant organ formation. *Cell* 115: 591-602.
- Bolte S, Talbot C, Boutte Y, Catrice O, Read ND, Satiat-Jeunemaitre B** (2004) FM-dyes as experimental probes for dissecting vesicle trafficking in living plant cells. *Journal of Microscopy* 214: 159-173.
- Berleth T, Scarpella E., Friml J, Marcos D** (2006) Control of leaf vascular patterning by polar auxin transport. *Developmental Biology* 1: 403.
- Bennett T, Hines G, Leyser O** (2014) Canalization: what the flux?. *Trends in Genetics* 30: 41-48.
- Bennett T, Hines G, van Rongen M, Waldie T, Sawchuk MG, Scarpella E, Ljung K, Leyser O** (2016) Connective auxin transport in the shoot facilitates communication between shoot apices. *PLoS Biology* 14, e1002446.
- Dhonukshe P, Aniento F, Hwang I, Robinson DG, Mravec J, Stierhof YD, Friml J** (2007) Clathrin-mediated constitutive endocytosis of PIN auxin efflux carriers in Arabidopsis. *Current Biology* 17: 520-527.
- El-Din El-Assal S, Le J, Basu D, Mallery EL, Szymanski DB** (2004) DISTORTED2 encodes an ARPC2 subunit of the putative Arabidopsis ARP2/3 complex. *The Plant Journal* 38: 526-538.
- Friml J, Benková E, Blilou I, Wisniewska J, Hamann T, Ljung K, Woody S, Sandberg G, Scheres B, Jürgens G, Palme K** (2002a) AtPIN4 mediates sink-driven auxin gradients and root patterning in Arabidopsis. *Cell*, 108, 661-673.
- Friml J, Wiśniewska J, Benková E, Mendgen K, Palme K** (2002b) Lateral relocation of auxin efflux regulator PIN3 mediates tropism in Arabidopsis. *Nature* 415: 806.
- Flaishman MA, Loginovsky K, Lev-Yadun S** (2003) Regenerative xylem in inflorescence stems of *Arabidopsis thaliana*. *Journal of Plant Growth Regulation* 22: 253-258.
- Geldner N, Friml J, Stierhof YD, Jürgens G, Palme K**. 2001. Auxin transport inhibitors block PIN1 cycling and vesicle trafficking. *Nature* 413: 425.
- Geldner N, Anders N, Wolters H, Keicher J, Kornberger W, Muller P, Delbarre A, Ueda T, Nakano A, Jürgens G** (2003) The Arabidopsis GNOM ARF-GEF mediates endosomal recycling, auxin transport, and auxin-dependent plant growth. *Cell* 112: 219-230.
- Jaqaman K, Loerke D, Mettlen M, Kuwata H, Grinstein S, Schmid SL, Danuser G** (2008) Robust single-particle tracking in live-cell time-lapse sequences. *Nature Methods* 5: 695.
- Kleine-Vehn J, Dhonukshe P, Swarup R, Bennett M, Friml J** (2006) Subcellular trafficking of the Arabidopsis auxin influx carrier AUX1 uses a novel pathway distinct from PIN1. *The Plant Cell* 18: 3171-3181.

- Kleine-Vehn J, Leitner J, Zwiewka M, Sauer M, Abas L, Luschnig C, Friml J (2008a)** Differential degradation of PIN2 auxin efflux carrier by retromer-dependent vacuolar targeting. *Proceedings of the National Academy of Sciences USA* 105: 17812-17817.
- Kleine-Vehn J, Łangowski Ł, Wiśniewska J, Dhonukshe P, Brewer PB, Friml J (2008b)**. Cellular and molecular requirements for polar PIN targeting and transcytosis in plants. *Molecular Plant* 1: 1056-1066.
- Kitakura S, Vanneste S, Robert S, Löffke C, Teichmann T, Tanaka H, Friml J (2011)** Clathrin mediates endocytosis and polar distribution of PIN auxin transporters in Arabidopsis. *The Plant Cell* 23: 1920-1931.
- Le J, El-Assal SED, Basu D, Saad ME, Szymanski DB (2003)** Requirements for Arabidopsis ATARP2 and ATARP3 during epidermal development. *Current Biology* 13: 1341-1347.
- Lanza M, Garcia-Ponce B, Castrillo G, Catarecha P, Sauer M, Rodriguez-Serrano M, et al (2012)** Role of actin cytoskeleton in brassinosteroid signaling and in its integration with the auxin response in plants. *Developmental Cell* 22: 1275-1285.
- Müller A, Guan C, Gälweiler L, Tänzler P, Huijser P, Marchant A, et al (1998)** AtPIN2 defines a locus of Arabidopsis for root gravitropism control. *The EMBO Journal* 17: 6903-6911.
- Mathur J, Mathur N, Kirik V, Kernebeck B, Srinivas BP, Hülskamp M (2003)** Arabidopsis CROOKED encodes for the smallest subunit of the ARP2/3 complex and controls cell shape by region specific fine F-actin formation. *Development* 130: 3137-3146.
- Marhavý P, Vanstraelen M, De Rybel B, Ding ZJ, Bennett MJ, Beeckman T, Benková E (2013)** Auxin reflux between the endodermis and pericycle promotes lateral root initiation. *The EMBO Journal* 32: 149-158.
- Marhavý P, Duclercq J, Weller B, Feraru E, Bielach A, Offringa R, Friml J, Schwechheimer C, Murphy A, Benková E (2014)** Cytokinin controls polarity of PIN1-dependent auxin transport during lateral root organogenesis. *Current Biology* 24: 1031-1037.
- Marhavý P, Montesinos JC, Abuzeineh A, Van Damme D, Vermeer JE, Duclercq J, Rakusová H, Nováková P, Friml J, Geldner N, Benková E (2016)** Targeted cell elimination reveals an auxin-guided biphasic mode of lateral root initiation. *Genes & Development* 30: 471-483.
- Mazur E, Benková E, Friml J (2016)** Vascular cambium regeneration and vessel formation in wounded inflorescence stems of Arabidopsis. *Scientific Reports* 6: 33754.
- Naramoto S, Otegui MS, Kutsuna N, De Rycke R, Dainobu T, Karampelias M, Fujimoto M, Feraru E, Miki D, Fukuda H, Nakano A, Friml J (2014)** Insights into the localization and function of the membrane trafficking regulator GNOM ARF-GEF at the Golgi apparatus in Arabidopsis. *The Plant Cell* 114
- Nagawa S, Xu T, Lin D, Dhonukshe P, Zhang X, Friml J, Scheres B, Fu Y, Yang ZB (2012)** ROP GTPase-dependent actin microfilaments promote PIN1 polarization by localized inhibition of clathrin-dependent endocytosis. *PLoS Biology* 10: e1001299.
- Paciorek T, Zažímalová E, Ruthardt N, Petrášek J, Stierhof YD, Kleine-Vehn J, Morris DA, Emans N, Jürgens G, Geldner N, Friml J (2005)** Auxin inhibits endocytosis and promotes its own efflux from cells. *Nature* 435; 1251.
- Pratap Sahi V, Cifrová P, García-González J, Kotannal Baby I, Mouillé G, Gineau E, Müller K, Baluška F, Soukup A, Petrášek J, Schwarzerová K (2017)** Arabidopsis thaliana plants lacking the ARP2/3 complex show defects in cell wall assembly and auxin distribution. *Annals of Botany* 122: 777-789

- Prát T, Hajný J, Grunewald W, Vasileva M, Molnár G, Tejos R, Schmid M, Sauer M, Friml J** (2018) WRKY23 is a component of the transcriptional network mediating auxin feedback on PIN polarity. *PLoS Genetics* 14: e1007177.
- Reboulet JC, Kumar P, Kiss JZ** (2010) DIS1 and DIS2 play a role in tropisms in *Arabidopsis thaliana*. *Environmental and Experimental Botany* 67: 474-478.
- Rakusová H, Gallego-Bartolomé J, Vanstraelen M, Robert HS, Alabadí D, Blázquez MA, Benková E, Friml J** (2011) Polarization of PIN3-dependent auxin transport for hypocotyl gravitropic response in *Arabidopsis thaliana*. *The Plant Journal* 67: 817-826.
- Robert HS, Grones P, Stepanova AN, Robles LM, Lokerse AS, Alonso JM, Alonso JM, Weijers D, Friml J**. 2013. Local auxin sources orient the apical-basal axis in *Arabidopsis* embryos. *Current Biology* 23: 2506-2512.
- Rotty JD, Wu C, Bear JE** (2013) New insights into the regulation and cellular functions of the ARP2/3 complex. *Nature Reviews Molecular Cell Biology* 14: 7.
- Rakusová, H, Abbas, M, Han, H, Song S, Robert H S, Friml J** (2016) Termination of shoot gravitropic responses by auxin feedback on PIN3 polarity. *Current Biology* 26: 3026-3032.
- Rakusová H, Han H, Valošek P, Friml J** (2019) Genetic screen for factors mediating PIN polarization in gravistimulated *Arabidopsis thaliana* hypocotyls. *The Plant Journal* 98:1048-1059
- Sachs T** (1975) The induction of transport channels by auxin. *Planta* 127: 201-206.
- Sachs T, Cohen D** (1982) Circular vessels and the control of vascular differentiation in plants. *Differentiation* 21: 22-26.
- Sachs T** (1986) Cellular interactions in tissue and organ development. In *Symposia of the Society for Experimental Biology* 40: 181-210.
- Szymanski DB** (2005) Breaking the WAVE complex: the point of *Arabidopsis* trichomes. *Current Opinion in Plant Biology* 8, 103-112.
- Sauer M, Balla J, Luschnig C, Wiśniewska J, Reinöhl V, Friml J, Benková E** (2006) Canalization of auxin flow by Aux/IAA-ARF-dependent feedback regulation of PIN polarity. *Genes & Development* 20: 2902-2911.
- Staiger CJ, Blanchoin L** (2006) Actin dynamics: old friends with new stories. *Current Opinion in Plant Biology* 9: 554-562.
- Smith RS, Bayer EM** (2009) Auxin transport-feedback models of patterning in plants. *Plant Cell & Environment* 32: 1258-1271.
- Sauer M, Friml J** (2010) Immunolocalization of proteins in plants. In *Plant Developmental Biology* 253-263. Humana Press, Totowa, NJ.
- Sun Y, Leong NT, Wong T, Drubin DG** (2015) A Pan1/End3/Sla1 complex links Arp2/3-mediated actin assembly to sites of clathrin-mediated endocytosis. *Molecular Biology of the Cell* 26: 3841-3856.
- Tominaga M, Kojima H, Yokota E, Orii H, Nakamori R, Katayama E, Anson M, Shimmen T, Oiwa K** (2003) Higher plant myosin XI moves processively on actin with 35 nm steps at high velocity. *The EMBO Journal* 22: 1263-1272.
- Ueda T, Uemura T, Sato MH, Nakano A** (2004) Functional differentiation of endosomes in *Arabidopsis* cells. *The Plant Journal* 40: 783-789.
- Wiśniewska J, Xu J, Seifertová D, Brewer PB, Růžička K, Blilou I, Rouquié D, Benková E, Scheres B, Friml J** (2006) Polar PIN localization directs auxin flow in plants. *Science* 312: 883-883.

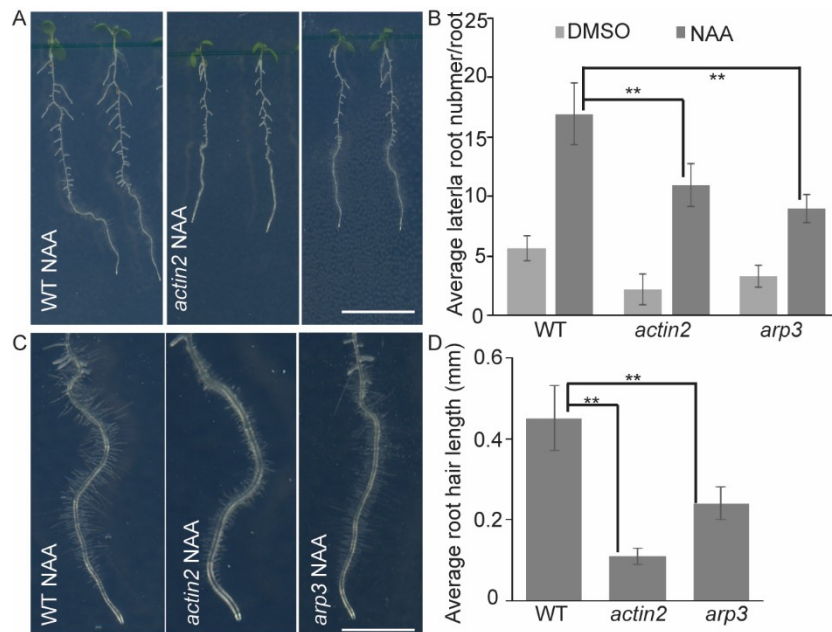
- Wabnik K, Robert HS, Smith RS, Friml J** (2013) Modeling framework for the establishment of the apical-basal embryonic axis in plants. *Current Biology* 23: 2513-2518.
- Wang P, Hussey PJ** (2015) Interactions between plant endomembrane systems and the actin cytoskeleton. *Frontiers in Plant Science* 6: 422.
- Yarar D, Waterman-Storer CM, Schmid SL** (2005) A dynamic actin cytoskeleton functions at multiple stages of clathrin-mediated endocytosis. *Molecular Biology of the Cell* 16: 964-975.
- Yanagisawa M, Zhang C, Szymanski DB** (2013) ARP2/3-dependent growth in the plant kingdom: SCARs for life. *Frontiers in Plant Science* 4: 166.
- Žádníková P, Petrášek J, Marhavý P, Raz V, Vandenbussche F, Ding ZJ, Schwarzerová K, Morita MT, Tasaka M, Hejátko J, Van Der Straeten D, Friml J, Benková E** (2010) Role of PIN-mediated auxin efflux in apical hook development of *Arabidopsis thaliana*. *Development* 137: 607-617.
- Zhu J, Geisler M** (2015) Keeping it all together: auxin–actin crosstalk in plant development. *Journal of Experimental Botany* 66: 4983-4998.
- Zou JJ, Zheng ZY, Xue S, Li HH, Wang YR, Le J** (2016) The role of Arabidopsis Actin-Related Protein 3 in amyloplast sedimentation and polar auxin transport in root gravitropism. *Journal of Experimental Botany* 67: 5325-5337.

5.6 Supplementary Figures



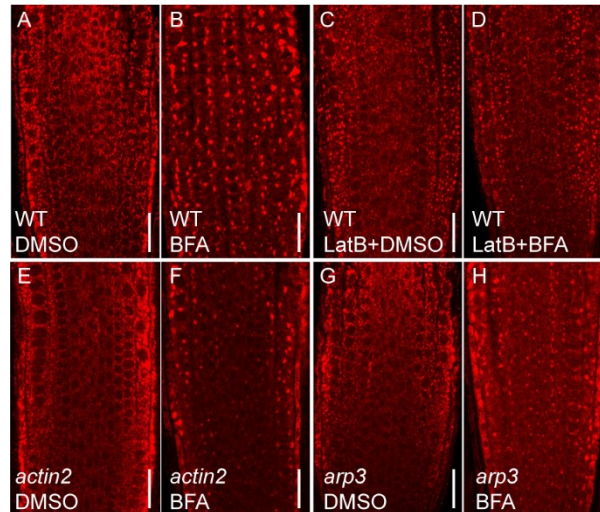
Supplementary Figure S1. Normal gravity-induced PIN3 polarization in *arp3* mutant.

3 days old etiolated seedlings were gravity stimulated for 6 hours or 24 hours. (A - B) Confocal image of PIN3-GFP in wild type (A) and *arp3* mutant (B) after 6 hours gravity stimulation. (C - D) Confocal image of PIN3-GFP in wild type (C) and *arp3* mutant (D) after 24 hours gravity stimulation. (E) Quantification of bending angle of *arp3* mutant after 24 hours gravity stimulation. (F - G) Quantification of PIN3 intensity in *arp3* mutant after 6 hours (F) and 24 hours (G) gravity stimulation. The ratio was calculated at outer side of endodermal cells between lower and upper side of hypocotyl. Data are means \pm the SD, N > 10, Students t-test, ** $P < 0.05$. Scale bars = 20 μ m. Arrowheads depict the PIN3-GFP at the outer sides of endodermal cells. Arrow indicates gravity direction.



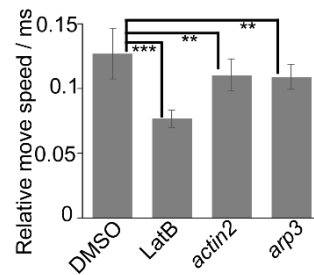
Supplementary Figure S2. Root phenotypes of *actin2* and *arp3* mutant upon auxin treatment.

3 days light grown seedlings were transferred onto new plates with DMSO or 100 nM of NAA and seedlings were kept growing for another 3 days, lateral root number and root hair length were quantified. (A) Representative images of lateral root of NAA treated wild type, *actin2* and *arp3* mutants. (B) Quantification of lateral root number after NAA treatment in *actin2* and *arp3* mutants. (C) Representative images of root hair elongation of NAA treated wild type, *actin2* mutant and *arp3* mutants. (D) Quantification of root hair length after NAA treatment in *actin2* and *arp3* mutants. Data are means \pm the SD, $N > 20$, Students t-test, $** P < 0.05$. Scale bars = 1 cm.



Supplementary Figure S3. Defective trafficking to TGN/EE in *actin2* and *arp3* mutants.

3 days light grown seedlings were pre-treated with 10 μM of LatB for 30minutes, then co-treated with 50μM BFA or DMSO, or only treated with 50 μM BFA or DMSO for another 60 minutes. Immunolocalization was performed using anti-ARF1. (A) DMSO treated wild type seedlings. (B) 50 μM BFA treated wild type seedlings. (C) LatB and DMSO co-treated wild type seedlings. (D) LatB and BFA co-treated wild type seedlings. (E - F) DMSO or BFA treated *actin2* mutant. (G - H) DMSO or BFA treated *arp3* mutant. Scare bar = 50 μm.



Supplementary Figure S4. Actin cytoskeleton, ACTIN2 and ARP3 are involved in late endosomes movement.

4 days light grown seedlings were pre-treated with 30 μM of LatB and DMSO for 30minutes, then late endosomes movement was tracked. Data are means ± the SD, N = 5, Students t-test, ** $P < 0.05$, *** $P < 0.01$.

6 Conclusions and future Perspectives

6.1 Conclusions

The main aim of this thesis is to gain a better understanding into processes that control cell polarity of auxin transporters PIN-FORMED (PIN) proteins during *Arabidopsis thaliana* development. Firstly, we study the physiological effect of PA, an inhibitor of phenylpropanoid pathway, on hypocotyl gravitropism. We demonstrate that PA inhibits auxin-mediated PIN3 repolarization via modulating flavonoid content and PID phosphorylation that ultimately leads to hypocotyl hyperbending. Secondly, we show the essential involvement of SCF^{TIR1/AFB} signalling in auxin-mediated PIN3 repolarization to terminate hypocotyl bending. By performing a phosphoproteomics, we characterize the role of Myosin XI protein and the MadB2 family myosin binding protein in PIN polarization regulation that ultimately leads to canalization-related developmental defects. Additionally, we uncover the vital role of actin cytoskeleton in PIN polarity regulation via modulating PIN trafficking. The results presented in this PhD thesis will provide novel insights into PIN polarity regulation during *Arabidopsis* development.

6.2 Further perspectives

Over the past decades, the mechanism underline PIN polarity regulation remains elusive. Genetic screen or chemical screen have been performed to identify novel factors mediating PIN subcellular localization. In Chapter 2, we investigate the physiological effect of PA on *Arabidopsis* hypocotyl gravitropism via modulating PIN-mediated intercellular polar auxin transport. However, it is also important to examine the PA effect on other kinases which have been reported to play essential roles in PIN polarity regulation. Meanwhile, under our experimental system, we only dissect the physiological effect of PA on hypocotyl gravitropism, we can't rule out whether PA also has impact on other developmental processes. On the other hand, the chemicals we used in the hypocotyl gravitropism assay also requires further study to uncover their role during *Arabidopsis* development.

In Chapter 4 and Chapter 5, we characterize the role of myosin complex and actin organization protein, ACTIN2 and ARP3, in PIN polarity regulation via modulating PIN trafficking. Despite the initial insights we obtained, some crucial questions needs more investigations in future, such as (1) which auxin signaling pathway is involved in the auxin-mediated myosin complex phosphorylation? (2) Which kinase phosphorylates myosin

protein? (3) How myosin protein and its binding protein transport cargoes, such as PINs? (4) How the tail-binding proteins are employed by myosin proteins to carry out their transport ability and cellular functions? (5) Is the interaction between myosin and myosin binding proteins is auxin dependent? (6) Are other known myosin proteins and its binding proteins also involved in PIN trafficking? (7) Is there any other actin-related proteins essential for PIN trafficking and polarity regulation? (8) What is the upstream of the ARP2/3 complex in PIN polarity regulation?

On the other hand, our phosphoproteomics approach identified many proteins are rapidly phosphorylated upon auxin treatment in a TIR1-dependent and -independent manner. The candidate proteins from our phosphoproteomics assay will provide novel and additional phosphorylation dependent regulation of PIN subcellular localization and polar auxin transport during *Arabidopsis* development and growth.

Overall, the answers to those fundamental questions will help us to understand how the PIN polarity is regulated by secondary metabolites, myosin transport network, and actin cytoskeleton. It will also bring new insights into phosphorylation-dependent regulation of PIN subcellular localization during plant development.